

**Towards a Formal Total Synthesis of Triptolide
Via a Gold-Catalyzed Cyclization Cascade**

By

Travis R. Schwantje

A thesis submitted to the Faculty of Graduate and Postdoctoral Studies
In partial fulfillment of the requirements for the
Master of Science (M.Sc.) degree in Chemistry

Candidate

Supervisor

Travis Schwantje

Dr. Louis Barriault

Ottawa-Carleton Chemistry Institute
Faculty of Science
University of Ottawa

© Travis Schwantje, Ottawa, Canada, 2013

Abstract

This thesis discusses the progress made towards a formal total synthesis of triptolide, a naturally occurring diterpenoid triepoxide molecule. Isolated from a Chinese vine, triptolide features some interesting structural characteristics and has demonstrated a broad range of interesting medicinal effects. It has demonstrated remarkable cytotoxicity against a number of cancer cell lines, immunosuppressive activity, and reversible male sterility. This biological activity has made it a target of a number of total syntheses spanning from 1980 to 2010.

Gold-catalyzed transformations are an emerging field in synthetic organic chemistry, but their efficacy and potential uses are gaining much recognition among the synthetic organic community. Our research group is extremely interested in the applications of such gold-catalyzed organic transformations in natural product synthesis. Here, we discuss our investigations towards accessing the tetracyclic core of triptolide using a gold-catalyzed cyclization cascade reaction.

We explored a number of synthetic routes towards a common linear precursor, and our successes and failures are discussed herein. We also report numerous unsuccessful efforts towards an oxidative gold-catalyzed cyclization cascade to form the tetracyclic core of triptolide. Finally, we investigated the use of a photocatalytic radical cyclization cascade to access the desired core. We report some promising preliminary results, and this study is ongoing in the Barriault group.

Acknowledgements

First and foremost, I want to extend the warmest of thanks to my supervisor, Dr. Louis Barriault, for taking me into his research group and providing guidance. Without an honours thesis, I had little experience in a synthetic chemistry lab when I entered grad school, but Louis took a chance on me and I am so grateful for this. He gave me freedom to pursue my own goals for this project, encouraged me to investigate new ideas and push my creativity as far as I possibly could. He let me make my own mistakes and learn from them, which I feel has helped me grow both as a chemist and as a person. Finally, under his guidance, my passion for organic chemistry has grown more than I ever imagined. Thank you, Louis.

The students in the Barriault group are equally important to recognize. From my first day in group, everyone was warm, welcoming, and willing to provide advice and assistance. Jason Poulin and Kassandra Lepack were the first two people I met when I toured the uOttawa campus in March 2010. Their warm reception went a long way in convincing me to join the group. My fumehood neighbours, Daniel Newbury and Geneviève Bétournay, were such great people to hang around and never failed to put a smile on my face. I greatly enjoyed working with Joel Marcotte and Boubacar Sow, with whom I had lively debates about the merits of iPhone vs. Android – by the way, Android is still better. During my time in the group, I had the opportunity to improve my French, and much of this is due to Francis Barabé; merci beaucoup pour l'expérience! Huge thanks go to our resident post-doc, Guillaume Révol, and former PhD student David Lapointe (now at U.C Berkeley) for all their input and suggestions. My office neighbours, Patrick Levesque and Mathieu Morin, were two great labmates and truly wonderful friends. Pat always encouraged me to keep pushing and to never give up when I was facing challenges. Mathieu never failed to put a smile on my face and, during my writing, helped out greatly by sending me some spectral data I had forgotten. Finally, I got to work with a great bunch of undergraduate students:

Stephanie Lanoix, Terry McCallum and Anika Tarasewicz were all such a pleasure to work with and I wish them all the best!

During my time at the University of Ottawa, I was privileged to interact with excellent faculty and support staff. I would like to first thank my committee members, Professors Christopher Boddy and Jeffrey Keillor, for their valuable input and comments on my work. On numerous occasions, I associated with Professors André Beauchemin and Derek Pratt, who were always willing to lend advice or suggestions when needed. Glenn Facey, our NMR Manager, is invaluable to the department: his organization and dedication kept the NMR facilities running smoothly. I want to thank also the crew in science stores for their hard work and cheery disposition, day in and out.

I would never have even gone to graduate school without the inspiration of a number of my teachers and professors from my undergraduate degree and before. First, I want to thank Professors Dennis Hore and Fraser Hof at the University of Victoria for being such excellent instructors and inspiring me to pursue a career in chemistry. To Professor Robin Hicks at UVic and Professor Mark McLachlan at UBC, I am grateful for giving me my first experiences in research labs, which helped me so much throughout both my undergraduate and graduate work. Finally, I want to thank Mr. Ray Mar, my high school chemistry teacher, who, though his excellent teaching and wonderful personality first ignited my passion for chemistry.

I am fortunate to have had a great support system of friends and family throughout my schooling. I want to extend thanks to my amazing friends back home in Ladner – Fabian Juren, Andrew Isaak, and Ryan Coleman, as well as all my friends from the University of Victoria, especially Emma Nicholls-Allison, whose drive and perseverance I admire in the utmost. I thank my brother, Kevin Schwantje, and my mother, Gayle Hubbard, for always supporting me and encouraging me to pursue my dreams.

Finally, I want to give my deepest thanks to my best friend in the world, Claire Gilmour. She means the world to me and I would have had a tough time getting through graduate school without her love and support.

Table of Contents

Abstract	ii
Acknowledgements	iii
Table of Contents	v
List of Schemes	vii
List of Figures	ix
List of Tables	xiv
List of Symbols and Abbreviations	xvi
Experimental Index	xix
1 Introduction	1
1.1 Triptolide.....	1
1.1.1 Biosynthesis.....	3
1.1.2 Medicinal Activity.....	5
1.1.3 Previous Syntheses	8
1.1.4 Our Approach.....	17
1.2 Proposed Gold Catalyzed Cyclization Cascade	18
1.2.1 Introduction to Gold(I) Catalyzed Organic Transformations	18
1.2.2 Oxidative Gold Transformations	23
1.2.3 Gouverneur Oxidative Cyclization.....	25
2 Synthesis	28
2.1 Retrosynthetic Analysis.....	28
2.1.1 Proposed extension of Gouverneur mechanism	28
2.1.2 Construction of Linear Precursor	31
2.2 Synthesis of Starting Materials	32
2.3 Cyclopropanation and Brady-Julia Olefination.....	35
2.3.1 Oxidative Cleavage of Terminal Alkene.....	36
2.3.2 Grignard Addition and Cyclopropanation	37
2.3.3 Brady-Julia Olefination	39
2.4 Orthoester Rearrangement and Homologation.....	41
2.4.1 Orthoester Rearrangement.....	41
2.4.2 One-Carbon Homologation	43

2.4.3	Attempted Acetylation and Conclusions	47
2.5	Global Cross-Metathesis	47
2.5.1	Synthesis of Type III partner and Proof of Concept.....	49
2.5.2	Optimization.....	50
2.5.3	Initial attempts at Allene synthesis.....	52
2.5.4	Initial work with Gold	55
2.6	Selection of a new protecting group.....	57
2.6.1	Bis-benzyl ether.....	58
2.6.2	Methylene acetal.....	58
2.6.3	Bis-methyl ether	59
2.7	Cross Metathesis-Wittig-Hydroboration Route.....	60
2.7.1	Cross-Metathesis with Methacrolein	61
2.7.2	Wittig Olefination to access 1,3-diene	63
2.7.3	Hydroboration-Oxidation of Diene	64
2.7.4	Accessing Allene target.....	65
2.8	Investigations into the Oxidative Gold Cyclization	68
2.8.1	Gold(I) Catalyzed Butenolide Cyclization	70
2.8.2	Isolation of the Vinyl Gold Intermediate and Oxidant Screening.....	71
2.8.3	Model Substrate Studies	76
2.9	Unexpected Radical Cyclization	77
2.9.1	Proposed Photochemical Cyclization	80
2.9.2	Possible Mechanisms.....	83
2.9.3	Control Studies: Current and Future Work.....	84
2.10	Synthetic Route Revisions.....	86
2.10.1	Direct Synthesis of halobutenolide.....	86
2.10.2	Redesigning the Synthesis.....	89
2.11	Summary and Outlook.....	98
3	Experimental Procedures and Supporting Information	103

List of Schemes

Scheme 1.1. General schematic biosynthetic pathway of plant terpene synthesis within the chloroplast. 4 Blocks represent 5-carbon subunits (IPP or DMAPP).....	4
Scheme 1.2. Bertochold synthetic approach to O-Me-triptophenolide.	10
Scheme 1.3 Bertochold method to access 1 from O-Me-triptophenolide.....	11
Scheme 1.4. van Tamelen synthesis of C20 precursor and Lewis acid promoted cyclization.	12
Scheme 1.5 Butenolide construction via mesylation, elimination, epoxidation, base-induced hydrolysis and lactonization for the van Tamelen synthesis.	12
Scheme 1.6. Yang method to access racemic tricycle 26 via Mn(OAc) ₃ mediated radical cyclization and subsequent butenolide construction.	13
Scheme 1.7. Yang asymmetric approach to triptophenolide utilizing a menthol-derived chiral auxiliary to control the enantioselectivity of the Mn(OAc) ₃ and Yb(OTf) ₃ -mediated radical cyclization of β-ketoester 27 to access tricycle 28.	14
Scheme 1.8. Yang protocol to access (-)-1 from (+)-4.	15
Scheme 1.9. Diels-Alder approach to the formal synthesis of 1 from the Sherburn group, featuring a convergent series of [4+2] cycloadditions to access tetracycle 34.....	16
Scheme 1.10. Dithiane approach to the formal synthesis of 1 from the Baati group.	17
Scheme 2.1. Formation of β-ketoester 50 via Brady-Julia olefination of cyclopropylcarbinol.	36
Scheme 2.2. Proposed Johnson-Claisen rearrangement and homologation to access desired β-ketoester 50 or allenolate 38.	42
Scheme 2.3. Proposed cross-metathesis of type I olefin 45 with type III olefin 56 to access β-ketoester 50	48
Scheme 2.4. Cross-Metathesis-Wittig-Hydroboration route to access dimethylated β-ketoester 72.....	61
Scheme 2.5. Stages of proposed gold cyclization cascade to be investigated and optimized. (1): Gold-catalyzed butenolide cyclization of 73 to access 74. (2): Isolation and oxidation of the vinyl gold species 75. (3): Synthesis and studies of model substrate 76.	69
Scheme 2.6. Possible products of attempted vinyl gold synthesis: desired organogold product 75 and protodeaurated species 74.....	72
Scheme 2.7. Synthesis of model substrate for gold cyclization (76) via β-ketoester 56 and attempted gold-catalyzed oxidative cyclization under the Gouverneur conditions.....	77

Scheme 2.8. Proposed radical cyclization cascade triggered by vinyl radical formation from a halobutenolide precursor 77 or 78.....	78
Scheme 2.9. Proposed tetronic acid coupling, reduction and halide formation from carboxylate starting material 82.	90
Scheme 2.10. Proposed <i>B</i> -alkyl Suzuki coupling between alkylborane 86 and bromoallenoate 87.....	93
Scheme 2.11. Proposed Cu(II) mediated/catalyzed alkyne-borane coupling to access alkynylcarbonate 90 and subsequent Pd-catalyzed carbonylation to access allenoate 88.....	95
Scheme 2.12. Proposed <i>B</i> -alkyl Suzuki-Miyaura coupling of alkylborane 86 with bromotetronic acid 91. Base = K ₂ CO ₃ , Cs ₂ CO ₃ or K ₃ PO ₄	98

List of Figures

Figure 1.1 <i>Tripterygium wilfordii</i> Hook F. leaves and inflorescence.....	1
Figure 1.2. Cytotoxic diterpenoids triptolide (1), triptidiolide (2) and triptonide (3) isolated from <i>Tripterygium wilfordii</i>	2
Figure 1.3. Structural motifs present in 1, including the oxygenated A ring (blue), <i>cis</i> - and <i>trans</i> -decalin junctions (green) and the γ -butenolide D ring (red).	2
Figure 1.4. Structural precursors to plant terpenes: geranylgeranyl pyrophosphate and 5-carbon subunits DMAPP and IPP.....	4
Figure 1.5. Examples of structural diversity among plant diterpenoids.	5
Figure 1.6. O-Me-triptophenolide (4), the key intermediate in all previously reported syntheses of 1, and triptophenolide (5), a naturally occurring product in <i>Tripterygium</i> and suspected intermediate in the biosynthesis of triptolide.	9
Figure 1.7. Enantioselective Diels-Alder cycloaddition utilized in Sherburn's synthesis.....	16
Figure 1.8. Proposed gold-catalyzed cascade cyclization of an allenolate 38 to construct the tetracyclic core of triptolide (12).	18
Figure 1.9. Generalized mechanism of gold(I)-catalyzed nucleophilic attack onto an allene.....	19
Figure 1.10. Highlights of recent publications on gold(I)-catalyzed carbocyclization reactions published by the Barriault group. (1) Selective 5- <i>exo</i> or 6- <i>endo</i> -dig carbocyclizations towards fused carbocycles. (2) Gold (I)-catalyzed 6- <i>endo</i> -dig cyclization of bicyclo[3,3,1]alkenone frameworks towards the synthesis of papuaforin A. ^b	20
Figure 1.11. Examples of gold(I) catalyzed en-yne polycyclization cascades to access fused tri- and tetracycles.	21
Figure 1.12. Cation-alkene mechanism of gold(I) catalyzed polycyclizations of 1,5-enynes. The chair-like transition state required to access the <i>trans</i> -decalin skeleton is denoted by the double-dagger symbol (\ddagger).	22
Figure 1.13. Enantioselective gold(I) catalyzed polycyclization of enynes published by Toste and co-workers in 2010.	22
Figure 1.14. Cyclizations of 2,3-allenolates catalyzed by cationic gold(I) and gold(III) species.	23
Figure 1.15. Oxidative gold-catalyzed cross-coupling reaction of allenolates and terminal alkynes.....	24
Figure 1.16. General catalytic cycle of a gold(I/III) catalyzed oxidative cross-coupling reaction of an allene.....	25

Figure 1.17. Oxidative gold-catalyzed intramolecular cross-coupling synthesis of dihydroindénofuranones reported by the Gouverneur group in 2010.....	26
Figure 1.18. Proposed mechanism of oxidative gold-catalyzed intramolecular cross coupling to form dihydroindénofuranones.....	26
Figure 2.1. Possible mechanisms for the proposed oxidative gold-catalyzed cyclization cascade to form the tetracyclic core of triptolide. Path A: Coordination of alkene ligand to gold(III), triggering Friedel-Crafts arylation forming 42 directly. Path B: Formation of carbocation 41 by nucleophilic attack of alkene, then Friedel-Crafts alkylation to seal up the tetracyclic backbone.....	30
Figure 2.2. Retrosynthetic analysis of linear allenolate precursor to proposed starting material 2-isopropylphenol.....	31
Figure 2.3. Retrosynthetic analysis of highly <i>E</i> -selective synthetic methods to access the desired trisubstituted alkene.....	32
Figure 2.4. MgCl ₂ and Et ₃ N-mediated <i>ortho</i> -formylation of 2-isopropylphenol using paraformaldehyde as the carbon source.....	33
Figure 2.5. Synthesis of allylated diol 43 via a Barbier-type allylation of salicylaldehyde 44.....	34
Figure 2.6. Installation of the acetonide protecting group using catalytic <i>p</i> -toluenesulfonic acid in neat 2,2-dimethoxypropane.....	35
Figure 2.7. Optimized oxidative cleavage conditions to access aldehyde 46.....	37
Figure 2.8. Optimized procedure for Grignard addition of isopropenylmagnesium bromide to aldehyde 46 to access diastereomeric alcohol 47 and Simmons-Smith cyclopropanation with diethylzinc to access cyclopropane 48.....	38
Figure 2.9. Accepted mechanism of Brady-Julia olefination of secondary cyclopropylcarbinols.....	39
Figure 2.10. Newman projections for determination of the stereochemical outcome of the Brady-Julia olefination.....	40
Figure 2.11. Mechanistic explanation of <i>E</i> -selectivity in the Johnson-Claisen rearrangement of secondary allylic alcohols.....	43
Figure 2.12. Optimized conditions for the Johnson-Claisen orthoester rearrangement reaction.....	43
Figure 2.13. Reduction of ester 51 to primary alcohol 52 with LiAlH ₄	44
Figure 2.14. Tosylation of primary alcohol 52 with <i>p</i> -toluenesulfonyl chloride, triethylamine and DMAP to access sulfonate ester 2.14-1.....	44
Figure 2.15. Nucleophilic cyanation of tosylate 2.14-1 to access primary nitrile 53. (Structure).....	45

Figure 2.16. Basic hydrolysis of alkyl cyanide 53 to access carboxylate 54.....	46
Figure 2.17. Esterification of carboxylate 54 with Boc ₂ O and MgCl ₂ to access homologated ester 55.	46
Figure 2.18. Unintended O-acetylation of <i>tert</i> -butyl ester 55 with acetyl chloride.....	47
Figure 2.19. Thermodynamic control of cross-metathesis between type I alkene 45 and type III alkene 56. 45 is able to homodimerize to form 2.19-1, which can react via secondary metathesis with 56, forming 50.	49
Figure 2.20. Conversion of 3-methyl-3-buten-1-ol to iodide 2.20-2 via the Appel reaction.....	50
Figure 2.21. Alkylation of <i>tert</i> -butyl acetoacetate with iodide 2.20-2 to access type III metathesis partner 56.....	50
Figure 2.22. Initial results of cross-metathesis of 45 and 56 with the 2 nd generation Grubbs catalyst.....	50
Figure 2.23. One-pot synthesis of 2,3-allenoates from substituted β-ketoesters as described by Maity and Lepore.	53
Figure 2.24. Two-step triflate formation and subsequent elimination protocol to access allenoate 38.....	53
Figure 2.25. Alternative one-pot method for allene synthesis via intermediate enol phosphonate 59.....	54
Figure 2.26. Failure of original Gouverneur conditions for the proposed gold cyclization cascade reaction.....	55
Figure 2.27. Au(I)/Au(III) catalyzed butenolide cyclization with unexpected deprotection of acetonide group.	56
Figure 2.28. Deprotection of 38 to allenoate diol 62 upon exposure of 38 to the Gagosz catalyst in acetonitrile and water.	56
Figure 2.29. Proposed alternative protecting groups for the phenolic/benzylic diol system.....	57
Figure 2.30. Unexpected mono-methylation of diol 43 while attempting to form methylene acetal 67 under acidic conditions.	58
Figure 2.31. Successful installation of methylene acetal protecting group under basic phase-transfer conditions.	59
Figure 2.32. Base-mediated bis-methylation of diol 43 with iodomethane.....	59
Figure 2.33. Telescoped multigram-scale three-step synthesis of bis-methyl ether 66.....	60
Figure 2.34. Stability test of bis-methyl ether protecting group with the Gagosz gold catalyst.....	60
Figure 2.35. Optimization protocol for the cross-methathesis of 66 with methacrolein, catalyzed by the 2 nd generation Grubbs catalyst.	62

Figure 2.36. Proposed <i>in situ</i> -generated chelate 2.36-1 and 2nd generation Hoveyda-Grubbs catalyst 2.36-2.	63
Figure 2.37. Optimized procedures for Wittig olefination of aldehyde 68 to access diene 69.....	64
Figure 2.38. Hydroboration-oxidation of 1,3-diene 69 with <i>in situ</i> generated dicyclohexylborane and oxidative workup to access homoallylic alcohol 70.....	65
Figure 2.39. Mesylation and alkylation synthetic process. Mesylate 71 was worked up by aqueous extraction and drying under vacuum. Sodium enolate 2.39-2 was prepared and used as a solution in THF.	66
Figure 2.40. Selectivity difficulties in "malonate-type" alkylation reactions of β -ketoesters. After an initial alkylation, reformation of a mono-substituted enolate can result in formation of dialkylated product, reducing synthetic efficiency.....	67
Figure 2.41. Successful one-pot allene formation following the Maity and Lepore method.	68
Figure 2.42. Failure of Gouverneur conditions to cyclize dimethyl-protected allenolate 73.	68
Figure 2.43. Cationic gold(I) catalysts utilized during screening of conditions for butenolide construction.	71
Figure 2.44. Optimized conditions for synthesis and isolation of vinyl gold complex 75 using 2,6-di- <i>tert</i> -butyl-4-methylpyridine as an acid scavenger.....	73
Figure 2.45. Dimeric butenolide 2.45-1 resulting from treatment of 75 with $\text{PhI}(\text{OAc})_2$	74
Figure 2.46. Suppression of degradation by Na_2CO_3 upon exposure of allenolate 73 to Gagosz catalyst and SelectFluor in THF/water solvent system.....	75
Figure 2.47. Model substrate for studying the oxidative gold cyclization reaction and the potential for alkene coordination or nucleophilic attack.	76
Figure 2.48. Transformation of vinyl gold complex 75 to iodobutenolide 77 using NIS.	78
Figure 2.49. Tris(bipyridine)ruthenium(II)chloride (Ru-bipy) and <i>fac</i> -tris[2-phenylpyridinato- <i>C-N</i>]iridium(III) (Ir-ppy) photoredox catalysts.....	79
Figure 2.50. Representative catalytic cycle of a photoredox radical cyclization of an indole. [O] represents a one-electron oxidation process. $\text{Ru}(\text{bpy})_3 = \text{tris}(\text{bipyridine})\text{Ruthenium}(\text{II})$	80
Figure 2.51. Proposed photoredox cyclization from iodobutenolide 77 to proposed tetracycle 79 using a gold species [Au] upon exposure to UV light.	81
Figure 2.52. Setup of photochemical cyclization reaction. The left image is immediately after initial exposure to sunlight. The right image is after 2.5 hours of exposure to sunlight.	81
Figure 2.53. Aromatic ^1H NMR signals of proposed tetracycle 79 and known tetracyclic diol 12.....	81

Figure 2.54. Karplus Equation for estimation of $^3J_{\text{H-H}}$ coupling constants in NMR spectrometry, where \emptyset is the dihedral angle between the two atoms in question; A, B and C are empirically defined parameters depending on the atoms in question.....	82
Figure 2.55. 1,2-diaxial coupling between H_X and H_{ax} in our proposed tetracycle and known structural relative.....	82
Figure 2.56. Potential 5- <i>exo</i> - and 6- <i>endo</i> -trig cyclization pathways for the vinyl radical 2.55-1, giving rise to radical intermediates 2.55-2 and 2.55-3.....	83
Figure 2.57. Intermolecular carbocation trapping by acetonitrile and water to form amide 80 via the Ritter reaction.....	84
Figure 2.58. Synthesis of bromobutenolide 78 from vinyl gold species 75 using NBS.....	85
Figure 2.59. Proposed synthesis of chlorobutenolide 81 for further study of catalyst activity.....	85
Figure 2.60. Attempts to access halobutenolides from allenates 73 and 76 using electrophilic halide sources "X".....	87
Figure 2.61. Attempts to access halobutenolides using a catalytic amount of gold and NIS to trap the vinyl gold species via iododauration.....	88
Figure 2.62. Attempts to access halobutenolides using copper(II) halides to induce lactonization.....	89
Figure 2.63. Literature precedent for coupling of a β - γ -unsaturated carboxylate to tetronic acid via a two-step coupling/Fries rearrangement and reduction protocol.....	90
Figure 2.64. Proposed mechanism of reduction of ketotetronic acid 2.63-1 by two equivalents of NaCNBH_3 in acidic conditions.....	91
Figure 2.65. Oxidation procedures performed on homoallylic alcohol to access carboxylate 82.....	92
Figure 2.66. Undesired formation of conjugated isomer of starting carboxylate during attempted tetronic acid coupling.....	92

List of Tables

Table 1. Optimization of oxidative cleavage reaction of allyl acetonide 45 using osmium tetroxide and sodium periodate.	37
Table 2. Optimization of global cross-metathesis reaction. All yields are isolated yields reported as a 2:1 E/Z mixture unless otherwise indicated. G2 = Grubbs 2nd generation catalyst, HG2 = Hoveyda-Grubbs 2nd generation catalyst, iPr-HG2 = Hoveyda-Grubbs 2nd generation catalyst with IPr NHC ligand. *(dg) indicates that the reaction mixture was degassed prior to heating. ^a Type I partner was added over 5 hours. ^b Type I partner added over 12 hours. ^c Catalyst was added over 5 hours. ^d Reaction performed under Schlenk conditions. ^e Reaction performed on 500mg scale. ^f Product isolated as a 4:1 E/Z mixture.	52
Table 3. Stability study of allenolate 38 to gold(I) and Selectfluor. *All reactions were run in ACN/H ₂ O (0.05M) at RT.	57
Table 4. Optimization and scale-up of cross-metathesis of 66 with methacrolein. *Isolated yields. All reactions proceeded with <100% conversion. Remaining 66 not recovered.	63
Table 5. Optimization of Wittig olefination of 68 to produce 1,3-diene 69. *n-BuLi and KOtBu were added as solutions in hexanes and THF, respectively. **KHMDs was added as a solid.	64
Table 6. Solvent and catalyst screening for gold-catalyzed butenolide formation from allenolate 73. ^a NMR Yield, ^b Isolated yield, ^c Degradation of starting material observed.	70
Table 7. Optimization of the synthesis and isolation of vinyl gold species 75. Py = 2,6-di- <i>t</i> -butyl-4-methylpyridine. *Generated <i>in situ</i> from PPh ₃ AuCl and AgOTf.	73
Table 8. Oxidant screening for gold(I-III) oxidation of vinyl gold species 75. ^a 2-3 equivalents of each oxidant used respective to vinyl gold. ^b NFSI = N-fluorobenzenesulfonamide. ^c KBARF = Potassium tetrakis[3,5-bis(trifluoromethyl)phenyl]borate.	74
Table 9. Summary of current and future work to study the photoredox radical cyclization and study the reactivity of [Au] compared to other photoredox catalysts.*Other Ir-centered photocatalysts have been reported. These will be investigated in due course.	86
Table 10. Failed attempts at halobutenolide formation using electrophilic halogenation and lactonization in the absence of gold.	87
Table 11. Failed attempts at a gold-catalyzed cyclization, trapping <i>in situ</i> -formed vinyl gold species with N-iodosuccinimide to access iodobutenolide.	88

Table 12. Failed attempts at conducting copper(II)halide-mediated synthesis of bromo- and chlorobutenolides from model substrate 76. Reactions were performed at 80-85°C in sealed vials.	89
Table 13. Conditions attempted for the B-alkyl Suzuki-Miyaura coupling of alkylborane 86 and bromoallenoate 87. *Reaction solutions were degassed by sparging with Ar for 15 minutes prior to mixing.	94
Table 14. Attempted optimization of copper(II)-mediated alkyne-borane coupling reaction. Deg. = degradation was observed. A=added a solution of alkyne and copper in DMA to borane solution in THF. B=added solution of borane to a solution of copper and alkyne in DMA. C=added DMA, followed by neat alkyne and copper to a solution of borane in THF. ^d Borane solution was degassed by sparging prior to adding other reagents. ^e Reaction was warmed to 45°C.....	96

List of Symbols and Abbreviations

δ : chemical shift

Δ : represents heating of a reaction

9-BBN: 9-borabicyclo[3.3.1]nonane

acac: acetylacetonate

Ac: acetyl

ACN: acetonitrile

AIBN: 2,2'-Azobisisobutyronitrile

BINOL: 1,1'-Bi-2-naphthol

Boc: tert-butyloxycarbonyl

br: broad

Bu: butyl

Bn: benzyl

calcd: calculated

CM: cross-metathesis

CTAB: cetyltrimethylammonium bromide

Cy: cyclohexyl

DCC: dicyclohexylcarbodiimide

DCE: 1,2-dichloroethane

DCM: dichloromethane or methylene chloride

DIPEA: diisopropylethylamine

DMA: N,N-dimethylacetamide

DMAP: 4-(dimethylamino)pyridine

DMAPP: dimethylallyl pyrophosphate

DMF: N,N-dimethylformamide

DMSO: dimethyl sulfoxide

dppf: 1,1'-Bis(diphenylphosphino)ferrocene

equiv. (eq): mole equivalent

er : enantiomeric ratio

Et: ethyl

FOD : 1,1,1,2,2,3,3-heptafluoro-7,7-dimethyl-4,6-octanedionate

Grubbs II (G2) : (1,3-Bis(2,4,6-trimethylphenyl)-2-imidazolidinylidene)dichloro(phenylmethylene)(tricyclohexylphosphine)ruthenium(II)

HMPA : hexamethylphosphoramide

Hoveyda-Grubbs II (HG2) : (1,3-Bis-(2,4,6-trimethylphenyl)-2-imidazolidinylidene)dichloro(*o*-isopropoxyphenylmethylene)ruthenium(II)

HRMS: high resolution mass spectrometry

IPP: isopentenyl Pyrophosphate

iPr: isopropyl

IPr: 2,6-diisopropylphenyl

IPr-Hoveyda-Grubbs II (IPr-HG2): Dichloro[1,3-bis(2,6-isopropylphenyl)-2-imidazolidinylidene](2-isopropoxyphenylmethylene)ruthenium(II)

KBARF: potassium tetrakis (3,5-bis(trifluoromethyl)phenyl)borate

KHMDS: potassium bis(trimethylsilyl)amide

LDA: lithium diisopropylamide

LiHMDS: lithium bis(trimethylsilyl)amide

mCPBA: *meta*-chloroperoxybenzoic acid

Me: methyl

MOM: methoxymethyl ether

Ms: methanesulfonyl (mesyl)
N-ABT: N-acetylbenzotriazole
NBS: N-bromosuccinimide
NIS: N-iodosuccinimide
NFSI: N-fluorobenzenesulfonimide
NHC: N-heterocyclic carbene
NMR: Nuclear Magnetic Resonance
Nu: nucleophile
Ph: phenyl
ppm: parts per million
RT: room temperature (19-25°C)
t-Bu: tertiary-butyl
TBS: *tert*-butyldimethylsilyl
TEA: triethylamine
tert: tertiary
Tf: trifluoromethanesulfonate (triflate)
TFEOH: 2,2,2-trifluoroethanol
THF: tetrahydrofuran
TIPS: triisopropylsilyl
TLC: Thin Layer Chromatography
TMS: trimethylsilyl
Ts: *para*-toluenesulfonyl (Tosyl)
UV: ultraviolet

Experimental Index

2-Hydroxy-3-isopropyl-benzaldehyde (44):	103
(±)-2-(1-Hydroxy-but-3-enyl)-6-isopropyl-phenol (43):	104
(±)-4-Allyl-8-isopropyl-2,2-dimethyl-4 <i>H</i> -benzo[1,3]dioxine (45):	105
(±)-(8-Isopropyl-2,2-dimethyl-4 <i>H</i> -benzo[1,3]dioxin-4-yl)-acetaldehyde (46):	106
(±)-11-(8-Isopropyl-2,2-dimethyl-4 <i>H</i> -benzo[1,3]dioxin-4-yl)-3-methyl-but-3-en-2-ol (47):	106
(±)-2-(8-Isopropyl-2,2-dimethyl-4 <i>H</i> -benzo[1,3]dioxin-4-yl)-1-(1-methyl-cyclopropyl)-ethanol (48):	107
(±)-(E)-Methyl 6-(8-isopropyl-2,2-dimethyl-4 <i>H</i> -benzo[d][1,3]dioxin-4-yl)-4-methylhex-4-enoate (51):	108
(±)-(E)-6-(8-Isopropyl-2,2-dimethyl-4 <i>H</i> -benzo[d][1,3]dioxin-4-yl)-4-methylhex-4-en-1-ol (52):	109
(±)-(E)-7-(8-Isopropyl-2,2-dimethyl-4 <i>H</i> -benzo[d][1,3]dioxin-4-yl)-5-methylhept-5-enoic acid (54):	111
(±)- <i>tert</i> -Butyl-2-acetyl-5-methylhex-5-enoate (56):	113
(±)-4-Allyl-8-isopropyl-4 <i>H</i> -benzo[d][1,3]dioxine (64):	116
(±)-1-Isopropyl-2-methoxy-3-(1-methoxybut-3-enyl)benzene	116
(±)-(E)-5-(3-Isopropyl-2-methoxyphenyl)-5-methoxy-2-methylpent-2-enal (68):	117
(±)-(E)-1-Isopropyl-2-methoxy-3-(1-methoxy-4-methylhexa-3,5-dienyl)benzene (69):	118
(±)-(E)-6-(3-Isopropyl-2-methoxyphenyl)-6-methoxy-3-methylhex-3-en-1-ol (70):	119
(±)-(E)-6-(3-Isopropyl-2-methoxyphenyl)-6-methoxy-3-methylhex-3-enyl methanesulfonate (71)	120
(±)-(E)- <i>tert</i> -Butyl-2-acetyl-8-(3-isopropyl-2-methoxyphenyl)-8-methoxy-5-methyloct-5-enoate (72)	120
(±)-(E)- <i>tert</i> -Butyl-8-(3-isopropyl-2-methoxyphenyl)-8-methoxy-5-methyl-2-vinylideneoct-5-enoate (73):	121
(±)-(E)-3-(6-(3-Isopropyl-2-methoxyphenyl)-6-methoxy-3-methylhex-3-enyl)furan-2(5 <i>H</i>)-one (74):	122
(±)-(E)-4-[(Triphenylphosphino)gold]-3-(6-(3-isopropyl-2-methoxyphenyl)-6-methoxy-3-methylhex-3-enyl)furan-2(5 <i>H</i>)-one (75):	123
<i>tert</i> -Butyl 5-methyl-2-vinylidenehex-5-enoate (76):	123
(±)-(E)-4-Iodo-3-(6-(3-isopropyl-2-methoxyphenyl)-6-methoxy-3-methylhex-3-enyl)furan-2(5 <i>H</i>)-one (77):	124

(±)-(E)-4-Bromo-3-(6-(3-isopropyl-2-methoxyphenyl)-6-methoxy-3-methylhex-3-enyl)furan-2(5H)-one (78):.....	125
(±)-(3b <i>R</i> ,9b <i>S</i>)-7-Isopropyl-5,6-dimethoxy-9b-methyl-3b,4,5,9b,10,11-hexahydrophenanthro[2,1- <i>c</i>]furan-1(3 <i>H</i>)-one (79):	125
(±)-(E)-6-(3-Isopropyl-2-methoxyphenyl)-6-methoxy-3-methylhex-3-enoic acid (82):.....	126
(±)-(E)-Ethyl-9-(3-isopropyl-2-methoxyphenyl)-9-methoxy-6-methylnon-6-en-2-ynyl carbonate (90):.....	127
(±)-(E)-Ethyl 8-(3-isopropyl-2-methoxyphenyl)-8-methoxy-5-methyl-2-vinylideneoct-5-enoate (88):.....	128

1 Introduction

1.1 Triptolide

Triptolide (**1**) is one of a number of natural diterpenoid molecules isolated from the Chinese plant *Tripterygium wilfordii* Hook F., known also as the Thunder God Vine or Lei Gong Teng (Figure 1.1). Kupchan and colleagues isolated this complex triepoxide, along with triptodiolide (**2**) and triptonide (**3**) in 1972 via an ethanolic extraction assisted by a cell activity assay against KB carcinoma cells and L-1210 and P-338 leukemia cell lines (Figure 1.2).¹ These cytotoxic effects were already documented for extracts of *Tripterygium*. Such extracts of *Tripterygium* have also been used extensively in traditional Chinese medicine. Biological activity assays of the individual natural molecules have demonstrated that many of them possess potent medicinal effects including anticancer, immunosuppression and male antifertility. Triptolide has demonstrated the most potent activity of the entire family of *Tripterygium* diterpenoids.



Figure 1.1 *Tripterygium wilfordii* Hook F. leaves and inflorescence.

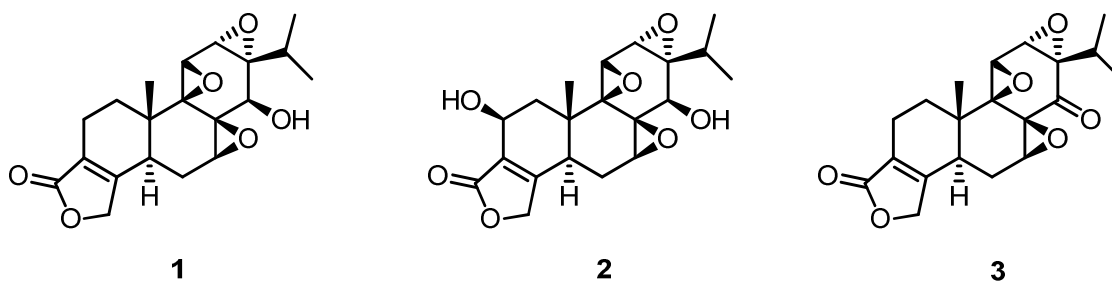


Figure 1.2. Cytotoxic diterpenoids triptolide (1), triptidiolide (2) and triptonide (3) isolated from *Tripterygium wilfordii*.

The three diterpenoids **1**, **2** and **3** possess some interesting structural features. They are the first reported natural products containing the 18(4 \rightarrow 3) *abeo*-abietane skeleton, and also the first reported natural triepoxides.¹ Triptolide features some noteworthy structural motifs, such as both *cis*- and *trans*-decalin ring junctions, nine contiguous stereocentres – three of which are quaternary carbons – as well as a highly oxygenated A ring (Figure 1.3). Finally, the D ring possesses a γ -butenolide structure, which has been found in a number of natural products with potent medicinal effects,² suggesting that this structure plays a particular role in the bioactivity of triptolide.

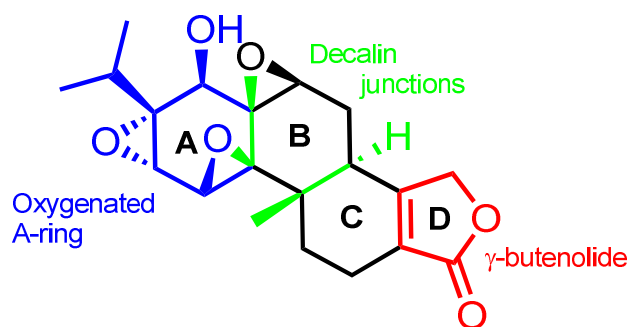


Figure 1.3. Structural motifs present in **1**, including the oxygenated A ring (blue), *cis*- and *trans*-decalin junctions (green) and the γ -butenolide D ring (red).

1.1.1 Biosynthesis

The biosynthesis of plant terpenes is a vast field of study in the natural sciences. Knowledge of the biosynthetic mechanisms of medicinally relevant compounds has led to substantial improvements in production of medications. A key example of this is in the production of paclitaxel; the primary source of this potent anticancer drug used to be direct extraction from the bark of the Pacific Yew, *Taxus brevifolia* Nutt N. This approach caused severe ecological destruction, and was highly expensive and impractical, as only about 10 g of pure paclitaxel could be isolated from nearly 1200 kg of tree bark.³ Elucidation of the biosynthetic pathway towards paclitaxel led to the discovery of a revolutionary plant cell fermentation method, whereby an advanced intermediate in the synthesis of paclitaxel could be extracted from leaves and twigs of the European Yew *Taxus baccata* L., vastly increasing yield, reducing cost and protecting millions of square kilometres of rainforest. This process was developed and patented in part by a Canadian biotechnology company, Phyton Biotech. This semisynthetic method is currently the only route utilized to fulfill the global demand for paclitaxel.

Significant effort has been expended to elucidate the specific biosynthetic pathway towards **1**, but the specific series of enzymes responsible for the production of this molecule has remained elusive. As such, this thesis will briefly discuss the general mechanisms towards plant terpene biosynthesis. Typically, it involves assembly of a number of five-carbon isoprene units (Figure 1.4) – themselves derived from glucose – by a variety of enzymes. Interestingly, terpene biosynthesis in higher plants is segregated by number of carbon atoms; physically separate sets of enzymes produce pools of chemically distinct natural products. The sesquiterpenes (C₁₅) and triterpenes (C₃₀) are synthesized within the cytosol, whereas isoprenes, monoterpenes (C₁₀), diterpenes (C₂₀) and tetraterpenes (C₄₀) – also called carotenoids – are synthesized within the chloroplasts. The communication between these two sets of biosynthetic machinery is of great importance to plant molecular biology.⁴

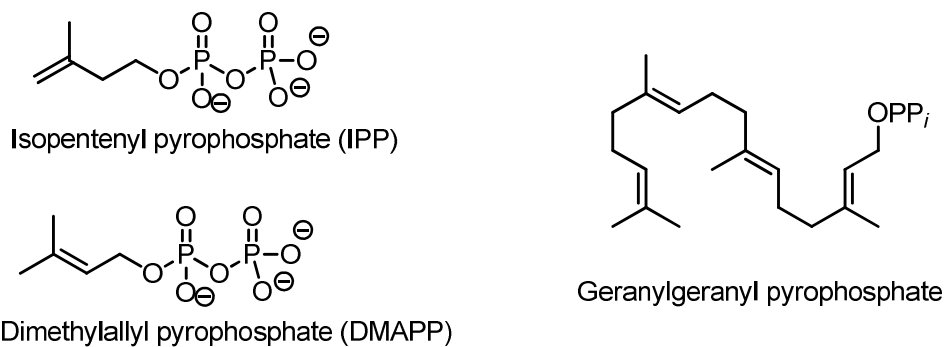
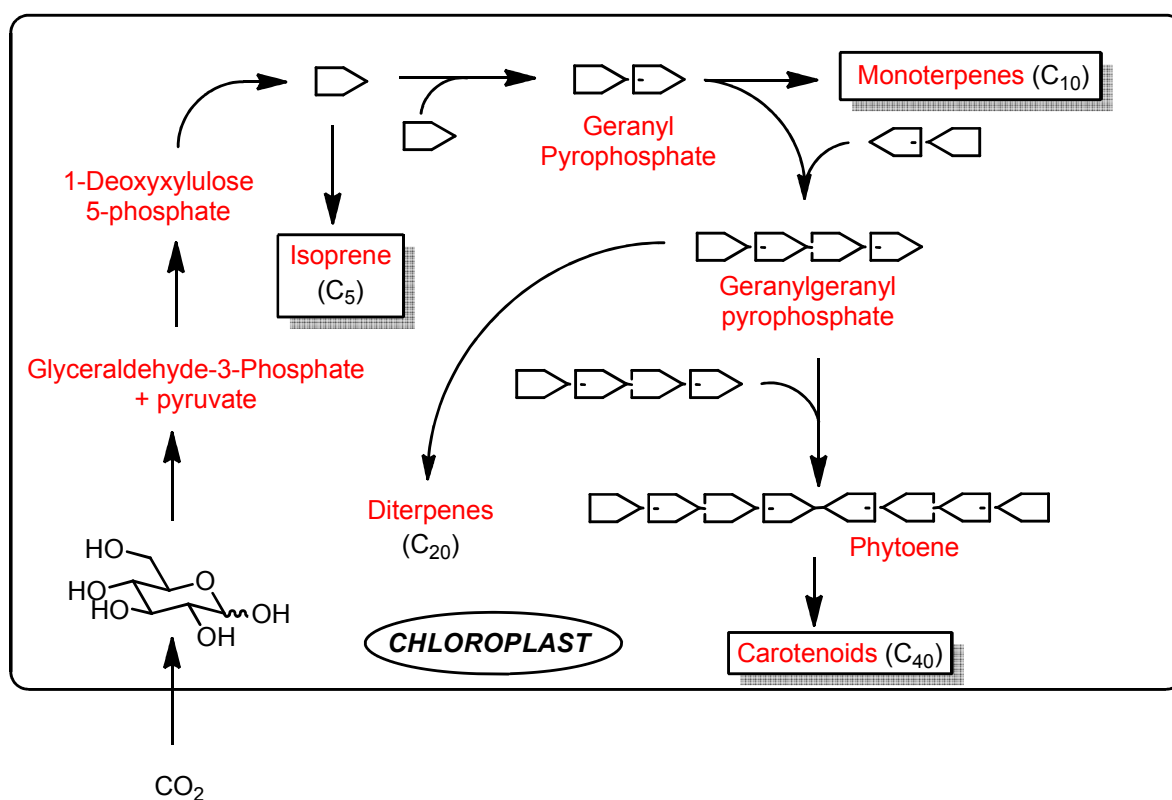


Figure 1.4. Structural precursors to plant terpenes: geranylgeranyl pyrophosphate and 5-carbon subunits DMAPP and IPP.



Scheme 1.1. General schematic biosynthetic pathway of plant terpene synthesis within the chloroplast. ⁴ Blocks represent 5-carbon subunits (IPP or DMAPP).

Diterpenes such as **1** are derived from a geranylgeranyl pyrophosphate precursor and can take many forms, including fused ring structures of various sizes, leading to a vast library of potential structures (Figure 1.5). Higher order structures are formed by a family of terpene synthase enzymes, particularly the terpene cyclases. These cyclase enzymes catalyze the

removal of pyrophosphate to generate a polyprenyl cation; they then force the hydrocarbon chain into a variety of desired conformations to trigger an intramolecular cyclization process. After formation of the cyclic skeleton, a number of downstream transformations can occur. Addition, migration or subtraction of methyl groups or oxidative modifications access products known as diterpenoids. This greatly increases the molecular diversity of the diterpene family.

The specific enzymatic pathway involved in the biosynthesis of **1** has not been elucidated, but these pathways are typically highly conserved, so it is reasonable to assume that the biosynthesis proceeds in a similar fashion. From *Tripterygium*, over 380 secondary metabolites have been isolated to date, and over 95% of these are terpenoid compounds.⁵ This demonstrates the importance of terpene-derived natural products in this genus.

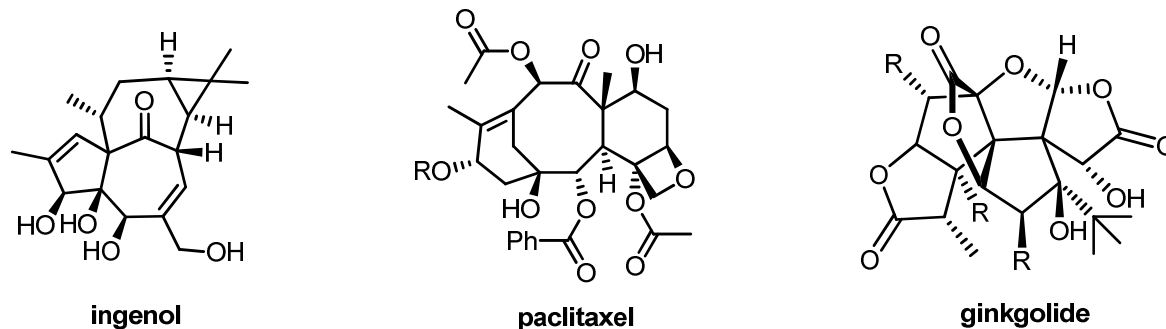


Figure 1.5. Examples of structural diversity among plant diterpenoids.

1.1.2 Medicinal Activity

Extracts of *Tripterygium* have been used in traditional Chinese medicine for thousands of years. Typically, these extracts were used as a generic “cure-all” for various ailments including fever, inflammation and joint pain – a common theme in traditional medicine⁵. In the 1960s, the medicinal uses of *Tripterygium* extracts expanded to include rheumatoid arthritis⁶ and have since grown further to include cancer, hepatitis and other disorders. Future studies demonstrated that the primary component in these plant extracts was, in fact, triptolide,⁷ and therefore this molecule was proposed as the key source of the observed bioactivity.⁸ In a number of cases, extracts of *Tripterygium* have demonstrated fewer side effects than pure **1**, but both are still widely used in medicinal studies. In this

section, we will discuss a selection of diseases and conditions against which triptolide has demonstrated notable bioactivity. A more comprehensive look at the history and biological effects of triptolide and *Tripterygium* can be found in a review by Brinker, Ma, Lipsky and Raskin, published in *Phytochemistry* in 2007.⁵

Cancer

During the isolation of triptolide and related natural products triptidiolide and triptonide, Kupchan and colleagues utilized a bioassay-directed approach against mouse L1210 and P388 leukemia cells and human KB carcinoma cells. They discovered that both triptolide and triptidiolide demonstrated cytotoxic activity against these cell lines – *in vivo* against L1210 and P338 (0.1 mg/kg) and *in vitro* against KB ($ED_{50} = 10^{-4}$ - 10^{-3} $\mu\text{g/mL}$).¹ Two years after this publication, Kupchan and Schubert proposed a potential mode of action of this anti-tumour activity, involving selective alkylation of cysteine residues via thiol-mediated opening of the 9,11-epoxy-14 β -hydroxy system.⁹ Conversely, the Bertochold group, who later reported the first total synthesis of **1**, proposed that the γ -butenolide D ring was responsible for the antileukemic activity, as an analogue lacking this functional group demonstrated no cytotoxicity against P388 leukemia cells.²⁴ Recently, triptolide has become a hot topic in cancer research, featured in dozens of publications over the past five years.¹⁰ Recent studies have shown that **1** alone has potential applications against a wide variety of cancers including prostate¹¹, colorectal¹², and lung¹³. In addition, triptolide appears to have a synergistic effect when co-administered with existing cancer drugs such as *cis*-platin.¹⁴

Immunosuppression

The historical use of *Tripterygium* extracts as anti-inflammatory agents alludes to its ability to suppress the immune response. In both animal and clinical trials, **1** has demonstrated remarkable activity against autoimmune diseases such as rheumatoid arthritis and also against transplant rejection. Studies of rheumatoid arthritis in mice and rats^{6,15} have yielded positive results after treatment with *Tripterygium* extracts. Results from human

clinical trials have also been positive, demonstrating good efficacy of extracts.¹⁶ In the transplant field, a high demand exists for immunosuppressive agents, where organ rejection and graft-vs.-host disease is an ever-present threat to patient longevity; the incidence rate of graft-vs.-host disease in transplant patients ranges from 30-60% and the mortality rate remains close to 50%.¹⁷ Extracts of *Tripterygium* have demonstrated potential in this area of medicine. In a 1994 clinical trial, graft function in kidney transplant patients normalized more quickly and experienced fewer complications during recovery when treated with *Tripterygium* extract.¹⁸ Another study demonstrated that similar extracts were beneficial to survival rates of diabetes patients with pancreas islet cell grafts.¹⁹

Contraception

During clinical trials of both triptolide and *Tripterygium* extracts, reversible sterility was noted as a common side effect in male patients. This prompted further study into the potential of **1** or extracts of *Tripterygium* as male contraceptives. A number of studies have documented that treatment of male rats and humans with a *Tripterygium* extract causes a significant drop in sperm motility and concentration, rendering the subjects infertile after an eight-week treatment with no apparent adverse side effects and full recovery of fertility within five weeks of stopping the treatment.²⁰ Furthermore, an *in vivo* rat assay of various pure components of a *Tripterygium* extract revealed that **1** alone demonstrates similar efficacy as an antifertility agent at a very low dose (30 µg/kg). A possible mode of action for this sterilization was suggested by Bai and Shi in the early 2000s: they demonstrated that *Tripterygium* extracts have an inhibitory effect on T-type Ca²⁺ ion channels in sperm cells, which is important for sperm-oocyte interaction as well as acrosome reaction and motility.²¹ It is noteworthy that the dosage required to induce sterility is substantially lower than that required to cause immunosuppression, which is a promising sign for future human consumption.

Recent Work

Modern bioanalytical methods have enabled a more detailed approach to elucidating the biological target of many natural molecules. In 2011, Liu and co-workers published an article in *Nature Chemical Biology* identifying the true molecular target of **1** - the XPB subunit of RNA transcription factor TFIIH.²² They describe this inhibition of TFIIH as a “unified molecular mechanism” for the variety of biological effects of triptolide. The identification process followed a general-to-specific sequence of screening against various cell processes; initial screens against HeLa cells revealed that **1** had an inhibitory effect on tritium-labelled uridine incorporation, suggesting that it selectively affected RNA synthesis. Narrowing their focus, they determined that **1** targeted a transcription factor of RNAPII and, after screening a variety of transcription factors, they identified TFIIH as the factor in question. A final detailed screen of the 10 TFIIH subunits revealed XPB (an ATP-dependent DNA helicase) as the specific subunit targeted by triptolide. In the article, they also described a previously unknown mode of action whereby **1** inhibits nucleotide excision repair, which is of interest in the field of cancer research.

1.1.3 Previous Syntheses

A number of research groups have made efforts towards the synthesis of **1** over the past 32 years. Inspired by the biosynthesis, many have incorporated cyclization cascades into their syntheses. Throughout all previous syntheses, one particular intermediate has been utilized as the synthetic target: O-Me-triptophenolide (**4**), is the anisole derivative of triptophenolide (**5**), a suspected intermediate in the biosynthesis of **1** found to occur naturally in *Tripterygium* (Figure 1.6).

The history of investigations into the total synthesis of **1** spans more than three decades. The first to report a total synthesis of triptolide was the Bertochold group, who had previously studied the cytotoxicity of the natural product and its source.²⁴ Shortly thereafter, the van Tamelen group published a series of three total syntheses, setting the standard for nearly two decades.²⁵ At the turn of the 21st century, the Yang group reported the first asymmetric synthesis, which rekindled interest in **1** within the synthetic organic

community.²⁷ The Sherburn group studied the synthesis of triptolide from a unique perspective, describing both a racemic and asymmetric synthesis in 2008.²⁸ Finally, the Baati group most recently reported their efforts towards **1**, publishing a formal synthesis in 2010.²⁹

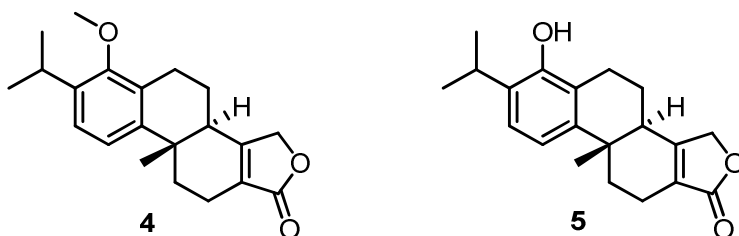
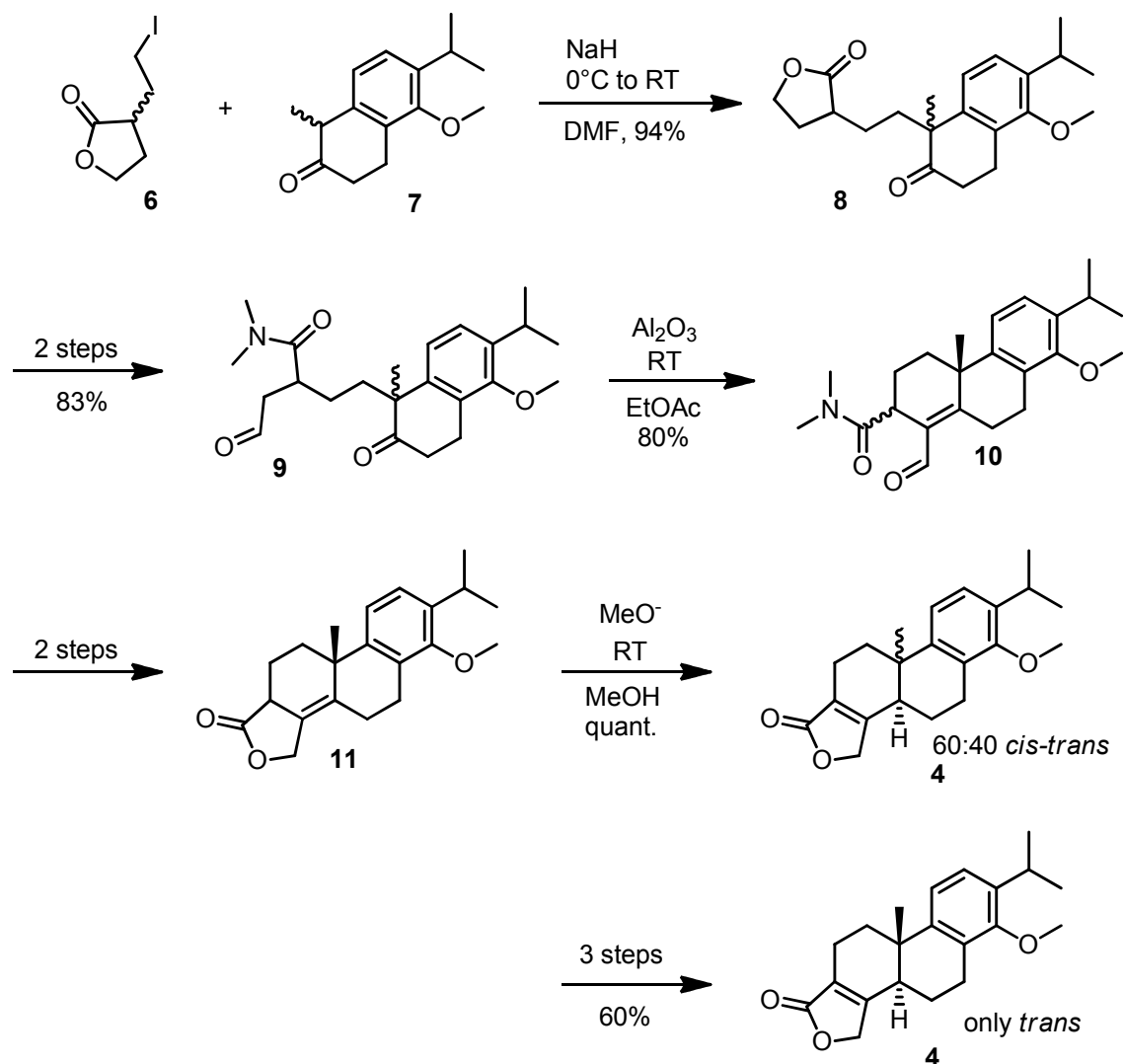


Figure 1.6. O-Me-triptophenolide (**4**), the key intermediate in all previously reported syntheses of **1**, and triptophenolide (**5**), a naturally occurring product in *Tripterygium* and suspected intermediate in the biosynthesis of triptolide.

Bertochold: The First

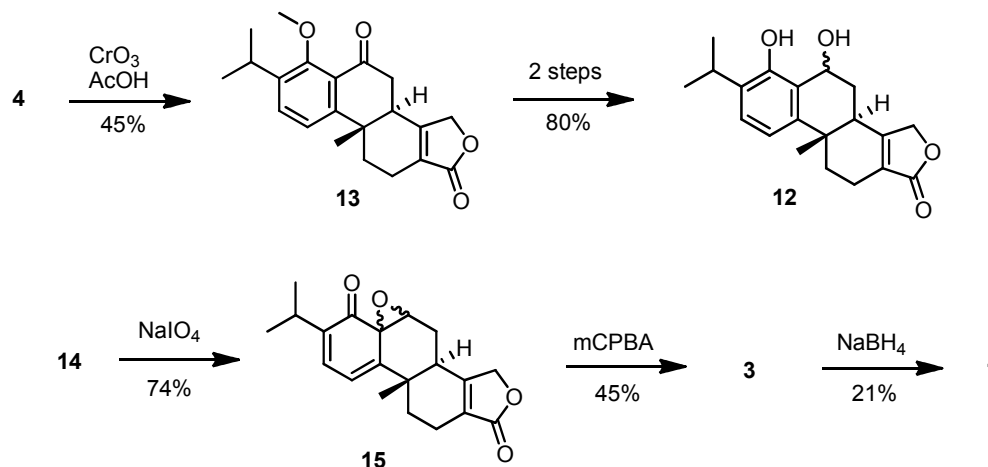
The Bertochold group at the Massachusetts Institute of Technology was the first to describe synthetic efforts towards triptolide. A report discussing their progress towards the natural product was published in the late 1970s²³, culminating in the completed total synthesis of racemic **1** in 1980; their method consisted of 28 steps in a linear synthesis (Scheme 1.2).²⁴ From **4**, they accessed the final product in seven steps.

The Bertochold group approached the synthesis of triptolide via the tetralone **7**, for which they had previously described a synthetic route.²³ Thermodynamic enolate alkylation with alkyl iodide **6** yielded the product **8**. After dimethylamine-promoted opening of the butyrolactone, oxidation and alumina-mediated Aldol condensation, they accessed the tricycle **10** in good yields. Reduction of the aldehyde and lactone closure formed the tetracycle **11**, but an additional alkene isomerization step was required to form the desired γ -butenolide moiety of **4**. Bertochold and co-workers were able to isomerize the double bond in the presence of methoxide ion in methanol in quantitative yield, but upon isolation of the product they discovered that the strongly basic conditions had induced isomerization of the decalin ring junction as well, producing the *cis*-decalin **12** along with the desired *trans* product **4** in a 60:40 *cis-trans* ratio. Fortunately, they were able to work around this step using an epoxidation, dehydration and Pd-catalyzed hydrogenation to afford only the desired *trans* product **4** in 60% yield.



Scheme 1.2. Bertochold synthetic approach to O-Me-triptphenolide.

From **4**, a benzylic oxidation was performed to access the ketone **13** (along with some quinone byproduct), followed by methyl ether cleavage and ketone reduction to access the diol **14**. An Alder periodate reaction followed by exposure to excess mCPBA afforded **3**, which could be reduced with NaBH_4 to produce **1**. This final reduction proceeded in poor yields, only producing 21% of the desired configuration. The remaining product (68%) could be re-oxidized to **3** for recycling (Scheme 1.3).



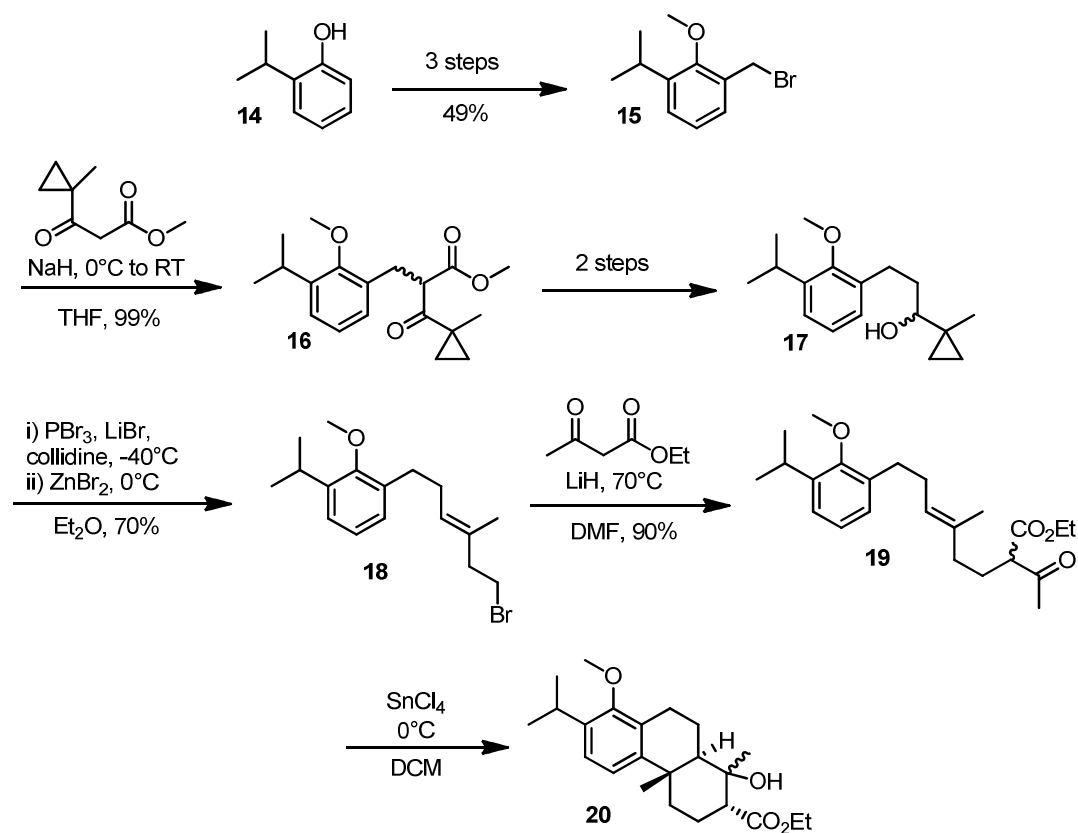
Scheme 1.3 Bertochold method to access **1** from O-Me-triptophenolide.

van Tamelen: “Biogenetic” Cyclization

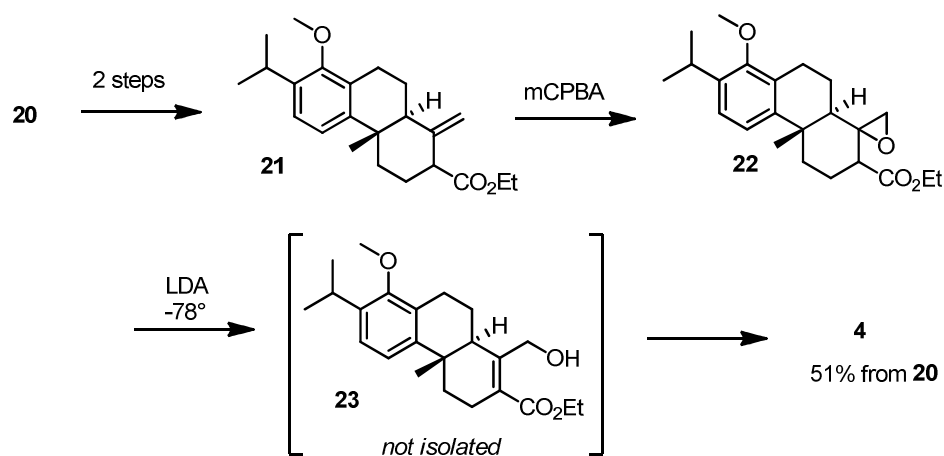
Shortly following publication of Bertochold’s synthesis, the van Tamelen group at Stanford University published three consecutive formal syntheses: two in 1980 and one in 1982.²⁵ Their ultimate synthesis is of particular note, as it was the first to utilize a cyclization cascade reaction to construct the *trans*-decalin skeleton present in the B and C rings, yielding racemic **4** in 13 steps from commercially available 2-isopropylphenol (**14**) (Scheme 1.4). As their synthetic plan involved construction of a geranylgeraniol surrogate **19**, van Tamelen and coworkers dubbed this synthesis a “biogenetic” method towards triptolide.

Functionalization of **14** to brominated anisole derivative **15** was accomplished via *ortho*-lithiation, quenching with formaldehyde, followed by bromination of the alcohol and methylation of the phenol to access **15** in 49% yield over three steps. Subsequent alkylation with cyclopropyl β -ketoester produced **16** in excellent yield. Decarboxylation and ketone reduction accessed cyclopropyl alcohol **17**, which was subjected to Brady-Julia olefination conditions to access homoallylic bromide **18**. After another β -ketoester alkylation, they accessed the C20 cyclization precursor **19**. At this point, van Tamelen and co-workers utilized a Lewis acid-promoted cyclization cascade with SnCl_4 to afford tricycle **20**. Construction of the D ring was accomplished using a three-step method via formation of the methanesulfonate ester and *in situ* elimination to form the terminal alkene **21**. Epoxidation with mCPBA formed the β - γ -epoxyester **22**, which was cleaved in the presence of LDA to

form the γ -hydroxyester **23**. This species was not isolated as it cyclized spontaneously to form the desired tetracycle **4**, completing the formal synthesis in reasonable yields (Scheme 1.5).



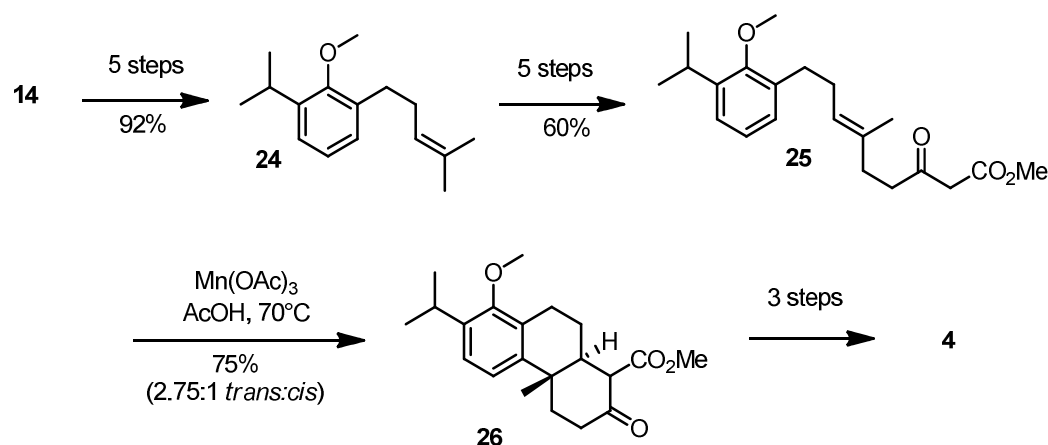
Scheme 1.4. van Tamelen synthesis of C20 precursor and Lewis acid promoted cyclization.



Scheme 1.5 Butenolide construction via mesylation, elimination, epoxidation, base-induced hydrolysis and lactonization for the van Tamelen synthesis.

Yang: Radical Cyclization and Asymmetric Synthesis

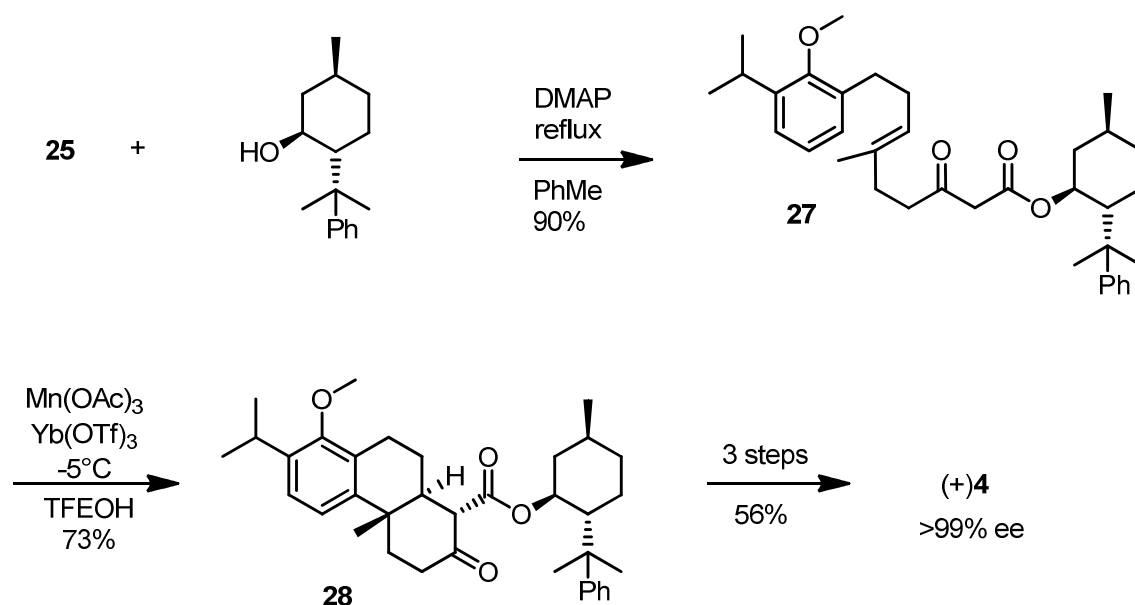
After van Tamelen's remarkable cationic cyclization approach to triptolide, interest in its synthesis waned for nearly two decades until 1998, when the Yang group published a racemic radical cyclization method to access the tricycle (Scheme 1.6).²⁶ Their synthetic route featured an *ortho*-lithiation of a methoxymethyl ether-protected derivative of **14**, quenching with methyl iodide, then benzylic deprotonation and alkylation with dimethylallyl bromide to access **24**. Allylic oxidation with SeO₂ selectively formed the *E*-allylic alcohol, which was transformed into β -ketoester **25**, the substrate for the Mn(OAc)₃-mediated radical cyclization, which proceeded in good yield and with reasonable selectivity for the *trans*-decalin. After cyclization, the butenolide ring was constructed in a further three steps via triflate formation, reduction and Pd-catalyzed carbonylation to access **4** in 14 steps.



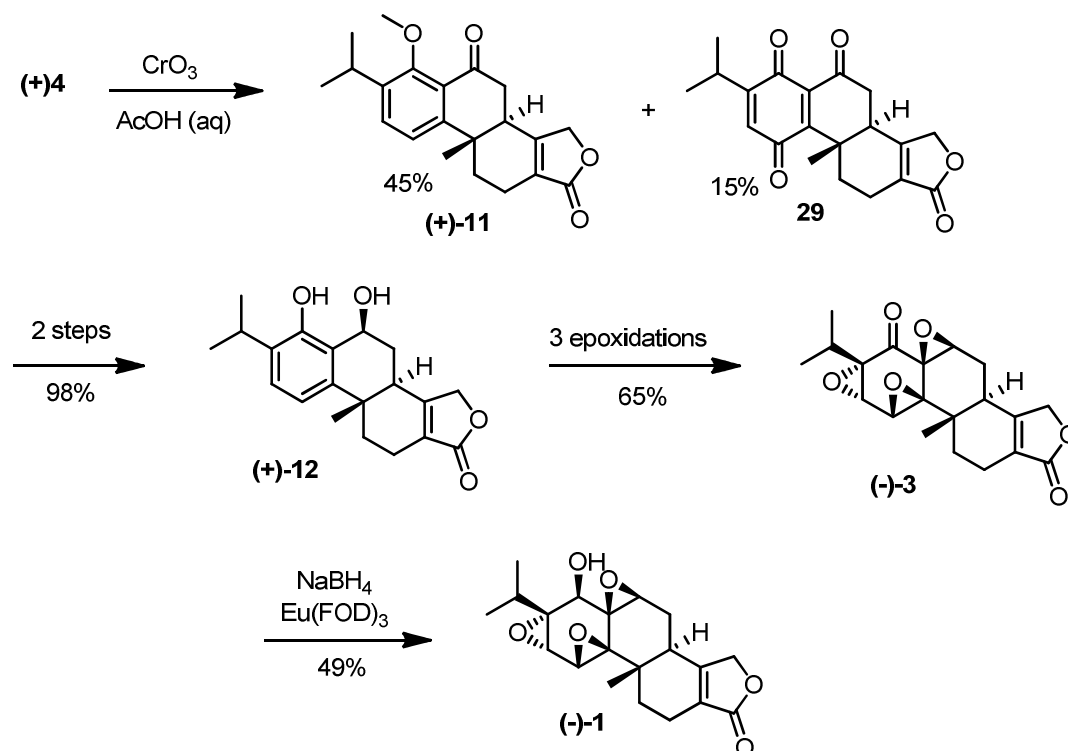
Scheme 1.6. Yang method²⁶ to access racemic tricycle **26** via Mn(OAc)₃ mediated radical cyclization and subsequent butenolide construction.

Two years later, the Yang group elaborated on this synthetic method with the first enantioselective synthesis of triptolide, where the stereochemistry of the radical cyclization was controlled through the use of a menthol-derived chiral auxiliary **27** (Scheme 1.7).^{27a,c} In addition, they found that using an additional stoichiometric amount of a lanthanide (III) triflate contributed to greatly increased diastereoselectivity in the cyclization due to strong chelation effects between such lanthanide salts and β -ketoesters.^{27b} Using this method, they

were able to synthesize (+)-**4** in reasonable yield and excellent diastereo- and enantioselectivity. In addition to this highly enantioselective cyclization method, the Yang group also described a new, more efficient method to construct the three epoxides from **4**, accessing the final product in seven steps in 14% yield (Scheme 1.8). This series of transformations is similar to the Bertochold method, but is more efficient and higher yielding, particularly in the final reduction step, where addition of a europium(III) salt more than doubled the isolated yield of the desired enantiomer. This series of transformations has become known as the “Yang protocol” for accessing the natural product **1**.



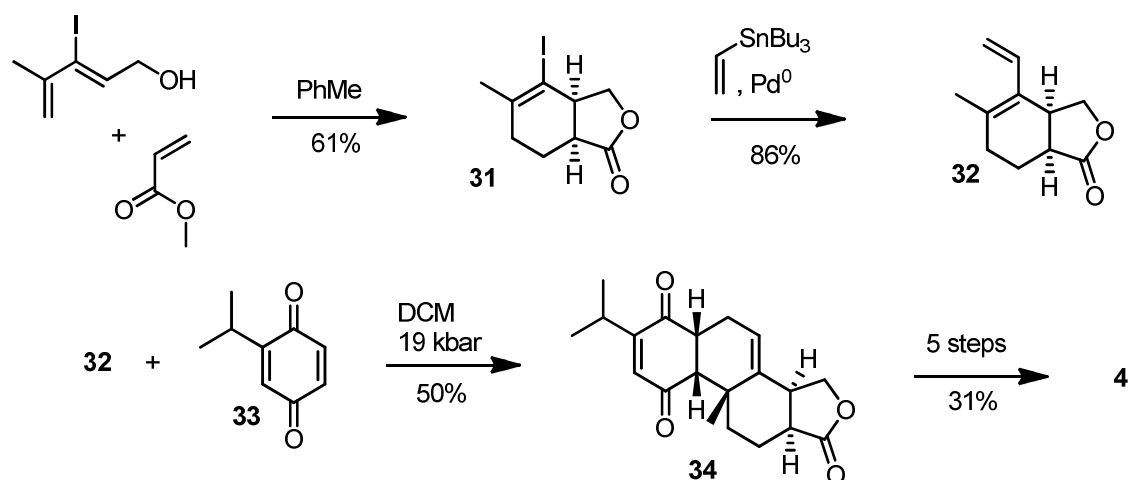
Scheme 1.7. Yang asymmetric approach to triptophenolide utilizing a menthol-derived chiral auxiliary to control the enantioselectivity of the Mn(OAc)_3 and Yb(OTf)_3 -mediated radical cyclization of β -ketoester **27** to access tricycle **28**.



Scheme 1.8. Yang protocol to access (-)-1 from (+)-4.

Sherburn: Convergence

Currently, the most unique approach to **1** originated from the Sherburn group at the Australia National University. In 2008, they published a convergent Diels-Alder approach to access **4** in ten linear steps, which currently holds the record for the shortest formal synthesis of triptolide.²⁸ This approach involves a series of [4+2] cycloaddition reactions, starting with the formation of the [4.3.0] bicyclic lactone **31**, followed by a Stille coupling with vinyltributyl tin to form diene **32** (Scheme 1.9). This diene was utilized in another [4+2] cycloaddition with the substituted *p*-benzoquinone **33** to form the tetracycle **34**. A further five steps were required to access **4**, thus completing the formal synthesis. In the same publication, Sherburn and co-workers also described an asymmetric variant of their synthesis. This was accomplished by a Diels-Alder cycloaddition to form bicyclic lactone **31**, which was performed in the presence of a mild Lewis acid and chiral ligand (Figure 1.7). Under these conditions, this cycloaddition was accomplished in excellent yield and enantioselectivity.



Scheme 1.9. Diels-Alder approach to the formal synthesis of **1** from the Sherburn group, featuring a convergent series of [4+2] cycloadditions to access tetracycle **34**.

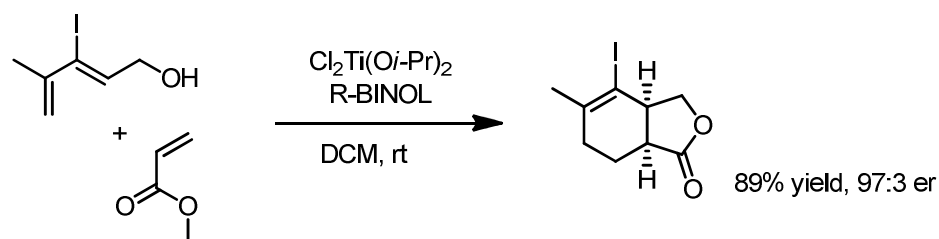
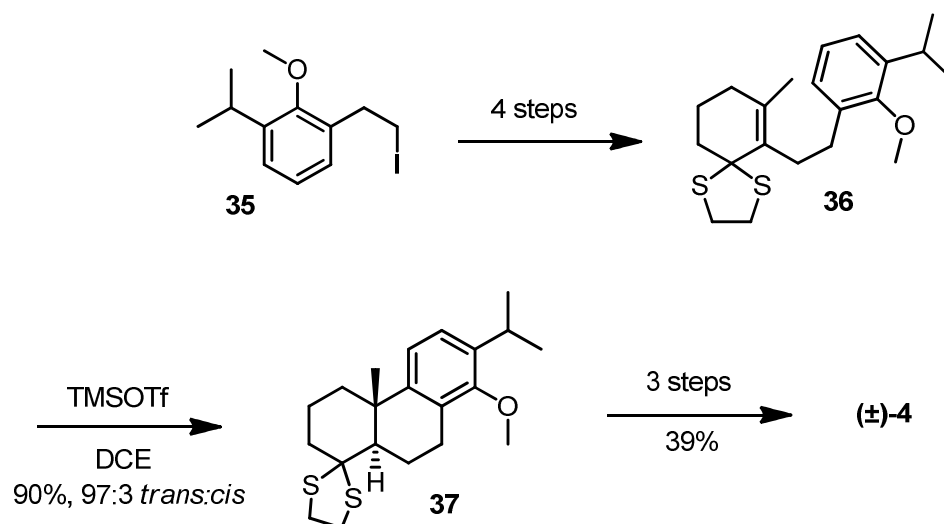


Figure 1.7. Enantioselective Diels-Alder cycloaddition utilized in Sherburn's synthesis.

Baati: Lewis Acid-promoted cationic dithiane cyclization

The most recent efforts towards triptolide were reported in 2010 from the Baati group at the University of Strasbourg in France. Their racemic approach featured a cationic *6-endo-trig* cyclization mediated by TMSOTf to form tricycle **37**, utilizing a dithiane protecting group to promote the reaction (Scheme 1.10).²⁹ Via this cyclization reaction, Baati and co-workers claimed that they accessed racemic **4** in 8 synthetic steps and, consequently, stated that they achieved the shortest formal synthesis to date. However, the raw material they reported for this synthesis, **35**, is not a commercially available product and requires a four-step synthesis to produce. As a result, we argue that this synthesis is, in fact, not the shortest reported.



Scheme 1.10. Dithiane approach to the formal synthesis of **1** from the Baati group.

1.1.4 Our Approach

Our approach to the synthesis of triptolide differs from the literature precedent in a number of critical aspects. Previous synthetic efforts utilizing cyclization cascades, namely the van Tamelen group, Yang group and Baati group, have only formed the B and C ring in a single step. The γ -butenolide D ring was constructed separately, adding at least three steps to the syntheses. We envisioned constructing the butenolide ring in a one-pot sequential process (Figure 1.8) with the *trans*-decalin moiety using a cascade cyclization method catalyzed by a cationic gold species.

In addition, we were aiming to intercept the Yang protocol at a later stage than the majority of previous syntheses. Instead of targeting triptophenolide as the key intermediate, we wished to target the diol **12**. This intermediate was previously targeted by the Yang group²⁶ and they highlighted the particular sensitivity of the benzylic ether to acid-induced cleavage of the C-O bond and subsequent elimination. This sensitivity was crucial to moderate during the synthesis. Furthermore, we envisioned this functionality as a useful synthetic handle for accessing the cyclization precursor and also as a simple point for asymmetric induction towards an enantioselective synthesis.

Our inspiration for this cyclization cascade stemmed from the ability of homogeneous gold complexes to catalyze particular transformations: polycyclization cascades forming

trans-decalin ring junctions, γ -butenolides from 2,3-allenoates, and intramolecular cross-coupling reactions.

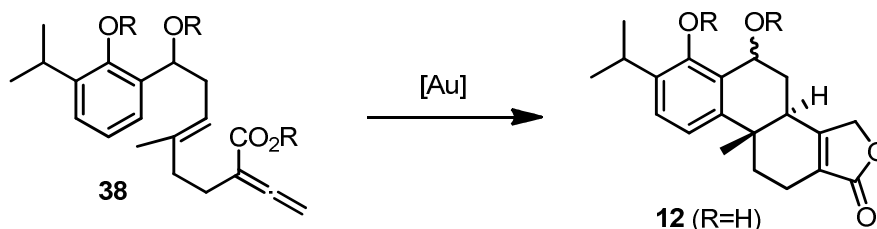


Figure 1.8. Proposed gold-catalyzed cascade cyclization of an allenoate **38** to construct the tetracyclic core of triptolide (**12**).

1.2 Proposed Gold Catalyzed Cyclization Cascade

1.2.1 Introduction to Gold(I) Catalyzed Organic Transformations

Organic transformations catalyzed by cationic gold species are very attractive to the modern synthetic chemist. The mild conditions, selectivity and tolerance of these reactions to water and atmospheric oxygen has resulted in a large amount of reaction and catalyst development from prominent chemists around the world including Echavarren, Gagosz, Hashmi, Shi, Toste, and Furstner.³⁰ The Barriault research group is also very interested in homogeneous gold-catalyzed transformations and, in particular, is interested in the applications of homogeneous gold catalysis in the total synthesis of natural products.³¹ Gold cations in solution act as soft Lewis acids, coordinating to electron-rich π systems. This π -acidity can activate carbon-carbon multiple bonds, increasing their susceptibility to nucleophilic attack in both an inter- and intramolecular fashion. Allenes and alkynes are the most common substrates for this type of reactivity.

Despite a wide variety of reactivity,³² the mechanisms of gold(I)-catalyzed reactions are highly conserved. A typical mechanism of gold-catalyzed nucleophilic attack onto an allene is outlined in Figure 1.9. Coordination of a cationic gold(I) species to the electron-rich π system begins the catalytic cycle. In the case of allenenes, the gold(I) coordinates to the centre

carbon of the allene. Nucleophilic attack occurs next, forming the vinyl gold species. These vinyl gold species are highly susceptible to protodeauration by water or Brønsted acids, but, under certain circumstances, can be isolated. This protodeauration step releases the cationic gold(I) species, forming the desired product and completing the catalytic cycle.

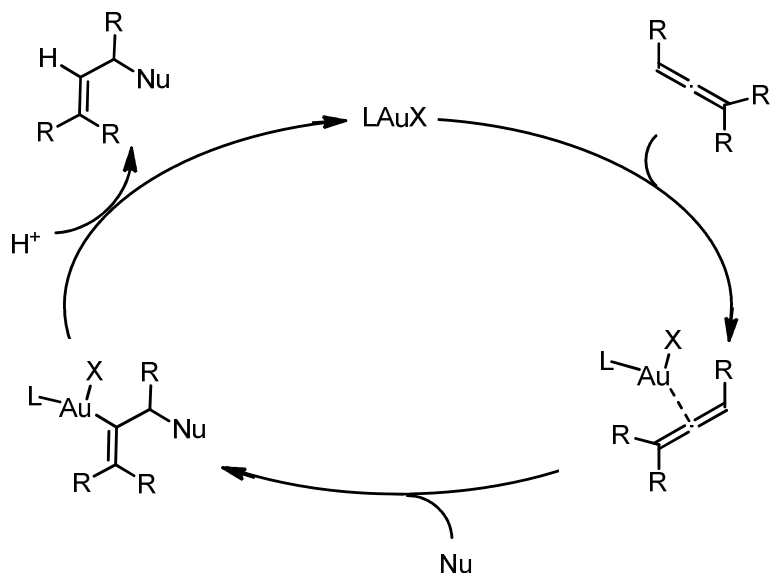


Figure 1.9. Generalized mechanism of gold(I)-catalyzed nucleophilic attack onto an allene.

A common application of gold(I) catalysis is intramolecular cyclization reactions involving carbon-based π systems. This field of synthetic organic chemistry is rapidly growing in popularity and gaining recognition for its vast spread of applications. Its unique reactivity has also been explored in a number of total syntheses, though the overall number of natural product syntheses utilizing gold-catalyzed cyclization reactions remains relatively small.³³ A key goal of the Barriault group is to increase awareness within the chemical community of the usefulness of homogeneous gold catalysis in the total synthesis of complex natural products. Indeed, our group has published a number of recent articles on intramolecular cyclization reactions catalyzed by gold(I) species to selectively generate various cyclic systems of interest for total synthesis (Figure 1.10).³⁴ When we considered triptolide as a synthetic target, we envisioned forming the tetracyclic core via a series of three gold-catalyzed transformations which are known individually, but a combination of all three was unprecedented in the literature. We pictured the general scope of the proposed reaction as a polyene-type cyclization cascade, but imagined it originating from a 2,3-

allenoate cyclization to form the butenolide. Based on the literature precedent, this combination of transformations seemed highly unlikely to be catalyzed by gold(I) alone, but recent developments in the field of gold(I/III) catalyzed oxidative transformations spurred us to investigate the possibilities of this reaction.

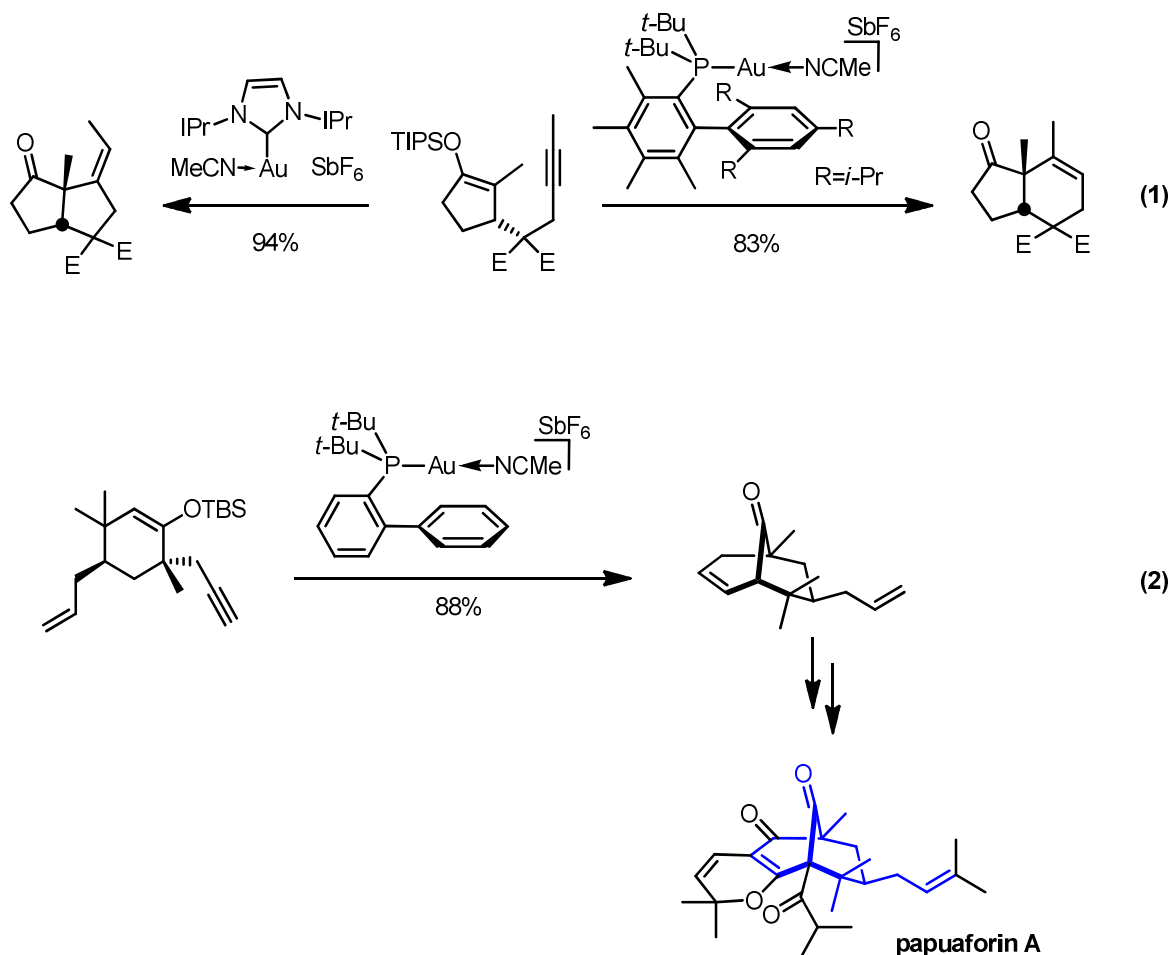


Figure 1.10. Highlights of recent publications on gold(I)-catalyzed carbocyclization reactions published by the Barriault group. (1) Selective 5-*exo*- or 6-*endo*-dig carbocyclizations towards fused carbocycles.³⁴ (2) Gold (I)-catalyzed 6-*endo*-dig cyclization of bicyclo[3,3,1]alkenone frameworks towards the synthesis of papuaforin A.^{31b,35}

Gold(I) catalyzed polycyclization reactions

The general class of cyclization reactions we are interested in are polyene-type cyclizations that utilize a cascade cyclization to form multiple fused cycles in a one-pot process. This topic has been of great interest to synthetic chemists for decades,³⁶ as this

synthetic method is analogous to the natural process catalyzed by enzymes to form terpenes as described in section 1.1.1. Typical synthetic polyene cyclizations are induced by Lewis³⁷ or Brønsted³⁸ acids or, more recently, transition metals complexes containing platinum³⁹ or titanium.⁴⁰ A number of asymmetric variations on this process have been developed as well.⁴¹ Many of these transformations have low functional group tolerance, high likelihood of side-reactions (due to non-selective alkene activation) and in some cases must be performed in strict absence of water and oxygen. It is in these aspects that gold has demonstrated remarkable value.

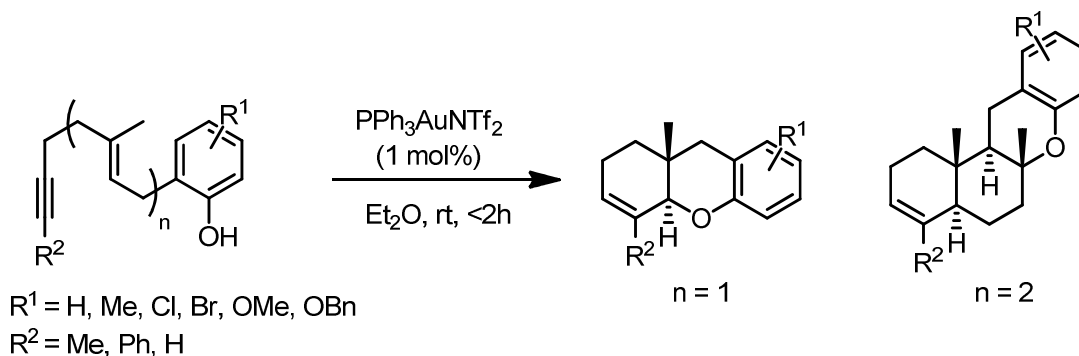


Figure 1.11. Examples of gold(I) catalyzed en-yne polycyclization cascades to access fused tri- and tetracycles.

The linear precursors for gold(I)-catalyzed polycyclizations feature an enyne functionality which negates the most problematic side-reaction of typical polyene reactions: non-selective alkene activation. Gold(I) binds to alkynes preferentially over alkenes, as they have more easily accessible π -orbitals, and this preference exclusively dictates the initiation site of the cyclization sequence. Michelet and co-workers recently demonstrated that gold(I) catalyzed polycyclizations of 1,5-enynes and 1,5,9-dienynes proceed with high diastereoselectivity and 6-*endo* selectivity in the synthesis of tri- and tetracycles containing one pyran ring - as the terminal nucleophile was a phenol (Figure 1.11).⁴² They described further that this transformation proceeds in a biomimetic fashion - via a cascade cation-alkene mechanism (Figure 1.12). This mechanism proceeds via a chair-like transition state, which heavily favours both the 6-*endo* cyclization pathway and the *trans*-decalin skeleton, leading to excellent region- and diastereoselectivity of these cyclizations. Toste and colleagues have also described a highly enantioselective variant of this gold(I) catalyzed

polycyclization of 1,5-enynes to form similar tricycles utilizing a chiral cationic bis-gold complex (Figure 1.13).⁴³

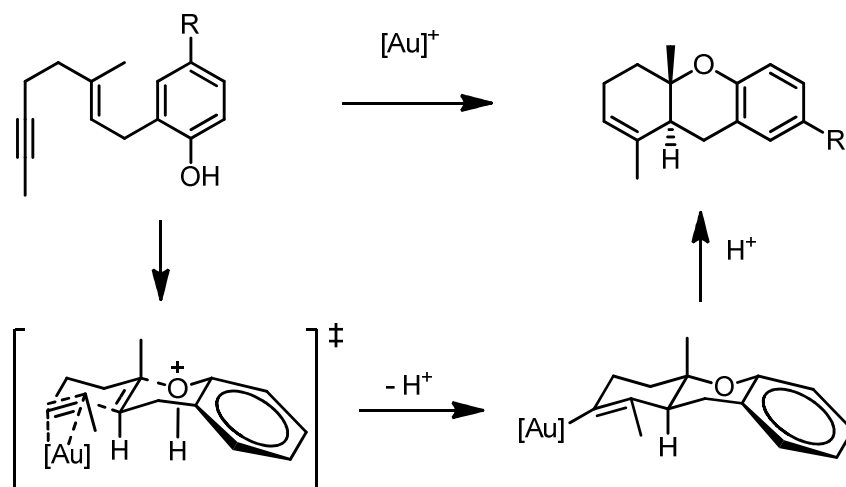


Figure 1.12. Cation-alkene mechanism of gold(I) catalyzed polycyclizations of 1,5-enynes. The chair-like transition state required to access the *trans*-decalin skeleton is denoted by the double-dagger symbol (\ddagger).

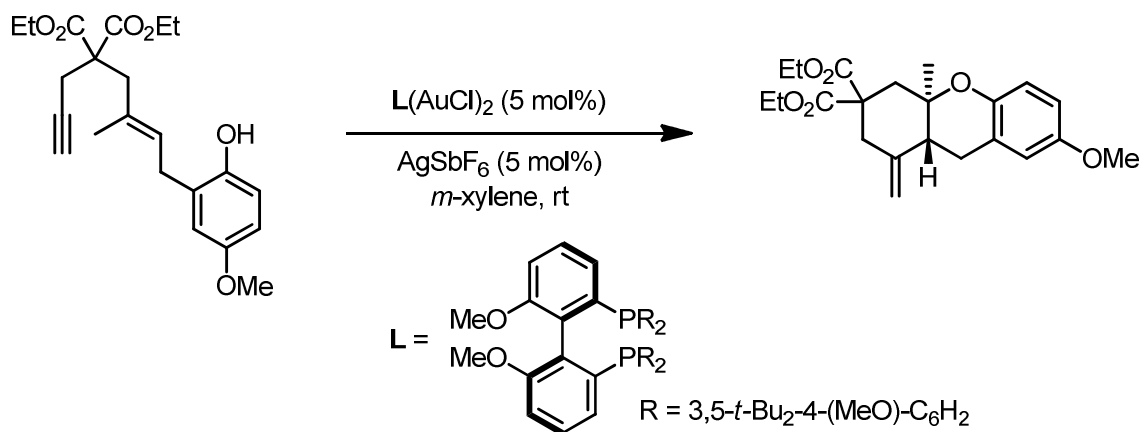


Figure 1.13. Enantioselective gold(I) catalyzed polycyclization of enynes published by Toste and co-workers in 2010.

Synthesis of γ -butenolides from 2,3-allenoates

We are interested in utilizing a gold(I) catalyzed polycyclization cascade to form the tetracyclic core of triptolide. As previously mentioned, past syntheses have utilized cyclization cascades to form rings B and C, but the γ -butenolide D ring has never been constructed as part of the cyclization cascade. Here, gold has the potential to play another key role: cationic gold species are known to catalyze the cyclizations of 2,3-allenoates to form γ -butenolides (Figure 1.14). This cyclization was first reported with allenic acids and transition metal salts such as Pd(II), Ag(I) and Au(III). In a 2005 publication, Shin and co-workers at Hanyang University in South Korea described the first cyclization of *tert*-butyl allenoates. Therein, they found that Au(III) was particularly effective in catalyzing this transformation over a wide variety of other transition metal species.⁴⁴ Later, Hammond and co-workers demonstrated that gold(I) is also capable of catalyzing this reaction, but under much milder conditions and in higher yields.⁴⁵ This precedent was encouraging for us, as we envisioned exploiting this reactivity of gold to initiate our cyclization cascade.

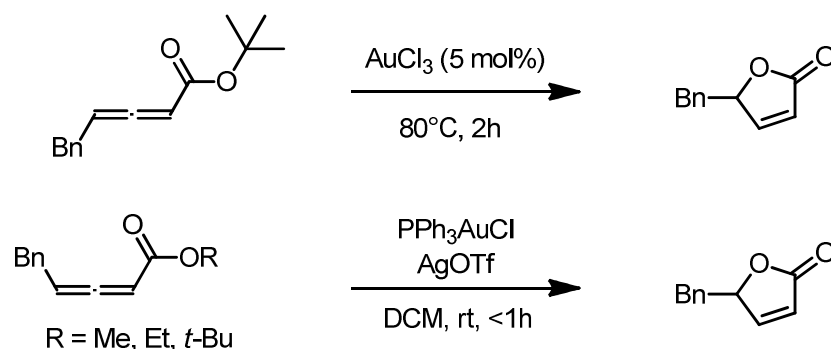


Figure 1.14. Cyclizations of 2,3-allenoates catalyzed by cationic gold(I) and gold(III) species.

1.2.2 Oxidative Gold Transformations

The desired cyclization cascade as described in section 1.1.4 requires a number of inherently difficult transformations. First, we wished to use an aromatic ring as the terminal nucleophile, whereas the majority of previous gold-catalyzed polycyclizations reports had cast an alcohol in this role. In addition, previous polycyclizations have utilized gold to activate an alkyne and prime it for nucleophilic attack by an alkene as per Figure 1.11; via

this method, the relatively stable vinyl gold species is generated *after* completion of the cyclization cascade. In our approach, the first cyclization to form the butenolide ring generates the vinyl gold species, which then must go on to cyclize the remainder of the tetracycle. As a result, we considered that gold(I) would likely be unable to catalyze this cyclization cascade. Instead, we wished to investigate an oxidative gold (I/III) process, whereby the different oxidation states of the catalyst possess different reactivity, which has the potential to catalyze our domino cyclization.

Oxidative gold(I/III) processes have been gaining good literature exposure in recent years and their potential is being recognized as an alternative to typical transition metal catalyzed reactions. Many of the benefits of gold(I) catalyzed reactions hold true for oxidative gold transformations: tolerance to oxygen and water are highly sought-after traits for modern synthetic organic transformations. This family of reactions typically utilizes an external sacrificial oxidant to form the gold(III) species during the catalytic cycle, which has different reactivity properties to gold(I). Gold(III) is a much stronger Lewis acid and is known to react in cross-coupling-type reactions, terminating the catalytic cycle with a reductive elimination to reform gold(I) (Figure 1.16).⁴⁶ An example of this reactivity was described by the Gouverneur group in 2010, wherein they described an oxidative cross-coupling reaction between an *in situ* generated vinyl gold species and terminal alkynes using SelectFluor[®] as a stoichiometric oxidant (Figure 1.15).⁴⁷ A number of other cross-coupling reactions have been reported, including intramolecular coupling reactions, which is the area of focus for this synthesis.

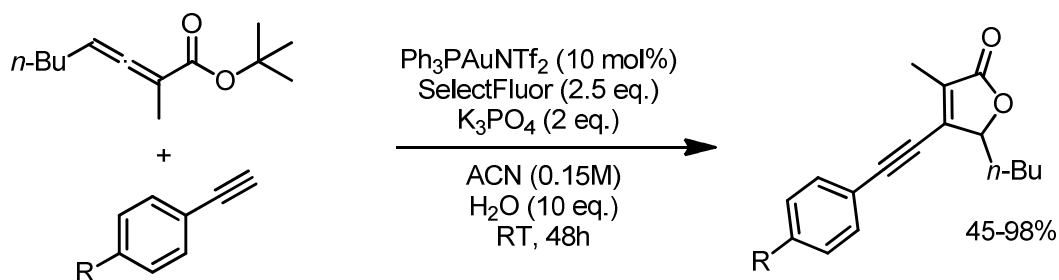


Figure 1.15. Oxidative gold-catalyzed cross-coupling reaction of allenolates and terminal alkynes.

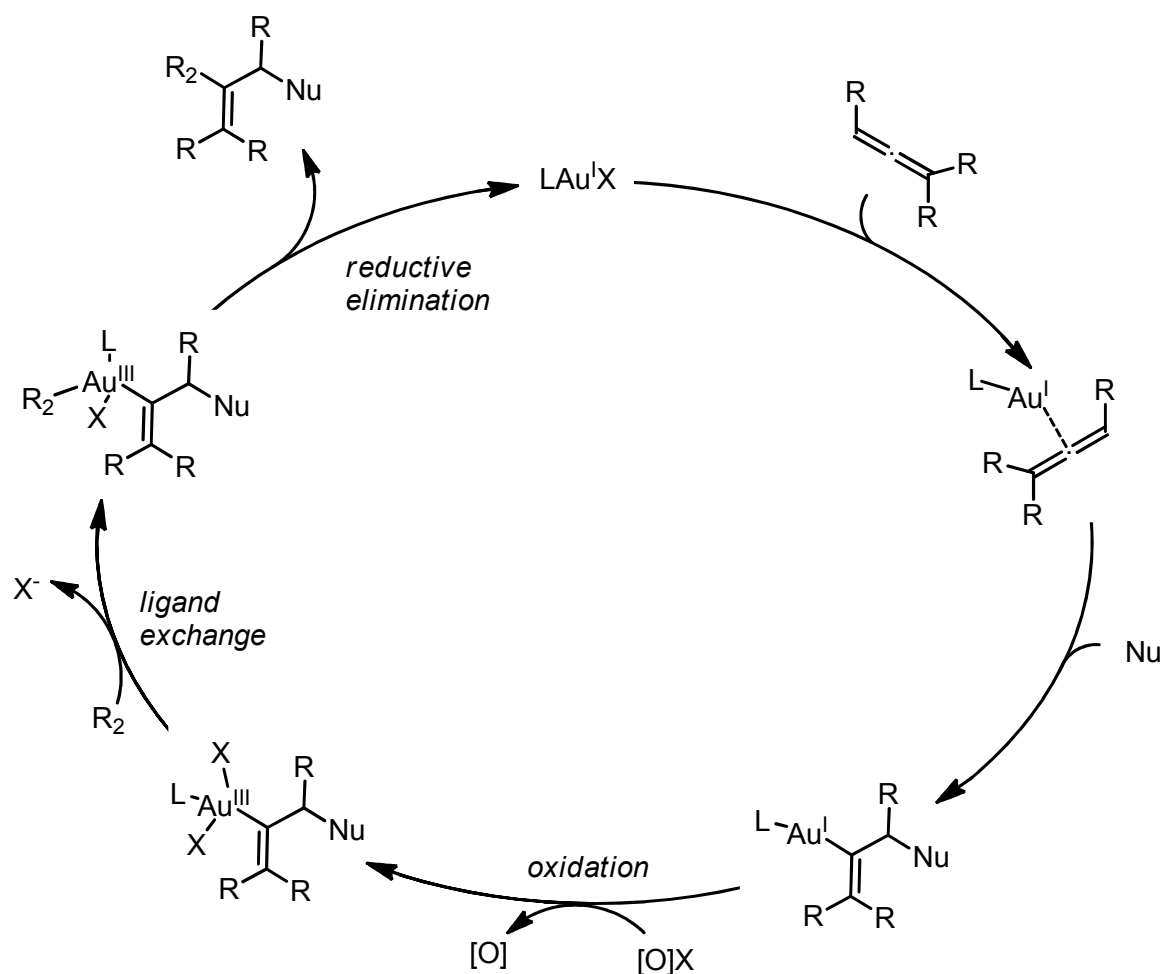


Figure 1.16. General catalytic cycle of a gold(I/III) catalyzed oxidative cross-coupling reaction of an allene.

1.2.3 Gouverneur Oxidative Cyclization

In 2010, Veronique Gouverneur and her group at Oxford University published an article in *Chemistry: A European Journal* entitled “Gold-Catalyzed Intramolecular Oxidative Cross-Coupling of Nonactivated Arenes”. Therein, they reported an oxidative cyclization process to synthesize dihydroindenofuranones from 1,3-disubstituted allenoates using cationic gold(I) complexes and SelectFluor[®] (Figure 1.17).⁴⁸ This cyclization cascade, they proposed, proceeds via a mechanism outlined in Figure 1.18.

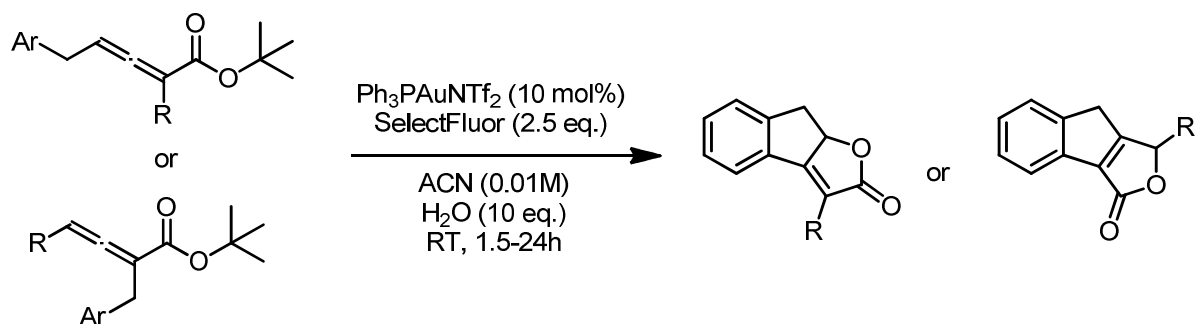


Figure 1.17. Oxidative gold-catalyzed intramolecular cross-coupling synthesis of dihydroindeno-furanones reported by the Gouverneur group in 2010.

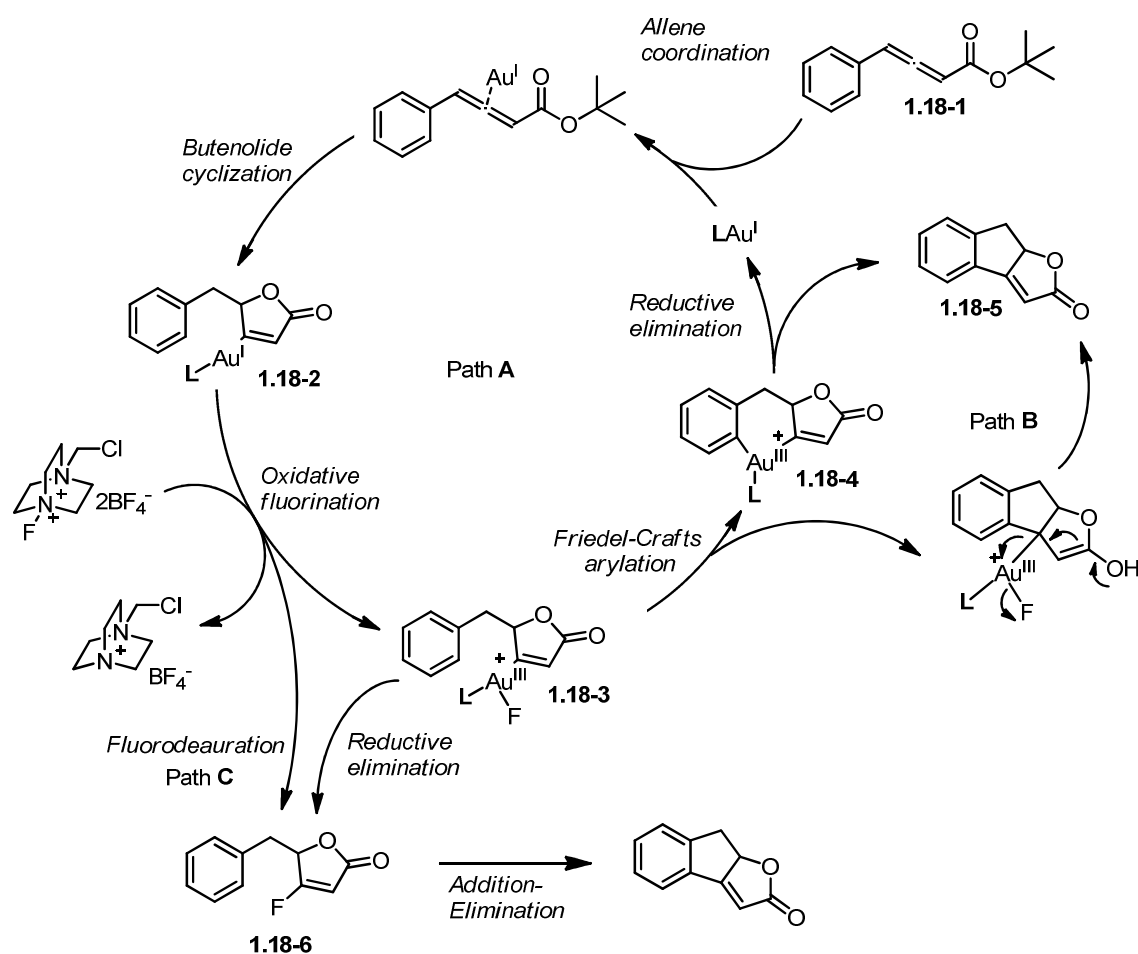
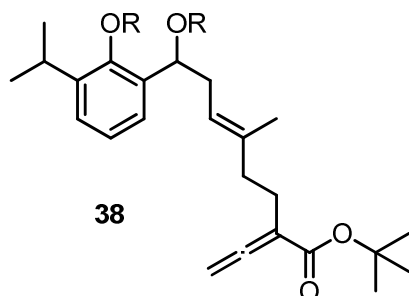


Figure 1.18. Proposed mechanism of oxidative gold-catalyzed intramolecular cross-coupling to form dihydroindeno-furanones.

The mechanism proposed by Gouverneur and co-workers is as follows. The allenoate is first cyclized with $\text{PPh}_3\text{AuNTf}_2$ (also known as the Gagosz catalyst⁴⁹) to form the vinyl gold

butenolide **1.18-2**. This gold(I) intermediate, they describe, is stable for long enough in solution to be oxidized to gold(III) by SelectFluor[®], which then enables an intramolecular Friedel-Crafts-type arylation onto the electron-poor gold species, displacing fluoride and forming the bis-organogold(III) species **1.18-4**. This species then undergoes reductive elimination to afford the desired product **1.18-5** and regenerate gold(I), thus completing the catalytic cycle (Path **A**). Alternatively, Gouverneur and colleagues proposed a conjugated addition-elimination mechanism whereby the gold(I) species is regenerated by elimination of fluoride ion (Path **B**). The authors supported their Friedel-Crafts arylation proposal by demonstrating the preference of this reaction for electron-rich over electron poor arenes, which agrees with the well-established body of knowledge for electrophilic aromatic substitution reactions. They also separately prepared fluorobutenolide **1.18-6** and exposed it to the reaction conditions to test for the activity of path **C**. They found that **1.18-6** did not react under these conditions, and as such discounted this pathway as a significant contributor to the overall mechanism. Gouverneur and colleagues have not published any further articles on this reaction and as such, the potential applications of this reaction in organic synthesis remain mostly unexplored.

Applying this methodology to our formal synthesis of triptolide will be challenging. The Lewis acidity of the gold species generated by the reaction may cause problems for the acid-sensitive homoallylic benzylic oxygen functionality present in the proposed precursor **38**. Furthermore, if we accept the proposed mechanism as accurate, the substitution of an alkene in place of an arene as the first coupling partner is likely to be challenging and will, in all likelihood, require in-depth study. Nevertheless, the possibility of extending this methodology to the total synthesis of a complex natural molecule such as triptolide is alluring and, if successful, may open up numerous avenues for further investigation into the synthetic applications of gold catalysis in organic chemistry.



2 Synthesis

Organic chemistry...is enough to drive one mad. It gives one the impression of a primeval, tropical forest full of the most remarkable things, a monstrous and boundless thicket, with no way of escape, into which one may well dare to enter.

German chemist Friedrich Wöhler, in a letter to his mentor, Berzelius. January 28, 1835

2.1 Retrosynthetic Analysis

At the start of any total synthesis, a retrosynthetic analysis must be performed in order to devise a route to access the desired target. This allows for a number of possible routes to be devised, which can be compared and validated separately to determine the optimal method for the proposed synthesis. Our retrosynthesis proceeded via two avenues: investigating potential mechanisms of our proposed cyclization cascade and exploring methods of accessing the desired allenolate precursor **38**.

2.1.1 Proposed extension of Gouverneur mechanism

In this formal synthesis of triptolide, we targeted a particular key step, so we needed to design the synthesis around this step. We proposed an extension of the aforementioned oxidative gold-catalyzed cyclization, utilizing an alkene linker to extend the cascade from the synthesis of a tricycle to a tetracycle. With this in mind, we proposed that our key step could proceed via an extension of the mechanism proposed by Gouverneur and co-workers (Figure 2.1).

After coordination of a cationic gold(I) species to the allene **38** and cyclization to form the vinyl gold-butenolide **39**, an oxidative fluorination could occur, forming the fluorogold(III) species **40**. Following formation of this highly electron-poor gold species, two possible mechanisms exist for formation of the desired tetracycle. The most likely route

is via coordination of the trisubstituted alkene to the gold, which would increase the susceptibility of this alkene to nucleophilic attack from the electron-rich aromatic ring, (Path **A**) forming the bis-organogold species **42**. Alternatively, nucleophilic attack could occur directly from the trisubstituted alkene onto the gold species, (path **B**) expelling fluoride and forming intermediate **41**. This method of nucleophilic addition onto vinyl gold(III) was proposed by Gouverneur; however, the nucleophile in our case, an alkene, is far less nucleophilic than an electron-rich arene, leading to our deduction that path **B** is less likely. Intermediate **41** contains a tertiary carbocation that is poised to undergo an intramolecular Friedel-Crafts alkylation to access **42**. Finally, reductive elimination can occur to regenerate gold(I) and, after rearomatization, form the desired tetracycle **12**.

We believe that coordination of the alkene to the gold(III) species is the most likely pathway for this reaction, as carbon π systems are well-known ligands for soft Lewis acids. Indeed, it is this exact property – coordination to carbon π systems – that forms the basis of gold-catalyzed reactions in general.³⁰ Compared to alkynes and allenes, however, alkenes are relatively poor ligands, but in the case of this reaction, the electron-poor gold(III) species **40** may be reactive enough to enable this transformation. Trapping a gold-catalyzed polyene cyclization with an arene nucleophile has also been described previously,⁴³ lending support for the proposed 6-*endo*-trig cyclization.

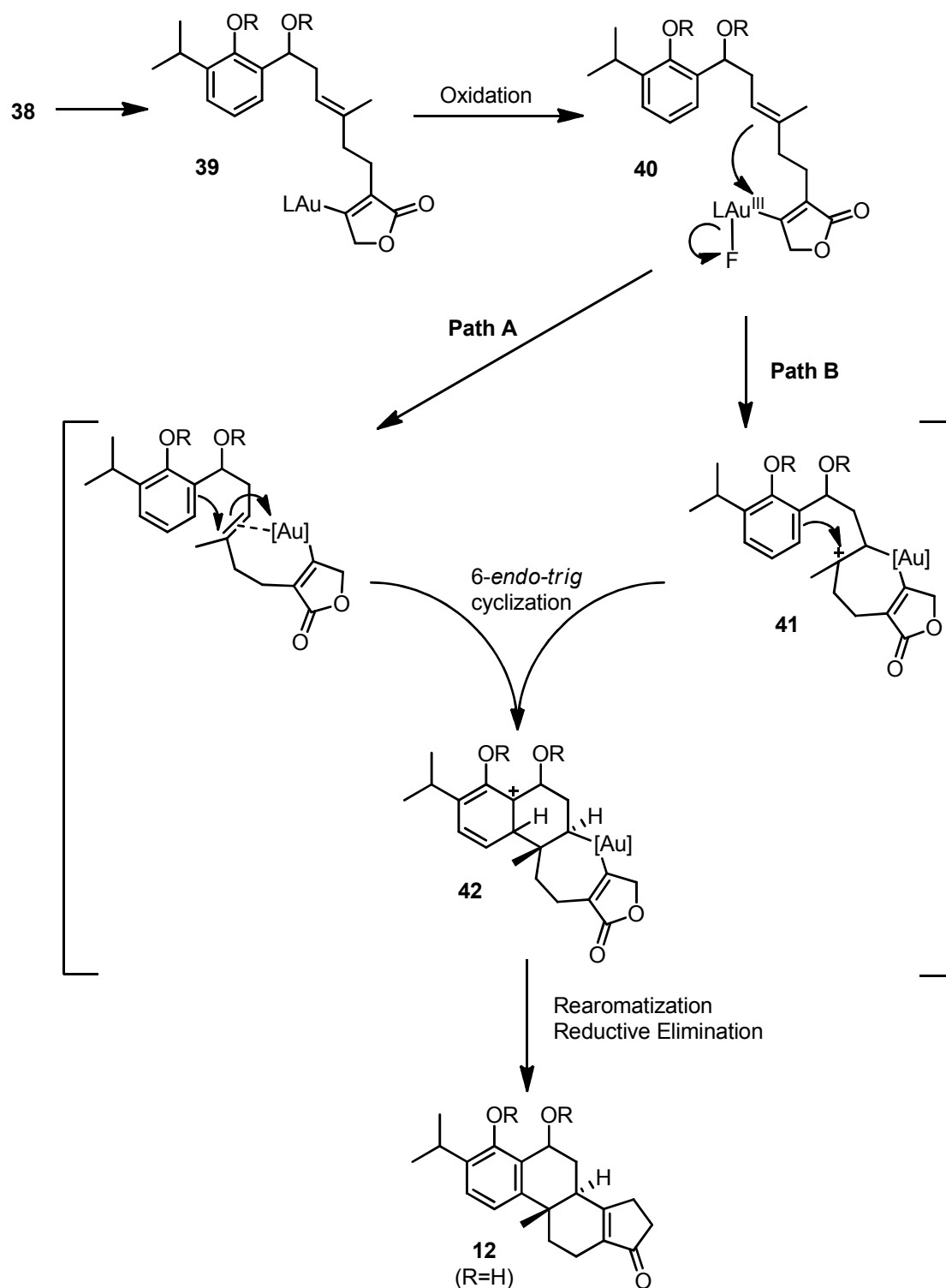


Figure 2.1. Possible mechanisms for the proposed oxidative gold-catalyzed cyclization cascade to form the tetracyclic core of triptolide. Path A: Coordination of alkene ligand to gold(III), triggering Friedel-Crafts arylation forming **42** directly. Path B: Formation of carbocation **41** by nucleophilic attack of alkene, then Friedel-Crafts alkylation to seal up the tetracyclic backbone.

2.1.2 Construction of Linear Precursor

During our investigation of potential synthetic routes to access **38**, we broke the molecule down into three components: an electron rich arene terminus, an electron poor allenolate terminus and an alkene linker segment. We wanted to synthesize this precursor in a “left-to-right” fashion, using the inexpensive and readily available **14** as our starting material - as did van Tamelen and Yang.²⁵⁻²⁷ This approach is logical, as the aromatic moiety and alkene linker do not feature any high-energy or reactive functional groups, unlike the allenolate terminus, which we elected to install later in the synthesis. Furthermore, the number of known methodologies for construction of 2,3-allenates is relatively small and the majority of existing protocols are reported only for the synthesis of internal allenes. We envisioned forming the allenolate via a substituted acetoacetate which, following a recently published procedure, could be converted to an allenolate in a one-pot process in good yields.⁵⁰ To form the benzylic alcohol functionality of **38**, we wished to perform an *ortho*-formylation of the starting phenol and allylation of the resulting salicylaldehyde **44**. This two-step method was supported by literature precedent and, we proposed, would provide a convenient and scalable route to access to diol **43**. The two alcohol groups could be protected either with identical protecting groups (from **43**) or with different groups (involving a separate protection of **44**) to provide suitable stability for further functionalization (Figure 2.2).

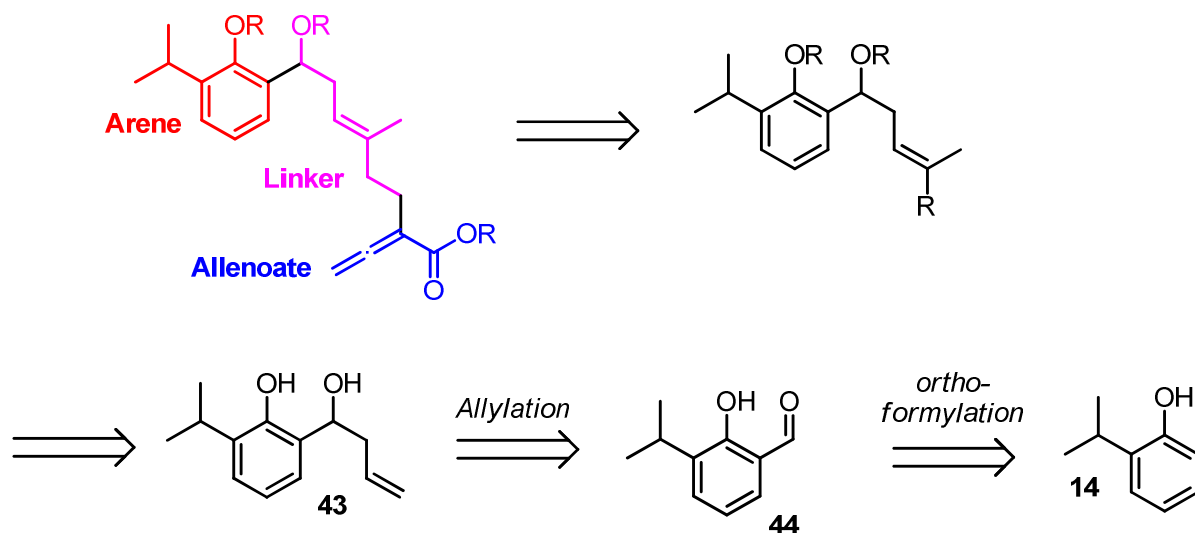


Figure 2.2. Retrosynthetic analysis of linear allenolate precursor to proposed starting material 2-isopropylphenol.

During our retrosynthetic analysis, we uncovered a number of viable options for the synthesis of the *E*-trisubstituted alkene. Use of a highly selective method for accessing the *E*-geometry of this alkene was of utmost importance, as this translates to the *trans* geometry of the desired decalin structure present in the B-C ring junction of **1**. Figure 2.3 outlines a selection of known methods for the synthesis of trisubstituted alkenes with good to excellent *E* selectivity. These methods were all investigated over the course of this synthesis, and each posed their own unique challenges.

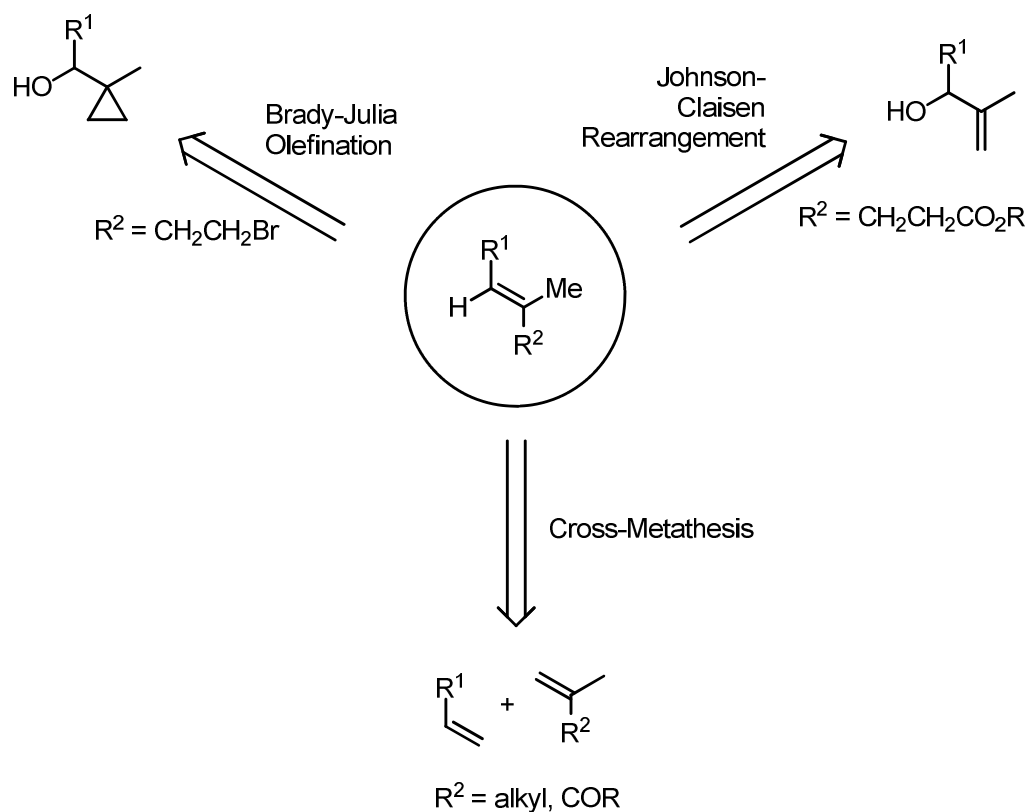


Figure 2.3. Retrosynthetic analysis of highly *E*-selective synthetic methods to access the desired trisubstituted alkene.

2.2 Synthesis of Starting Materials

Over the course of our retrosynthetic analysis, we discovered that all the proposed synthetic pathways originated from a shared starting material. The allylated diol **43** could be accessed through a simple two-step synthesis from **14**. A method to formylate the phenol

selectively at the *ortho* position was sought as the first synthetic transformation. Typical Lewis acid-catalyzed Friedel-Crafts aromatic formylation conditions were unsuitable for this synthesis, as they are known to react preferentially at the position *para* to the phenol. The isopropyl substituent at the 2-position made this method even more undesirable, as the steric influence of similar groups was known to further disfavor substitution at the *ortho* position.

Fortunately, we discovered a procedure - reported by the Skattebøel group⁵¹ - which utilized the inherent hydrogen-bonding characteristics of the phenol to direct the *ortho*-formylation reaction with exclusive selectivity. This report described the synthesis of a number of related salicylaldehydes in good yields using magnesium chloride and triethylamine to form an enhanced phenoxide base and directing agent.^{51a} A superstoichiometric amount of paraformaldehyde was required as it served as both the source of the formyl group and oxidant in an Oppenauer-type process to furnish the desired salicylaldehyde. Adapting this method to our synthesis was highly successful; employing six equivalents of paraformaldehyde and performing the reaction at reflux in THF afforded **44** in excellent yield (Figure 2.4). This reaction has one important safety issue which needed to be monitored carefully. During the reflux, paraformaldehyde decomposes to release formaldehyde gas, which, under the reaction conditions employed, condenses and re-polymerizes on the walls of the reflux condenser. A wide-bore condenser was required for this reaction when performing it on large scale, as the polymer is able to plug the condenser, cause a buildup of pressure and rupture the flask. A side-arm round bottom flask is also recommended as the reaction vessel. Lightly stoppering the side-arm with a rubber septum can act as a pressure release mechanism in case the pressure does increase during the reaction.

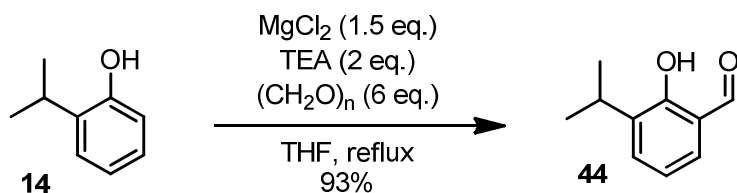


Figure 2.4. MgCl_2 and Et_3N -mediated *ortho*-formylation of 2-isopropylphenol using paraformaldehyde as the carbon source.

To form the diol **43**, a simply allylation reaction was required. We elected to use a method which would tolerate the phenol moiety in order to avoid extra protection steps. The Barbier allylation was the targeted method for this transformation, as it was known to have much higher functional group tolerance than the ubiquitous Grignard reaction. In addition, Barbier allylations are often performed in aqueous or biphasic conditions, utilize inexpensive reagents, and are often performed open to air, allowing for an operationally simple and scalable process. The allylation proceeded smoothly in a biphasic mixture of THF and saturated aqueous ammonium chloride, using two equivalents of zinc dust and adding allyl bromide in one portion while controlling the exotherm with a cold water bath. Upon scale-up of this process (ca. 50 g), this exotherm proved much more difficult to control, owing to a reduced rate of heat transfer in the larger reaction vessel. However, metering the addition of allyl bromide over 30 minutes while cooling the reaction vessel in an ice bath proved highly effective, affording the desired product **43** in good yields (Figure 2.5).

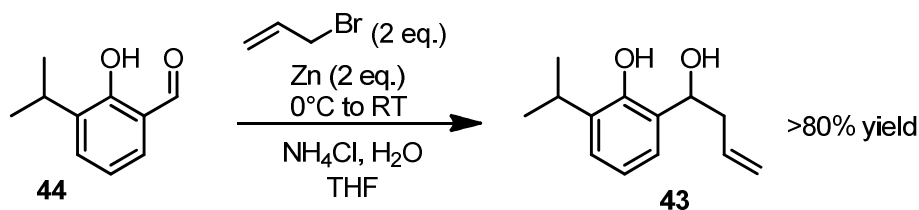


Figure 2.5. Synthesis of allylated diol **43** via a Barbier-type allylation of salicylaldehyde **44**.

Selection of protecting groups is often a critical factor in total synthesis. A chemist must choose protecting groups to maximise stability during the synthesis, but also allow for relatively simple deprotection at a later stage. For 1,3-diols, the typical protecting group described in the literature is a dimethyl acetal – also known as an acetonide - group, as this affords good stability towards base, oxidation, reduction and nucleophilic attack.⁵² It is, however, known to be relatively acid sensitive. Nevertheless, the well-documented ease of installation and future removal of this group were very appealing; in practice, the acetonide was indeed simple to install, with little optimization needed to achieve good results (Figure 2.6). Upon scale-up of these processes, isolation and purification of the salicylaldehyde and allyl diol intermediates proved unnecessary; a 67% yield of the acetonide-protected product **45** could be attained over the three steps, requiring chromatographic purification only of the final product.

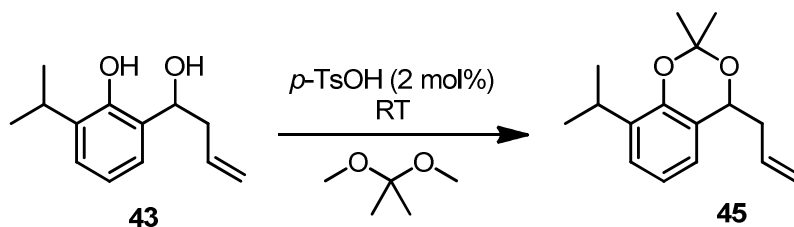
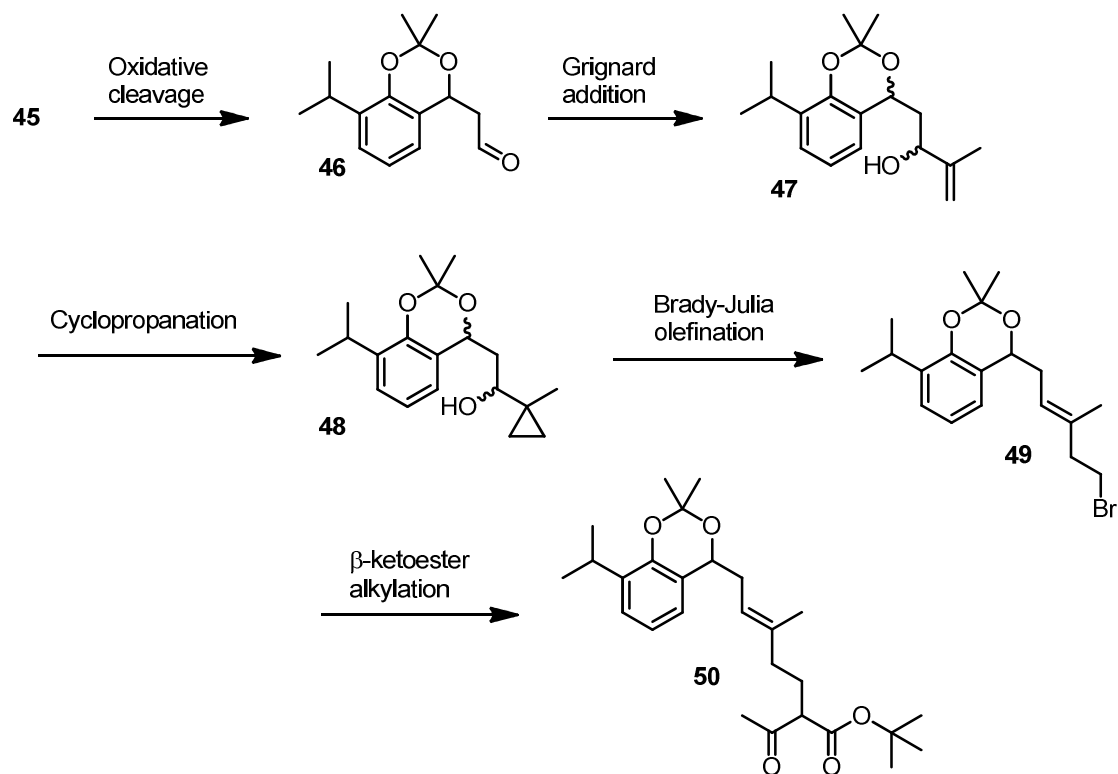


Figure 2.6. Installation of the acetonide protecting group using catalytic *p*-toluenesulfonic acid in neat 2,2-dimethoxypropane.

2.3 Cyclopropanation and Brady-Julia Olefination

The first synthetic route we investigated was analogous to that explored by van Tamelen and co-workers in their landmark 1982 synthesis of triptolide.²⁵ As described in section 1.1.3, their method involved formation of cyclopropylcarbinol **17**, followed by a highly *E*-selective one-pot bromination-ring opening-elimination process to form homoallylic bromide **18**. We desired a method to access cyclopropylcarbinol **48**, at which point we envisioned forming bromide **49**, followed by β -ketoester alkylation and allene formation to form the desired cyclization precursor, as per Scheme 2.1. We proposed a route whereby we would cleave the alkene **45** to form an aldehyde, access secondary alcohol **47** via Grignard addition, then cyclopropanate the alkene under Simmons-Smith conditions to form the precursor for the Brady-Julia reaction. After formation of the homoallylic bromide **49**, alkylation with *tert*-butyl acetoacetate would access **50**, the desired substrate for allene formation followed by cyclization.



Scheme 2.1. Formation of β -ketoester **50** via Brady-Julia olefination of cyclopropylcarbinol.

2.3.1 Oxidative Cleavage of Terminal Alkene

The initial method selected for the oxidative cleavage reaction was ozonolysis. This method is operationally simple and avoids the use of toxic and expensive osmium tetroxide (OsO_4). Unfortunately, this method did not yield positive results, so we were forced to seek a method utilizing OsO_4 and excess sodium periodate (NaIO_4) (Figure 2.7). This method worked very well, producing the desired aldehyde on the first attempt in 75% yield. Upon scale-up of this procedure, optimization of solvent choice, concentration and catalyst loading was performed, the results of which are summarized in Table 1. The optimal method was found to be a 1:1 mixture of THF and water, approximately 3 equivalents of NaIO_4 and 1.5 mol% of OsO_4 . The aldehyde product **46**, however, was found to be somewhat unstable, and degraded rapidly upon silica gel chromatography. As a result, this product was carried on as crude material to the following step without purification.

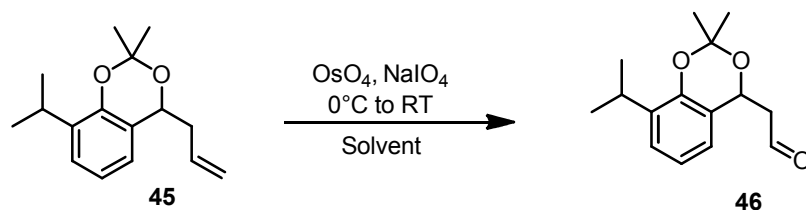


Figure 2.7. Optimized oxidative cleavage conditions to access aldehyde **46**.

Entry	Solvent	Concentration /M	Eq. NaIO_4	Mol% OsO_4	Yield / (crude)
1	EtOAc/ H_2O (1:1)	0.01	3.1	2.3	75
2	EtOAc/ H_2O (2.5:1)	0.1	3.4	0.9	83
3	THF/ H_2O (1:1)	0.1	2.8	1.5	88

Table 1. Optimization of oxidative cleavage reaction of allyl acetonide **45** using osmium tetroxide and sodium periodate.

2.3.2 Grignard Addition and Cyclopropanation

In theory, the Grignard addition desired for this synthesis (Figure 2.8) was very simple. The required Grignard reagent, isopropenylmagnesium bromide, is commercially available and a vast body of literature precedent existed to support this transformation.⁵³ However, this reaction proved difficult in practice. Initial attempts – using THF solvent at 0°C – yielded a crude mixture which was difficult to purify due to severe streaking during silica gel column chromatography. After purification, the yield was poor - 35% from acetonide **45**. Early scale-up attempts were disastrous – the yield dropped to 14%. Suspecting that the basicity of the organomagnesium species was causing degradation of **46**, an organocerium species was prepared *in situ* following a previously reported procedure by our group.⁵⁴ This protocol improved the yield to 45% but was difficult to reproduce on scale. Finally, by omitting cerium, switching solvents to Et_2O and dropping the reaction temperature to -78°C , the yield was improved. We succeeded in isolating **47** as a 1:1 mixture of diastereomers in 68% yield over two steps after purification, which was much cleaner than our earlier efforts. This yield was reproducible on multi-gram scale.

The cyclopropanation of **47** with diiodomethane occurred very cleanly. An initial attempt using zinc-copper couple – the classical Simmons-Smith reagent – yielded only degradation, but employing Et_2Zn worked extremely well – 97% on the first attempt. No chromatography was required for purification of **48**. This reaction proved reproducible and robust - the use of diethylzinc as a premade solution or neat reagent proved inconsequential to the outcome of the reaction. Interestingly, this cyclopropanation reaction is reported to be highly diastereoselective,⁵⁵ the oxygen moiety is known to coordinate to the zinc species and direct the facial selectivity of cyclopropanation. Our results are in agreement with this report, as we observed only two diastereomers both on TLC and in the NMR spectra – diastereomers were generated by the previous Grignard reaction. At this point, we had established a robust and scalable procedure to access the substrate for the Brady-Julia reaction, and began our investigation of this key transformation.

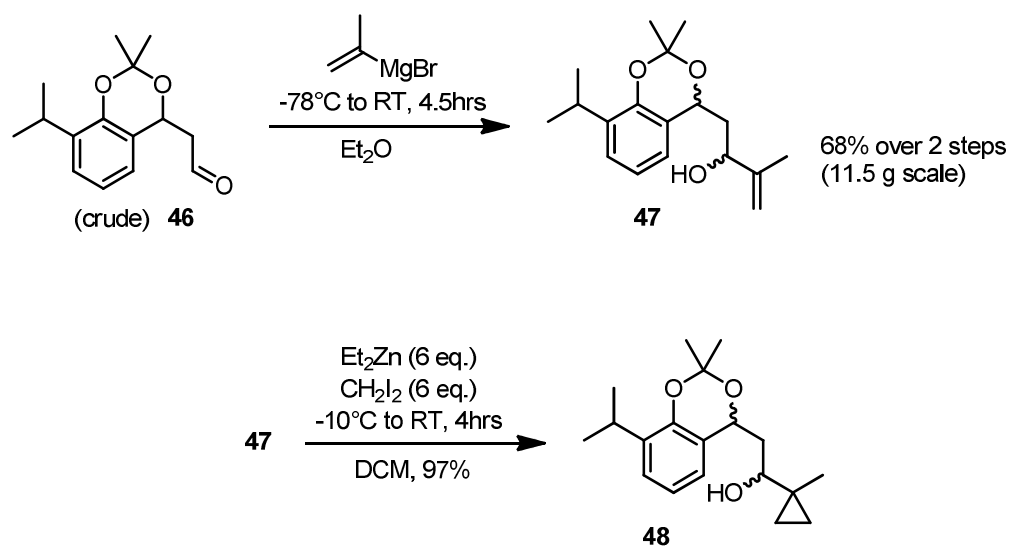


Figure 2.8. Optimized procedure for Grignard addition of isopropenylmagnesium bromide to aldehyde **46** to access diastereomeric alcohol **47** and Simmons-Smith cyclopropanation with diethylzinc to access cyclopropane **48**.

2.3.3 Brady-Julia Olefination

The one-pot bromination-ring opening-elimination of cyclopropylcarbinols to form homoallylic bromides is a lesser-known transformation in synthetic organic chemistry. It was first described by Brady and co-workers in 1968.⁵⁶ In this publication, the authors describe this transformation as a modification to the Julia reaction, hence the moniker “Brady-Julia Olefination”. Brady and colleagues document the high propensity of this reaction to form homoallylic bromides with excellent *E*-selectivity, which no doubt attracted the attention of the van Tamelen group and, likewise, us. This transformation is known to occur under a variety of conditions (HBr⁵⁶ or MgBr₂⁵⁷) but the most often-used (and highest yielding) method uses PBr₃, pyridine base and ZnBr₂. In some cases, an additional source of bromide ion is present, often LiBr. The literature describe that exposure of the alcohol to PBr₃ forms the bromocyclopropane, which is then opened upon exposure to the Lewis acidic conditions afforded by the ZnBr₂. The additional bromide ion provided by LiBr is thought to assist in the nucleophilic ring-opening step, as illustrated in Figure 2.9.

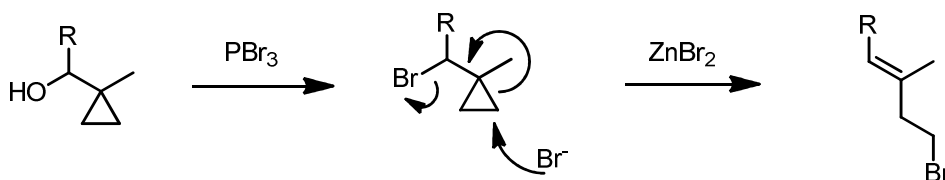


Figure 2.9. Accepted mechanism of Brady-Julia olefination of secondary cyclopropylcarbinols.

The high stereoselectivity of this transformation originates from the transition state geometry of the cyclopropyl group upon ring opening (denoted by double dagger in Figure 2.9). Attack of bromide occurs in a pseudo-antiperiplanar fashion to the leaving group, therefore if we examine the transition state geometry in a Newman projection, two such projections can be drawn (Figure 2.10). Projection **A** leads to formation of the *E* product, and projection **B** leads to the *Z* product. It is clear that projection **B** contains a highly unfavourable eclipsing interaction between the R group and the cyclopropane ring. As a result, the **A** pathway is lower in energy, and thus the *E* product is formed preferentially.

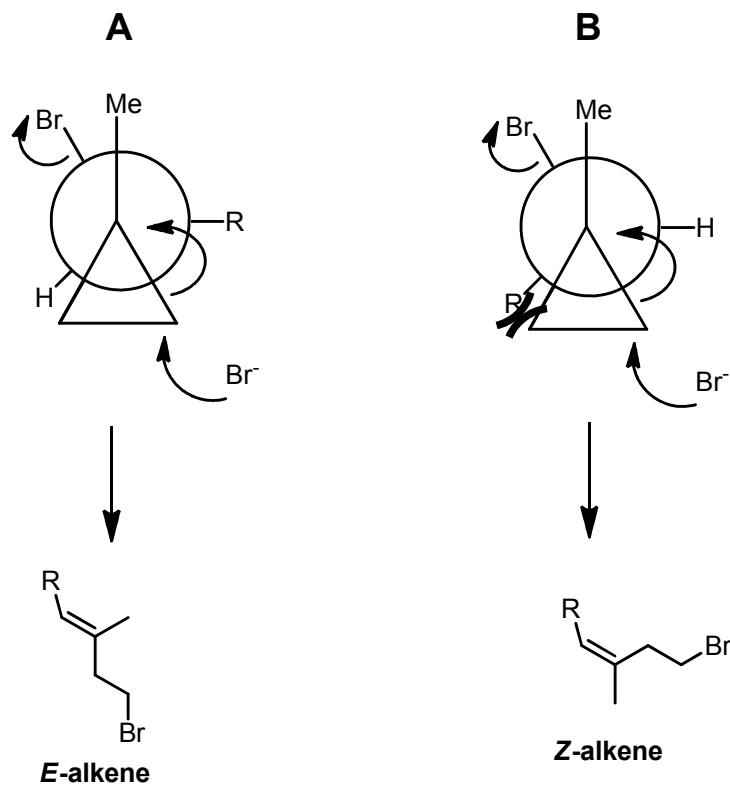


Figure 2.10. Newman projections for determination of the stereochemical outcome of the Brady-Julia olefination.

This reaction held much promise, since the van Tamelen group had already utilized it in their landmark formal synthesis of triptolide. However, all attempts to carry out this reaction failed. The desired product was never observed in the ^1H NMR of the crude reaction mixture. We suspect that the reaction conditions required for this transformation were too acidic, leading to loss of the protecting group and further degradation. This suspicion was confirmed by performing a synthesis of van Tamelen's cyclopropylcarbinol **17** and attempting the same reaction with that substrate. The known homoallylic bromide **18** was indeed detected in the crude reaction mixture. However, we elected to not pursue this reaction further.

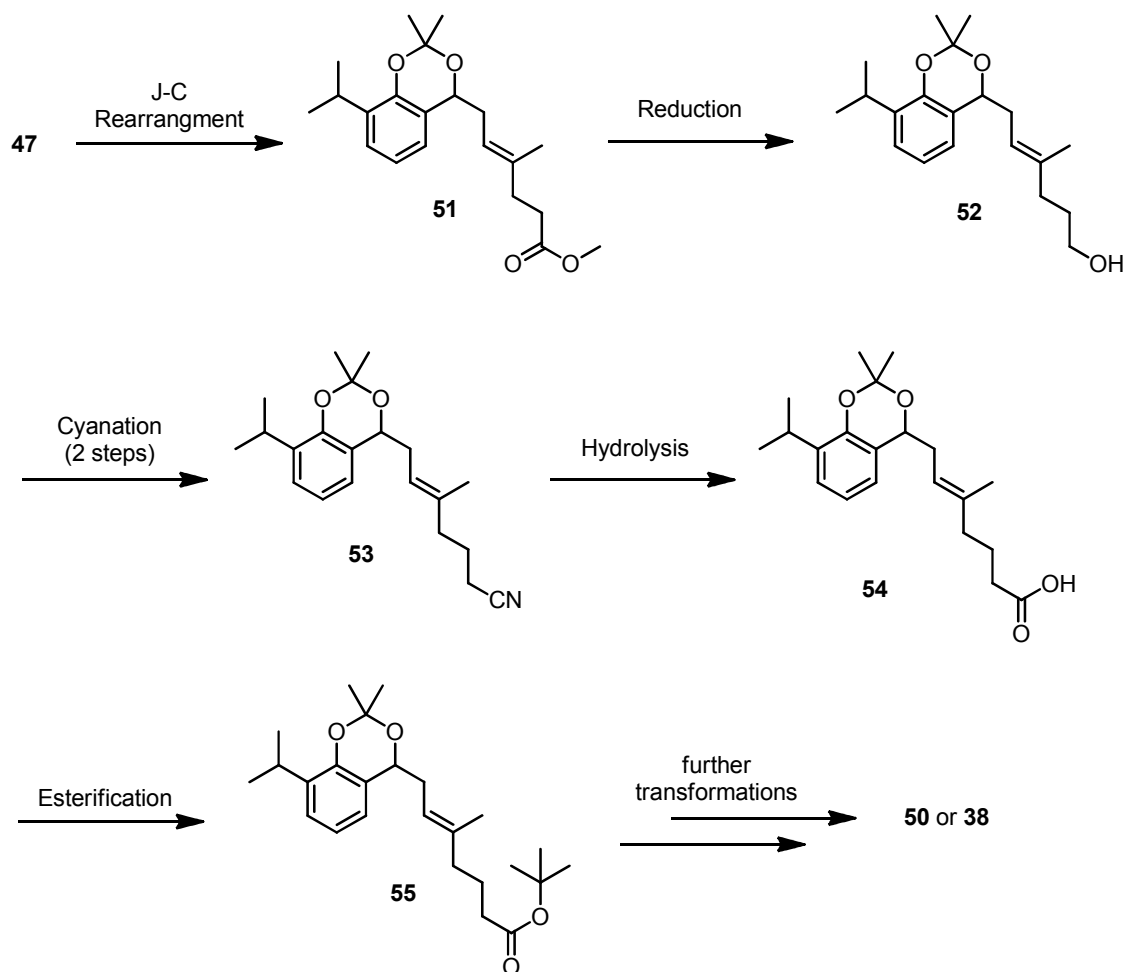
2.4 Orthoester Rearrangement and Homologation

After the failure of the Brady-Julia route, we revisited the literature in search of another method to access trisubstituted alkenes which would suit our purpose. In a short time, we came across the Johnson-Claisen orthoester rearrangement reaction. This transformation attracted our attention because we already had access to the desired precursor: isopropenyl alcohol **47**. Using this, we could easily access the unsaturated ester **51** (Scheme 2.2). Unfortunately, this ester is not in the correct position for our desired target, so we sought out a synthetic route to perform a one carbon homologation. Known methods exist for a one-pot homologation of esters – the Kowalski ester homologation⁵⁸ and the Arndt-Eistert homologation⁵⁹ – but these reactions are known to be operationally complex, highly temperature sensitive and, in the case of the Arndt-Eistert reaction, utilize dangerous reagents such as diazomethane. A simpler, yet longer homologation route was investigated, accessing the homologated *t*-butyl ester **55** via reduction, cyanation, hydrolysis and esterification (Scheme 2.2). At that point, a number of methods were available to us for installation of either an acetyl group to access **50** or direct formation of the allene **38** via alkynylation and subsequent isomerization.

2.4.1 Orthoester Rearrangement

The Johnson-Claisen rearrangement is mechanistically related to the ubiquitous Claisen rearrangement with which it shares its name; it features a [3,3]-sigmatropic rearrangement of a 1,5-diene to yield a γ - δ -unsaturated carbonyl compound. However, the true substrate for this rearrangement, **2.11-2**, is formed *in situ*, as it is a relatively unstable species (Figure 2.11). The 1,5-diene is formed by heating the allylic alcohol starting material with a trialkyl orthoacetate (commonly trimethyl orthoacetate) with a catalytic amount of a weak organic acid – commonly propionic acid. The acid present triggers the formation of an oxonium species, which is attacked by the alcohol and, after a proton shift and loss of methanol, forms intermediate **2.11-2**. This species is primed for rearrangement, which, given the high temperatures employed in this reaction, occurs rapidly, forming the desired *E*-alkene. This high *E*-selectivity originates from the energy difference present in the two

possible chair-like transition states through which the [3,3]-sigmatropic rearrangement occurs. Transition state **2.11-4** is configured such to place its substituents in equatorial positions, whereas **2.11-5** contains an unfavourable pseudo-1,3-diaxial interaction between the groups denoted R_2 and OR, increasing the energy of this transition state. This energy difference is dramatic for secondary allylic alcohol precursors ($R_1 \neq H$), heavily favouring transition state **2.11-4** and the *E*-alkene product. We were successful in performing this rearrangement in our synthesis using trimethyl orthoacetate, cleanly affording the desired ester **51** in 78% yield. No other alkyl orthoacetates were attempted, as the identity of the ester group was irrelevant for the subsequent reactions. We were also able to perform this reaction neat in trimethyl orthoacetate, as it was a suitable high-boiling solvent for this transformation.



Scheme 2.2. Proposed Johnson-Claisen rearrangement and homologation to access desired β -ketoester **50** or allenoate **38**.

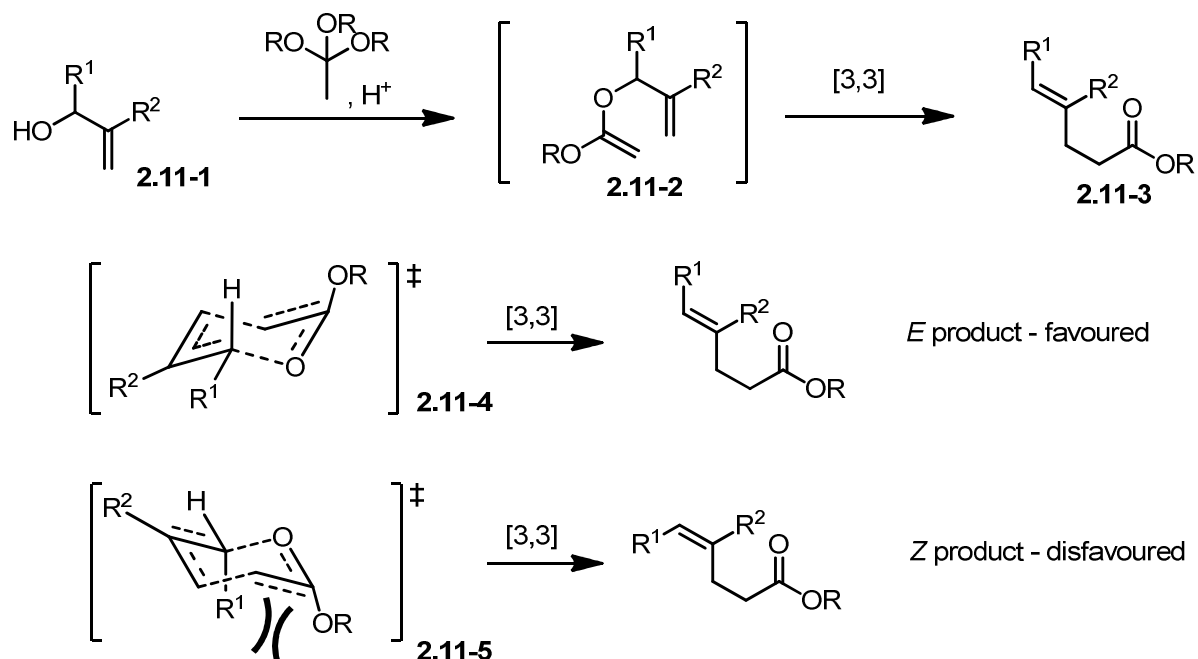


Figure 2.11. Mechanistic explanation of *E*-selectivity in the Johnson-Claisen rearrangement of secondary allylic alcohols.

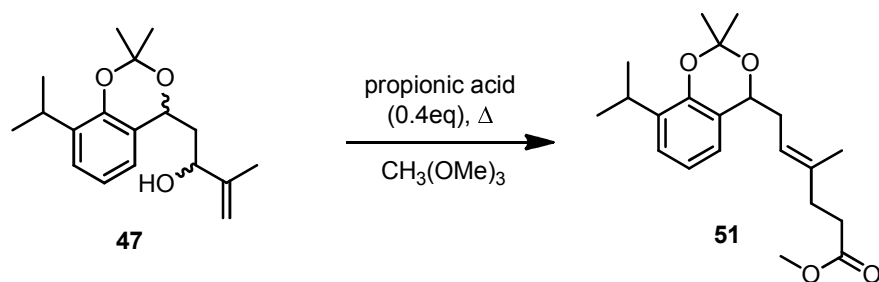


Figure 2.12. Optimized conditions for the Johnson-Claisen orthoester rearrangement reaction.

2.4.2 One-Carbon Homologation

The route proposed for the homologation of **51** is lengthy, with five total steps. However, each step is operationally simple and well known, thus we hoped this would grant us a useable pathway to access the desired allenoate target and test the cyclization.

Reduction

The initial transformation we desired was reduction of the ester to a primary alcohol. This was easily accomplished by using the strong reducing agent LiAlH₄. Exposure of **51** to

LiAlH_4 at 0°C in THF for one hour afforded complete conversion to the alcohol **52**, which was isolated in 72% yield (Figure 2.13).

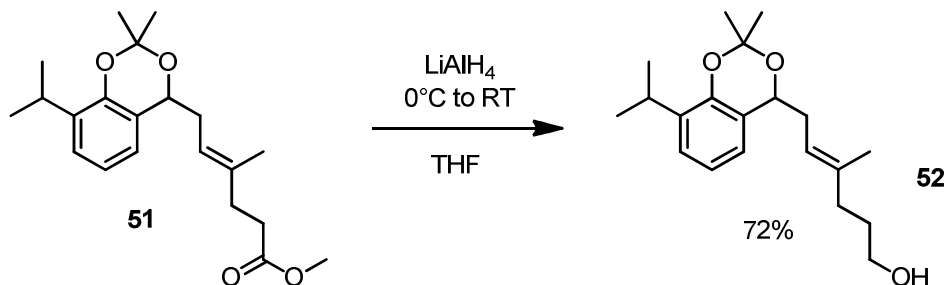


Figure 2.13. Reduction of ester **51** to primary alcohol **52** with LiAlH_4 .

Tosylation

Conversion of a primary alcohol to a sulfonate ester is a simple and ubiquitous reaction in synthetic organic chemistry. This transformation was required as part of this homologation procedure to convert the alcohol into a better leaving group for the subsequent cyanation reaction. Treatment of **52** with *p*-toluenesulfonyl chloride in the presence of TEA and DMAP cleanly converted the alcohol to tosylate **2.14-1** (Figure 2.14). This product, however, was not isolated, as we found that it was somewhat unstable on silica gel. As such, it was carried on as crude material to the next reaction in sequence.

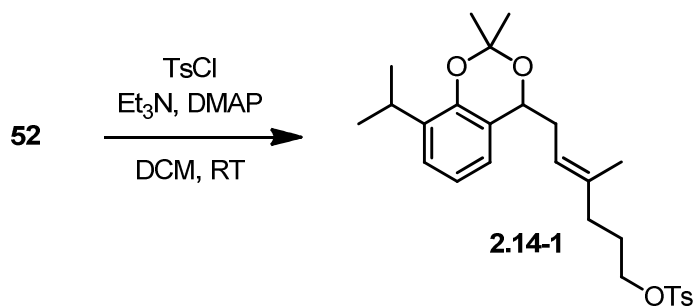


Figure 2.14. Tosylation of primary alcohol **52** with *p*-toluenesulfonyl chloride, triethylamine and DMAP to access sulfonate ester **2.14-1**.

Cyanation

The next reaction in the homologation sequence is a simple S_N2 displacement of the tosylate group with a cyanide group. Typical procedure for this transformation is heating of the tosylate in the presence of a cyanide salt (usually sodium or potassium cyanide) at high temperatures. DMSO is a common solvent choice for this reaction, as it is a polar, aprotic solvent that readily solubilizes the cyanide salt and easily accommodates the high reaction temperature. These exact conditions worked perfectly for our purposes. Refluxing **2.14-1** with 1.2 equivalents of KCN in DMSO for four hours cleanly afforded the desired product **53** in 94% yield over two steps (Figure 2.14, Figure 2.15).

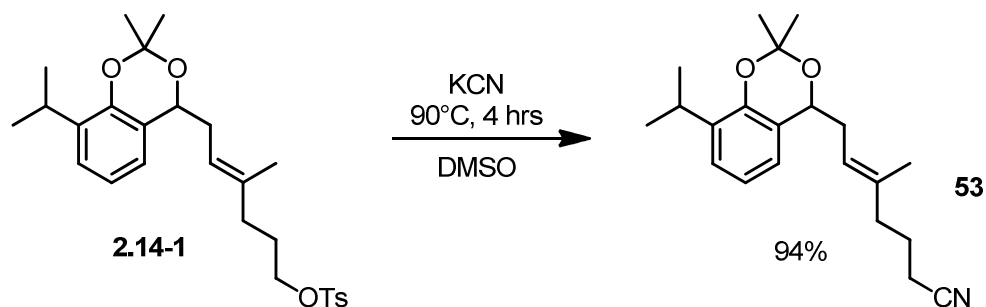


Figure 2.15. Nucleophilic cyanation of tosylate **2.14-1** to access primary nitrile **53**. (Structure)

Hydrolysis

Hydrolysis of a nitrile to a carboxylic acid is typically performed by heating the substrate in aqueous strong acid or strong base. Considering the known acid sensitivity of the acetonide protecting group, strong base was the preferred method for this synthesis. In the presence of excess potassium hydroxide, heating nitrile **53** in a 4:1 mixture of ethanol and water for 20 hours led to complete consumption of the starting material. Aqueous workup in basic conditions, followed by acidification and re-extraction isolated the desired product cleanly in 58% yield (Figure 2.16). This yield was somewhat disappointing, but we did not spend any time to optimize this transformation.

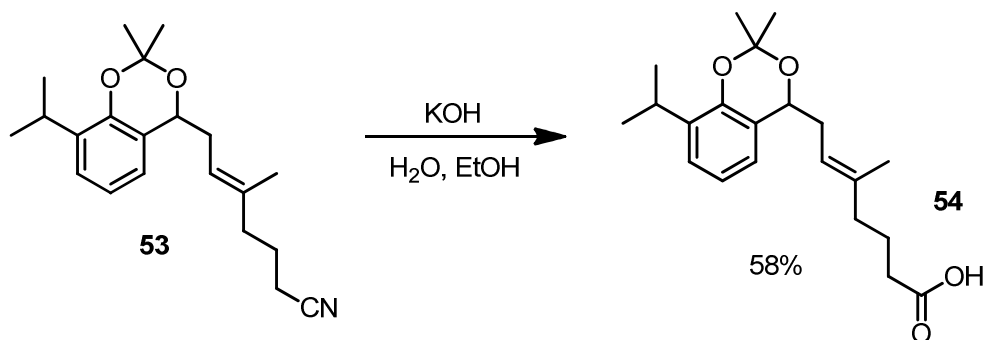


Figure 2.16. Basic hydrolysis of alkyl cyanide **53** to access carboxylate **54**.

Esterification

Classical esterification conditions involve prolonged exposure of the carboxylate precursor to heat and strong acid – commonly sulfuric acid. These conditions are undesirable for this substrate due to the aforementioned acid sensitivity. Moreover, these conditions are not applicable for the formation of *tert*-butyl esters; *tert*-butanol is a very poor nucleophile and, as such, is unable to undergo esterification in the usual way. Fortunately, an alternative method exists for this process. Esterification of carboxylic acids to *tert*-butyl esters can be performed in the presence of di-*tert*-butyl carbonate (Boc₂O) and catalytic magnesium chloride at room temperature, using Boc₂O as the source of the *t*-butyl group.⁶⁰ Exposing **54** to these conditions gave clean conversion to the *t*-butyl ester **55** in 86% yield, thus completing the homologation. Any remaining starting material was easy to recover and resubmit to the reaction conditions.

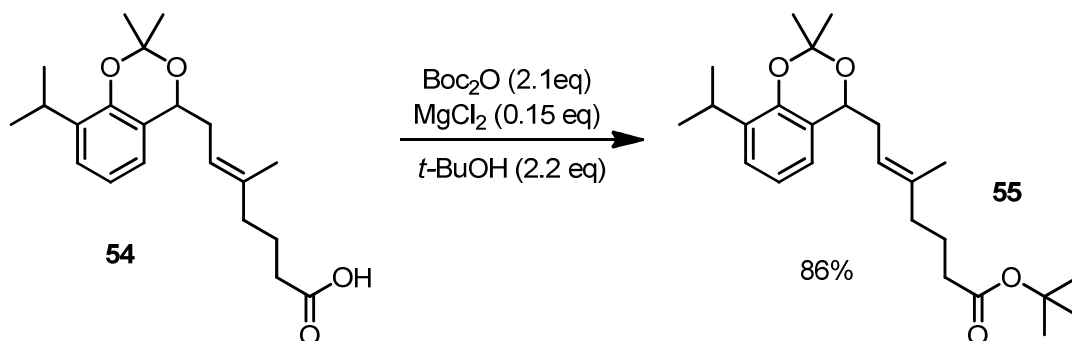


Figure 2.17. Esterification of carboxylate **54** with Boc₂O and MgCl₂ to access homologated ester **55**.

2.4.3 Attempted Acetylation and Conclusions

After completing the five-step homologation, we were left with only a small amount of material, and as such concluded that it was a lengthy, linear and low-yielding method to access ester **55**. Acknowledging that it was unlikely to be the final synthetic method, we began an investigation into methods to acetylate **55** to access β -ketoester **50**. A number of acetylating reagents were investigated, including common reagents such as acetyl chloride and acetic anhydride to unusual ones such as *N*-acetylbenzotriazole.⁶¹ None of these acetylating agents yielded the desired product. No reaction was observed with acetic anhydride and *N*-ABT; acetyl chloride yielded what we suspect was the *O*-acetylated product **2.18-1** rather than the *C*-acetylated product – a known side reaction with this type of transformation.⁶² This undesired product was not fully characterized. These disappointing acetylation results combined with the low yields of the homologation procedure drove us to seek a more concise method to access our desired target.

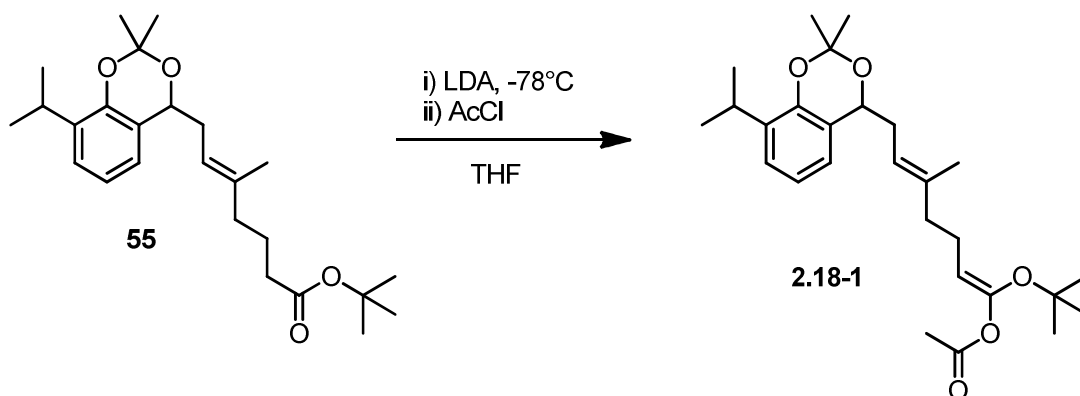


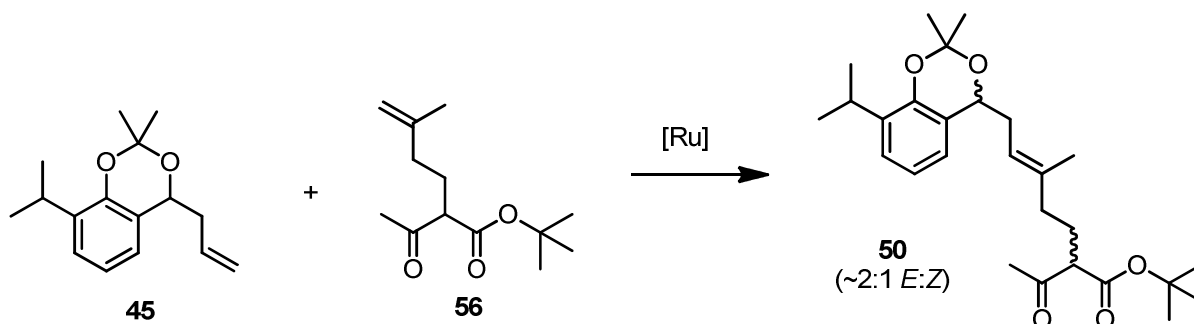
Figure 2.18. Unintended *O*-acetylation of *tert*-butyl ester **55** with acetyl chloride.

2.5 Global Cross-Metathesis

After the disappointing and lengthy homologation route, we turned our attention to seeking a more expedient method to access the desired β -ketoester **50**. Revisiting our retrosynthetic analysis (Figure 2.3), we decided to investigate the possibility of synthesizing the central alkene using an olefin cross-metathesis process. The synthesis of trisubstituted alkenes with cross-metathesis is well documented in the literature^{63,64} and the subject has

attracted much attention in recent years for its atom economy and functional group tolerance.⁶⁵ The synthesis of trisubstituted alkenes with high *E*-selectivity, however, remains highly substrate-dependent: typically, only coupling partners with considerable steric bulk at the allylic position or α,β -unsaturated carbonyl compounds give synthetically useful *E/Z* ratios.⁶⁴

The substrates for the desired cross-metathesis (**Scheme 2.3**) featured neither of these characteristics, so we accepted that optimizing the *E/Z* ratio would present a challenge – typically, without any steric or electronic driving force, cross-metathesis reactions yield thermodynamic *E/Z* ratios, in the range of 1.5:1 to 4:1⁶⁶. On the upside, we recognized that this metathesis process would, in theory, be selective for the desired product (**50**), as the starting material **45** is a type I alkene for second-generation metathesis catalysts and the coupling partner **56** is a type III alkene. The desired product is, according to the literature, a type IV alkene, and as such should constitute a thermodynamic minimum for the reaction, funneling both reactants into the desired product.



Scheme 2.3. Proposed cross-metathesis of type I olefin **45** with type III olefin **56** to access β -ketoester **50**

This thermodynamic control of ruthenium-catalyzed metathesis reactions is outlined in Figure 2.19. In addition to a direct cross-metathesis to form the desired product, **50** can be accessed in a two-part metathesis cascade. Type I alkene **45** can undergo rapid self-metathesis to form homodimer **2.19-1**. This homodimer constitutes a type II alkene, which is still reactive to further metathesis reactions, a phenomenon known as secondary metathesis. The homodimer can react in a cross-metathesis with **56** to form the desired product. In this manner, the desired product should be formed in a highly selective manner. In comparison, the type III partner does not undergo homodimerization⁶⁴ and is available to react

exclusively to form the desired product. With the theoretical limits of the reaction well understood, we then moved on to the synthesis of the type III coupling partner.

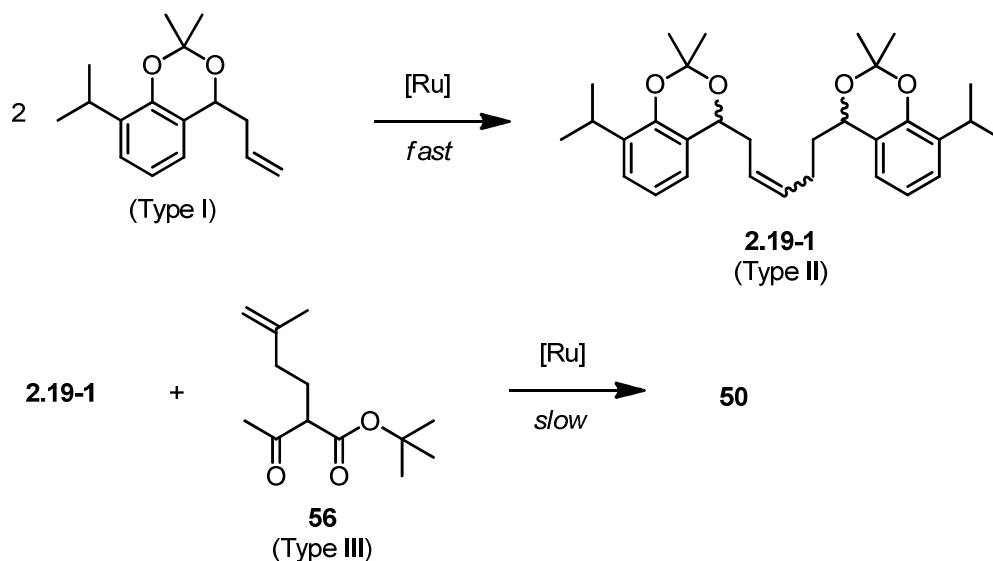


Figure 2.19. Thermodynamic control of cross-metathesis between type I alkene **45** and type III alkene **56**. **45** is able to homodimerize to form **2.19-1**, which can react via secondary metathesis with **56**, forming **50**.

2.5.1 Synthesis of Type III partner and Proof of Concept

The synthesis of homoallylic β -ketoester **56** proved very simple. Conversion of inexpensive 3-methyl-3-buten-1-ol (**2.20-1**) to the iodide **2.20-2** proceeded smoothly using Appel conditions: triphenylphosphine, imidazole, and iodine (Figure 2.20).⁶⁷ This product was volatile, and as such was used without further purification to alkylate *tert*-butyl acetoacetate. This reaction was accomplished under slightly unconventional conditions – potassium *tert*-butoxide in *tert*-butanol⁶⁸ - but was nevertheless successful, affording **56** in 52% yield over two steps (Figure 2.21).

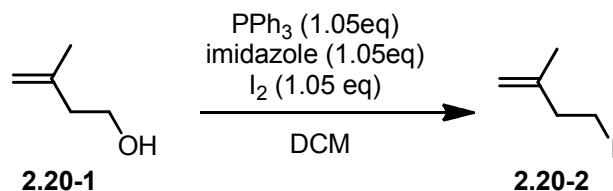


Figure 2.20. Conversion of 3-methyl-3-buten-1-ol to iodide **2.20-2** via the Appel reaction.

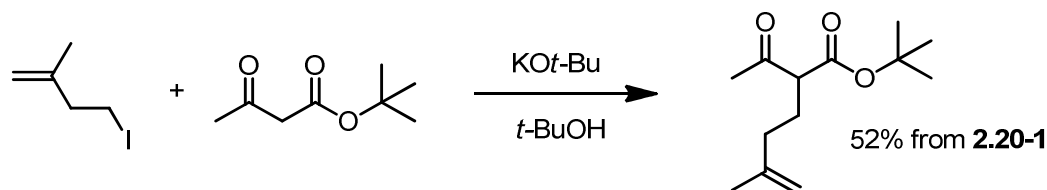


Figure 2.21. Alkylation of *tert*-butyl acetoacetate with iodide **2.20-2** to access type III metathesis partner **56**.

Subjecting **56** to typical cross-metathesis conditions (5 mol% Grubbs II, DCM, reflux) in the presence of two equivalents of type I partner **45** yielded a mixture of products on TLC. The type III partner was not fully consumed and a substantial amount of Type II homodimer was present. However, we were pleased to discover that the desired product was also produced and was isolated in 16% yield as a 2:1 *E/Z* mixture (Figure 2.22).

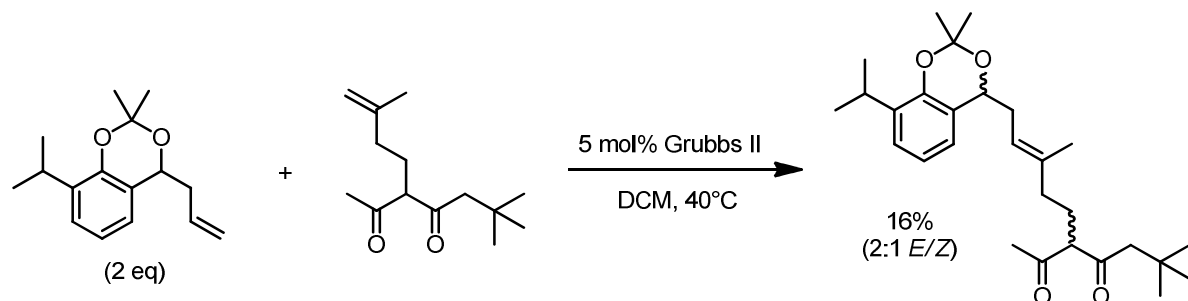


Figure 2.22. Initial results of cross-metathesis of **45** and **56** with the 2nd generation Grubbs catalyst.

2.5.2 Optimization

Encouraged by our initial success, we pushed forward to optimize this cross-metathesis reaction (Table 2). We first tested the effect of degassing the dichloromethane solvent, as the presence of oxygen is known to accelerate degradation of the active catalytic species (Entry

2). This did not appear to improve the result, despite running the reaction over several days. Unsurprisingly, it did not have a detrimental effect on the result either, and as such we opted to degas the reaction mixtures for most of our attempts. Interestingly, increasing the loading of Grubbs II appeared to have a detrimental effect on the yield and this drop in yield was consistent when we switched solvents to toluene and increased temperature. (Entries 3-4). Subjecting the 2nd generation Grubbs catalyst to high temperatures is known to accelerate decomposition so we switched catalysts to the 2nd generation Hoveyda-Grubbs catalyst, which possesses better thermal stability.⁶⁹ This catalyst was inactive at the reflux temperature of DCM (Entry 5), but performing the reaction toluene dramatically improved the yield to 39% (Entry 6). We attempted to reproduce these results under rigorous Schlenk conditions, decreasing catalyst loading and increasing the A:B ratio, but the yield from this attempt was a mediocre 15% (Entry 7). Further optimization of this reaction under Schlenk conditions was not performed as it was operationally complicated and not amenable to scale-up. An attempted 0.5 g scale-up of the successful conditions resulted in a modest yield of 24% (Entry 8).

Consulting the literature again, we learned of the existence of a modified Hoveyda-Grubbs catalyst which featured a bulkier NHC ligand and was reported to be more efficient for the synthesis of trisubstituted olefins by cross-metathesis.⁷⁰ Testing this catalyst in our synthesis required switching back to DCM and lower temperatures, as these were the suggested conditions. Entries 9 and 10 of Table 2 outline our attempts made with this catalyst – both demonstrated a decreased yield compared to the standard Hoveyda catalyst in toluene. Finally, we investigated an unusual combination of solvents for metathesis reactions: running this reaction in 1:1 THF/toluene gave similar yields as most attempts, but the *E/Z* ratio increased from 2:1 to 4:1 (Entry 11). This was a very exciting result, as it effectively doubled the yield of our desired *E* product compared to similar yields in previous trials. We were able to increase the yield to 22% (Entry 12) but were unfortunately unable to reproduce or surpass the 39% yield obtained previously. We performed one final test, running this reaction under microwave conditions (Entry 13), but this yielded poor results.

Despite extensive optimization, we were, regrettably, unable to achieve good results with this global cross-metathesis method. However, over the course of the optimization, we were able to collect a reasonable amount of the desired product and the inseparable *Z* isomer. Both

these materials were of acceptable purity for continuation of the synthesis, testing the desired allene formation reaction and for some initial investigation of the proposed gold cyclization.

Entry	A:B	Catalyst	Mol % catalyst	Solvent*	T /°C	Reaction time (h)	AB yield
1	2:1	G2	5	DCM	40	24	16
2	2:1	G2	7	DCM(dg)	40	96	13 ^a
3	2:1	G2	8	DCM	40	18	7 ^c
4	2:1	G2	10	PhMe(dg)	80	18	11.6
5	3:1	HG2	7	DCM(dg)	40	18	0
6	2:1	HG2	5	PhMe(dg)	110	18	39
7	9:1	HG2	1	PhMe(dg)	110	84	15 ^{b,d}
8	3:1	HG2	5	PhMe(dg)	110	18	24 ^e
9	3:1	iPr-HG2	5	DCM(dg)	40	48	13.4
10	3:1	iPr-HG2	5	DCM(dg)	40	72	18
11	3:1	HG2	5	THF/PhMe	80	24	17 ^f
12	2:1	HG2	2	THF/PhMe	85	72	22 ^f
13	2:1	HG2	9	THF/PhMe	μ w	3.5	6 ^f

Table 2. Optimization of global cross-metathesis reaction. All yields are isolated yields reported as a 2:1 E/Z mixture unless otherwise indicated. G2 = Grubbs 2nd generation catalyst, HG2 = Hoveyda-Grubbs 2nd generation catalyst, iPr-HG2 = Hoveyda-Grubbs 2nd generation catalyst with IPr NHC ligand. *(dg) indicates that the reaction mixture was degassed prior to heating. ^aType I partner was added over 5 hours. ^bType I partner added over 12 hours. ^cCatalyst was added over 5 hours. ^dReaction performed under Schlenk conditions. ^eReaction performed on 500mg scale. ^fProduct isolated as a 4:1 E/Z mixture.

2.5.3 Initial attempts at Allene synthesis

With the material collected over the course of optimizing the global cross-metathesis method, we turned our attention towards the synthesis of the desired allenolate **38**. The precedent for this transformation was set by Maity and Lepore in 2007⁵⁰ where they documented clean conversion of a series of substituted β -ketoesters to the corresponding 2,3-allenolates in moderate to good yields. Their publication reported a one-pot transformation involving formation of an external enol triflate **2.23-2** under basic conditions, and then a

subsequent deprotonation and elimination of the triflate group to form the desired product (Figure 2.23).

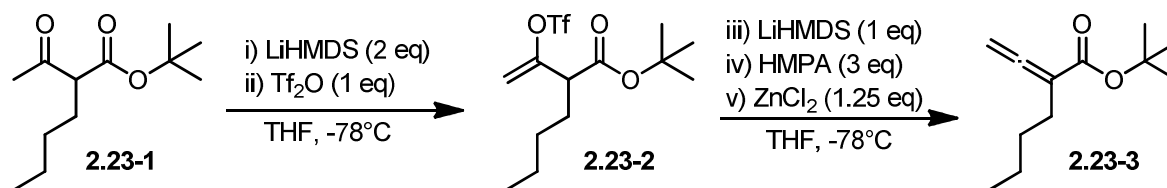


Figure 2.23. One-pot synthesis of 2,3-allenoates from substituted β -ketoesters as described by Maity and Lepore.

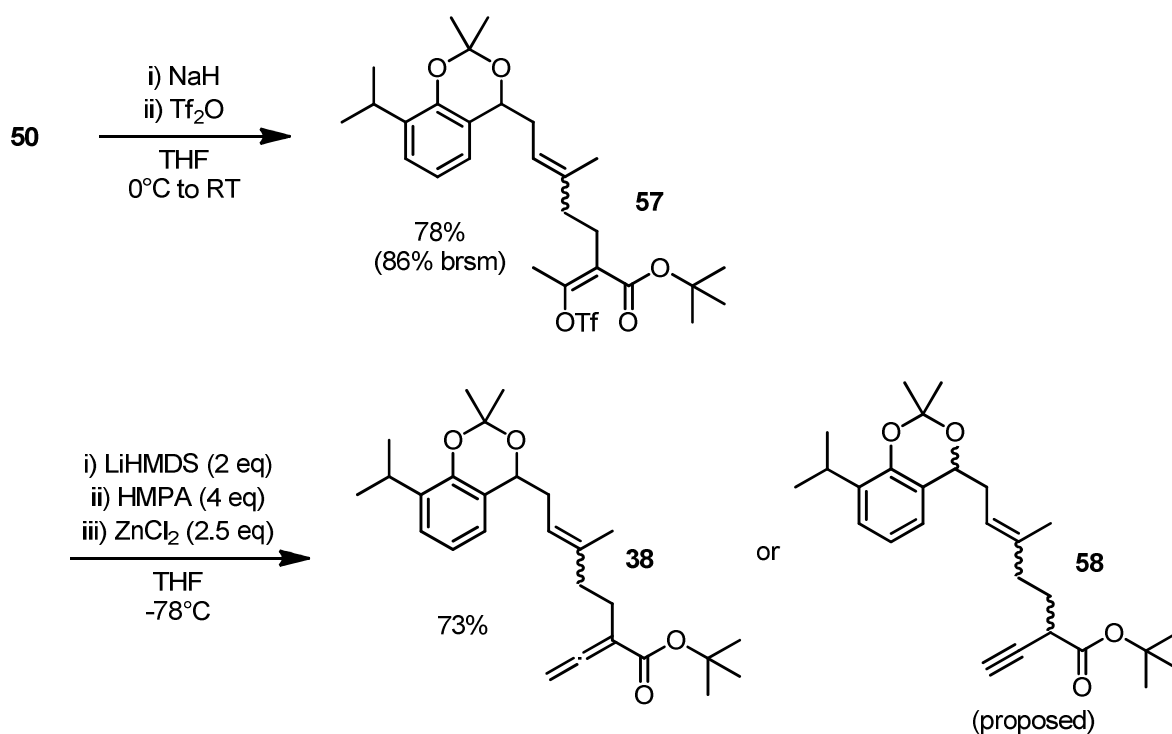


Figure 2.24. Two-step triflate formation and subsequent elimination protocol to access allenoate **38**.

Our initial attempts to reproduce this procedure met with little success: the only product isolated from the reaction mixture was suspected to be the internal enol triflate **57** (Figure 2.24). Further attempts yielded small amounts of **38** (< 2%) but **57** remained the major product. Fortunately, we discovered that this species could be isolated and resubmitted to the second set of reaction conditions to afford the desired product **38**. This two-step procedure

was sufficient for the time being, and we performed some optimization of the reaction conditions: formation of **57** was performed using sodium hydride, yielding the internal enol triflate in 78% yield (86% brsm). This material could be converted to the desired allenolate in 73% yield by exposure to the second half of the aforementioned one-pot protocol.

During the optimization, we learned that this reaction is highly temperature-sensitive. Quenching of the reaction from -78° directly into an ice-cold mixture of diethyl ether and saturated aqueous ammonium chloride provided the desired product, but allowing the mixture to warm to 0°C before quenching yielded a different, unidentified product – we suspected this may be the isomeric alkyne **58**, but exposure of this unknown product to basic conditions did not form the allene as would be expected.⁵⁰

An alternative one-pot approach to accessing allene **38** was also explored, using an enol phosphonate intermediate in place of an enol triflate. This method is known for the formation of allenes from isolated ketones and also from 1,3-diketones, but not from β -ketoesters.⁷¹ Initial attempts with these conditions (Figure 2.25) yielded similar, but slightly improved results to the Maity and Lepore method. Small amounts of the desired allenolate were formed, along with a similar amount of recovered starting material. The majority of material present appeared to be the intermediate enol phosphonate **59**. We did not pursue this method further.

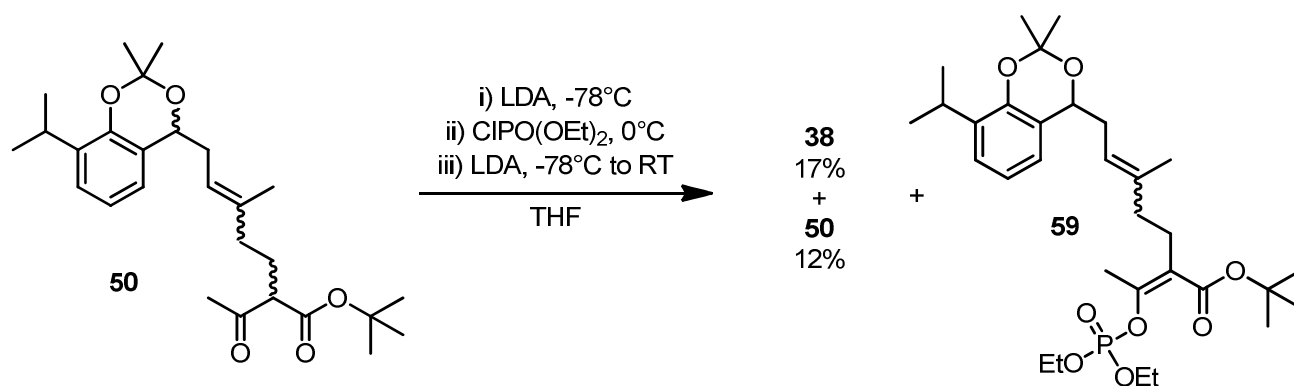


Figure 2.25. Alternative one-pot method for allene synthesis via intermediate enol phosphonate **59**.

2.5.4 Initial work with Gold

The proposed gold cyclization, as described in section 1.2, was inspired by a publication from the Gouverneur group; as such, once we had precursor **38** in our possession, we attempted the exact conditions described in the aforementioned paper as a starting point in the investigation of the key step (Figure 2.26). To our dismay, these conditions yielded only degradation of the starting material and no product of any kind of was detectable.

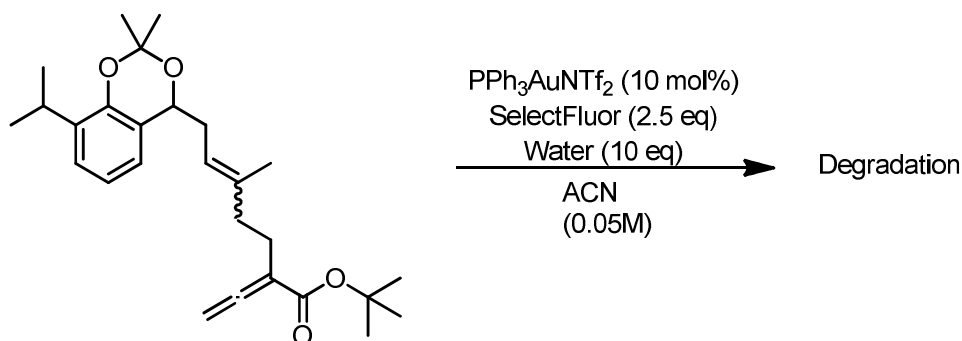


Figure 2.26. Failure of original Gouverneur conditions for the proposed gold cyclization cascade reaction.

In an attempt to understand the cause of this degradation, we tried to break the cascade down into individual reactions and analyze each part. We understood that the proposed cascade would commence with a gold(I)-catalyzed cyclization of the allenoate to form a γ -butenolide, as described in section 1.2.1. We performed two parallel attempts at this cyclization using AuCl and AuCl_3 , both of which are known catalysts for this reaction.^{44,48} To our surprise, we isolated a mixture of products, both the desired butenolide **60** and the deprotected butenolide **61** (Figure 2.27). From this result, we hypothesized that the acetonide group was sensitive to the Lewis acidity of gold(I) and gold(III), and that the deprotected diol underwent further degradation in the presence of SelectFluor.

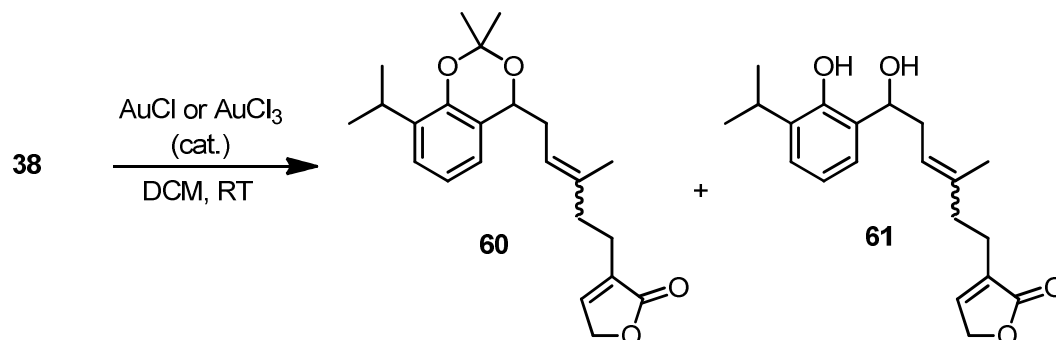


Figure 2.27. Au(I)/Au(III) catalyzed butenolide cyclization with unexpected deprotection of acetonide group.

To test this hypothesis, we performed a series of stability tests as described in Table 3. Subjecting the allenoate **38** to PPh₃AuNTf₂ in the absence of SelectFluor[®] yielded only the deprotected allenoate **62** (Figure 2.28): no traces of cyclized product were detected in the ¹H NMR. This deprotected allenoate, when exposed to only SelectFluor, degraded rapidly, confirming our hypothesis. Interestingly, the protected allenoate was stable to SelectFluor in the absence of gold – no degradation was observed. Finally, we exposed the cyclized, protected butenolide to SelectFluor, where a slow degradation of the starting material was observed, suggesting that this intermediate is potentially unstable to the cyclization conditions as well.

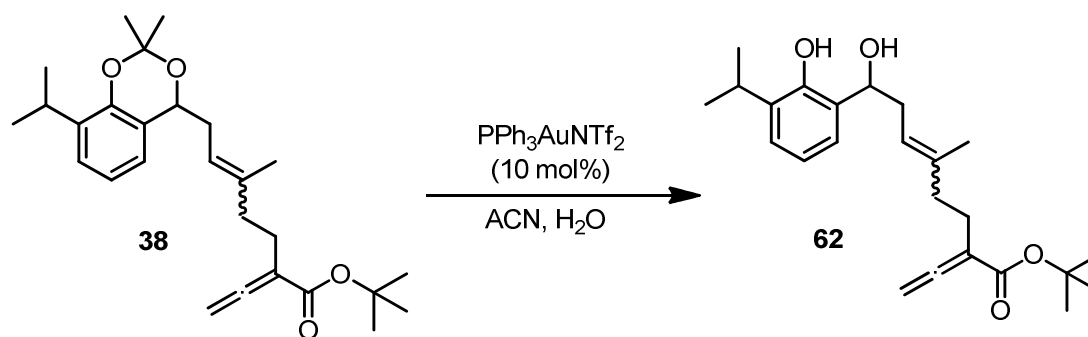


Figure 2.28. Deprotection of **38** to allenoate diol **62** upon exposure of **38** to the Gagosz catalyst in acetonitrile and water.

Entry	Substrate	Conditions*	Result
1	38	PPh ₃ AuNTf ₂	Deprotection to 62
2	38	SelectFluor	No reaction
3	62	SelectFluor	Degradation
4	60	SelectFluor	Slow degradation

Table 3. Stability study of allenolate **38** to gold(I) and Selectfluor. *All reactions were run in ACN/H₂O (0.05M) at RT.

2.6 Selection of a new protecting group

After conducting stability studies of the acetonide protecting group, we concluded that this protecting group was insufficiently stable for the proposed gold-catalyzed cyclization cascade. As a result, we were forced to re-think our synthetic strategy. We proposed a number of alternative protecting groups for the 1,3-diol moiety (Figure 2.29): bis-benzyl ether **63**, methylene acetal **64**, bis-MOM ether **65**, and bis-methyl ether **66**.

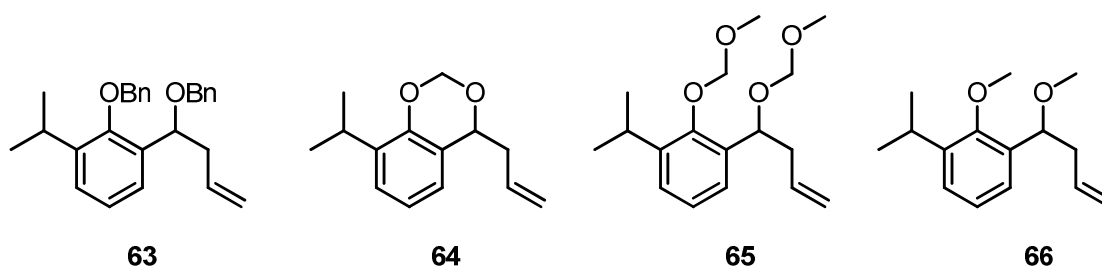


Figure 2.29. Proposed alternative protecting groups for the phenolic/benzylic diol system.

Of these ideas, we decided that the bis-MOM ether protecting group **65** was likely to be the least stable due to the known deprotection methods - strong Brønsted acids⁵² - and as such, it was quickly rejected.

2.6.1 Bis-benzyl ether

We attempted to synthesize the bis-benzyl derivative **63** first, as this protecting group is known to be stable to nearly all conditions save for hydrogenolysis, thus the group should be stable to our gold conditions.⁵² Unfortunately, our efforts towards this bis-benylation yielded poor results, consisting of mixed mono-benzylated products – either the phenol or the benzylic alcohol were protected, but not both. This is likely due to the strong steric influence imposed by one benzyl group upon the unprotected hydroxyl moiety.

2.6.2 Methylene acetal

Both the methylene acetal and bis-methyl ether derivatives (**64** and **66**, respectively) are known to be very robust and, as such, are difficult to remove without using harsh reagents such as BBr_3 .⁵² The robustness of these groups was, at this point, highly attractive, as we desired a protective group that would remain intact when exposed to the Lewis acidic nature of cationic gold. The methylene acetal was investigated first. Consulting the literature, we first attempted to install this group using a modified set of acidic conditions, similar to those used to install the original acetonide group: excess dimethoxymethane in the presence of catalytic *p*-toluenesulfonic acid and lithium bromide.⁷² This reaction, unexpectedly, yielded the incorrect product **67**, featuring a mono-methylation at the benzylic position (Figure 2.30). We proposed that the dimethoxymethane used contained a large amount of methanol that reacted with a benzylic carbocation formed *in situ* to form the undesired product.

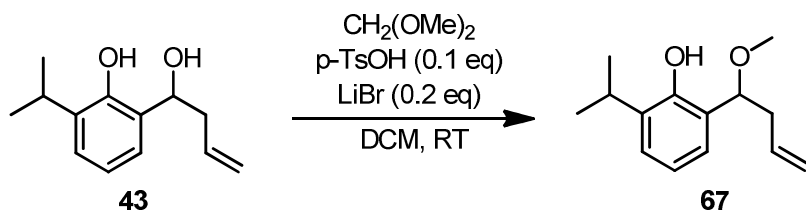


Figure 2.30. Unexpected mono-methylation of diol **43** while attempting to form methylene acetal **67** under acidic conditions.

After the failure of the acidic method, we turned to a base-induced, phase-transfer method using dibromomethane as the methylene source. The first protocol we investigated utilized a water/1,4-dioxane solvent mixture at high temperatures in the presence of excess sodium hydroxide and catalytic tetrabutylammonium iodide (Figure 2.31).⁷³ This method was successful in producing the desired methylene acetal **64**, albeit in low yields. We attempted to improve upon this result using a modified set of conditions – water and DCM at 50°C using CTAB as a phase-transfer catalyst,⁷⁴ but we observed low conversion to product. Additionally, **64** proved difficult to purify on column chromatography.

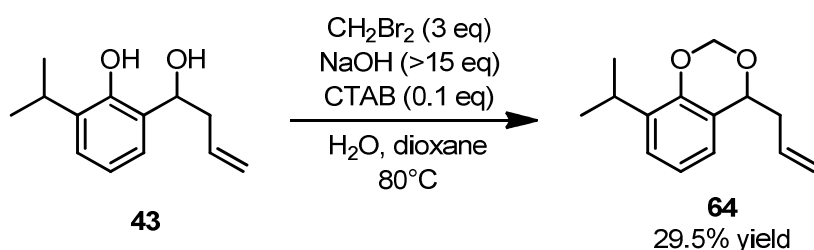


Figure 2.31. Successful installation of methylene acetal protecting group under basic phase-transfer conditions.

2.6.3 Bis-methyl ether

The low yield and complicated purification of **64** pushed us towards the bis-methyl ether protective group. We expected these groups to be much simpler to install, due to the vast literature precedence for methylations of alcohols at ambient temperatures. On our first attempt, we were successful in synthesizing bis-methyl ether **66** from a crude sample of diol **43** under basic conditions (Figure 2.32).

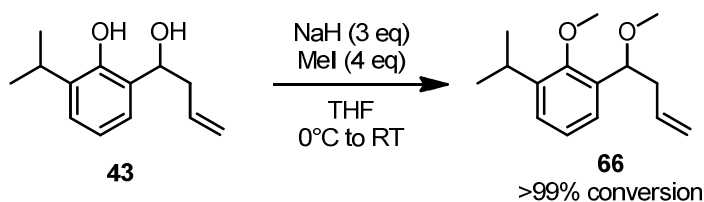


Figure 2.32. Base-mediated bis-methylation of diol **43** with iodomethane.

We quickly investigated the compatibility of telescoping this methylation with the initial two synthetic steps as per section 2.2. This methylation protocol proved viable and high yielding – we were able to access the methylated product **66** in 78% yield over the three steps, only requiring chromatographic purification of the final product.

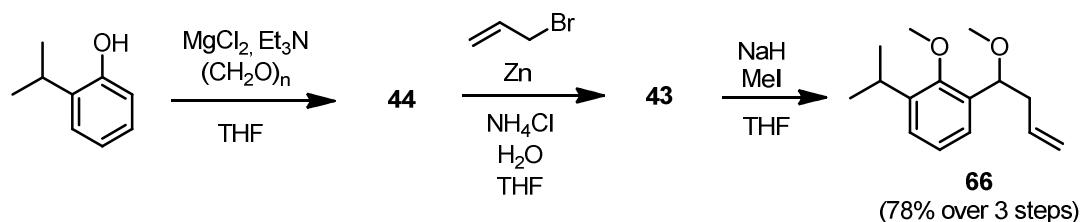


Figure 2.33. Telescoped multigram-scale three-step synthesis of bis-methyl ether **66**.

With hindsight from the failed acetonide protecting group, we decided to investigate the stability of the protecting group to gold(I) immediately. To our delight, when we exposed **66** to the Gagosz catalyst in ACN and water (Figure 2.34), no reaction whatsoever was observed over several days, suggesting that the bis-methyl ether groups possessed good stability to gold(I) salts.

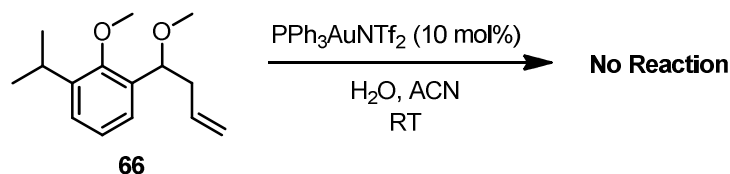
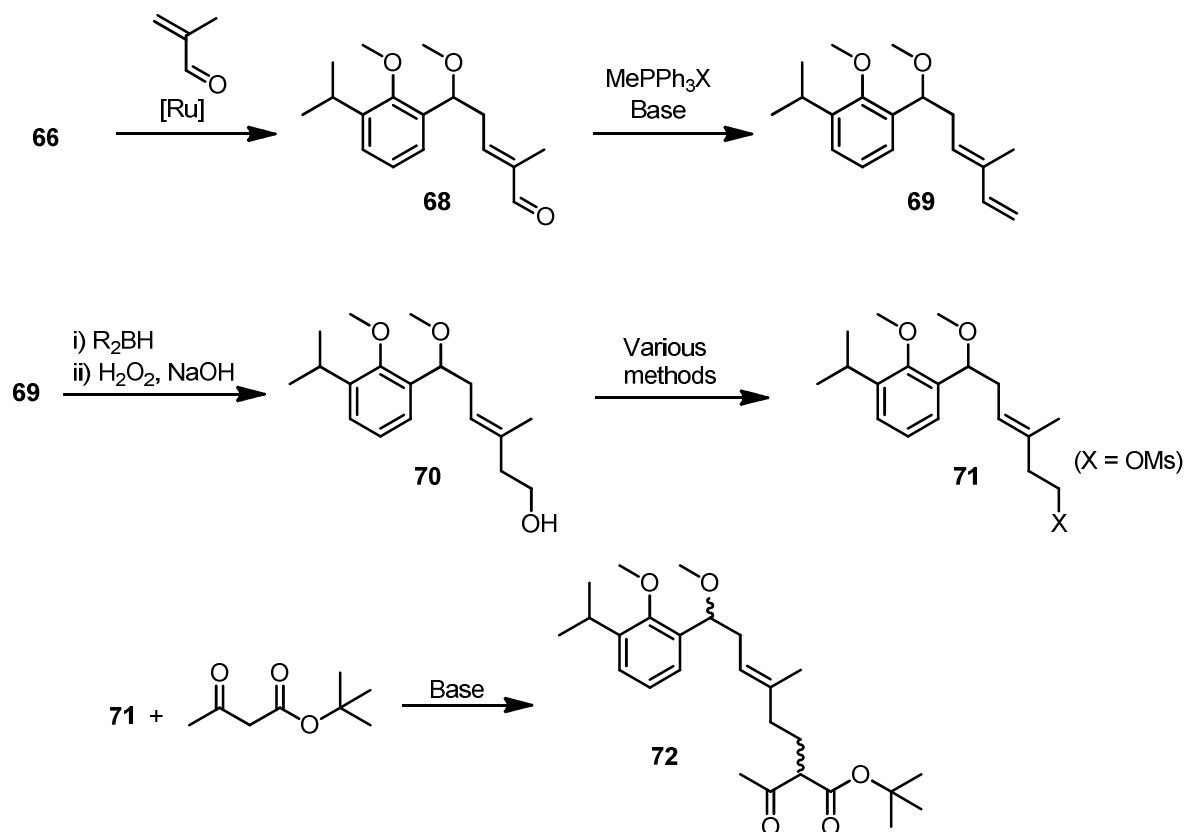


Figure 2.34. Stability test of bis-methyl ether protecting group with the Gagosz gold catalyst.

2.7 Cross Metathesis-Wittig-Hydroboration Route

With a new, stable protecting group in our possession, we returned to the drawing board to seek a simple and reliable method to access the allenolate cyclization precursor. Drawing on the knowledge we gained from the global cross metathesis method, we elected to utilize a cross-metathesis again to establish the *E*-trisubstituted alkene. In this case, however, we elected to use methacrolein as the metathesis partner, due to its low cost, availability and functionality (Scheme 2.4). From the α,β -unsaturated aldehyde **68** generated in this step, we

envisioned doing a methylene Wittig reaction to form the *E*-1,3-diene **69**, which would afford the two-carbon linker group between the alkene and the β -ketoester functionality. From there, we proposed a selective hydroboration-oxidation protocol of the terminal alkene to access the homoallylic alcohol **70**, at which point the primary hydroxyl group could be converted to a leaving group and subsequently displaced to form **72**.



Scheme 2.4. Cross-Metathesis-Wittig-Hydroboration route to access dimethylated β -ketoester **72**.

2.7.1 Cross-Metathesis with Methacrolein

Olefin cross-metathesis of type I alkenes such as **66** with methacrolein is well-documented in the metathesis literature.⁶⁴ This transformation is known to proceed in good yields and with synthetically useful *E/Z* selectivity, typically favouring the *E* geometry in a 9:1 ratio or greater.⁶⁴ There are, however, some issues to consider for the scale-up of metathesis processes, chiefly among which is the high cost of the catalysts. As such, the main area of focus in the optimization of this cross-metathesis was in reducing the catalyst

loading while maximizing yield. Typical conditions for this transformation would involve refluxing a mixture of **66** for ca. 18-24 hours with excess methacrolein (≥ 9 equivalents) in the presence of 5 mol% Grubbs 2 in DCM. Our goal was to reduce the catalyst loading to below 1% and reduce the reaction time to minimize degradation of the aldehyde product. These two goals are typically opposing forces – reducing catalyst loading leads to increased reaction times – and to circumvent this problem we sought a method to accelerate the reaction.

Bruce Lipshutz and his research group at the University of California Santa Barbara have recently developed some interesting methodology for improving the rates of olefin metathesis reactions. In 2011, they reported a method to accelerate the rates of CM processes with enones, acrylates, and acrylic acids by introducing copper(I) iodide as a co-catalyst and running the reactions in Et₂O, an uncommon solvent for olefin metathesis reactions.⁷⁵ This caught our attention and we investigated the applications of this protocol to our synthesis. On the first try, we achieved a reasonable 60% yield of **68** reproducing the Lipshutz conditions: 2 mol% Grubbs II, 3 mol% CuI, 0.1 M in Et₂O at reflux for three hours. We noted that the conversion of this reaction was not absolute, but the unreacted **66** was easy to remove with chromatography. Optimization and scale-up of this reaction proceeded very well (Table 4). The reaction appeared to perform best on a 2 g scale (Entry 1), where it reached 73% yield. However, the yield did not decrease dramatically up to a 10 g scale, where we were still able to reliably run this process at 67% isolated yield using only 0.9 mol% loading of Grubbs II.

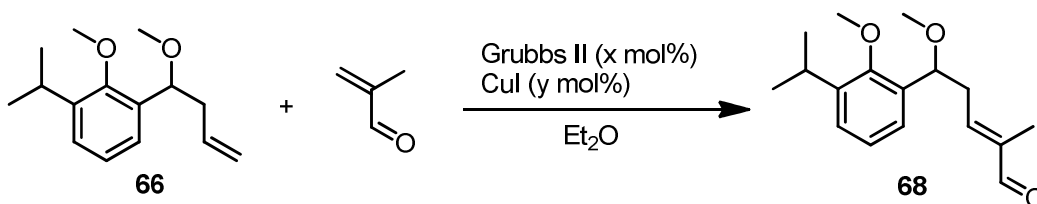


Figure 2.35. Optimization protocol for the cross-methathesis of **66** with methacrolein, catalyzed by the 2nd generation Grubbs catalyst.

Entry	Scale /g 66	Mol% G2/CuI	Catalyst addition	Total reaction time (h)	% Yield*
1	2.0	1.0/2.4	2 portions/1 h	2.5	73
2	3.5	1.0/2.3	4 portions/2 h	2.5	66
3	4.1	1.0/2.4	4 portions/2 h	2.5	61
4	5.0	1.0/2.0	4 portions/1 h	2.5	69
5	10.2	0.9/2.0	3 portions/2 h	4	67

Table 4. Optimization and scale-up of cross-metathesis of **66** with methacrolein. *Isolated yields. All reactions proceeded with <100% conversion. Remaining **66** not recovered.

During optimization of this reaction, we deduced that the benzylic ether moiety is able to coordinate to the ruthenium centre, forming 5-membered chelate **2.36-1** (Figure 2.36). We noticed, when running the reaction in degassed ether, the formation of a dark green colour in the reaction mixture. This colour was nearly identical to that of the 2nd generation Hoveyda-Grubbs catalyst **2.36-2**, which features a 5-membered chelate as well. We did not attempt to isolate and characterize this species, but it is clear from a visual comparison of the proposed chelate **2.36-1** to the Hoveyda catalyst **2.36-2** that they share a great deal of structural characteristics.

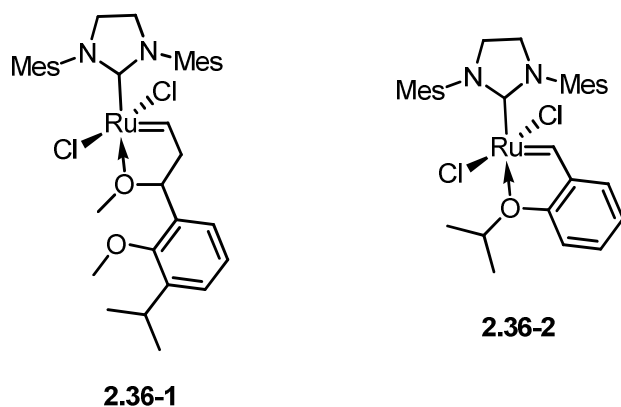


Figure 2.36. Proposed *in situ*-generated chelate **2.36-1** and 2nd generation Hoveyda-Grubbs catalyst **2.36-2**.

2.7.2 Wittig Olefination to access 1,3-diene

The Wittig olefination reaction is one of the best-known and most widely used synthetic organic transformations. As a result, when we investigated the literature for precedence of performing a methylene Wittig olefination for this synthesis (Figure 2.37), we were

inundated with procedures.⁷⁶ Many procedures utilized *n*-butyllithium (*n*-BuLi) as a base at low temperatures to form the active phosphorus ylide reagent, and as such we began our investigation with this base (Table 5). Initial results were disappointing: the desired 1,3-diene **69** was isolated in sub-40% yields. Switching to potassium *tert*-butoxide yielded similarly poor results. Finally, using KHMDS returned a good result. Using this base also allowed for an extremely operationally simple reaction: the base could be added as a solid to a slurry of aldehyde and MePPh₃I at room temperature and, within 20 minutes, the product could be cleanly isolated in nearly quantitative yield. Moreover, these conditions proved highly robust and reproducible on multi-gram scale, varying only $\pm 3\%$ in yield.

Entry	Base (eq.)	Temperature	Isolated Yield
1	<i>n</i> -BuLi*(1.05)	0°C	39.7%
2	<i>n</i> -BuLi* (1.25)	-10°C	37%
3	KOtBu* (3.15)	0°C	24%
4	KHMDS** (1.15)	25°C	93%

Table 5. Optimization of Wittig olefination of **68** to produce 1,3-diene **69**. **n*-BuLi and KOtBu were added as solutions in hexanes and THF, respectively. **KHMDS was added as a solid.

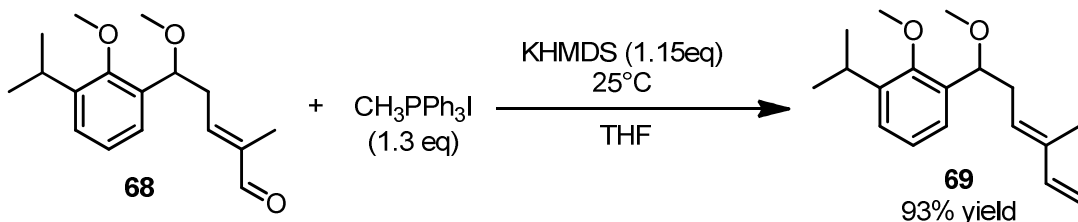


Figure 2.37. Optimized procedures for Wittig olefination of aldehyde **68** to access diene **69**.

2.7.3 Hydroboration-Oxidation of Diene

Hydroboration and oxidation of an alkene is another ubiquitous reaction in synthetic organic chemistry. Our intended application, however, is substantially less common: the selective hydroboration of a 1,3-diene to access a homoallylic alcohol requires particular conditions to achieve the desired results (Figure 2.38). Literature precedence for this transformation does exist, however, describing success in similar hydroboration/oxidation

processes using 9-BBN⁷⁷ or an *in situ* generated dicyclohexylborane (Cy₂BH)⁷⁸. We first attempted this transformation with a solution of commercially available 9-BBN - 0.5M in THF. The desired product was not identified in the crude reaction mixture. However, generating Cy₂BH *in situ* followed by introducing the substrate **69** proved highly effective, cleanly producing the desired homoallylic alcohol **70** after oxidative workup in 98% yield. We noticed that while the oxidative workup of hydroboration reactions is usually performed at low temperatures, our process required heat to go to completion – reflux at 55-60°C for two hours. Like the two previous steps, this process was also highly scalable, maintaining this near-quantitative yield on multi-gram scale.

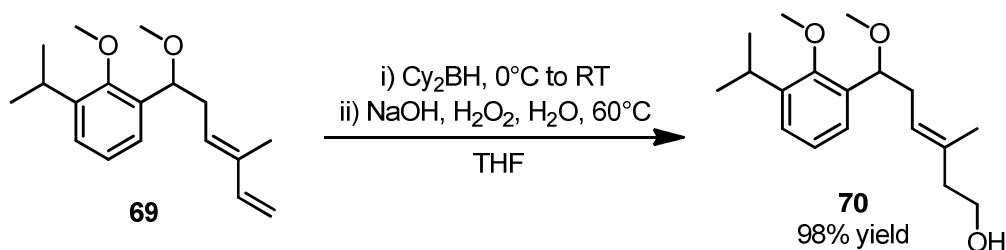


Figure 2.38. Hydroboration-oxidation of 1,3-diene **69** with *in situ* generated dicyclohexylborane and oxidative workup to access homoallylic alcohol **70**.

2.7.4 Accessing Allene target

With the alcohol **70** in our possession, accessing the allene target was only three synthetic steps away. The first two steps we directed towards accessing β -ketoester **72** via formation of a leaving group and displacement under basic conditions. We selected a methanesulfonate ester (mesylate) as the leaving group of choice: the formation of mesylates from primary alcohols is known to proceed in excellent yields and is often the leaving group of choice for alkylations of similar malonate substrates.⁷⁹ Formation of the mesylate was straightforward: complete consumption of the alcohol was achieved using MsCl and TEA in DCM at 0°C. We did not isolate **71**, but, following a brief aqueous workup, carried it on as crude material to the alkylation step (Figure 2.39).

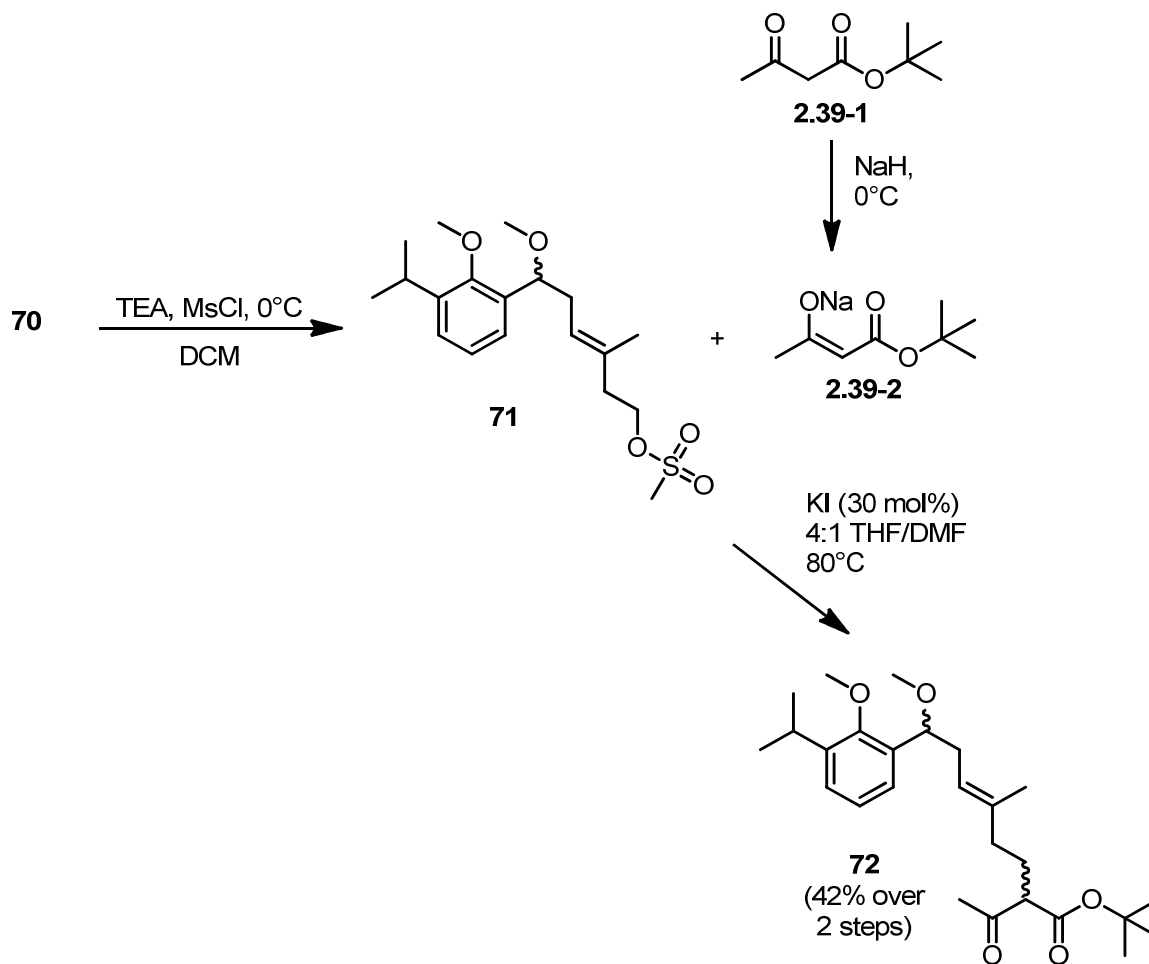


Figure 2.39. Mesylation and alkylation synthetic process. Mesylate **71** was worked up by aqueous extraction and drying under vacuum. Sodium enolate **2.39-2** was prepared and used as a solution in THF.

To perform the alkylation, we prepared a solution of the sodium enolate of *t*-butyl acetoacetate in THF, and then added the crude mesylate to this mixture. We also added a catalytic amount of potassium iodide to the reaction mixture before heating.⁷⁹ This induces an *in situ* Finkelstein reaction, displacing the mesylate with an iodide, which in turn is displaced by the enolate nucleophile. Addition of such halide salts are reported to improve the yield of this type of alkylation with mesylate or tosylate leaving groups.⁷⁹ Selective mono-alkylations of enolates are difficult reactions to optimize and often the crude reaction mixtures contain both mono- and di-substituted products. Any excess base in solution is able to re-form the enolate of a mono-substituted acetoacetate, enabling it to react with another equivalent of electrophile (Figure 2.40). As a result, many of these “malonate” or

“acetoacetate” type alkylations have low synthetic efficiency, often peaking at 50% yield. We were delighted, then, to isolate the desired product **72** in 42% yield on our first attempt. Further attempts demonstrated that this yield was reproducible on multi-gram scale, albeit with a slight reduction in yield. (38% yield over 2 steps) **72** also proved difficult to purify, as the chromatographic separation of this product from acetoacetate starting material **2.39-1** was very small. This was partially rectified by distilling off most of the remaining acetoacetate at high temperature under vacuum (bp = 71-72°C at 11mm Hg), but multiple chromatographic separations were often required to isolate pure **72**.

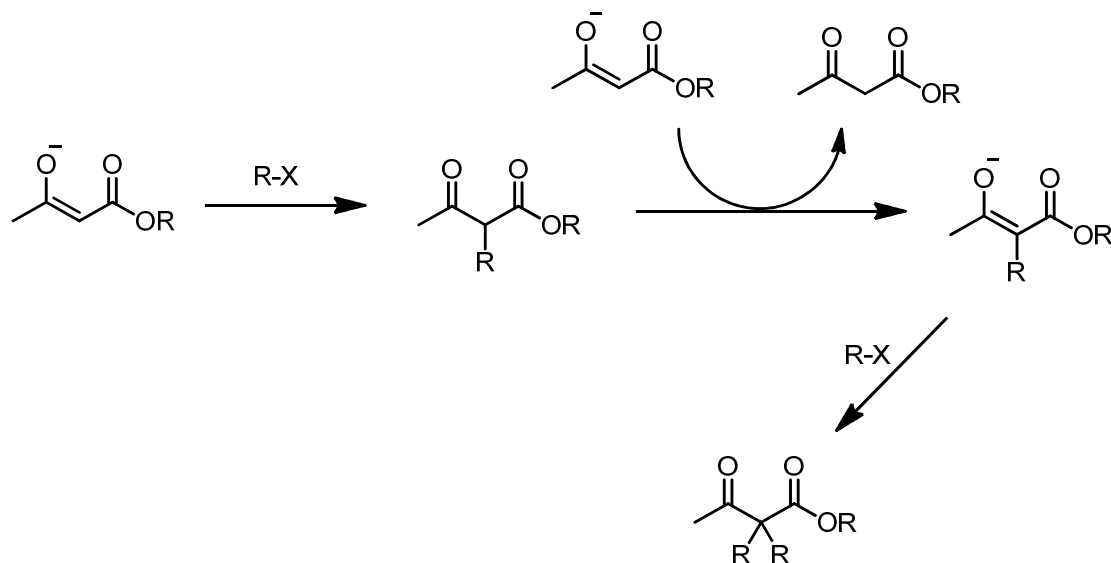


Figure 2.40. Selectivity difficulties in "malonate-type" alkylation reactions of β -ketoesters. After an initial alkylation, reformation of a mono-substituted enolate can result in formation of dialkylated product, reducing synthetic efficiency.

With experience of this difficult allene formation gained previously (Section 2.5.3), we approached the synthesis of this allene cautiously. Re-investigating the Maity and Lepore conditions,⁵⁰ we were surprisingly able to access the desired allene in 53% yield on our first attempt. This yield was, however, difficult to reproduce, with future attempts and scale-up only reaching 40-45% yield. Often, some of the β -ketoester starting material could be recovered, increasing the effective reaction yield by 10-20%. This transformation has a significant flaw that we encountered in late spring and early summer 2012. The reaction is extremely moisture sensitive to such extent that an increase in atmospheric humidity within the laboratory had a highly detrimental effect on the result. Yields of this reaction

plummeted to 0-5%, combined with severe degradation of the starting material such that none could be recovered from the reaction mixture. However, during dry seasons this reaction was reproducible in the range of 40-45% yield on gram scale.

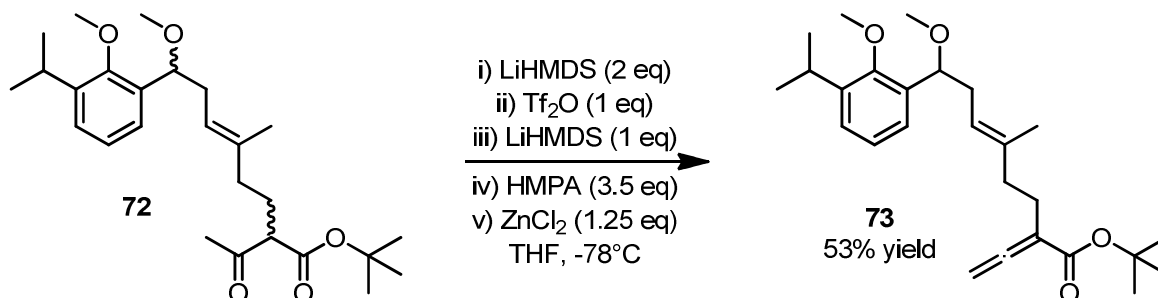


Figure 2.41. Successful one-pot allene formation following the Maity and Lepore method.

2.8 Investigations into the Oxidative Gold Cyclization

With the new, stable protecting group in place, we returned to the Gouverneur gold cyclization conditions to attempt our cyclization reaction. We were dismayed to find that, upon exposure to the conditions as per Figure 2.42, the starting material degraded in a similar fashion as with the acetonide protecting group. This time, we knew that the protecting group was stable to the reaction conditions, so this result prompted us to scrutinize the proposed mechanism (Section 2.1.1, Figure 2.1) to identify potential causes of this failed reaction and, in turn, sites for further investigation.

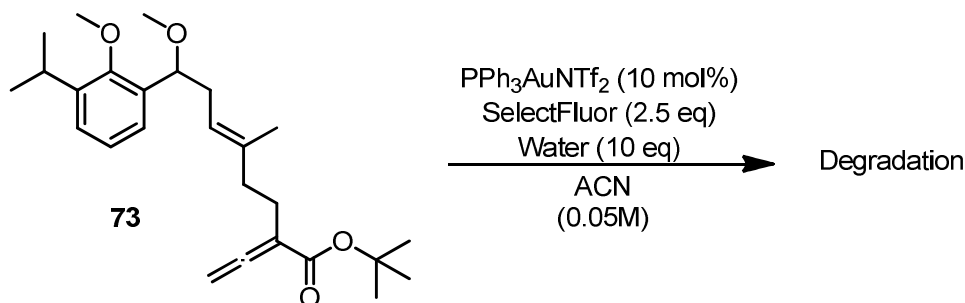
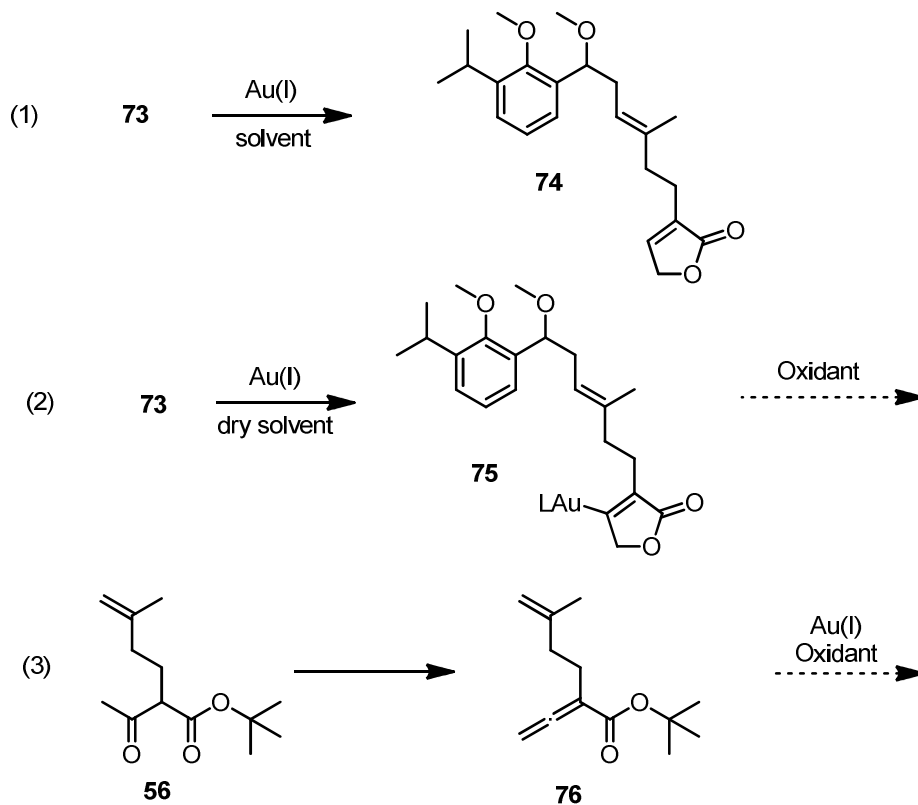


Figure 2.42. Failure of Gouverneur conditions to cyclize dimethyl-protected allenoate **73**.

We identified three stages in the proposed key step where problems could arise (Scheme 2.5). First, the lactonization of the allenolate starting material to access **74** is the first entry point for the catalytic cycle and is known to proceed at varying rates in different solvents, as well as with electron-rich and electron-poor Au(I) species. Investigation and optimization of both these parameters was required (Equation 1). Second, the Gouverneur mechanism describes the oxidation of the vinyl gold(I) species **75** occurring before protodeauration. This conflicts with the literature, where it has been documented that the protodeauration of Au(I) cyclizations of allenolates proceeds rapidly.⁸⁰ To study vinyl gold species **75** and the oxidation process, we desired a method to synthesize **75** and exposed it to a variety of oxidants (Equation 2). Finally, once oxidation of the vinyl gold species occurred, we proposed either a coordination of the internal alkene to the gold, triggering a nucleophilic attack from the aromatic ring, or a direct attack of the alkene onto gold, forming a carbocation. We proposed studying a model substrate **76** to study and compare these two proposed mechanistic pathways (Equation 3).



Scheme 2.5. Stages of proposed gold cyclization cascade to be investigated and optimized. (1): Gold-catalyzed butenolide cyclization of **73** to access **74**. (2): Isolation and oxidation of the vinyl gold species **75**. (3): Synthesis and studies of model substrate **76**.

2.8.1 Gold(I) Catalyzed Butenolide Cyclization

For our study of the gold(I)-catalyzed lactonization process, we primarily wished to investigate the effect of varying the reaction solvent. Gouverneur and co-workers reported their gold cyclization reaction in acetonitrile and water – a solvent mixture in which SelectFluor is highly soluble. Typically, this type of cyclization is performed in dichloromethane, in which SelectFluor is insoluble. While studying solvent effects we also screened several different gold species to examine any electronic effects on this reaction. The results are summarized in Table 6. We found that this reaction proceeded remarkably well in the presence of ligandless gold(I) chloride and gold(III) chloride using DCM solvent. In fact, adding any ligand appeared to retard the reaction substantially, as treating **73** with the Gagosz catalyst in DCM (Entry 3) afforded the product in only 58% yield. Entry 4 is of particular interest: exposing **73** to the Gagosz catalyst in acetonitrile and water – the Gouverneur conditions minus any oxidant – yielded no reaction and complete recovery of the starting material. We also found that using a more activated catalyst such as JohnPhosAuSbF₆ (Entry 5) or a highly electron poor phosphite catalyst (tBu₂PhO)₃AuNTf₂ (Entry 6) afforded, respectively, low yields or complete degradation of the starting material (Figure 2.43).

Entry	Gold species (mol%)	Solvent	% Yield
1	AuCl (10)	DCM	90 ^a
2	AuCl ₃ (10)	DCM	72 ^a
3	PPh ₃ AuNTf ₂ (10)	DCM	58 ^b
4	PPh ₃ AuNTf ₂ (10)	ACN/H ₂ O	0
5	JohnPhosAuSbF ₆ (5)	DCM	<30
6	(tBu ₂ PhO) ₃ AuNTf ₂ (5)	DCM	- ^c

Table 6. Solvent and catalyst screening for gold-catalyzed butenolide formation from allenolate **73**. ^aNMR Yield, ^bIsolated yield, ^cDegradation of starting material observed.

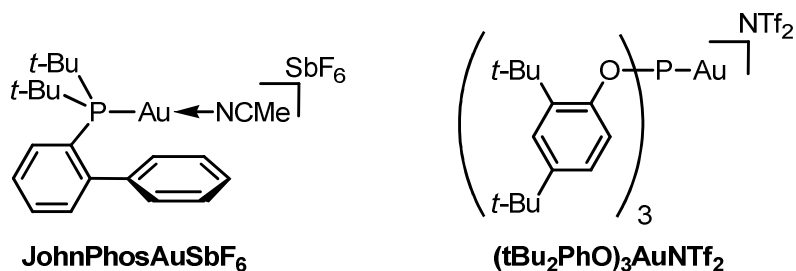


Figure 2.43. Cationic gold(I) catalysts utilized during screening of conditions for butenolide construction.

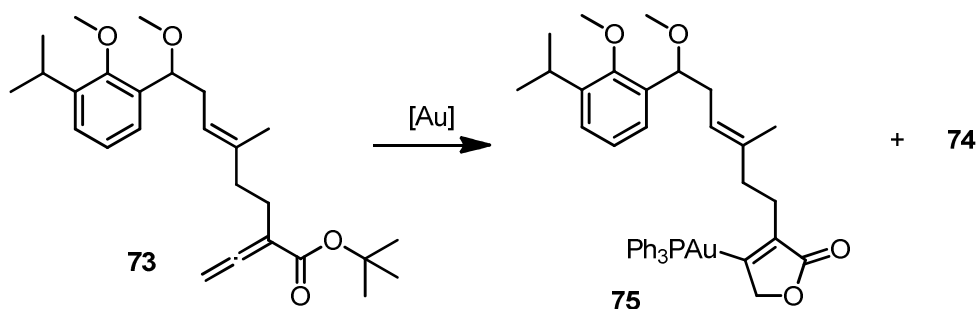
The data described in Table 6, particularly entry 4, cast doubt on the validity of the mechanism proposed by the Gouverneur group. If the gold(I) species catalyzes the butenolide formation and is oxidized afterwards to gold(III), the cyclization must be sufficiently rapid as to outcompete premature gold oxidation by SelectFluor. We have demonstrated that this cyclization is extremely slow in the solvent system required. Interestingly, the Gouverneur group observed a similar result: in the supporting information for their 2010 publication, they note that the butenolide cyclization catalyzed by PPh₃AuNTf₂ in ACN/H₂O is extremely slow, affording only 46% of the desired product after six days at room temperature, compared to 91% achieved over 16 hours if the reaction was run in DCM.⁴⁸ The exact nature of this mechanism is questionable, as both gold(I) and gold(III) species could be involved in this first stage of the cyclization.

2.8.2 Isolation of the Vinyl Gold Intermediate and Oxidant Screening

While the mechanism for butenolide construction is somewhat ambiguous in terms of which oxidation state is catalyzing the reaction, there is little doubt that the proposed cascade process to form the tetracycle requires the formation of a gold(III) species. We set out to synthesize and isolate the vinyl gold species **75** in order to study the gold(I-III) oxidation process.

Isolation of the Vinyl Gold Complex

Typical procedures for the synthesis of stable vinyl gold complexes of the type required involve exposing the allenolate precursors to a stoichiometric amount of a ligand-bound gold(I) species under anhydrous conditions.⁸¹ These conditions are designed to minimize or eliminate the presence of water – the chief agent responsible for protodeauration – leading to the butenolide product **74** (Scheme 2.6). Our initial efforts towards the vinyl gold species were disappointing (Table 7, Entries 1-3): submitting allenolate **73** to known conditions resulted in a mixture of products containing predominately the protodeaured product.



Scheme 2.6. Possible products of attempted vinyl gold synthesis: desired organogold product **75** and protodeaured species **74**.

Upon further investigation of the literature, we discovered that the isolation of a vinyl gold-butenolide species accessed from a terminal allene (i.e. featuring a CH₂ group at the 3-position adjacent to the carbon bearing the gold) had never been reported. We suspected that this lack of any steric presence at this position increased the rate of protodeauration of the *in situ* generated vinyl gold complex, making it more difficult to isolate. The presence of a *tert*-butyl ester in **73** also presented some difficulties. The Hammond group at the University of Louisville, Kentucky reported that these types of allenolates tended to afford lower yields of vinyl gold product than ethyl or benzyl analogues.⁸² Considering the character of the *tert*-butyl group, this result is not surprising. Upon lactonization, the *tert*-butyl group will rapidly dissociate from the parent molecule as a *tert*-butyl cation, which is able to lose a proton to form isobutylene. This proton is able to induce protodeauration, causing erosion of the yield of the desired vinyl gold species. We were thrilled, then, to find that introducing an excess of a hindered pyridine base as an acid scavenger afforded clean **75** in 52% yield with no trace

of the protodeaurated compound.⁸³ Further optimization of these conditions allowed us to increase the isolated yield to 77.3% simply by extending the reaction time (Figure 2.44, Table 7 Entries 4-6). Chromatography of the product was very simple and we isolated pure **75** as a white semi-crystalline solid. We made numerous attempts to obtain a fully crystalline form of **75** in order to record an X-ray crystal structure, but were unsuccessful. Nevertheless, we are happy to report the first successful synthesis of a room-temperature stable γ -butenolide-organogold product from a terminal allenolate precursor.

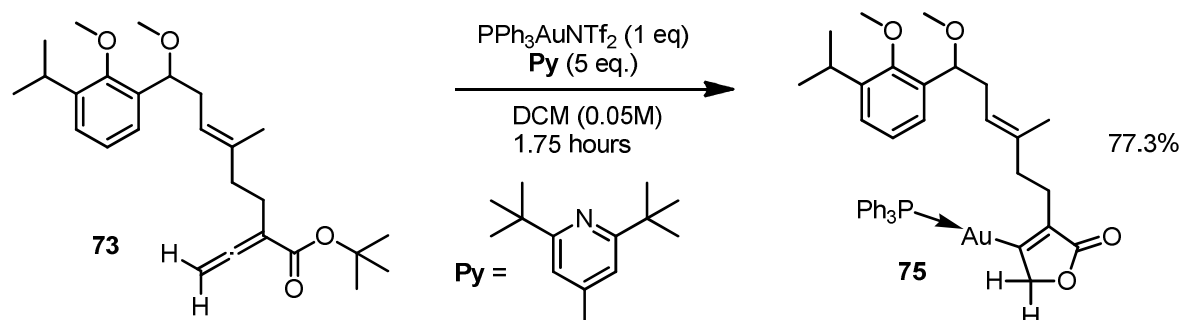


Figure 2.44. Optimized conditions for synthesis and isolation of vinyl gold complex **75** using 2,6-di-*tert*-butyl-4-methylpyridine as an acid scavenger.

Entry	Gold(I) Species	Additive	Reaction Time	Major Product	Isolated Yield #
1	$\text{PPh}_3\text{AuOTf}^*$	-	5 mins	74	-
2	$\text{PPh}_3\text{AuNTf}_2$	-	5 mins	74	-
3	JohnPhosAuSbF_6	-	60 mins	74	-
4	$\text{PPh}_3\text{AuOTf}^*$	Py	5 mins	75	52
5	$\text{PPh}_3\text{AuNTf}_2$	Py	5 mins	75	52
6	$\text{PPh}_3\text{AuNTf}_2$	Py	105 mins	75	77

Table 7. Optimization of the synthesis and isolation of vinyl gold species **75**. Py = 2,6-di-*t*-butyl-4-methylpyridine. *Generated *in situ* from PPh_3AuCl and AgOTf .

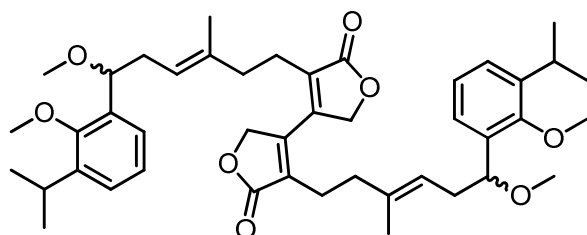
Oxidation Study

Once we had established a reproducible process for accessing **75**, we began our investigation of the gold(I-III) oxidation process. The oxidants we selected to screen were

also studied in the Gouverneur paper,⁴⁸ so we were able to directly compare any results we obtained. We also investigated other solvents or solvent mixtures such as DCM and THF/water. We employed the addition of sodium carbonate (Na_2CO_3) as an additive to reactions using SelectFluor to sequester any HF potentially released during the reaction.⁸⁴ Finally, we attempted to employ an anionic phase transfer reagent to help solubilize SelectFluor in DCM.⁸⁵ The results are summarized in Table 8.

Entry	Oxidant ^a	Solvent	Additive	Temperature	Results
1	$\text{PhI}(\text{OAc})_2$	DCM	-	RT	SM + Dimer 2.45-1
2		ACN/ H_2O	-	RT	2.45-1
3	tBuOOH	DCM	-	RT	NR
4	Ph_2SO	DCM	-	RT	NR
5		ACN/ H_2O	-	RT	NR
6	NFSI ^b	DCM	-	RT	NR
7		ACN/ H_2O	-	RT	Degradation
8	Oxone	ACN/ H_2O	-	RT	Degradation
9	SelectFluor	ACN/ H_2O	-	RT	Degradation
10		ACN/ H_2O	Na_2CO_3	RT	Degradation
11		THF/ H_2O	-	RT	Slow degradation
12		THF/ H_2O	Na_2CO_3	RT to 40°C	NR
13		THF/ H_2O	Na_2CO_3	60°C	Slow degradation
14		DCM	KBARF ^c	RT	Degradation

Table 8. Oxidant screening for gold(I-III) oxidation of vinyl gold species **75**. ^a2-3 equivalents of each oxidant used respective to vinyl gold. ^bNFSI = N-fluorobenzenesulfonamide. ^cKBARF = Potassium tetrakis[3,5-bis(trifluoromethyl)phenyl]borate.



2.45-1

Figure 2.45. Dimeric butenolide **2.45-1** resulting from treatment of **75** with $\text{PhI}(\text{OAc})_2$.

From the oxidation data collected, one important datum stood out: we did not observe any protodeauration occurring in any of the trials. This was quite unexpected, as we anticipated observing some traces of butenolide **74** in the crude NMR of some trials. The remainder of the data unfortunately provided little insight into the mechanism of this reaction. Using a hypervalent iodine species resulted in dimerization of the butenolides, a result also observed by Gouverneur. No reaction was observed using diphenyl sulfoxide (Ph_2SO) or NFSI, which also agrees with the results from Gouverneur. Using SelectFluor alone, again only degradation of the starting material was observed, regardless of solvent choice. However, the rate of degradation was retarded using a THF/water solvent system. The addition of sodium carbonate had no effect on the reaction in acetonitrile, but in THF, we observed complete suppression of the degradation: only starting material was recovered after stirring at room temperature for 16 hours. Heating the reaction mixture to 60°C did induce degradation, but the mixture was stable to 40°C . We were able to reproduce this suppression of degradation when the allenolate starting material was subjected to gold(I) and SelectFluor in THF and Na_2CO_3 (Figure 2.46). The origin of this stability afforded by adding Na_2CO_3 is unclear.

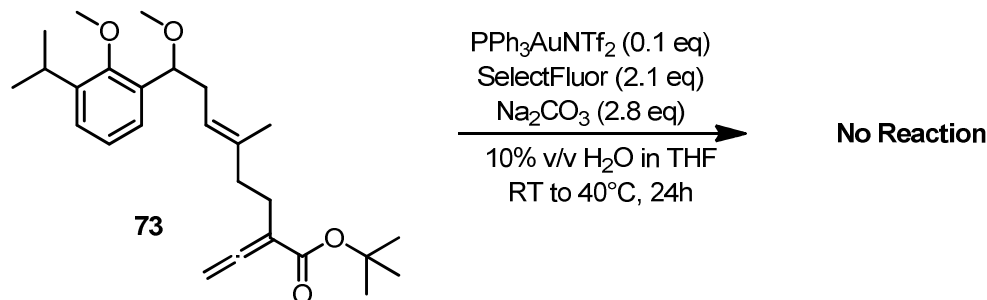


Figure 2.46. Suppression of degradation by Na_2CO_3 upon exposure of allenolate **73** to Gagosz catalyst and SelectFluor in THF/water solvent system.

Conclusions of Oxidation Study

The results of the oxidant screening were disappointing. No meaningful data were collected to begin drawing conclusions on the mechanism of this reaction, nor were any of the degradation products successfully identified to elucidate any possible side reactions. However, some inferences can be made regarding the chemistry at work here: Exposure of

the vinyl gold species to oxidants such as SelectFluor and $\text{PhI}(\text{OAc})_2$ causes further reactivity, which suggests that the gold(I) is, in fact, being oxidized to gold(III) by these reagents. As a result, we concluded that the most likely downfall of the proposed cyclization cascade is in the cascade itself. Earlier, we proposed two potential mechanisms for this cascade process to form the tetracycle (Figure 2.1), one via activation of the alkene by coordination to gold and the other via direct nucleophilic attack onto the organogold(III) species. We concluded that the key to understanding this reaction must lie in this final aspect.

2.8.3 Model Substrate Studies

To study the final stage of the proposed cyclization mechanism, we elected to synthesize a model substrate lacking the aromatic moiety. This would potentially allow us to differentiate between our two proposed mechanisms and help understand why we had been unable to isolate any products – desired or otherwise – from our previous attempts.

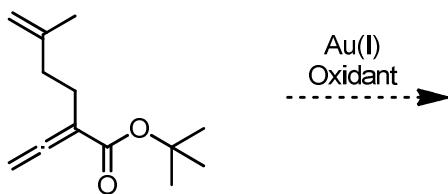
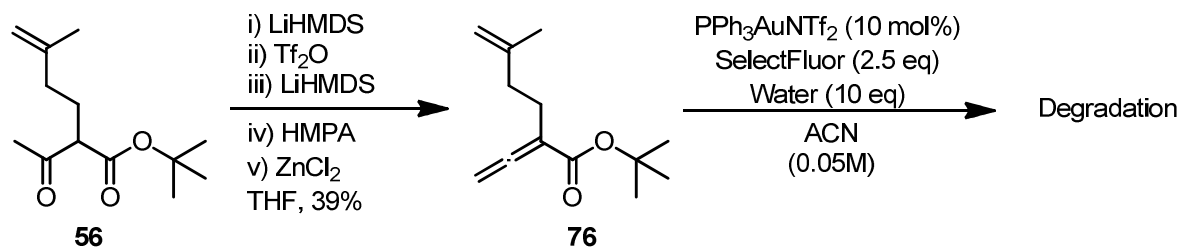


Figure 2.47. Model substrate for studying the oxidative gold cyclization reaction and the potential for alkene coordination or nucleophilic attack.

Fortunately, the synthesis of this allenolate **76** was trivial, as the β -ketoester precursor **56** had been previously synthesized in large quantities for use in the global cross metathesis method (Section 2.5.1). Allene formation was conducted as before and we isolated **76** in 39% yield (Scheme 2.7). If our proposed cyclization cascade was, in fact, viable, we anticipated that we should be able to isolate some product from exposing this model substrate to the Gouverneur conditions. We performed this experiment and, after normal workup, we examined the crude ^1H NMR and observed no discernible products whatsoever. From this result, we were forced to accept the disappointing conclusion that our proposed

oxidative gold(I-III) catalyzed cascade cyclization reaction was, to the best of our knowledge, not possible.



Scheme 2.7. Synthesis of model substrate for gold cyclization (**76**) via β -ketoester **56** and attempted gold-catalyzed oxidative cyclization under the Gouverneur conditions.

2.9 Unexpected Radical Cyclization

After disappointing results from the proposed oxidative gold cyclization method, we began to consider alternative methods of forming the tetracyclic core of triptolide. Since we still possessed a reasonable supply of the vinyl gold species **75**, we decided to investigate the possibility of performing a radical cyclization to form the tetracyclic core. We envisioned transforming the vinyl gold species into a halogen, which would be an appropriate functional group handle for generation of a vinyl radical which, in theory, could be used to form the desired tetracycle **79** (Scheme 2.8). This transformation has been reported previously in modest yield using elemental iodine.⁸² We wanted to avoid any potential side reactions with the internal alkene, so we initially investigated using *N*-iodosuccinimide as the electrophile. We were able to achieve this transformation in excellent yield using one equivalent of NIS in acetone (Figure 2.48). Unknown to us at the time, these reaction conditions had never been reported for the synthesis of vinyl halides from vinyl gold species. We then began to investigate potential conditions for carrying out this proposed radical redox cyclization cascade.

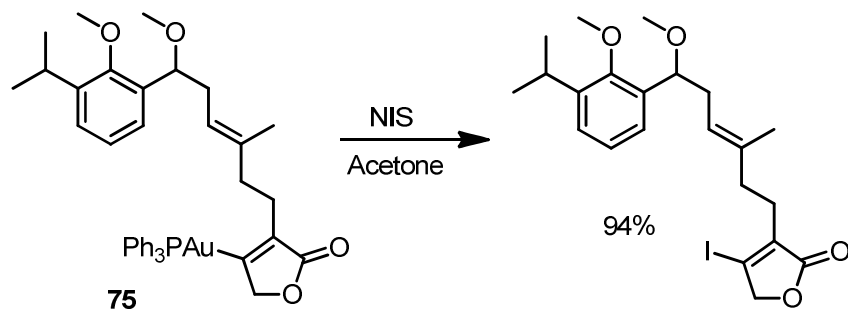
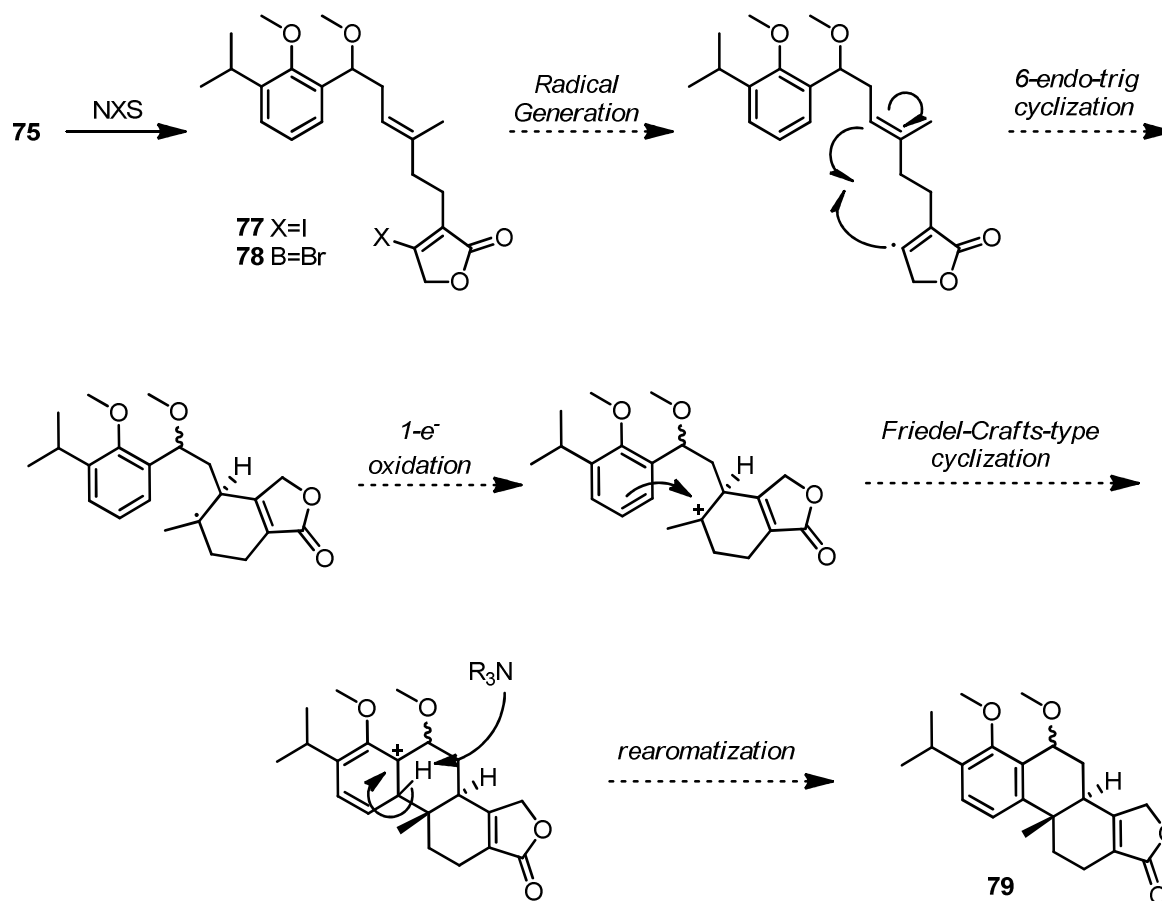


Figure 2.48. Transformation of vinyl gold complex **75** to iodobutenolide **77** using NIS.



Scheme 2.8. Proposed radical cyclization cascade triggered by vinyl radical formation from a halobutenolide precursor **77** or **78**.

Radical cyclizations with alkenes are ubiquitous synthetic organic transformations,⁸⁶ and a number of methods exist for generation of such radicals from vinyl halides. A popular, classical method involves the use of an organotin species such as tributyltin hydride and an initiator such as azobisisobutyronitrile (AIBN)⁸⁷. This method, however, suffers from the

generation of a stoichiometric amount of toxic tin waste and is rapidly losing favour in the synthetic organic chemistry community. Samarium(II) iodide is also commonly applied to generate these types of radicals, but is expensive and often required in superstoichiometric amounts, thus it suffers from poor atom economy and similar generation of metal waste.⁸⁸ A new and promising field in radical chemistry is the generation of radicals through the use of photoredox catalysts, which generate radicals in the presence of light and, typically, an amine base. Two prime examples of such catalysts are tris(bipyridine)-ruthenium(II)chloride (**Ru-bipy**) and *fac*-tris[2-phenylpyridinato-C,*N*]iridium(III) (**Ir-ppy**) (Figure 2.49). These photoredox catalysts have demonstrated great potential for catalyzing a vast scope of organic transformation, including halide reductions,⁸⁹ cycloadditions,⁹⁰ intermolecular cross-coupling reactions,⁹¹ functional group interconversions⁹² and intramolecular radical cyclizations.⁹³ An example of a catalytic cycle and mechanism for a photoredox radical cyclization is shown in Figure 2.50. These photosensitive metal complexes have demonstrated remarkable efficacy in catalyzing radical reactions under mild conditions and with high yield and selectivity. The current mindset of designing “green” chemistry processes has also cast a positive light on this family of reactions.⁹⁴

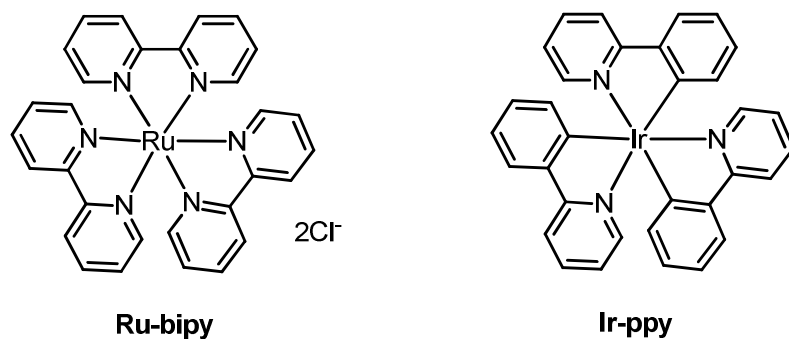


Figure 2.49. Tris(bipyridine)ruthenium(II)chloride (**Ru-bipy**) and *fac*-tris[2-phenylpyridinato-C-*N*]iridium(III) (**Ir-ppy**) photoredox catalysts.

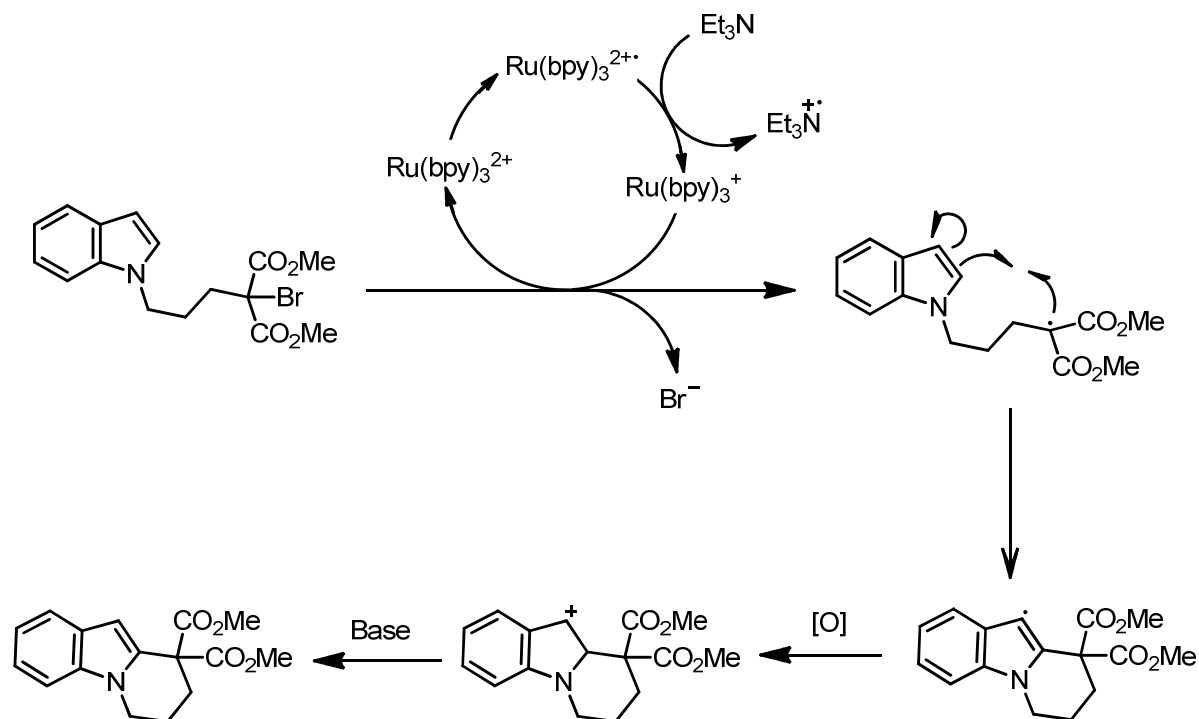


Figure 2.50. Representative catalytic cycle of a photoredox radical cyclization of an indole. [O] represents a one-electron oxidation process.⁹⁴ Ru(bpy)₃ = tris(bipyridine)Ruthenium(II)

2.9.1 Proposed Photochemical Cyclization

The timing of this investigation proved extremely convenient, as our postdoctoral fellow at the time, Dr. Guillaume Révol, along with Terry McCallum, an undergraduate summer student, had recently undertaken a new project studying light-promoted radical cyclization and coupling reactions with a novel gold-centered photoredox catalyst.⁹⁵ Their work had demonstrated some positive initial results, so we decided to try out their conditions with iodobutenolide **77**. Experiments thus far⁹⁶ had demonstrated that the catalyst is activated by ultraviolet light, and preliminary trials had performed best when exposed to direct sunlight using degassed acetonitrile as the reaction solvent and DIPEA as the base (Figure 2.51). We elected to try this method, hopeful that we could still accomplish this formal synthesis using a gold-catalyzed cyclization cascade. The reaction was performed in a sealed Pyrex tube as per Figure 2.52. Prior to light exposure, the reaction mixture was clear and colourless, but quickly turned yellow once exposed to sunlight.

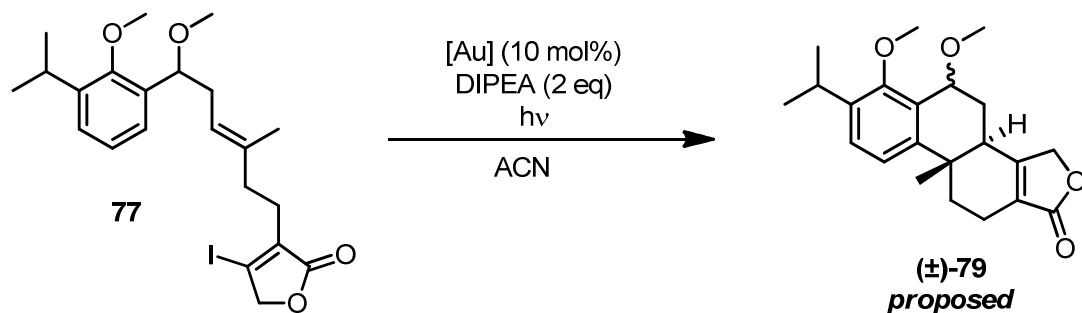


Figure 2.51. Proposed photoredox cyclization from iodobutenolide **77** to proposed tetracycle **79** using a gold species $[Au]$ upon exposure to UV light.



Figure 2.52. Setup of photochemical cyclization reaction. The left image is immediately after initial exposure to sunlight. The right image is after 2.5 hours of exposure to sunlight.

Workup of this reaction was simple; concentration of the reaction mixture and dilution with diethyl ether precipitated out any catalyst, which could be removed – and theoretically recovered – by filtration. To our surprise, the crude NMR of the reaction mixture appeared relatively clean and exhibited only two aromatic C-H signals. We anticipated this resonance pattern for a successful cyclization (Figure 2.53), as the diol relative **12** is known²⁷ and features two aromatic protons, resonating at 6.85 ppm and 7.14 ppm.

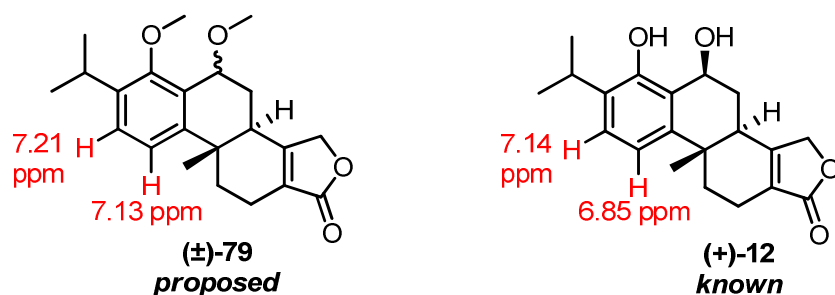


Figure 2.53. Aromatic 1H NMR signals of proposed tetracycle **79** and known tetracyclic diol **12**.

In addition, the crude reaction mixture appeared to contain two diastereomers, which we also expected in the desired product, as we had not specifically defined the configuration at the benzylic position. The majority of the ^1H NMR spectrum was difficult to process and has not yet been fully deduced. We were, however, able to extract some evidence from the spectra that support our proposed product: diol **12** features a characteristic splitting pattern for the proton H_X (2.78 ppm) indicated in Figure 2.55. We observed a similar splitting pattern in our NMR spectra, where a proton resonating at 2.8 ppm splits into a doublet with a J value of 13.2 Hz. The protons on the adjacent carbon sit at approximately 90° and 180° dihedral angle to H_X which, according to the Karplus equation (Figure 2.54), causes the observed 13 Hz splitting of the proton at 180° dihedral angle, residing in a pseudo 1,2-diaxial relationship. The proton at 90° dihedral angle does not split with H_X according to this equation. HRMS analysis of the product after chromatography – a white, waxy solid – clearly demonstrated the molecular ion of the desired product, which provides good evidence of a successful radical cyclization. More spectral data is required to confirm the correct structure, which is ongoing in the Barriault group.

$$J(\phi) = A \cos^2 \phi + B \cos^2 \phi + C$$

Figure 2.54. Karplus Equation for estimation of $^3J_{\text{H-H}}$ coupling constants in NMR spectrometry, where ϕ is the dihedral angle between the two atoms in question; A, B and C are empirically defined parameters depending on the atoms in question

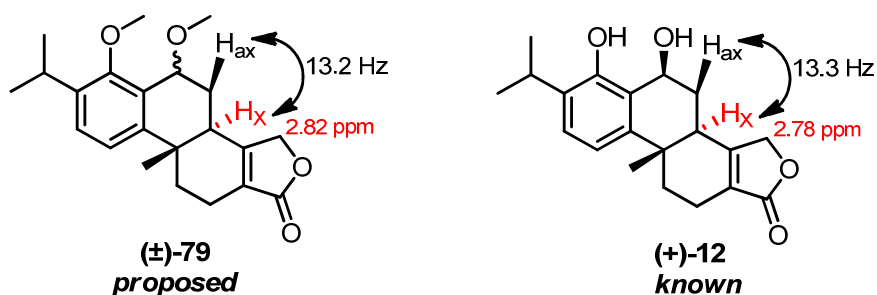


Figure 2.55. 1,2-diaxial coupling between H_X and H_ax in our proposed tetracycle and known structural relative.

2.9.2 Possible Mechanisms

This mechanism of this photoredox cyclization is simple to elucidate, as the mechanisms of similar photoredox catalysts like **Ru-bipy** and **Ir-ppy** have been studied in detail.⁸⁹⁻⁹⁴ The metal catalyst – in an excited state after absorbing a photon of light – donates an electron into the carbon-halogen bond, forming a vinyl radical and oxidizing the catalyst. The catalyst is regenerated via reduction mediated by the amine base. Once formed, the vinyl radical reacts in an intramolecular cyclization with the internal alkene as per Scheme 2.8, generating a tertiary radical via a 6-*endo*-trig process. A 5-*exo*-trig pathway is inherently possible as well (Figure 2.56). In many cases of gold catalysis, this route occurs preferentially over the 6-*endo* due to enhanced kinetics of the 5-*exo* reaction.⁸⁶ We believe that, for this cyclization, the 6-*endo* route dominates due to the possible chair-like transition state which is available exclusively through this pathway. A number of radical-mediated cascade cyclizations have been reported⁹⁷ with exclusive 6-*endo* selectivity, citing this transition state as the key factor in this high selectivity, including the Yang synthesis²⁷ of triptolide. We therefore conclude that this cyclization cascade is, in all likelihood, highly selective for the 6-*endo* pathway. At this time, however, we cannot unequivocally confirm the absence of the 5-*exo* pathway as we have not yet fully characterized the isolated product.

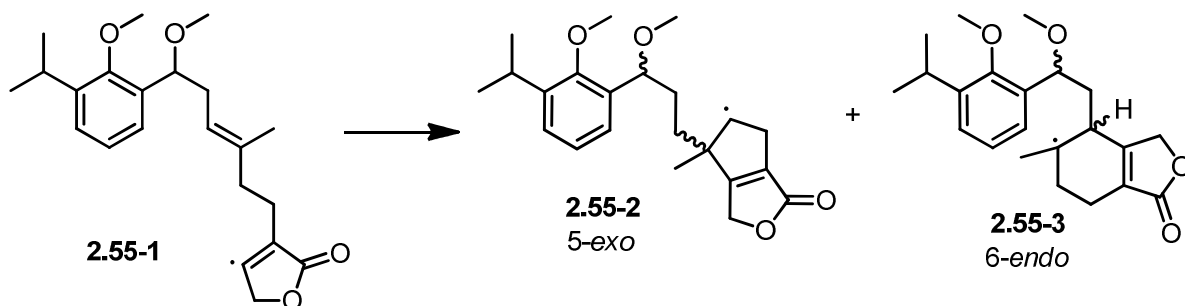


Figure 2.56. Potential 5-*exo*- and 6-*endo*-trig cyclization pathways for the vinyl radical **2.55-1**, giving rise to radical intermediates **2.55-2** and **2.55-3**.

After this first cyclization, two potential mechanistic pathways are possible to form the final ring. A continuation of the radical mechanism is one possibility, where an analogous cyclization occurs with the aromatic ring – again in a 6-*endo* fashion – producing the desired tetracycle after rearomatization. A more likely mechanism, however, is that the tertiary alkyl radical is quenched by a 1-electron oxidation, forming a tertiary carbocation. This cation is a

prime electrophile for a Friedel-Crafts-type arylation, again forming the desired tetracycle. This mechanism is documented for other photoredox catalysts, due to the redox potential of the photocatalyst.⁹³ Fortunately, both mechanisms yield the same final product, so differentiating between them is unnecessary. If a carbocation does form, however, we propose that it must be extremely short-lived, as we did not observe any formation of product **80**, which would result from trapping of the cation by a molecule of acetonitrile which, as the solvent, is present in large excess in the reaction mixture (Figure 2.57). This process is known as the Ritter reaction.⁵⁹ Since the radical cyclization was not performed under strict anhydrous conditions, water was likely present in the reaction mixture – a requirement for the Ritter reaction.

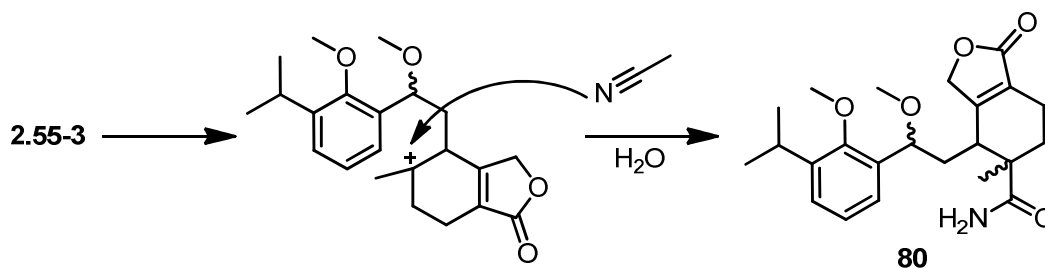


Figure 2.57. Intermolecular carbocation trapping by acetonitrile and water to form amide **80** via the Ritter reaction.

2.9.3 Control Studies: Current and Future Work

In order to establish the efficacy of our bimetallic gold catalyst in this cyclization cascade, we have designed a series of experiments that must be performed in the future. Alkyl, alkenyl, alkynyl, and aryl iodides are generally known to be light sensitive, and the direct photolysis of vinyl iodides with UV light to form vinyl radicals has been reported on a number of occasions.⁹⁸ As such, a control study must be performed using a catalyst-free sample as a baseline to ascertain the rate enhancement – if any – of our catalyst.

In addition, the effect of different halogen precursors must be studied. We were able to perform the cyclization on the vinyl bromide **78**, which was accessed from vinyl gold species **75** using *N*-bromosuccinimide in acetone in an analogous procedure to the formation of **77**. The yield of **78** was lower than that of the vinyl iodide and some protodeauration was

observed. This was primarily due to the quality of the NBS – it was not recrystallized prior to use, and likely contained some residual HBr.

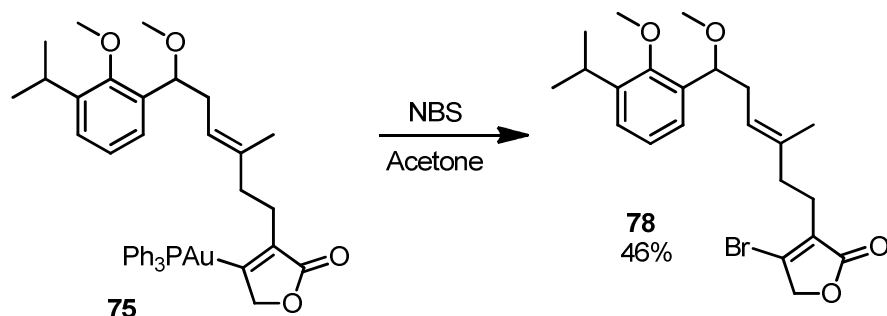


Figure 2.58. Synthesis of bromobutenolide **78** from vinyl gold species **75** using NBS.

Interestingly, after exposing **78** to the radical cyclization conditions alongside the iodide, we found that **78** afforded a smoother reaction in equal time: both the TLC and ^1H NMR of the crude reaction mixture appeared cleaner. This suggests that iodobutenolide **77** suffers from some degradation in the presence of UV light. Vinyl bromides are known to have higher stability to light, and this promising result offers support that our catalyst does afford a significant rate enhancement over baseline degradation. It is not a complete control study, however. To study the activity of the catalyst further, we wish to synthesize the chlorobutenolide **81** as well. Currently, the bromobutenolide **78** should work as a suitable and stable model for further study.

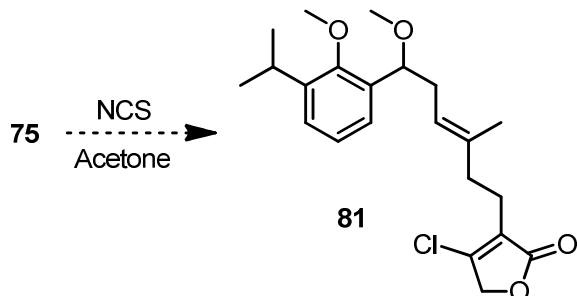


Figure 2.59. Proposed synthesis of chlorobutenolide **81** for further study of catalyst activity.

The number of photoredox catalysts in the literature today presents a particular challenge for our new catalyst: how does its reactivity compare to the well-established ruthenium and iridium catalysts? We plan to study this by running parallel trials, exposing **78** to **Ru-bipy** and **Ir-ppy** photoredox conditions in addition to our gold catalyst and directly compare the results of each trial.

Current/Future	Substrate	Catalyst	Result
Current	77	[Au]	Cyclization, some degradation
Current	78	[Au]	Clean cyclization
Future	77	None	Pending
Future	81	[Au]	Pending
Future	78	Ru-bipy	Pending
Future	78	Ir-ppy*	Pending
Future	78	Other photocatalysts	Pending

Table 9. Summary of current and future work to study the photoredox radical cyclization and study the reactivity of [Au] compared to other photoredox catalysts. *Other Ir-centered photocatalysts have been reported. These will be investigated in due course.

2.10 Synthetic Route Revisions

While we believe we have found strong evidence for the successful synthesis of the tetracyclic core of triptolide, the current synthetic method suffers in a number of key aspects. The formation of the halobutenolide substrate for the radical cyclization currently requires a stoichiometric amount of gold, as we access the vinyl gold complex **75** as an intermediate. This is expensive and highly impractical, so we sought a way to circumvent this problem. Also, the current route is linear and features two late-stage low-yielding steps – the β -ketoester alkylation and allene formation. Finding alternative methods for one or both of these steps would be highly advantageous to improve the elegance and overall yield of the synthesis.

2.10.1 Direct Synthesis of halobutenolide

The direct formation of halobutenolides from 2,3-allenoates or allenic acids has been previously reported via a number of protocols. The first method we attempted for this transformation is direct exposure of allenoates **73** and **76** to a stoichiometric amount of halogen source such as Br₂, I₂, NBS or NIS (Figure 2.60). Literature precedent for this

transformation exists on substrates without other competing nucleophiles, such as alkenes. Unfortunately, our substrate does contain an alkene, which posed a potential cross-reactivity problem. Our suspicions were confirmed, as exposing substrates **73** or **76** to I₂, NBS or NIS in a variety of solvents produced a number of products, none of which were the desired halobutenolides (Table 10). We propose that the allene is too electron poor to act as the primary coordination site for the halogen, and as such the richer alkene reacts preferentially over the allene. We did not observe this cross-reactivity with the vinyl gold species **75** due to the nucleophilic carbanion character of the carbon bearing the gold.

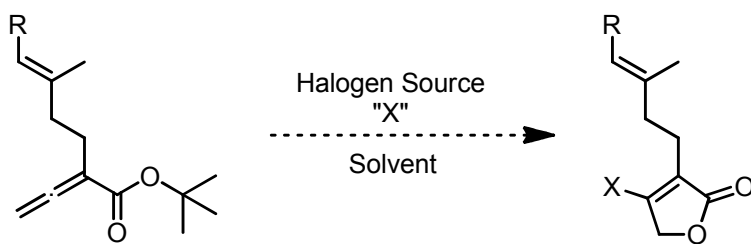


Figure 2.60. Attempts to access halobutenolides from allenolates **73** and **76** using electrophilic halide sources "X".

Entry	Substrate	X	Solvent
1	73	I ₂	ACN
2			DCM
3	76	NBS	H ₂ O
4			ACN
5		I ₂	ACN/H ₂ O
6		NIS	Acetone
7			ACN

Table 10. Failed attempts at halobutenolide formation using electrophilic halogenation and lactonization in the absence of gold.

We also investigated the gold-catalyzed cyclization of allenolates, introducing an electrophilic halogen source as well to trap the *in situ* formed vinyl gold species, forming the desired halobutenolide and regenerating the gold catalyst. We envisioned performing the reaction under identical conditions to those used for the isolation of the vinyl gold species,

but using a catalytic amount of gold and a source of electrophilic iodine (Figure 2.61). These attempts were unsuccessful, so we tested a more active biarylphosphine catalyst, JohnPhosAuSbF₆ and also attempted this cyclization with the bimetallic gold catalyst used in the photoredox cyclization. These attempts were entirely unsuccessful; no trace of product was detected in any of the trials outlined in Table 11. We propose that catalyst turnover was hindering reaction progress, as counterion exchange with halide could occur in solution; halogen counterions are known to depress the reaction rates of cationic gold species in comparison to non-coordinating anions.⁹⁹

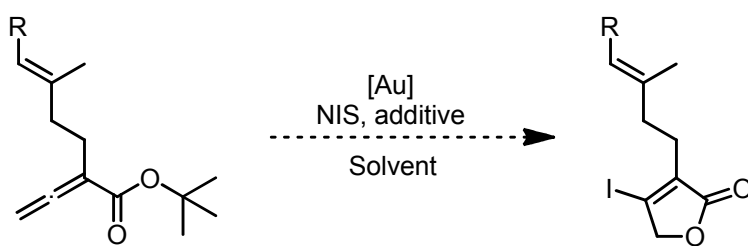


Figure 2.61. Attempts to access halobutenolides using a catalytic amount of gold and NIS to trap the vinyl gold species via iododauration.

Entry	R	Au	Additive	Solvent
1	Ar	PPh ₃ AuNTf ₂	-	DCM
2		JohnPhosAuSbF ₆	Py	DCM
3			Py	Acetone
4	H	PPh ₃ AuNTf ₂	Py	DCM
5		[(dppm)AuCl] ₂	-	Acetone
6			-	CH ₃ CN

Table 11. Failed attempts at a gold-catalyzed cyclization, trapping *in situ*-formed vinyl gold species with N-iodosuccinimide to access iodobutenolide

The final method we pursued in our search for a more efficient butenolide synthesis was utilizing copper(II) halides to mediate the allenolate cyclization. A clean and high-yielding synthesis of bromo- and chlorobutenolides from 2,3-allenoic acids and allenolates has been previously reported by Ma and Wu using a stoichiometric amount of CuBr₂ and CuCl₂ under aqueous conditions.¹⁰⁰ We attempted the synthesis of both halobutenolides using a model

substrate (Figure 2.62, Table 12) but to no avail: no trace of the desired product was detected in the reaction mixture by ^1H NMR.

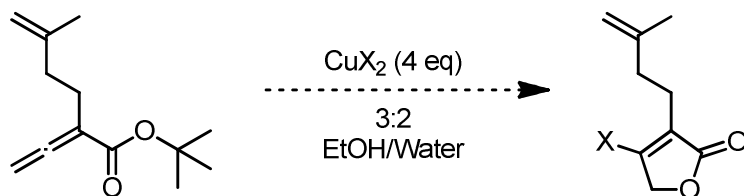


Figure 2.62. Attempts to access halobutenolides using copper(II) halides to induce lactonization.

Entry	Cu(II) source	Result
1	CuBr_2	Degradation
2	$\text{CuCl}_2 \cdot \text{H}_2\text{O}$	Degradation

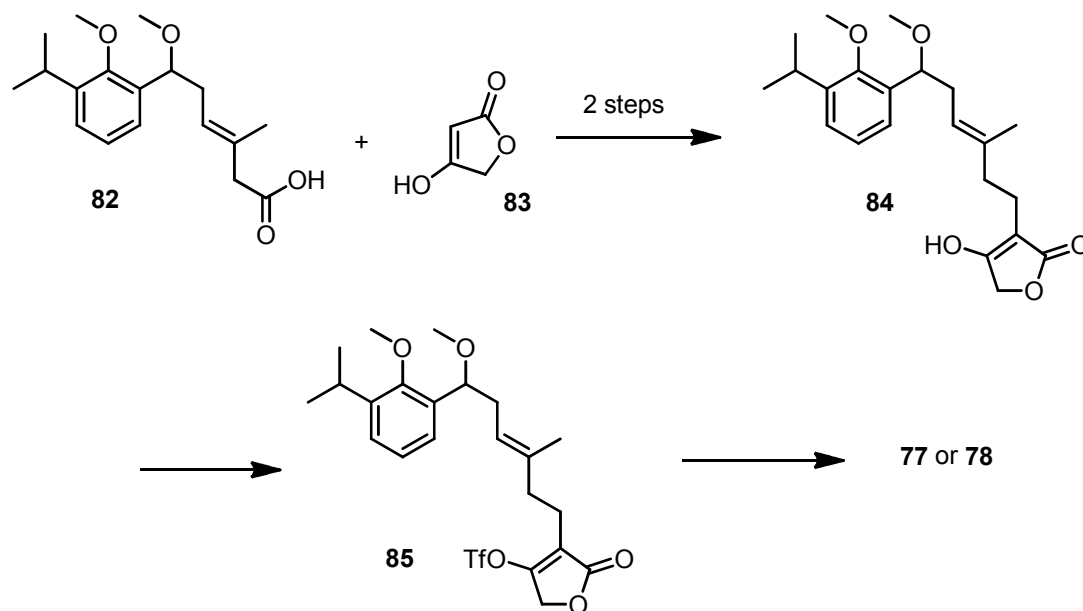
Table 12. Failed attempts at conducting copper(II)halide-mediated synthesis of bromo- and chlorobutenolides from model substrate **76**. Reactions were performed at 80-85°C in sealed vials.

2.10.2 Redesigning the Synthesis

After the failure of all our attempts to circumvent the isolation of the vinyl gold intermediate, we were forced to conclude that the current synthetic route did not allow us to avoid this particular step. We then turned our attention to designing a new synthetic route to bypass the allene entirely or, failing that, access the allene in fewer synthetic steps, bypassing the current low-yielding steps.

Tetronic Acid coupling

The first revised route we investigated involved bypassing the allenolate species entirely, accessing a 3-substituted tetronic acid derivative instead. We envisioned accessing these tetronic acid derivatives via an ester coupling reaction of a homoallylic carboxylate **82**, followed by an *in situ* Fries-type rearrangement and subsequent reduction with sodium cyanoborohydride (NaCNBH_3), as reported by the Baati group in 2011.¹⁰¹ The 4-hydroxyl group could then be transformed into a triflate¹⁰¹ or halogen¹⁰² - suitable substrates for photoredox cyclization – following known procedures (Scheme 2.9).



Scheme 2.9. Proposed tetronic acid coupling, reduction and halide formation from carboxylate starting material **82**.

The literature precedent for this synthetic route was extremely promising, as the Baati group had performed the coupling/rearrangement reaction on a β - γ -unsaturated carboxylate, a similar substrate to ours in terms of sensitivity to isomerization (Figure 2.63).¹⁰¹ This was encouraging for us, as we feared that the basic conditions required for the ester coupling reaction would cause alkene isomerization to the α,β -unsaturated species. Baati and co-workers did not report the mechanism of the reduction process, but it is simple to deduce (Figure 2.64): The ketotetronic acid **2.63-1**, formed after the Fries rearrangement, is reduced to alcohol **2.63-2** by NaCNBH_3 . The acidic conditions cause protonation of this alcohol, generating a reasonable leaving group, which is expelled to form an unsaturated ketoester. This species is an excellent Michael acceptor, and is readily reduced by NaCNBH_3 via a 1,4-hydride addition to form the desired product.

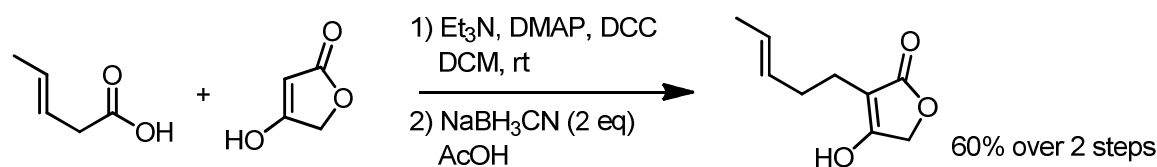


Figure 2.63. Literature precedent for coupling of a β - γ -unsaturated carboxylate to tetronic acid via a two-step coupling/Fries rearrangement and reduction protocol.

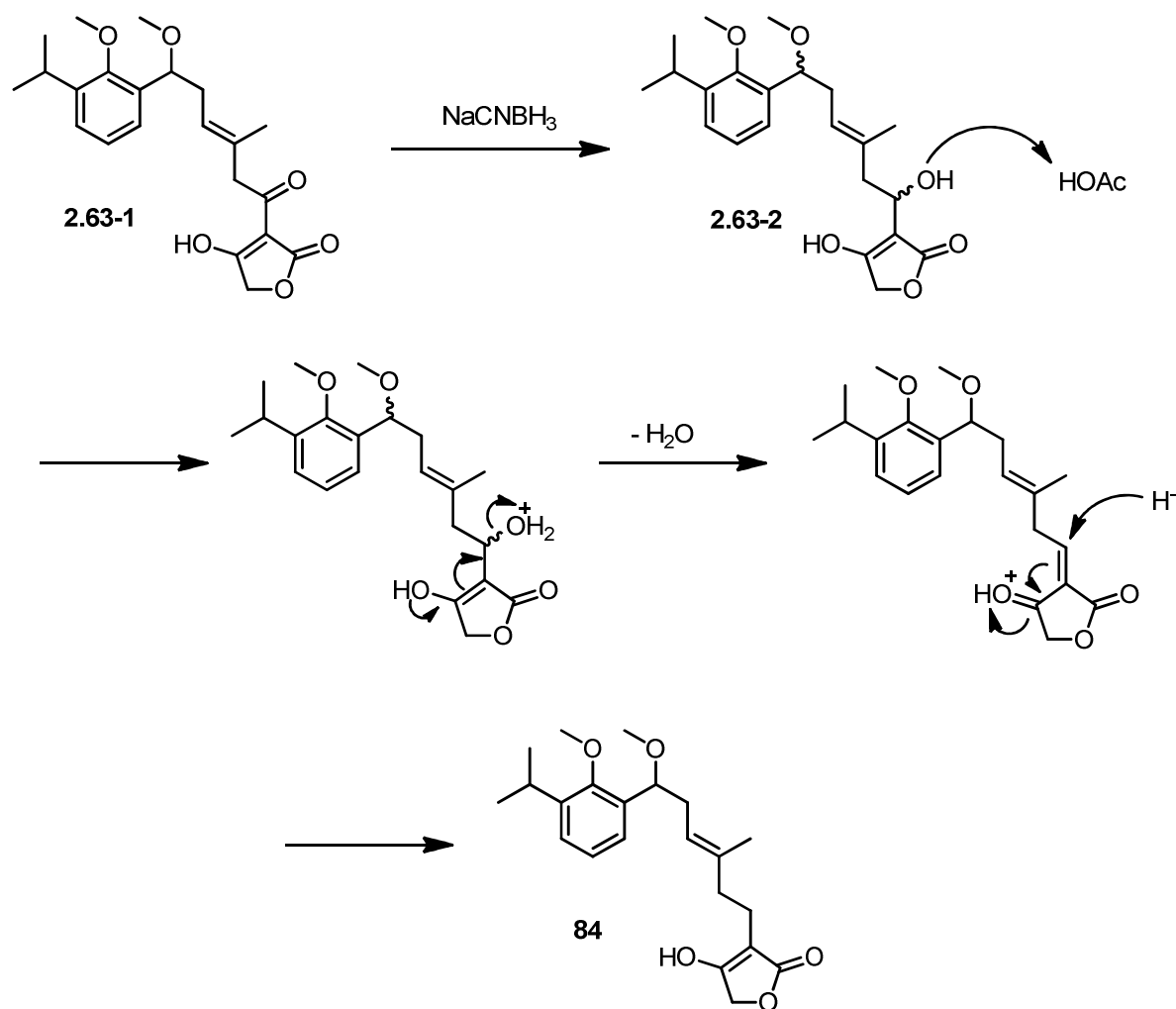


Figure 2.64. Proposed mechanism of reduction of ketotetronic acid **2.63-1** by two equivalents of NaCNBH_3 in acidic conditions

We successfully synthesized the substrate for this coupling reaction via oxidation of homoallylic alcohol **70** (Figure 2.65). We initially attempted the oxidation following an unusual protocol designed for substrates sensitive to isomerization, utilizing a catalytic amount of sodium dichromate and nitric acid and stoichiometric periodate.¹⁰³ This protocol yielded the desired product in 31% yield. A slightly higher yield of 43% was obtained using the Jones reagent, and with substrate in hand we pushed forward to attempt the coupling reaction. Unfortunately, NMR analysis of the crude reaction mixture did not suggest a successful reaction. Upon further analysis, we concluded that the predominant component in the reaction mixture was the conjugated isomer of the starting material (Figure 2.66). This

was extremely disappointing for us, as the literature suggested that this procedure was tolerant to homoallylic carboxylate substrates.

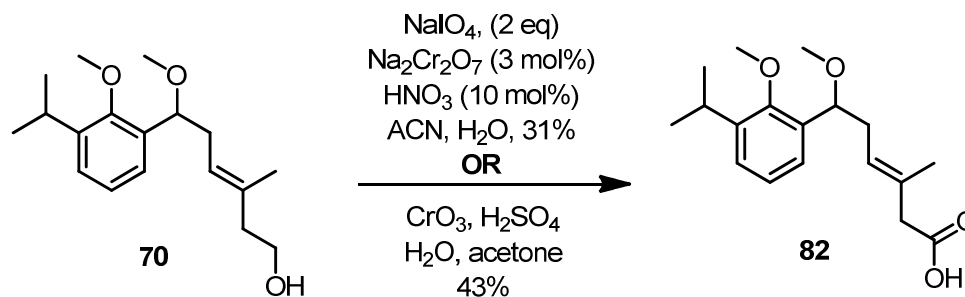


Figure 2.65. Oxidation procedures performed on homoallylic alcohol to access carboxylate **82**.

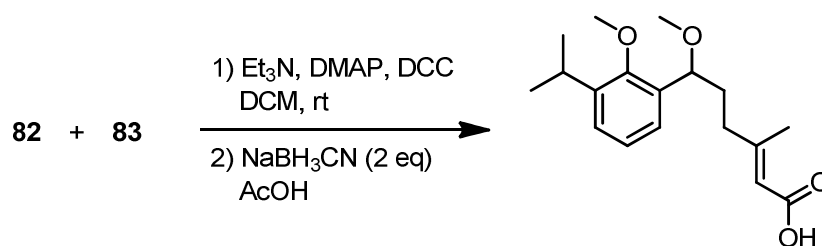


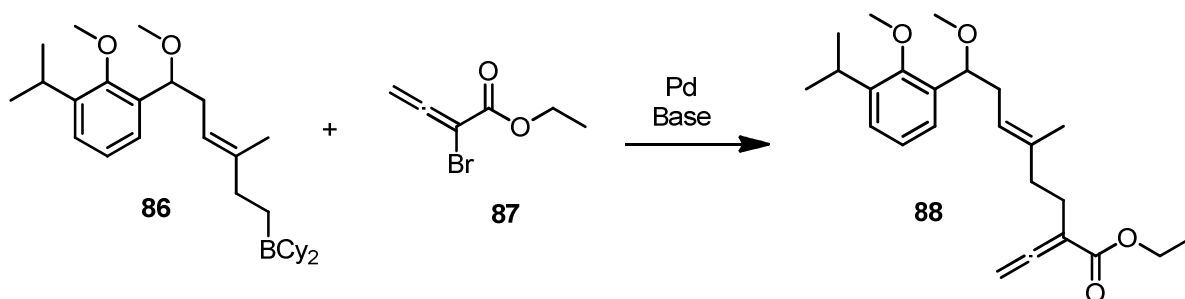
Figure 2.66. Undesired formation of conjugated isomer of starting carboxylate during attempted tetronic acid coupling.

Exploiting the Potential of the Hydroboration

After the failure of the tetronic acid coupling, we elected to seek a shorter method of accessing the allenolate **73**. We considered the current synthetic route – particularly the diene hydroboration – and we considered methods of exploiting the inherent reactivity of the *in situ* generated alkylborane. The current route generates a reactive carbon-boron bond that is wasted in the oxidative workup and must be re-activated by formation of a leaving group. We envisioned utilizing the reactive borane character to perform further chemistry without quenching the borane. We investigated two borane coupling reactions: a *B*-alkyl Suzuki reaction and an uncommon borane-alkyne coupling process.

One of the most widely used transformations involving carbon-boron bonds in modern synthetic organic chemistry is the Suzuki-Miyaura coupling reaction. This palladium-catalyzed reaction is most commonly used with alkyl, alkenyl or aryl boronic acids and

esters, but is also reported with alkyl boranes, where it gained the name of *B*-alkyl Suzuki-Miyaura reaction. This transformation was first reported in 1989 by Suzuki and Miyaura, who reported this reaction as an efficient method of performing selective sp^3 - sp^2 couplings under mild conditions, in good yields and with high selectivity.¹⁰⁴ Alkylboranes, they reported, are sensitive to β -hydride elimination, but this proclivity could be tamed with the use of a palladium precatalyst such as [1,1-bis(diphenylphosphino)ferrocene]-dichloropalladium(II) [PdCl₂(dppf)]. They also studied the effect of various hydroboration reagents, concluding that alkyl-9-BBN and alkyl-dicyclohexylboranes gave similarly good yields of coupled products. Suzuki and Miyaura concluded that the rate of transmetalation of primary alkyl groups is substantially faster than that of secondary alkyl groups, such that they did not observe any coupling of secondary alkyl boranes. The reaction proved highly robust in the presence of various bases, solvents, coupling partners and temperatures. Since its discovery, the *B*-alkyl Suzuki reaction has been utilized in numerous total syntheses; these applications are summarized in a 2001 review by Danishefsky.¹⁰⁵ We envisioned utilizing this coupling reaction with the *in situ*-generated alkylborane **86** and bromoallenoate **87** - synthesized according to literature procedures¹⁰⁶ - to access ethyl allenoate **88** as per Scheme 2.10.



Scheme 2.10. Proposed *B*-alkyl Suzuki coupling between alkylborane **86** and bromoallenoate **87**.

Following the literature precedent, we opted to avoid the use of strong bases such as sodium hydroxide due to the potential for ester saponification. We also selected PdCl₂(dppf) as the catalyst of choice and a THF/DMF/water solvent system, as the use of these components have been reported extensively in the literature.¹⁰⁵ We performed numerous attempts at this coupling reaction, primarily screening base, temperature, additives and

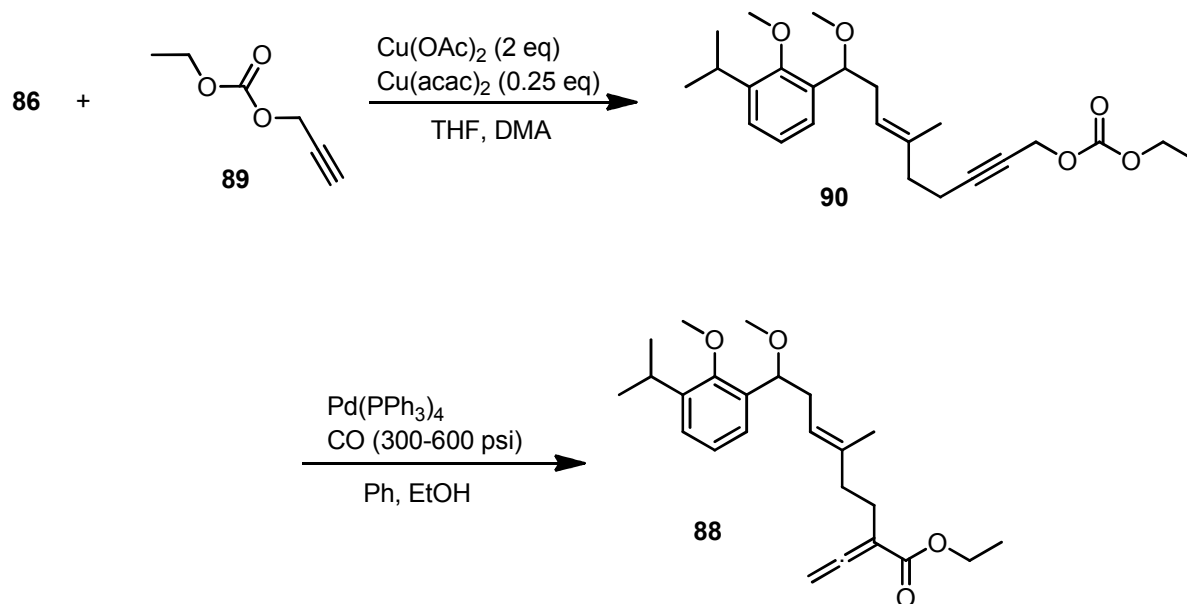
degassing of the reaction mixture (Table 13). Consulting the literature, we found only one report of a Suzuki coupling to a haloallenoate, where the authors reported that the use of silver oxide as the base was beneficial to the coupling reaction.¹⁰⁷ Unfortunately, we were not able to detect the product in any of the trials.

Entry	Pd source	Base	Additive	Temperature
1	PdCl ₂ (dppf)	K ₂ CO ₃	-	RT
2*	PdCl ₂ (dppf)	K ₂ CO ₃	-	50°C
3*	PdCl ₂ (dppf)	K ₂ CO ₃	AsPh ₃	RT
4*	PdCl ₂ (dppf)	Ag ₂ O	AsPh ₃	RT
5*	PdCl ₂ (dppf)	Cs ₂ CO ₃	AsPh ₃	50°C
6	PdCl ₂ (dppf)	K ₃ PO ₄	-	RT
7	PdCl ₂ (PPh ₃) ₂	K ₃ PO ₄	-	RT

Table 13. Conditions attempted for the B-alkyl Suzuki-Miyaura coupling of alkylborane **86** and bromoallenoate **87**. *Reaction solutions were degassed by sparging with Ar for 15 minutes prior to mixing.

Our final attempt to improve the synthesis also involved utilizing the inherent reactivity of the alkylborane. We discovered an interesting publication by Masuda *et al.* where they reported the coupling of a terminal alkyl or vinyl borane with a terminal alkyne, mediated by copper(II) acetate.¹⁰⁸ This coupling reaction was demonstrated with good functional group tolerance towards carbonyls and even free alcohols. We envisioned coupling **86** with ethyl propargyl carbonate **89** to access enyne **90**. This substrate is primed to undergo a known Pd-catalyzed carbonylation reaction to form the desired 2,3-allenoate **88** (Scheme 2.11).^{109,110} The difficulty posed by this proposed route was the lack of a published experimental procedure for the key alkyne-borane coupling. Masuda and co-workers report the use of two mole equivalents of copper(II) acetate, 0.25 mole equivalents of copper(II)acetoacetate to perform the coupling, the use of THF and DMA as the solvent, reaction temperature, and rough workup, but they do not report a full experimental procedure or a mechanism.¹⁰⁸ The authors propose the generation of an organocopper species via transmetalation of the alkylborane, but offer no evidence to support this. In a footnote, they also mention that the addition of galvinoxyl, a radical scavenger, significantly hinders the coupling reaction,

suggesting a radical-type mechanism. We elected to pursue this reaction and devise our own procedure en route.



Scheme 2.11. Proposed Cu(II) mediated/catalyzed alkyne-borane coupling to access alkyne-carbonate **90** and subsequent Pd-catalyzed carbonylation to access allenoate **88**.

We synthesized propargyl carbonate **89** via literature procedures¹¹¹ and began our investigation of the coupling process (Table 14). Our first attempt (adding copper and **89** to a solution of borane **86**) yielded the correct product, but in extremely low yield; the major components in the reaction mixture were starting material and homoallylic alcohol **70**, resulting from oxidation of the alkylborane. We found that reversing the order of addition, adding borane to a solution of carbonate and copper, was deleterious to the reaction. Our best yield was obtained by diluting a THF solution of alkylborane with DMA, then adding neat carbonate and copper directly to the reaction mixture – we isolated the desired product in 16% yield. Again, the oxidation product **70** was present in the reaction mixture as well, suggesting that the coupling reaction was slow. We attempted running the coupling at slightly elevated temperature, increasing the stoichiometry of alkyne coupling partner or copper species, increasing concentration and changing solvent composition but were sadly unable to reproduce our results. The slight success of this reaction encouraged us that this unusual coupling process was feasible, but we did not have the time to study it in further detail.

Entry	Eq. alkyne	Mole eq. Cu		THF:DMA ratio	Concentration (M)	Addition order	Result
		Cu(OAc) ₂	Cu(acac) ₂				
1	1.2	2.3	0.35	3:2	0.5	A	5%
2	1.5	2.1	0.30	3:2	0.5	B	0
3	1.5	2.0	0.5	1:1	0.5	C	16%
4	1.5	2.0	0.5	1.25:1	0.5	C	7 ^{d,e}
5	2.9	3.1	0.38	1:2	0.1	C	Deg.
6	1.2	2.0	0.30	1:5	0.1	C	0
7	1.2	2.0	0.30	4:1	0.5	C	0
8	1.2	2.0	0.30	5:1	0.5	C	0

Table 14. Attempted optimization of copper(II)-mediated alkyne-borane coupling reaction. Deg. = degradation was observed. A=added a solution of alkyne and copper in DMA to borane solution in THF. B=added solution of borane to a solution of copper and alkyne in DMA. C=added DMA, followed by neat alkyne and copper to a solution of borane in THF.^dBorane solution was degassed by sparging prior to adding other reagents.^eReaction was warmed to 45°C.

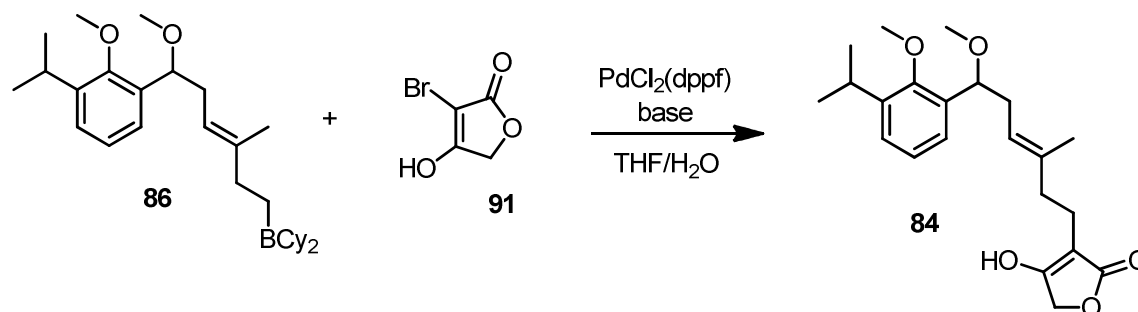
Over the course of the optimization, we were able to isolate a small amount of the alkynyl carbonate product **90**, which allowed us to try the carbonylation reaction. The mechanism of this reaction is, fortunately, known, and we learned that the alkyl group on the allenolate product originates from the alcoholic solvent and that the selection of this alcohol is known to affect the reaction rate. Poorly nucleophilic alcohols such as *tert*-butanol require elevated temperatures (100°C) and prolonged reaction times to undergo this carbonylation.¹⁰⁹ In the interest of preserving our small stock of starting material, we elected to run the reaction in ethanol, which is much more nucleophilic and allows this reaction to occur more readily. We were only able to conduct a single trial of this reaction, which we performed at 60°C under a 400 psi atmosphere of carbon monoxide. We were able to identify the desired product in the reaction mixture, and isolated it in low yield. This result was highly encouraging and we have little doubt this yield could be greatly improved with little effort. We suspected that the ethyl allenolate would be equally effective in the synthesis and isolation and the vinyl gold species, and we confirmed this with a small-scale trial.

Future work

We have demonstrated a proof of concept that the inherent reactivity of the *in situ*-generated alkyldicyclohexylborane **86** can be exploited in a cross-coupling process with terminal alkynes to access disubstituted alkynes such as **90**. This sp-sp³ coupling reactivity is largely unexplored in the literature, but has the potential to be very powerful, as it bridges two of the most common families of cross-coupling reactions, the Suzuki-Miyaura reaction and the Sonogashira reaction. We were able to achieve a successful cross-coupling reaction in 16% yield, but, with further study, the yield of this reaction could surely be improved dramatically. The subsequent carbonylation step to access allenolate **88** also holds much promise and has not been optimized for use in this synthesis. Reduction in reaction temperature is likely a key factor to improving the yield of **88**.

Based on the knowledge we gained from these recent revisions to the synthetic route, we propose another modification to the synthetic route. We propose a *B*-alkyl Suzuki coupling reaction of alkylborane **86** with bromotetronic acid **91** to access the coupled product **84**. We believe that our *B*-alkyl Suzuki coupling failed due to the instability of the bromoallenolate coupling partner or to cross-reactivity of the bromoallenolate with the palladium catalyst. Bromotetronic acid **91** is a known, stable compound and can be synthesized easily on gram-scale.^{112,113} Furthermore, it does not contain any reactive functional groups which would promote untoward side reactions. Literature precedent for *B*-alkyl Suzuki reactions with similar bromide coupling partners describes couplings occurring at room temperature with the use of mild bases such as potassium or caesium carbonate or potassium phosphate tribasic.¹⁰⁵ The success of this coupling process would bypass the entire β-ketoester/allene/vinyl gold sequence, vastly improving the yield of the synthesis and removing the requirement of a stoichiometric amount of gold. It would also allow for easy access to a variety of halogens or pseudohalogens (OMs, OTs, OTf) for in-depth study of the radical cyclization process. If this synthetic route is indeed successful, we would also be able to return to using the acetonide protecting group, as we would no longer use any strongly acidic conditions during this synthesis. This would greatly facilitate the endgame of the

synthesis, as we have yet to investigate methods to cleave the bis-methyl ether protecting groups to access our true desired product **12**.



Scheme 2.12. Proposed *B*-alkyl Suzuki-Miyaura coupling of alkyborane **86** with bromotetronic acid **91**. Base = K₂CO₃, Cs₂CO₃ or K₃PO₄.

2.11 Summary and Outlook

Our initial goal of accessing the tetracyclic core of **1** via an oxidative cyclization cascade unfortunately did not pan out. Time after time, our attempts met with failure and we were sadly unable to gain any insight into the workings of the process, unable to even identify any of the degradation products. Investigating this route, however, bore certain fruits. We succeeded in synthesizing the vinyl gold species **75**, which is the first reported vinyl gold complex of its type synthesized from a terminal allene. Our ability to access this substrate gave us the starting block to access the family of halobutenolides **77**, **78**, and, in the future, **81**. Inadvertently, we also discovered a hitherto unknown method for forming these halobutenolides from vinyl gold species such as **75**. These halobutenolide substrates were critical to the investigation of our newly discovered photoredox catalyst and its potential to induce intramolecular radical cyclizations. Our study of this photoredox cyclization is incomplete, but the data we have collected thus far are extremely promising. We believe that we have been successful in accessing the tetracyclic core of triptolide via a photoredox radical cyclization cascade of **77** and **78**. Further study of this reaction is still required to confirm the structure of the product and investigate the substrate scope of the reaction. With the synthetic revisions discussed in section **Error! Reference source not found.**, we demonstrated some methods for potential dramatic improvements to the synthetic route. The

culmination of these ideas has resulted in a promising cross-coupling method from alkylborane **86** and bromotetronic acid **91**. This method has great potential to improve this synthesis and allow us to study the radical cyclization in detail.

Claims to Original Research

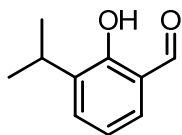
1. The first synthesis and isolation of a vinyl-gold butenolide species from cyclization of a *terminal* 2,3-allenoate.
2. The first reported use of *N*-iodosuccinimide and *N*-bromosuccinimide to transform a vinyl gold species to a vinyl iodide or bromide, respectively.

-
- ¹ Kupchan, S.M.; Court, W.A.; Dailey, R.G, Jr.; Gilmore, C.J.; Bryan, R.F. *J. Am. Chem. Soc.* **1972**, *94*, 7194
- ² Kupchan, S.M. *Pure. Appl. Chem.* **1970**, *21*, 227
- ³ Goodman, J.; and Walsh, V. *The Story of Taxol: Nature and Politics in the Pursuit of an Anti-Cancer Drug.* **2001**, Cambridge University Press
- ⁴ Humphrey, A.J. and Beale, M.H. *Plant Secondary Metabolites: Occurrence, Structure and Role in the Human Diet.* **2006**, Wiley-Blackwell: Boston, MA
- ⁵ Brinker, A.M.; Ma, J.; Lipsky, P.E.; Raskin, I. *Phytochemistry* **2007**, *68*, 732
- ⁶ Tao, X. and Lipsky, P.E. *Rheum. Dis. Clin. N. Amer.* **2000**, *26*, 29
- ⁷ Tao, X.; Cai, J.J.; Lipsky, P.E. *J. Pharmacol. Exp. Ther.* **1991**, *272*, 1305
- ⁸ Tao, X. S-K, H.; Ma, L.; Cai, J.; Mao, Y.; Lipsky, P.E. *Arthritis Rheum.* **1998**, *41*, 130
- ⁹ Kupchan, S.M. *Science*, **1974**, *185*, 791
- ¹⁰ A Scifinder Scholar search conducted on July 24, 2012 lists 218 hits for “triptolide cancer” from 2005 to present
- ¹¹ Huang, W.; He, T.; Chai, C.; Yang, Y.; Zheng, Y.; Zhou, P.; Qiao, X.; Zhang, B.; Liu, Z.; Wang, J.; Shi, C.; Lei, L.; Gao, K.; Li, H.; Zhong, S.; Yao, L.; Huang, M.; Lei, M. *PLoS One* **2012**, *7*, 1
- ¹² a) Wang, Z.; Jin, H.; Xu, R.; Mei, Q.; Fan, D. *Exp. Mol. Med.* **2009**, *41*, 717 b) Liu, J.; Shen, M.; Yue, Z.; Yang, Z.; Wang, M.; Li, C.; Xin, C.; Wang, Y.; Mei, Q.; Wang, Z. *Phytomedicine* **2012**, *19*, 756
- ¹³ a) Sun, L.; Zhang, S.; Jiang, Z.; Huang, X.; Wang, T.; Huang, X.; Li, H.; Zhang, L. *Biochem. Bioph. Res. Co.* **2011**, *416*, 99. b) Aoyagi, Y.; Hitotsuyanagi, Y.; Hasuda, T.; Fukaya, H.; Takeya, K.; Aiyama, R.; Matsuzaki, T.; Hashimoto, S. *Bioorg. Med. Chem. Lett.* **2011**, *21*, 3046
- ¹⁴ a) Li, C.; Chu, C.; Huang, L.; Wang, M.; Sheu, L.; Yeh, J.; Hsu, H. *Cancer Lett.* **2012**, *319*, 203. b) Matsui, Y.; Watanabe, J.; Ikegawa, M.; Kamoto, T.; Ogawa, O.; Nishiyama, H. *Oncogene* **2008**, *27*, 4603
- ¹⁵ a) Gu, W.Z.; Brandwein, S.R.; Banerjee, S. *J. Rheumatol.* **1992**, *19*, 682. b) Yu, K.T.; Nuss, G.; Boyce, R.; Jariwala, N.; Owens, G.; Pennetti, A.; Chan, W.; Zhang, D.C.; Chang, M.N.; Zilberstein, A. *Gen. Pharmacol.* **1994**, *25*, 1115. c) Lin, N.; Liu, C.; Xiao, C.; Jia, H.; Imada, K.; Wu, H.; Ito, A. *Biochem. Pharmacol.* **2007**, *73*, 136
- ¹⁶ a) Tao, X.; Cush, J.J.; Garret, M.; Lipsky, P.E. *J. Rheumatol.* **2001**, *28*, 2160. b) Tao, X.; Younger, J.; Fan, F.Z.; Wang, B.; Lipsky, P.E. *Arthritis Rheum.* **2002**, *46*, 1735
- ¹⁷ Barton-Burke, M.; Dwinell, D.; Kafkas, L.; LAvalley, C.; Sands, H.; Proctor, C.; Johnson, E. *Oncology* **2008**, *22* (*11 Suppl. Nurse Ed*), 31
- ¹⁸ Ao, J.H.; Li, Y.T.; Xiao, X.R.; *Zhonghua Waiké Zazhi* **1994**, *32*, 175
- ¹⁹ Zhang, X.Z.; Li, S.; Wu, X.Z. *Chung-kuo Chung His I Chieh Ho Tsa Chih* **1994**, *14*, 451
- ²⁰ Qian, S.Z.; Xu, Y.; Zhang, J.W. *Contraception* **1995**, *51*, 121 and references therein
- ²¹ Bai, J-P. and Shi, Y-L. *Contraception* **2002**, *65*, 441
- ²² Titov, D.V.; Gilman, B.; He, Q.; Bhat, S.; Low, W.; Dang, Y.; Smeaton, M.; Demain, A.L.; Miller, P.S.; Kugel, J.F.; Goodrich, J.A.; Liu, J.O. *Nature Chem. Biol.* **2011**, *7*, 182
- ²³ a) Sher, F.T. and Bertochold, G.A. *J. Org. Chem.* **1977**, *42*, 2569. b) Lai, C.; Buckanin, R.; Chen, S.; Zimmerman, D.; Sher, F.; Bertochold, G. *J. Org. Chem.* **1982**, *47*, 2364
- ²⁴ Buckanin, R.S.; Chen, S.J.; Freize, D.M.; Sher, F.T.; Bertochold, G.A. *J. Am. Chem. Soc.* **1980**, *102*, 1200
- ²⁵ a) van Tamelen, E.E.; Demers, J.P.; Taylor, E.G.; Koller, K. *J. Am. Chem. Soc.* **1980**, *102*, 5424. b) Garver, L.C. and van Tamelen, E.E. *J. Am. Chem. Soc.* **1980**, *104*, 867. c) van Tamelen, E.E. and Leiden, T.M. *J. Am. Chem. Soc.* **1982**, *104*, 1785
- ²⁶ Yang, D.; Ye, X-Y.; Xu, M.; Pang, K-W.; Zou, N.; Letcher, R. *J. Org. Chem.* **1998**, *63*, 6446
- ²⁷ a) Yang, D.; Ye, X-Y.; Gu, S.; Xu, M. *J. Am. Chem. Soc.* **1999**, *121*, 5579. b) Yang, D.; Ye, X-Y.; Xu, M.; Pang, K-W.; Cheung, K-K. *J. Am. Chem. Soc.* **2000**, *122*, 1658. c) Yang, D.; Ye, X-Y. and Xu, M. *J. Org. Chem.* **2000**, *65*, 2208
- ²⁸ Miller, N.A.; Willis, A.C. and Sherburn, M.S. *Chem. Comm.* **2008**, *44*, 1226
- ²⁹ Goncalves, S.; Hellier, P.; Nicolas, M.; Wagner, A.; Baati, R. *Chem. Comm.* **2010**, *46*, 5778
- ³⁰ Hashmi, S. *Chem. Rev.* **2007**, *107*, 3180. Li, Z.; Brouwer, C. and Chuan, H. *Chem. Rev.* **2008**, *108*, 3239
- ³¹ Barriault, L. and Grisé, C. *Org. Lett.* **2006**, *8*, 5905. Barriault, L.; Barabé, F.; Bétournay, G.; Bellavance, G. *Org. Lett.* **2009**, *11*, 4236. b) Barriault, L.; Sow, B.; Bellavance, G.; Barabé, F. *Beils. J. Org. Chem.* **2011**, *7*, 1007
- ³² Hashmi, A.S.K. *Chem. Rev.* **2007**, *107*, 3180
- ³³ Rudolph, M. and Hashmi, S. *Chem. Soc. Rev.* **2012**, *41*, 2448
- ³⁴ Barabé, F.; Levesque, P.; Korobkov, I.; Barriault, L. *Org. Lett.* **2011**, *13*, 5580
- ³⁵ Bellavance, G.; Sow, B. and Barriault, L. Unpublished work.
- ³⁶ Stork, G. and Burgstahler, A. *J. Am. Chem. Soc.* **1955**, *77*, 5068

- ³⁷ Zhao, Y. and Loh, T. *J. Am. Chem. Soc.* **2008**, *130*, 10024
- ³⁸ Muhammet, U.; Hideaki, I.; Kazuaki, I.; Hisashi, Y. *Org. Lett.* **2005**, *7*, 1601
- ³⁹ Feducia, J. and Gagné, M. *J. Am. Chem. Soc.* **2008**, *130*, 592
- ⁴⁰ Gansauer, A.; Justicia, J.; Rosales, A.; Worgull, D.; Rinker, B.; Cuerva, J.; Oltra, J. *Eur. J. Org. Chem.* **2006**, *18*, 4115
- ⁴¹ Maddaford, S.; Andersen, N.; Cristofoli, W.; Keay, B. *J. Am. Chem. Soc.* **1996**, *118*, 10766. Domingo, V.; Arteaga, J.; Lopez Perez, J.; Pelaez, R.; Quillez de Moral, J.; Barrero, A. *J. Org. Chem.* **2012**, *77*, 341
- ⁴² Toullec, P.Y.; Blarre, T. and Michelet, V. *Org. Lett.* **2009**, *11*, 2888
- ⁴³ Sethofer, S.G.; Mayer, T. and Toste, F.D. *J. Am. Chem. Soc.* **2010**, *132*, 8276
- ⁴⁴ Kang, J.; Lee, E.; Park, S.; Shin, S. *Tet. Lett.* **2005**, *46*, 7431
- ⁴⁵ a) Liu, L.; Xu, B.; Mashuta, M.S.; Hammond, G.B. *J. Am. Chem. Soc.* **2008**, *130*, 17642. b) Liu, L. and Hammond, G.B. *Chem. Asian. J.* **2009**, *4*, 1230
- ⁴⁶ Hopkinson, M.N.; Gee, A.D. and Gouverneur, V. *Chem. Eur. J.* **2011**, *17*, 8248
- ⁴⁷ Hopkinson, M.N.; Ross, J.E.; Giuffredi, G.T.; Gee, A.D.; Gouverneur, V. *Org. Lett.* **2010**, *12*, 4904
- ⁴⁸ Hopkinson, M.N.; Tessier, A.; Salisbury, A.; Giuffredi, G.T.; Combettes, L.E.; Gee, A.D.; Gouverneur, V. *Chem. Eur. J.* **2010**, *16*, 4739
- ⁴⁹ Mezaillas, N.; Ricard, L. and Gagosz, F. *Org. Lett.* **2005**, *7*, 4133
- ⁵⁰ Maity, P. and Lepore, S. D. *J. Org. Chem.* **2009**, *74*, 158
- ⁵¹ A) Hofsløkken, N.U. and Skattebøl, L. *Acta. Chim. Scand.* **1999**, *53*, 258. B) Hansen, T.V. and Skattebøl, L. *Org. Synth.* **2005**, *82*, 64
- ⁵² Wuts, P.G.M and Theodora, W. Greene. *Greene's Protective Groups in Organic Synthesis* (Various Editions). Wiley: 1981 - 2006
- ⁵³ A Reaxys search performed on October 7, 2012 for a similar transformation yielded 334 reaction hits from 216 citations.
- ⁵⁴ Sauer, E.L.O. and Barriault, L. *J. Am. Chem. Soc.* **2004**, *126*, 8569
- ⁵⁵ Charette, A. and Lebel, H. *J. Org. Chem.* **1995**, *60*, 2996
- ⁵⁶ Brady, S.F. Ilton, M.A. and Johnson, W.S. *J. Am. Chem. Soc.* **1968**, *90*, 2882
- ⁵⁷ McCormick, J.P. and Barton, D.L. *J. Org. Chem.* **1980**, *45*, 2566
- ⁵⁸ Kowalsky, C.J. and Reddy, R.E. *J. Org. Chem.* **1992**, *57*, 7194
- ⁵⁹ Kürti, L. and Czako, B. *Strategic Applications of Named Reactions in Organic Synthesis.* **2005**, Elsevier Academic Press: Burlington, MA.
- ⁶⁰ Bartoli, G.; Bosco, M.; Carlone, A.; Dalpozzo, R.; Marcantoni, E.; Melchiorre, P.; Sambri, L. *Synthesis* **2007**, 3489
- ⁶¹ Katritzky, A. and Pastor, A. *J. Org. Chem.* **2000**, *65*, 3679
- ⁶² House, H.; Auerbach, R.; Gall, M.; Peet, N. *J. Org. Chem.* **1973**, *38*, 514
- ⁶³ Chatterjee, A.K. and Grubbs, R.H. *Org. Lett.* **1999**, *1*, 1751
- ⁶⁴ Chatterjee, A.K.; Choi, T-L.; Sanders, D.P.; Grubbs, R.H. *J. Am. Chem. Soc.* **2003**, *125*, 11360
- ⁶⁵ Fürstner, A. *Angew. Chem. Int. Ed.* **2000**, *39*, 3012
- ⁶⁶ Blackwell, H.E.; O'Leary, D.J.; Chatterjee, A.K.; Washenfelder, R.A.; Bussmann, D.A.; Grubbs, R.H. *J. Am. Chem. Soc.* **2000**, *122*, 58
- ⁶⁷ Helmboldt, H.; Köhler, D. and Hiersemann, M. *Org. Lett.* **2006**, *8*, 1573
- ⁶⁸ Chou, T.; Lee, S. and Yao, N. *Tetrahedron* **1989**, *45*, 4113
- ⁶⁹ Kingsbury, J.; Harrity, J.; Bonitatebus, P.; Hoveyda, A. *J. Am. Chem. Soc.* **1999**, *121*, 791. Garber, S.; Kingsbury, J.; Gray, B.; Hoveyda, A. *J. Am. Chem. Soc.* **2000**, *122*, 8168
- ⁷⁰ Stewart, I.C.; Douglas, C.J. and Grubbs, R.H. *Org. Lett.* **2008**, *10*, 441
- ⁷¹ Brummond, K.M.; Dingess, E.A. and Kent, J.L. *J. Org. Chem.* **1996**, *61*, 6096
- ⁷² Gras, J.; Nougier, R. and Mchich, M. *Tet. Lett.* **1987**, *28*, 6601
- ⁷³ Fleet, G.W. and Shing, T.K.M. *J. Chem. Soc. Chem. Comm.* **1984**, 835
- ⁷⁴ Norman, D.G.; Reese, C.B. and Serafinowska, H.T. *Synthesis* **1985**, 751
- ⁷⁵ Voigtritter, K.; Ghorai, S. and Lipshutz, B.H. *J. Org. Chem.* **2011**, *76*, 4697
- ⁷⁶ A Reaxys search for the conversion of a similar E-enal to 1,3-diene performed on September 20, 2012 gave 278 reactions from 116 citations.
- ⁷⁷ Kim, P.; Zhang, Y.; Shenoy, G.; Nguyen, Q.; Boshoff, H.; Manjunatha, U.; Goodwin, M.; Lonsdale, J.; Price, A.; Miller, D.; Duncan, K.; White, S.; Rock, C.; Barry, C.; Dowd, C. *J. Med. Chem.* **2006**, *49*, 159
- ⁷⁸ Cole, K. and Hsung, R. *Org. Lett.* **2003**, *5*, 4843
- ⁷⁹ Marsault, E. and Deslongchamps, P. *Org. Lett.* **2000**, *2*, 3317

-
- ⁸⁰ Wang, W.; Hammond, G.B. and Xu, B. *J. Am. Chem. Soc.* **2012**, *134*, 5697
- ⁸¹ Liu, L.; Xu, B.; Mashuta, M.; Hammond, G. *J. Am. Chem. Soc.* **2008**, *130*, 17642
- ⁸² Liu, L. and Hammond, G. *Chem. Asian. J.* **2009**, *4*, 1230
- ⁸³ Roth, K. and Blum, S. *Organometallics* **2010**, *29*, 1712
- ⁸⁴ Zhang, G.; Luo, Y.; Wang, Y.; Zhang, L. *Angew. Chem.* **2011**, *123*, 4542
- ⁸⁵ Nishida, H.; Takada, N.; Yoshimura, M.; Sonoda, T.; Kobayashi, H. *Bull. Chem.Soc. Jpn.* **1984**, *57*, 2600
- ⁸⁶ Clayden, J.; Greeves, N.; Warren, S.; Wothers, P. *Organic Chemistry*. **2001**. Oxford University Press: Oxford.
- ⁸⁷ Lin, H.; Schall, A. and Reiser, O. *Synlett*. **2005**, 2603
- ⁸⁸ Capella, L.; Montecocchi, P. and Navacchia, M. *J. Org. Chem.* **1995**, *60*, 7424
- ⁸⁹ Nguyen, J.; D'Amato, E.; Narayanam, J.; Stephenson, C. *Nature Chemistry* **2012**, *4*, 854
- ⁹⁰ Lin, S.; Ischay, M.; Fry, C.; Yoon, T. *J. Am. Chem. Soc.* **2011**, *133*, 19350
- ⁹¹ Andrew, R.S.; Becker, J. and Gagné, M. *Angew. Chem. Int. Ed.* **2010**, *49*, 7274. Nguyen, J.; Tucker, J.; Konieczynska, M.; Stephenson, C. *J. Am. Chem. Soc.* **2011**, *133*, 4160. Furst, L.; Narayanam, J. and Stephenson, C. *Angew. Chem. Int. Ed.* **2011**, *50*, 9655
- ⁹² Dai, C. Narayanam, J. and Stephenson, C. *Nature Chemistry* **2011**, *3*, 140
- ⁹³ Wallentin, A.; Nguyen, J.; Finkbeiner, P.; Stephenson, C. *J. Am. Chem. Soc.* **2012**, *134*, 8875
- ⁹⁴ Narayanam, J. and Stephenson, C. *Chem. Soc. Rev.* **2011**, *40*, 102
- ⁹⁵ Patent pending
- ⁹⁶ Révol, G.; McCallum, T. and Barriault, L. Unpublished work, **2012**.
- ⁹⁷ Pattenden, G.; Roberts, L. and Blake, A. *J. Chem. Soc., Perkin Trans. 1* **1998**, 863. Snider, B. and Kiselgof, J. *Tetrahedron* **1998**, *54*, 10641
- ⁹⁸ Yamashita, S. *Chem. Lett.* **1975**, 967. Roberge, P. and Herman, J. *Can. J. Chem.* **1964**, *42*, 2262
- ⁹⁹ Gorin, G.; Sherry, B. and Toste, F.D. *Chem. Rev.* **2008**, *108*, 3351
- ¹⁰⁰ Ma, S. and Wu, S. *J. Org. Chem.* **1999**, *64*, 9314. Ma, S. and Wu, S. *Tet. Lett.* **2001**, *42*, 4075
- ¹⁰¹ Ghobril, C. Kister, J. and Baati, R. *Eur. J. Org. Chem.* **2011**, 3416
- ¹⁰² Jas, G. *Synthesis* **1991**, 965. Shirakawa, E.; Imazaki, Y. and Hayashi, T. *Chem. Comm.* **2009**, 5088
- ¹⁰³ de Vondervoort, L.; Bouttemy, S.; Padron, J.; Le Bras, J.; Muzart, J.; Alsters, P. *Synlett*. **2002**, 243
- ¹⁰⁴ Miyaura, N.; Ishiyama, T.; Sasaki, H.; Ishakawa, M.; Satoh, M.; Suzuki, A. *J. Am. Chem. Soc.* **1989**, *111*, 314
- ¹⁰⁵ Chemler, S.; Trauner, D. and Danishefsky, S. *Angew. Chem. Int. Ed.* **2001**, *40*, 4554
- ¹⁰⁶ Abell, A.; Houlst, D.; Morris, K.; Taylor, J.; Trent, J. *J. Org. Chem.* **1993**, *58*, 1531
- ¹⁰⁷ Gillmann, T. and Weeber, T. *Synlett* **1994**, 649
- ¹⁰⁸ Masuda, Y.; Murata, M.; Sato, K.; Watanabe, S. *Chem. Comm.* **1998**, 807
- ¹⁰⁹ Tsuji, J. Sugiura, T. and Minami, I. *Tet. Lett.* **1986**, *27*, 731
- ¹¹⁰ Chai, G.; Wu, S.; Fu, C.; Ma, S. *J. Am. Chem. Soc.* **2011**, *133*, 3740
- ¹¹¹ Le Ravalec, V. Fischmeister, C. and Bruneau, C. *Adv. Synth. Catal.* **2009**, *351*, 1115
- ¹¹² Ge, P. and Kirk, K. *J. Fluorine Chem.* **1997**, *84*, 45
- ¹¹³ Gillespie, J.; Price, C. *J. Org. Chem.* **1957**, *22*, 780

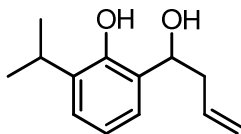
3 Experimental Procedures and Supporting Information



2-Hydroxy-3-isopropyl-benzaldehyde (44):

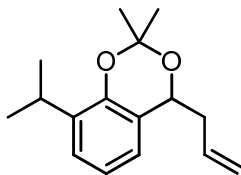
A dry 1L side-arm round-bottom flask equipped with a wide-bore condenser was charged with 2-isopropylphenol (25.0 mL, 180 mmol), 400 mL dry THF, MgCl_2 (26.24 g, 270.1 mmol) and TEA (50.5 mL, 362 mmol). The mixture was stirred at room temperature for 15 minutes, by which time a pale blue/white colour had formed. To this mixture was added solid paraformaldehyde (32.95 g, 1.043 mol) and the resultant slurry was warmed slowly to reflux with stirring. As it warmed, the suspension turned dark blue, then green, then bright yellow once reflux was attained. Reflux was continued for 1 hour until TLC showed complete consumption of starting phenol. At this point, the reaction mixture was cooled to room temperature and poured into 700 mL of 5% aqueous HCl. The pale yellow, cloudy mixture was stirred for 2 hours, then extracted with 5x100 mL Et_2O . The combined organic fractions were washed twice with brine, dried with MgSO_4 and concentrated to an orange oil. The residue was flushed through a plug of silica gel with Et_2O and concentrated *in vacuo* to isolate the title compound as a yellow oil. Spectral information matches that of a previously reported characterizationⁱ. Product was used directly to synthesize **43** without further purification.

ⁱ Knight, P.D. et al. *J. Organomet. Chem.* **2003**, 683, 103-113



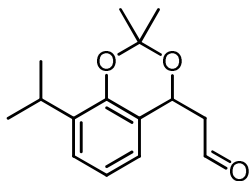
(±)-2-(1-Hydroxy-but-3-enyl)-6-isopropyl-phenol (43):

A 1 L round-bottom flask was charged with **44** (crude, ~180 mmol), 400 mL THF and 250 mL saturated aqueous ammonium chloride. The biphasic mixture was cooled in an ice-water bath and zinc dust (23.57 g, 360.6 mmol) was added. With vigorous agitation, allyl bromide (32 mL, 367 mmol) was charged to the reaction mixture via an addition funnel over 30 minutes. After addition completed, the mixture was warmed to room temperature over 1.5 hours until TLC showed complete consumption of the aldehyde. The heterogeneous mixture was filtered through a Celite pad to remove Zn and NH₄Cl solids and the filtrate was diluted with 100 mL Et₂O to cause layer separation. The aqueous fraction was extracted twice with 200 mL Et₂O, then the combined organic fractions were washed twice with brine, dried with anhydrous Na₂SO₄ and concentrated to a yellow oil, which was used without further purification to access either **45** or **66**. A small portion was purified by column chromatography on silica gel (4:1 Hexanes:Et₂O) to isolate the title compound as a colourless oil. IR (neat, cm⁻¹) 3525 (br, sh), 3375 (br), 3077 (w), 3047 (w), 1642 (m), 1593 (m), 920 (s), ; ¹H NMR (400 MHz, CDCl₃) δ = 8.20 (s, 1 H), 7.16 (t, J = 4.7 Hz, 1 H), 6.83 (d, J = 4.9 Hz, 2 H), 5.94 - 5.81 (m, 1 H), 5.30 - 5.21 (m, 2 H), 4.87 (ddd, J = 2.1, 4.6, 9.0 Hz, 1 H), 3.37 (spt, J = 6.9 Hz, 1 H), 2.69 (d, J = 2.4 Hz, 1 H), 2.68 - 2.56 (m, 2 H), 1.26 (d, J = 6.9 Hz, 3 H), 1.25 (d, J = 7.0 Hz, 3 H); ¹³C NMR (101 MHz, CDCl₃) δ = 152.9 (C), 136.5 (C), 134.0 (CH), 125.7 (CH), 125.5 (C), 124.5 (CH), 119.5 (CH₂), 119.4 (CH), 75.1 (CH), 41.9 (CH₂), 26.5 (CH), 22.7 (CH₃), 22.6 (CH₃). HRMS (EI) m/z calcd for C₁₃H₁₈O₂ (M)⁺ 206.1307, found 206.1310.



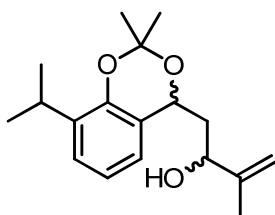
(±)-4-Allyl-8-isopropyl-2,2-dimethyl-4H-benzo[1,3]dioxine (45):

Crude **43** was dissolved in 40 mL of 2,2-dimethoxypropane (326.1 mmol) in a 250 mL round-bottom flask. To this solution was added *p*-toluenesulfonic acid monohydrate (250 mg, 1.31 mmol) and the resulting yellow solution was stirred at room temperature for 2 hours until TLC showed complete consumption of the diol. The reaction was quenched by addition of 100 mL saturated aqueous NaHCO₃; the layers were separated and the aqueous fraction extracted twice with 100 mL Et₂O. The combined organic fractions were washed with brine, dried with MgSO₄ and concentrated. The residue was flushed through a plug of silica gel with dichloromethane to obtain racemic **45** (16.54 g, 67.1% over 3 steps) as a yellow oil which was used without further purification. A pure sample was obtained by column chromatography on silica gel (4:1 hexanes:Et₂O) to isolate a colourless oil. IR (neat, cm⁻¹) 3077 (w), 1640 (m), 1592 (m), 916 (s) ¹H NMR (400 MHz, CDCl₃) δ = 7.11 (dd, J = 1.9, 7.3 Hz, 1 H), 6.93 (ddd, J = 0.7, 2.0, 7.7 Hz, 1 H), 6.89 (t, J = 7.4 Hz, 1 H), 5.93 (tdd, J = 6.7, 10.3, 17.1 Hz, 1 H), 5.16 (qd, J = 1.7, 17.2 Hz, 1 H), 5.09 (tdd, J = 1.2, 2.1, 10.2 Hz, 1 H), 4.98 (dd, J = 3.6, 7.5 Hz, 1 H), 3.26 (spt, J = 6.9 Hz, 1 H), 2.76 (dddd, J = 1.2, 1.7, 3.6, 6.5, 14.9 Hz, 1 H), 2.57 (dddd, J = 1.2, 1.7, 6.5, 7.5, 15.0 Hz, 1 H), 1.63 (s, 3 H), 1.49 (s, 3 H), 1.24 (d, J = 7.0 Hz, 3 H), 1.20 (d, J = 7.0 Hz, 3 H). ¹³C NMR (101 MHz, CDCl₃) δ = 148.6 (C), 136.6 (C), 134.6 (CH), 124.5 (CH), 122.6 (C), 121.8 (CH), 119.9 (CH), 117.0 (CH₂), 99.1 (C), 69.5 (CH), 39.7 (CH₂), 28.4 (CH₃), 26.6 (CH₃), 22.9 (CH₃), 22.0 (CH₃). HRMS (EI) m/z calcd for C₁₆H₂₂O₂ (M)⁺ 246.1620, found 246.1631.



(±)-(8-Isopropyl-2,2-dimethyl-4H-benzo[1,3]dioxin-4-yl)-acetaldehyde (46):

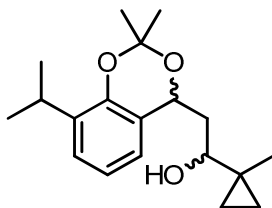
A mixture of **45** (0.52 g, 2.1 mmol) in 50 mL of 1:1 THF:H₂O was stirred and cooled to 0° C in the dark. To this was added NaIO₄ (1.26 g, 5.89 mmol) and OsO₄ (4% wt. aqueous solution, 0.2 mL, 0.03 mmol). The reaction mixture was stirred overnight in the dark, slowly warming to room temperature. The resultant yellow heterogeneous mixture was filtered through a pad of Celite to remove the white precipitate and the filtrate was diluted with 10 mL Et₂O to separate the layers. The aqueous fraction was extracted twice with 20 mL Et₂O, the combined organic fractions washed twice with 5 mL saturated aqueous Na₂SO₃ to remove remaining osmium, then once with saturated NaHCO₃, once with brine, and dried with MgSO₄ and concentrated to isolate the title compound as a dark yellow/orange oil which was used immediately in the subsequent reaction without further purification. ¹H NMR (300 MHz, CDCl₃) δ = 9.77 (t, J = 2.2 Hz, 1 H), 7.13 (dd, J = 1.6, 7.5 Hz, 1 H), 6.95 - 6.86 (m, J = 7.4, 7.4 Hz, 1 H), 6.82 (ddd, J = 0.8, 1.6, 7.7 Hz, 1 H), 3.24 (spt, J = 7.1 Hz, 1 H), 1.60 (s, 3 H), 1.51 (s, 3 H), 1.23 (d, J = 6.9 Hz, 3 H), 1.19 (d, J = 6.9 Hz, 3 H).



(±)-11-(8-Isopropyl-2,2-dimethyl-4H-benzo[1,3]dioxin-4-yl)-3-methyl-but-3-en-2-ol (47):

To a solution of isopropenylmagnesium bromide (120 mL, 0.5 M in THF) – cooled in a -78°C dry ice-acetone bath – was charged *slowly* a solution of aldehyde **46** (~47 mmol) in Et₂O (100 mL) via cannula. Addition rate was metered by watching dry ice bath for bubbling, slowing addition if bubbling became vigorous. The reaction mixture was stirred at -78°C for 20 minutes, then warmed to room temperature and stirred 4.5 hours. The resultant cloudy yellow mixture was cooled in an ice-water bath and quenched by addition of 50 mL

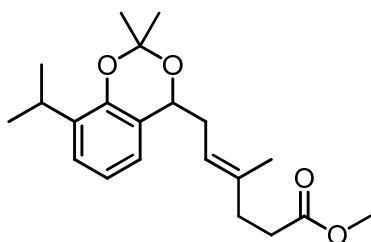
saturated aqueous NH_4Cl . After layer separation, the aqueous phase was extracted twice with 100 mL Et_2O . The combined organic fractions were washed with brine, dried with MgSO_4 and concentrated. The residue was chromatographed on silica gel with 1% Et_2O in DCM to isolate **47** as a yellow, waxy oil as a mixture of diastereomers (9.32 g, 68% yield over 2 steps). IR (neat, cm^{-1}) 3368 (br), 3072 (m), 1652 (m), 1592 (m), 906 (s). ^1H NMR (400MHz, CDCl_3) δ = 7.11 (dd, J = 1.6, 7.4 Hz, 1 H), 6.90 (t, J = 7.4 Hz, 1 H), 6.85 (ddt, J = 0.8, 1.6, 7.6 Hz, 1 H), 5.22 (dd, J = 3.1, 7.5 Hz, 1 H), 5.11 (dd, J = 2.6, 10.2 Hz, 1 H), 5.05 (d, J = 0.8 Hz, 1 H), 4.87 (d, J = 1.5 Hz, 1 H), 4.47 (dd, J = 2.9, 9.1 Hz, 1 H), 4.26 (d, J = 9.0 Hz, 1 H), 3.24 (spt, J = 13.9 Hz, 1 H), 2.28 - 1.90 (m, 2 H), 1.83 - 1.73 (m, 3 H), 1.82 - 1.73 (m, 3 H), 1.63 (s, 3 H), 1.64 - 1.60 (m, 3 H), 1.52 - 1.47 (m, 3 H), 1.52 - 1.47 (m, 3 H), 1.23 (d, J = 7.0 Hz, 3 H), 1.23 (d, J = 7.0 Hz, 3 H), 1.21 - 1.16 (m, J = 6.9 Hz, 3 H), 1.18 (d, J = 7.0 Hz, 3 H); ^{13}C NMR (101MHz, CDCl_3) δ = 148.5, 147.9, 147.1, 146.7, 136.9, 136.8, 124.9, 124.7, 122.3, 122.0, 121.5, 120.3, 120.3, 111.3, 110.1, 99.1, 99.0, 75.4, 71.9, 70.9, 68.5, 41.3, 39.9, 28.6, 28.5, 26.6, 22.9, 22.8, 22.1, 22.0, 21.7, 18.7, 17.7. HRMS (EI) m/z calcd for $\text{C}_{18}\text{H}_{26}\text{O}_3$ (M)+ 290.1882, found 290.1878.



(±)-2-(8-Isopropyl-2,2-dimethyl-4H-benzo[1,3]dioxin-4-yl)-1-(1-methyl-cyclopropyl)-ethanol (48):

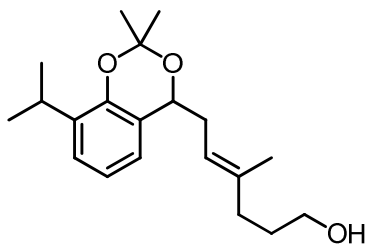
A dry round-bottom flask under argon was charged with **47** (0.467 g, 1.61 mmol) and 10 mL dry CH_2Cl_2 . The mixture was cooled to -15°C in an ice/acetone bath and a solution of diethylzinc (1M in hexanes, 8 mL, 8 mmol) was added dropwise, followed by diiodomethane (0.6 mL, 8.33 mmol). The resultant solution was stirred, slowly warming to room temperature over 3 hours, and then stirred an additional hour at room temperature. The mixture was quenched with saturated aqueous NH_4Cl , diluted with Et_2O and the layers were separated. The organic fraction was washed with saturated Na_2SO_3 , NaHCO_3 and brine, then dried with MgSO_4 and concentrated to isolate **12** as a pale yellow, waxy oil (0.4703 g, 96.1%, mixture of diastereomers). IR (neat, cm^{-1}): 3465br, 3066, 2993, 2960, 2870. ^1H NMR

(300 MHz, CDCl₃) δ ppm 0.16 - 0.65 (m, 4 H) 1.09 (s, 3 H) 1.15 - 1.27 (m, 6 H) 1.49 (s, 3 H) 1.62 (s, 3 H) 1.80 - 2.14 (m, 1 H) 2.19 - 2.37 (m, 1 H) 2.70 (s, 1 H) 3.08 (d, $J=9.63$ Hz, 1 H) 3.14 - 3.35 (m, 2 H) 5.11 (dd, $J=10.38, 2.27$ Hz, 1 H) 5.23 (dd, $J=6.67, 3.23$ Hz, 1 H) 6.80 - 6.96 (m, 2 H) 7.05 - 7.17 (m, 1 H). ¹³C NMR (76 MHz, CDCl₃) δ = 148.6, 147.8, 136.8, 136.7, 124.8, 124.6, 122.5, 122.1, 121.6, 120.3, 120.2, 99.0, 98.9, 74.2, 70.9, 68.5, 40.0, 39.0, 28.5, 28.4, 26.6, 26.5, 22.9, 22.8, 22.0, 21.9, 21.8, 21.6, 20.3, 20.1, 17.7, 17.5, 12.5, 12.3, 10.4, 10.2. HRMS (EI) m/z calcd for C₁₉H₂₈O₃ (M)⁺ 304.2038, found 304.20294



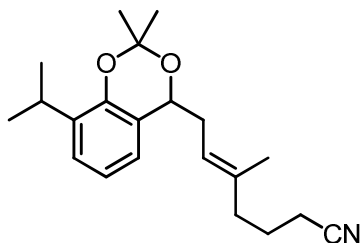
(±)-(E)-Methyl 6-(8-isopropyl-2,2-dimethyl-4H-benzo[d][1,3]dioxin-4-yl)-4-methylhex-4-enoate (51):

To a solution of **47** (0.274 g, 0.945 mmol) in trimethylorthoacetate (11 mL, 10 mmol) was added propionic acid (0.03 mL, 0.4 mmol) and the mixture was heated to reflux for 12 hours. The clear, yellow solution was then cooled to room temperature. Ethyl acetate was added and the mixture was washed twice with 1M HCl, once each with saturated aqueous NaHCO₃ and brine. The combined organic fractions were dried with MgSO₄ and concentrated *in vacuo* to isolate **51** as a pungent yellow oil (0.254 g, 78%). IR (neat, cm⁻¹): 2960, 2867, 1742. ¹H NMR (400 MHz, CDCl₃) δ = 7.08 (dd, $J = 1.8, 7.3$ Hz, 1 H), 6.92 - 6.88 (m, 1 H), 6.86 (t, $J = 7.5$ Hz, 1 H), 5.30 (t, $J = 6.2$ Hz, 1 H), 4.91 (dd, $J = 3.9, 7.3$ Hz, 1 H), 3.65 (s, 3 H), 3.23 (sxt, $J = 7.0$ Hz, 1 H), 2.67 (ddd, $J = 4.0, 6.7, 15.4$ Hz, 1 H), 2.46 (ddd, $J = 6.7, 7.0, 15.4$ Hz, 1 H), 2.42 - 2.36 (m, 2 H), 2.35 - 2.26 (m, 2 H), 1.64 (s, 3 H), 1.60 (s, 3 H), 1.46 (s, 3 H), 1.23 (d, $J = 6.9$ Hz, 3 H), 1.18 (d, $J = 6.9$ Hz, 3 H). ¹³C NMR (101 MHz, CDCl₃) δ = 173.9, 148.6, 136.5, 135.4, 124.4, 123.0, 121.8, 121.0, 119.9, 99.1, 69.8, 51.5, 34.7, 34.1, 33.0, 28.5, 26.6, 22.9, 22.0, 22.0, 16.4. HRMS (EI) m/z calcd for C₂₁H₃₀O₄ (M)⁺ 346.2144, found 346.2156



(±)-(E)-6-(8-Isopropyl-2,2-dimethyl-4H-benzo[d][1,3]dioxin-4-yl)-4-methylhex-4-en-1-ol (52):

To a suspension of LiAlH_4 (129.6 mg, 3.24 mmol) in 8 mL dry THF at 0°C was added dropwise a solution of methyl ester **51** (2.72 mmol) in 5 mL dry THF. The mixture was stirred for 1 hour at 0°C , and then quenched by the slow addition of a saturated aqueous solution of Rochelle salt. The layers were separated and the aqueous fraction extracted three times with ethyl acetate. The combined organic fractions were washed with water and brine, then dried with Na_2SO_4 , filtered and concentrated. The residue was purified by flash column chromatography on silica gel with 20% Ethyl acetate/hexane to isolate 0.6264 g of a pale yellow oil. (72.3% yield) IR (neat, cm^{-1}): 3384br, 2966, 2939. ^1H NMR (400 MHz, CDCl_3) δ = 7.09 (dd, J = 2.0, 7.3 Hz, 1 H), 6.91 (dd, J = 2.0, 7.5 Hz, 1 H), 6.87 (t, J = 7.5 Hz, 1 H), 5.31 (t, J = 6.5 Hz, 1 H), 4.94 (dd, J = 3.7, 7.3 Hz, 1 H), 3.56 (dt, J = 1.3, 6.2 Hz, 2 H), 3.24 (spt, J = 6.9 Hz, 1 H), 2.68 (ddd, J = 3.4, 7.4, 14.9 Hz, 1 H), 2.51 (td, J = 7.4, 14.9 Hz, 1 H), 2.10 (t, J = 7.1 Hz, 2 H), 1.65 (quin, J = 6.8 Hz, 2 H), 1.60 (s, 3 H), 1.46 (s, 3 H), 1.23 (d, J = 7.0 Hz, 3 H), 1.18 (d, J = 7.0 Hz, 3 H). ^{13}C NMR (101 MHz, CDCl_3) δ = 148.6, 137.3, 136.5, 124.4, 122.9, 121.8, 120.7, 119.9, 99.1, 69.9, 62.6, 36.6, 34.0, 30.2, 28.4, 26.6, 22.9, 22.0, 21.9, 16.2. HRMS (EI) m/z calcd for $\text{C}_{20}\text{H}_{30}\text{O}_3$ (M) $^+$ 318.2194, found 318.21969.

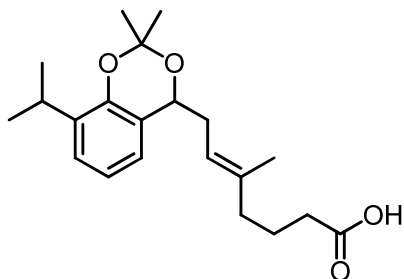


(±)-(E)-7-(8-Isopropyl-2,2-dimethyl-4H-benzo[d][1,3]dioxin-4-yl)-5-methylhept-5-enenitrile (53):

To a solution of **52** (2.52 g, 7.91 mmol) in 30 mL DCM at room temperature was charged *p*-toluenesulfonyl chloride (1.853 g, 9.52 mmol), TEA (1.37 mL, 9.83 mmol), and

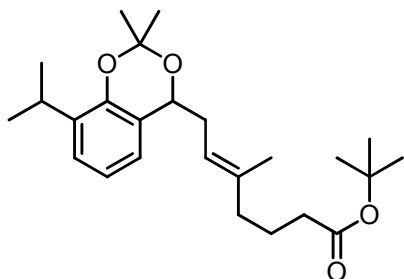
DMAP (99.2 mg, 0.81 mmol). The mixture was stirred overnight (ca. 15h) at room temperature, and then poured into 50 mL water. The layers were separated and the aqueous fraction extracted 3 times with DCM (60 mL total). The combined organic fractions were washed with brine, dried with Na₂SO₄ and concentrated *in vacuo* to isolate the sulfonate ester **2.14-1**.

To a solution of **2.14-1** (2.50 g, 5.30 mmol) in 20 mL DMSO was added solid potassium cyanide (0.425 g, 6.52 mmol) and the reaction mixture was heated to 90°C for 4 hours. After cooling to room temperature, 50 mL saturated aqueous sodium carbonate was added to quench the reaction and the resulting mixture was poured into 100 mL Et₂O. The fractions were separated (3 layers total: ether, DMSO and sat. aqueous NaHCO₃) and the ether fraction set aside. The aqueous and DMSO layers were extracted with Et₂O 3x (150 mL total) and the combined ether fractions were washed with water and brine, then dried with Na₂SO₄ and concentrated. The residue was flushed through a plug of silica gel with the following: 3 volumes petroleum ether to remove low polarity by-products, then with 2-3 volumes 20-50% Et₂O/pet ether to recover the title compound, which was isolated after concentration as a yellow oil (1.624 g, 94% yield). IR (neat, cm⁻¹): 2867, 2246, 1457. ¹H NMR (400 MHz, CDCl₃) δ = 7.09 (dd, *J* = 3.6, 5.6 Hz, 1 H), 6.91 - 6.83 (m, 2 H), 5.25 (t, *J* = 6.5 Hz, 1 H), 4.98 (dd, *J* = 3.7, 6.5 Hz, 1 H), 3.23 (spt, *J* = 6.9 Hz, 1 H), 2.67 (ddd, *J* = 3.4, 7.4, 14.6 Hz, 1 H), 2.55 (td, *J* = 7.4, 14.6 Hz, 1 H), 2.10 (t, *J* = 6.5 Hz, 2 H), 2.08 - 1.94 (m, 2 H), 1.69 (sxttd, *J* = 7.0, 13.8 Hz, 2 H), 1.60 (s, 6 H), 1.46 (s, 3 H), 1.23 (d, *J* = 7.0 Hz, 3 H), 1.18 (d, *J* = 6.9 Hz, 3 H). ¹³C NMR (101 MHz, CDCl₃) δ = 148.7, 136.6, 134.3, 124.5, 122.7, 122.3, 121.8, 119.9, 99.0, 69.7, 38.1, 33.7, 28.5, 26.6, 23.1, 22.9, 22.0, 21.9, 15.9, 15.4. HRMS (EI) *m/z* calc for C₂₁H₂₉NO₂ (M)⁺ 327.2198, found 327.21867.



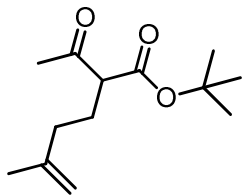
(±)-(E)-7-(8-Isopropyl-2,2-dimethyl-4H-benzo[d][1,3]dioxin-4-yl)-5-methylhept-5-enoic acid (54**):**

To a solution of **53** (1.62 g, 4.96 mmol) in 25 mL EtOH, 6 mL H₂O was added solid KOH (2.54 g, 45.3 mmol) and the mixture heated to reflux, stirring for 20 hours. The mixture was then cooled to room temperature and poured into a biphasic mixture of 75 mL Et₂O, 50 mL water. The organic phase was extracted 3x with 30 mL 15% aq. NaOH. The combined aqueous fractions were acidified to pH 2 with 2M HCl and this cloudy white mixture was extracted with EtOAc (3 x 100 mL). The combined organic fractions were washed with water and brine, dried with Na₂SO₄, filtered and concentrated to isolate **54** as a reddish oil (0.9898 g, 58% yield). IR (neat, cm⁻¹): 3400br, 2962, 2867, 1557. ¹H NMR (400 MHz, CDCl₃) δ = 7.08 (dd, *J* = 1.9, 7.3 Hz, 1 H), 6.91 (dd, *J* = 1.9, 7.3 Hz, 1 H), 6.86 (t, *J* = 7.3 Hz, 1 H), 5.26 (t, *J* = 7.0 Hz, 1 H), 4.93 (dd, *J* = 3.7, 7.3 Hz, 1 H), 3.23 (spt, *J* = 7.0 Hz, 1 H), 2.68 (ddd, *J* = 3.5, 6.0, 14.8 Hz, 1 H), 2.49 (td, *J* = 7.2, 14.9 Hz, 1 H), 2.23 (t, *J* = 6.5 Hz, 2 H), 2.05 (t, *J* = 7.1 Hz, 2 H), 1.73 (quin, *J* = 7.3 Hz, 2 H), 1.62 (s, 3 H), 1.60 (s, 3 H), 1.46 (s, 3 H), 1.22 (d, *J* = 7.1 Hz, 3 H), 1.17 (d, *J* = 7.0 Hz, 3 H). ¹³C NMR (101 MHz, CDCl₃) δ = 136.5, 124.4, 121.8, 121.0, 119.9, 99.1, 69.9, 34.2, 28.5, 26.6, 22.9, 22.0, 16.1. HRMS (EI) *m/z* calcd for C₂₁H₃₀O₄ (M)⁺ 346.2144, found 288.1701 (M-58)⁺



(±)-(E)-tert-Butyl-7-(8-isopropyl-2,2-dimethyl-4H-benzo[d][1,3]dioxin-4-yl)-5-methylhept-5-enoate (55):

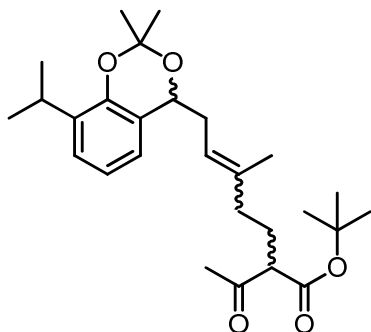
To a solution of **54** (663.2 mg, 1.914 mmol) and Boc_2O (896 mg, 4.11 mmol) in *t*-butanol (0.4 mL, 4.18 mmol) was added solid MgCl_2 (27 mg, 0.278 mmol) and the mixture was stirred at 40°C overnight. The reaction was quenched by the addition of water and the resulting biphasic mixture was extracted 3x with EtOAc. The combined organic fractions were washed twice with water, once with brine, then dried with Na_2SO_4 , filtered and concentrated. The residue was chromatographed on silica gel with 20%-100% EtOAc/hexane to isolate the desired ester as a viscous yellow oil (658.6 mg, 85.5% yield). IR (neat, cm^{-1}) 2970, 2935, 2867, 1734. ^1H NMR (400 MHz, CDCl_3) δ = 7.08 (dd, J = 1.7, 7.3 Hz, 1 H), 6.91 (dd, J = 1.7, 7.6 Hz, 1 H), 6.87 (q, J = 7.4 Hz, 1 H), 5.26 (t, J = 7.1 Hz, 1 H), 4.91 (dd, J = 3.9, 7.4 Hz, 1 H), 3.23 (spt, J = 7.1 Hz, 1 H), 2.68 (ddd, J = 4.0, 7.0, 15.2 Hz, 1 H), 2.47 (td, J = 7.1, 15.2 Hz, 1 H), 2.12 (dt, J = 2.7, 7.5 Hz, 2 H), 2.02 (t, J = 7.3 Hz, 2 H), 1.67 (quin, J = 7.4 Hz, 2 H), 1.62 (s, 3 H), 1.60 (s, 3 H), 1.48 - 1.46 (m, 3 H), 1.46 - 1.43 (m, 9 H), 1.23 (d, J = 7.0 Hz, 3 H), 1.18 (d, J = 7.1 Hz, 3 H). ^{13}C NMR (101 MHz, CDCl_3) δ = 173.3, 148.6, 136.5, 136.3, 124.4, 123.1, 121.8, 121.0, 119.9, 99.1, 79.8, 69.9, 38.9, 34.6, 34.2, 28.5, 28.1, 26.6, 23.1, 22.9, 22.0, 16.1. HRMS (EI) m/z calcd for $\text{C}_{25}\text{H}_{38}\text{O}_4$ (M) $^+$ 402.2770, found 402.27434.



(±)-tert-Butyl-2-acetyl-5-methylhex-5-enoate (56):

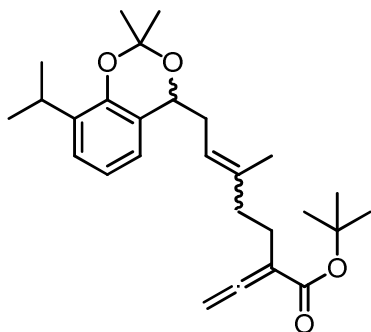
2.20-1: To a solution of PPh₃ (15.98 g, 56.9 mmol) and triethylamine (8.0 mL, 57.4 mmol) in 150 mL DCM at 0°C was added solid iodine (6.16 g, 24.16 mmol) portionwise. The mixture was stirred for 25 minutes, by which time a yellow slurry had formed. To this, 3-methyl-3-buten-1-ol (5.9 mL, 56.7 mmol) was charged dropwise, and then the mixture was allowed to warm to ambient temperature and stir 4-5 hours in the dark. At this time, TLC showed complete consumption of the alcohol starting material. Most of the DCM was removed on a rotary evaporator (700 mbar, 35°C) - *Caution: product is volatile!* – and pet ether was added to precipitate out PPh₃O. The solids were removed via filtration through a Celite pad and the filtrate was concentrated again. This precipitation, filtration, concentration process was repeated once more to isolate the title compound as a pale pink oil (9.26 g, 83% yield), which was used without further purification to access **56**.

To a solution of potassium *t*-butoxide (5.10 g, 44.07 mmol) in *t*BuOH (70 mL) at room temperature was added *t*-butyl acetoacetate (7.7 mL, 45.5 mmol) dropwise, whereby a solid mixture formed. The mixture was warmed slightly to melt the solid and the crude iodide **2.20-1** was charged dropwise via syringe. The reaction was heated to reflux (~80-85°C), stirred overnight, then cooled to room temperature. Water was added to dissolve any solids present and the mixture was acidified with 1M HCl until the orange colour disappeared (pH=1). The layers were separated and the aqueous fraction extracted 3x with Et₂O (150 mL total). The combined organic fractions were washed with 50% brine/water and brine, dried with Na₂SO₄ and concentrated. The residue was chromatographed on silica gel with 5% ethyl acetate/hexanes to isolate the title compound as a yellow oil (6.23 g, 52% yield over 2 steps). IR (neat, cm⁻¹): 2979, 2937 ¹H NMR (400 MHz, CDCl₃) δ = 4.76 (d, *J* = 1.0 Hz, 1 H), 4.70 (d, *J* = 1.0 Hz, 1 H), 3.33 (t, *J* = 7.3 Hz, 1 H), 2.23 (s, 3 H), 2.05 - 1.91 (m, 4 H), 1.72 (s, 3 H), 1.48 (s, 9 H). ¹³C NMR (101 MHz, CDCl₃) δ = 203.5, 168.9, 144.4, 111.1, 81.9, 60.0, 35.2, 28.9, 27.9, 25.8, 22.1. HRMS (EI) *m/z* calcd for C₁₃H₂₂O₃ (M)⁺ 226.1569, found 153.0938 (M-73)



(±)-*tert*-Butyl-2-acetyl-7-(8-isopropyl-2,2-dimethyl-4*H*-benzo[*d*][1,3]dioxin-4-yl)-5-methylhept-5-enoate (4:1 *E/Z* ratio) (50):

Charged a clean, dry 25 mL round bottom flask with 15.7 mg of the 2nd generation Hoveyda-Grubbs catalyst (0.025 mmol). To this, a solution of **45** (526.6 mg, 2.14 mmol) and **56** (236.2 mg, 1.04 mmol) in 5 mL THF, 5 mL toluene was charged via cannula. The resulting mixture was heated to reflux (87°C) for 72 hours then cooled, concentrated and passed through a plug of silica gel with DCM to remove catalyst. The filtrate was concentrated again and the residue chromatographed on silica gel with 5-15% ethyl acetate/hexanes. The title compound was isolated as a 4:1 *E/Z* mixture as a clear, pale yellow oil (102 mg, 22% yield, mixture of diastereomers). IR (neat, cm⁻¹): 2694, 2937, 2869, 1737, 1716. ¹H NMR (400 MHz, CDCl₃) δ = 7.08 (d, *J* = 7.3 Hz, 1 H), 6.91 (td, *J* = 1.8, 7.6 Hz, 1 H), 6.86 (dt, *J* = 1.1, 7.6 Hz, 1 H), 5.24 (t, *J* = 6.8 Hz, 1 H), 4.92 (dd, *J* = 3.1, 7.2 Hz, 1 H), 3.32, 3.27 (t, *J* = 7.2 Hz, 1 H), 3.23 (spt, *J* = 7.0 Hz, 1 H), 2.75 - 2.61 (m, 1 H), 2.49 (ddd, *J* = 6.8, 7.1, 14.7 Hz, 1 H), 2.17 (s, 3 H), 1.98 (m, 2 H), 1.95 - 1.85 (m, 2 H), 1.63 (m, 3 H), 1.60 (s, 3 H), 1.47 (s, 9 H), 1.46 (s, 3 H), 1.22 (d, *J* = 6.9 Hz, 3 H), 1.17 (d, *J* = 6.9 Hz, 3 H). ¹³C NMR (101 MHz, CDCl₃) δ = 203.8, 169.0, 148.5, 136.5, 135.8, 135.7, 124.4, 122.9, 122.9, 121.8, 121.8, 121.7, 121.6, 119.9, 99.1, 81.6, 69.8, 69.7, 59.4, 59.1, 37.1, 37.0, 34.0, 34.0, 29.3, 29.2, 28.5, 27.9, 27.9, 26.6, 26.5, 26.0, 25.9, 23.0, 23.0, 22.0, 21.9, 21.9, 16.0, 16.0. HRMS (EI) *m/z* calcd for C₂₇H₄₀O₅ (M)⁺ 444.2876, found 444.2828

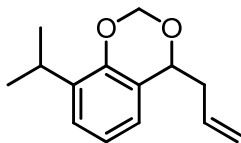


(±)-*tert*-Butyl-7-(8-isopropyl-2,2-dimethyl-4*H*-benzo[*d*][1,3]dioxin-4-yl)-5-methyl-2-vinylidenehept-5-enoate (4:1 *E:Z* ratio) (38):

To a suspension of NaH (40.8 mg, 1.02 mmol) in 4 mL dry Et₂O at 0°C was added a solution of **50** (181.6 mg, 0.408 mmol) in 4 mL dry Et₂O dropwise. The resulting solution was stirred for 30 minutes, then trifluoromethanesulfonic anhydride (1.05 eq.) was added dropwise. The mixture was stirred for 1 hour at 0°C, 1 hour at RT, then quenched by addition of saturated aqueous NH₄Cl. Separated layers, extracted aqueous fraction twice with Et₂O. Washed combined organic fractions with 1M HCl and brine. Dried with MgSO₄ and concentrated to isolate enol triflate **57** as a yellow oil, which was used without further purification.

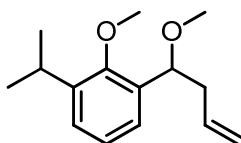
To a solution of LiHMDS (0.121 g, 0.701mmol) in 2 mL dry THF at -78°C was added a solution of **57** (199 mg, 0.347 mmol) in 2 mL dry THF. The yellow solution was stirred 1 hour at -78°C, then HMPA (0.24 mL, 1.38 mmol) was added and stirring continued at -78°C 1 hour. A ZnCl₂ solution (1M in Et₂O, 0.9 mL) was added, then the mixture was stirred a final hour at -78°C and quenched by pouring the cold reaction mixture quickly into a biphasic mixture of saturated aqueous NH₄Cl and Et₂O at 0°C. The phases were separated and the aqueous fraction extracted twice with Et₂O. The combined organic fractions were washed with brine, dried with MgSO₄ and concentrated. The residue was purified by chromatography on silica gel with 2% ethyl acetate/hexanes to isolate 108 mg of the title compound as a pale yellow oil (57% over 2 steps). ¹H NMR (400 MHz, CDCl₃) δ = 7.08 (d, *J* = 7.3 Hz, 1 H), 6.93 (dd, *J* = 1.5, 7.8 Hz, 1 H), 6.86 (t, *J* = 7.5 Hz, 1 H), 5.31 (t, *J* = 7.3 Hz, 1 H), 5.07 (t, *J* = 2.9 Hz, 1 H), 5.04 (t, *J* = 2.9 Hz, 2 H), 4.90 (dd, *J* = 4.0, 7.5 Hz, 1 H), 4.88 (dd, *J* = 3.8, 7.4 Hz, 1 H), 3.24 (spt, *J* = 7.1 Hz, 1 H), 2.69 (ddd, *J* = 3.8, 6.9, 15.3 Hz, 1 H), 2.46 (td, *J* = 7.4, 14.3 Hz, 1 H), 2.33 - 2.23 (m, 2 H), 2.23 - 2.10 (m, 2 H), 1.73 (d, *J* = 1.1 Hz, 1 H), 1.65 (s, 2 H), 1.60 (s, 3 H), 1.50 - 1.44 (m, 12 H), 1.23 (d, *J* = 7.0 Hz, 3 H), 1.18

(d, $J = 7.0$ Hz, 3 H). ^{13}C NMR (101 MHz, CDCl_3) $\delta = 213.7, 213.7, 166.5, 148.5, 136.4, 136.2, 124.4, 123.2, 121.9, 121.8, 121.6, 121.0, 119.9, 101.4, 101.3, 99.1, 80.7, 78.6, 70.0, 69.9, 38.0, 34.3, 34.1, 30.8, 28.5, 28.1, 26.6, 26.5, 23.4, 22.9, 22.0, 22.0, 16.3$.



(±)-4-Allyl-8-isopropyl-4H-benzo[d][1,3]dioxine (64):

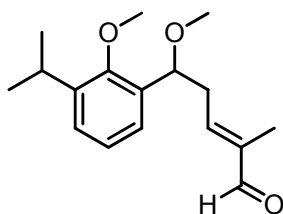
A 100 mL round bottom flask was charged with diol **43** (0.74 g, 3.59 mmol), dibromomethane (10 mL, 142.1 mmol), tetrabutylammonium iodide (267 mg, 0.71 mmol) and 30 mL 1,4-dioxane. The resulting mixture was heated to 80-100°C, at which point a solution of NaOH (3.6 g, 90 mmol) in 25 mL water was charged over 30 minutes. The reaction mixture was stirred vigorously overnight, cooled to RT, and then the layers were separated. The aqueous fraction was extracted 3x with Et_2O and the combined organic fractions washed 3x with water, once with brine, then dried with MgSO_4 and concentrated. The residue was chromatographed on silica gel with 3% ethyl acetate/hexanes and the title compound was isolated as a colourless oil (231.5 mg, 29.5% yield). ^1H NMR (400 MHz, CDCl_3) $\delta = 7.12$ (dd, $J = 2.1, 7.1$ Hz, 1 H), 6.93 (t, $J = 7.6$ Hz, 1 H), 6.90 (dd, $J = 2.3, 7.7$ Hz, 1 H), 5.94 (tdd, $J = 6.8, 10.3, 17.1$ Hz, 1 H), 5.36 (d, $J = 5.7$ Hz, 1 H), 5.20 (d, $J = 5.7$ Hz, 1 H), 5.20 (ddd, $J = 1.7, 3.4, 17.0$ Hz, 1 H), 5.15 (tdd, $J = 1.1, 2.0, 10.3$ Hz, 1 H), 5.05 (dd, $J = 3.5, 8.5$ Hz, 1 H), 3.27 (spt, $J = 6.9$ Hz, 1 H), 2.78 - 2.68 (m, 1 H), 2.65 - 2.55 (m, 1 H), 1.23 (d, $J = 7.0$ Hz, 18 H), 1.22 (d, $J = 7.0$ Hz, 6 H). ^{13}C NMR (101 MHz, CDCl_3) $\delta = 150.2, 136.7, 134.2, 124.5, 124.2, 122.7, 120.9, 117.6, 89.3, 74.6, 40.2, 26.3, 22.7, 22.5$. HRMS (EI) m/z calcd for $\text{C}_{14}\text{H}_{18}\text{O}_2$ (M) $^+$ 218.1307, found 218.1290.



(±)-1-Isopropyl-2-methoxy-3-(1-methoxybut-3-enyl)benzene (66):

(Telescoped from commercial **14**). To a suspension of NaH (18.37 g, 459 mmol) in 250 mL dry THF at 0°C was added dropwise a solution of freshly prepared crude **43** (\leq

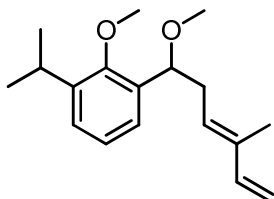
152.6 mmol) and iodomethane (40 mL, 640 mmol) in 60 mL THF. The resulting solution was stirred 30 minutes at 0°C, then warmed to RT and stirred overnight. The mixture was poured into 500 mL saturated aqueous NH₄Cl, then the layers separated and the aqueous fraction extracted twice with Et₂O (250 mL total). The combined organic fractions were washed with brine, dried with MgSO₄ and concentrated. The residue was chromatographed on a short silica gel column with 4% ethyl acetate/hexanes to isolate the title compound as a colourless oil (28.85 g, 78% yield over 3 steps from **14**). IR (neat, cm⁻¹): 3070, 2961, 2820, 1455. ¹H NMR (400 MHz, CDCl₃) δ = 7.24 (dd, *J* = 2.0, 7.3 Hz, 1 H), 7.21 (dd, *J* = 2.1, 7.3 Hz, 1 H), 7.15 (t, *J* = 7.6 Hz, 1 H), 5.87 (tdd, *J* = 7.1, 10.2, 17.3 Hz, 1 H), 5.14 - 5.00 (m, 2 H), 4.61 (dd, *J* = 5.0, 8.0 Hz, 1 H), 3.76 (s, 3 H), 3.33 (spt, *J* = 7.0 Hz, 1 H), 3.25 (s, 3 H), 2.60 - 2.49 (m, 1 H), 2.49 - 2.39 (m, 1 H), 1.26 (d, *J* = 6.9 Hz, 6 H), 1.24 (d, *J* = 6.9 Hz, 6 H). ¹³C NMR (101 MHz, CDCl₃) δ = 141.7, 135.4, 126.0, 124.7, 124.5, 116.5, 62.3, 56.7, 42.0, 29.1, 26.2, 24.1, 23.9. HRMS (EI) *m/z* calcd for C₁₅H₂₂O₂ (M)⁺ 234.1620, found 193.1231 (M-41)



(±)-(E)-5-(3-Isopropyl-2-methoxyphenyl)-5-methoxy-2-methylpent-2-enal (68**):**

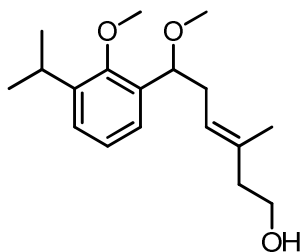
A solution of **66** (1.9945 g, 8.51 mmol) and methacrolein (4.4 mL, 42.7 mmol) in 50 mL dry Et₂O was degassed by bubbling argon through the solution with stirring for 30 minutes. To this solution was added half of a mixture of Grubbs 2nd Generation Catalyst (72.3 mg, 0.0852 mmol total) and CuI (39.0 mg, 0.205 mmol) and the mixture was heated to reflux for 1 hr. At this point, the rest of the catalyst mixture was added and the mixture refluxed for another 1.5 hrs, after which time TLC showed the reaction was complete. The mixture was cooled to RT, quenched with 10 mL ethyl vinyl ether, stirred 10 minutes, then concentrated. The residue was chromatographed on silica gel (neutralized with Et₃N) with 5-10% EtOAc/Hexanes to isolate the title compound as a yellow oil. (1.7251g, 73.3% yield) ¹H NMR (400 MHz, Benzene-d₆) δ = 9.32 (s, 1 H), 7.30 (dd, *J* = 1.9, 7.3 Hz, 1 H), 7.09 (dd, *J* = 2.2, 7.7 Hz, 1 H), 7.05 (t, *J* = 7.4 Hz, 1 H), 6.35 (dt, *J* = 1.4, 7.3 Hz, 1 H), 4.57 (dd, *J* =

4.7, 8.0 Hz, 1 H), 3.41 - 3.39 (m, 3 H), 3.30 (spt, $J = 7.1$ Hz, 1 H), 3.07 (s, 3 H), 2.68 - 2.48 (m, 2 H), 1.58 (d, $J = 1.3$ Hz, 3 H), 1.17 (t, $J = 7.1$ Hz, 6 H). ^{13}C NMR (101 MHz, Benzene- d_6) $\delta = 194.3, 156.2, 149.9, 142.5, 141.2, 135.0, 126.9, 125.6, 125.2, 77.6, 62.2, 57.0, 37.8, 26.9, 24.7, 24.1, 9.6$.



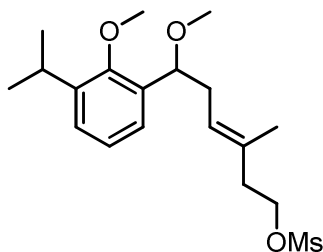
(±)-(E)-1-Isopropyl-2-methoxy-3-(1-methoxy-4-methylhexa-3,5-dienyl)benzene (69):

To a suspension of methyltriphenylphosphonium iodide (5.28 g, 13.3 mmol) in 130 mL dry THF at 0°C was added solid KHMDS (2.4082 g, 11.47 mmol). The resulting yellow suspension was warmed to RT and stirred 30 minutes. At this point, a solution of aldehyde **68** (2.7415 g, 9.92 mmol) in 20 mL THF was charged via cannula at RT, forming a thick yellow/white slurry. This mixture was stirred 20 minutes, then poured into 400 mL hexanes, forming a white slurry. The solids were removed by filtration through a pad of Celite and the filtrate was concentrated and chromatographed on a short silica gel column, eluting with 5% EtOAc/Hexane. The title compound was isolated as a clear, colourless oil (2.531 g, 93%). ^1H NMR (400 MHz, CDCl_3) $\delta = 7.25$ (dd, $J = 1.9, 7.3$ Hz, 1 H), 7.21 (dd, $J = 2.0, 7.7$ Hz, 1 H), 7.15 (t, $J = 7.5$ Hz, 1 H), 6.39 (dd, $J = 10.7, 17.4$ Hz, 1 H), 5.61 (t, $J = 7.2$ Hz, 1 H), 5.08 (d, $J = 17.4$ Hz, 1 H), 4.93 (d, $J = 10.7$ Hz, 1 H), 4.60 (dd, $J = 5.4, 7.7$ Hz, 1 H), 3.75 (s, 3 H), 3.33 (spt, $J = 6.9$ Hz, 1 H), 3.26 (s, 3 H), 2.68 - 2.49 (m, 2 H), 1.67 (s, 3 H), 1.27 (d, $J = 7.0$ Hz, 3 H), 1.24 (d, $J = 7.1$ Hz, 3 H). ^{13}C NMR (101 MHz, CDCl_3) $\delta = 155.4, 141.7, 141.5, 135.5, 134.7, 129.1, 125.9, 124.7, 124.5, 110.8, 77.6, 62.2, 56.8, 36.5, 26.2, 24.2, 23.8, 11.7$.



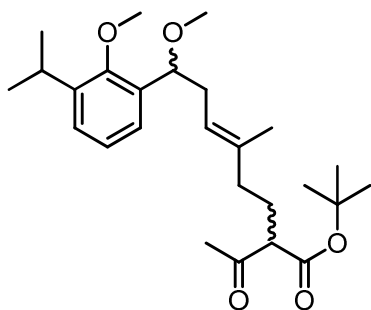
(±)-(E)-6-(3-Isopropyl-2-methoxyphenyl)-6-methoxy-3-methylhex-3-en-1-ol (70):

To a solution of $\text{BH}_3 \cdot \text{DMS}$ (0.98 mL, 9.71 mL) in 33 mL dry THF at 0°C was added cyclohexene (1.96 mL, 19.4 mmol) slowly over ca. 5 minutes. The resulting mixture was stirred 1 hr at 0°C , by which time a white slurry had formed. To this was added a solution of diene **69** (2.531 g, 9.23 mmol) in 25 mL dry THF quickly via syringe and the mixture was stirred overnight, slowly warming to RT, forming a clear solution. This solution was re-cooled to 0°C and quenched by addition of 30 mL of a 2M aqueous solution of NaOH – slowly at first, though little effervescence occurred – and 13 mL of a 35 wt. % aqueous solution of H_2O_2 . A reflux condenser was equipped to the flask and the mixture was heated to 55°C for 3 hours, adding a second 13 mL portion of H_2O_2 through the condenser after 1.5 hours. The mixture was then cooled to RT, diluted with water and extracted 3x with Et_2O . The combined organic fractions were washed with brine, dried with Na_2SO_4 and concentrated. The residue was purified by column chromatography on a short silica gel column with 20% EtOAc/Hexane. Isolated **70** as a clear, colourless oil (2.65 g, 98.3%). IR (neat, cm^{-1}): 3391br, 2937, 2860. ^1H NMR (400 MHz, CDCl_3) δ = 7.26 (dd, J = 2.2, 7.4 Hz, 1 H), 7.21 (dd, J = 2.3, 7.4 Hz, 1 H), 7.16 (t, J = 7.4 Hz, 1 H), 5.26 (t, J = 7.1 Hz, 1 H), 4.54 (t, J = 6.8 Hz, 1 H), 3.75 (s, 3 H), 3.66 - 3.51 (m, 2 H), 3.31 (spt, J = 6.9 Hz, 1 H), 3.27 (s, 3 H), 2.58 (ddd, J = 6.8, 7.1, 14.4 Hz, 1 H), 2.39 (ddd, J = 6.8, 7.1, 14.4 Hz, 1 H), 2.26 - 2.09 (m, 2 H), 2.00 (br. s, 1 H), 1.39 (s, 3 H), 1.27 (d, J = 7.0 Hz, 3 H), 1.22 (d, J = 6.9 Hz, 3 H). ^{13}C NMR (101 MHz, CDCl_3) δ = 155.0, 141.7, 134.7, 133.6, 126.0, 125.0, 124.4, 123.2, 77.6, 62.1, 59.6, 56.7, 42.7, 36.6, 26.1, 24.3, 23.8, 15.5. HRMS (EI) m/z calcd for $\text{C}_{18}\text{H}_{28}\text{O}_3$ (M) $^+$ 292.2038, found 260.1757 (M-32)



(±)-(E)-6-(3-Isopropyl-2-methoxyphenyl)-6-methoxy-3-methylhex-3-enyl methanesulfonate (71):

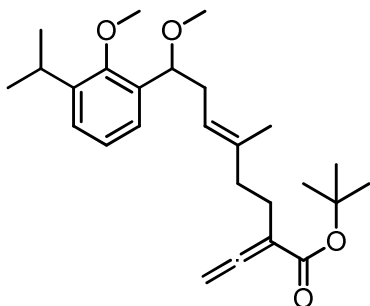
To a solution of **70** (4.25 g, 14.55 mmol) and Et₃N (3.0 mL, 21.5 mmol) in 50 mL dry CH₂Cl₂ at 0°C was added methanesulfonyl chloride (1.8 mL, 23.2 mmol) dropwise. The resulting solution was stirred at 0°C for 2 hours, then poured into 50 mL ice water. After layer separation, the aqueous phase was extracted 3x with DCM and the combined organic fractions washed with 50% saturated brine, dried with Na₂SO₄, and concentrated. The crude mesylate was used directly in the subsequent reaction without further purification.



(±)-(E)-tert-Butyl-2-acetyl-8-(3-isopropyl-2-methoxyphenyl)-8-methoxy-5-methyloct-5-enoate (72):

To a suspension of NaH (1.69 g, 42.18 mmol) in 80 mL dry THF at 0°C was added dropwise *t*-butyl acetoacetate (7.5 mL, 44.32 mmol). The resultant yellow solution was warmed to RT and stirred 1 hour, then 40 mL DMF, a solution of mesylate **71** (14.55 mmol, 0.5M in THF) and KI (775 mg, 4.67 mmol) were charged sequentially to the reaction mixture, which was then heated to 70°C overnight. The mixture was cooled to RT, quenched with saturated aqueous NH₄Cl, then extracted 3x with Et₂O. The combined organic fractions were washed twice with water, once with brine, dried with Na₂SO₄ and concentrated. Residual acetoacetate was removed by vacuum distillation at ~100°C and the residue was chromatographed on silica gel with 7% ethyl acetate/hexanes. The title compound was

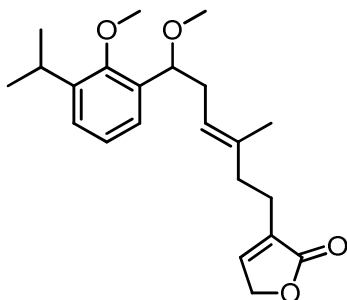
isolated as a yellow oil (2.41 g, 38% over 2 steps from **70**). IR (neat, cm^{-1}): 2968, 2827, 1737, 1715. ^1H NMR (400 MHz, CDCl_3) δ = 7.23 (dd, J = 1.9, 7.3 Hz, 1 H), 7.20 (dd, J = 1.9, 7.3 Hz, 1 H), 7.13 (t, J = 7.5 Hz, 1 H), 5.24 (d, J = 5.5 Hz, 1 H), 4.58 - 4.51 (m, 1 H), 3.75 (s, 3 H), 3.30 (spt, J = 7.1 Hz, 2 H), 3.24 (s, 3 H), 2.42 (d, J = 5.5 Hz, 2 H), 2.20 (d, J = 3.7 Hz, 3 H), 2.00 - 1.92 (m, 2 H), 1.92 - 1.84 (m, 2 H), 1.47 (d, J = 3.2 Hz, 9 H), 1.26 (d, J = 6.9 Hz, 3 H), 1.22 (d, J = 7.0 Hz, 3 H). ^{13}C NMR (101 MHz, CDCl_3) δ = 203.7, 169.0, 169.0, 155.4, 155.4, 141.6, 141.6, 135.6, 134.9, 125.8, 125.8, 124.6, 122.1, 122.1, 81.7, 77.9, 62.2, 59.9, 59.9, 56.7, 37.1, 36.1, 36.1, 29.0, 28.9, 27.9, 26.2, 24.2, 23.8, 23.8, 15.8, 15.8. HRMS (EI) m/z calcd for $\text{C}_{26}\text{H}_{40}\text{O}_5$ (M) $^+$ 432.2876, found 327.1971 (M-105)



(±)-(E)-tert-Butyl-8-(3-isopropyl-2-methoxyphenyl)-8-methoxy-5-methyl-2-vinylideneoct-5-enoate (73**):**

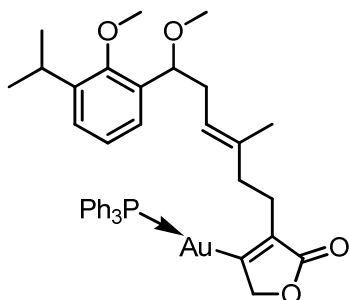
To a solution of LiHMDS (104.1 mg, 0.6035 mmol) in 1 mL THF at -78°C was charged dropwise a solution of **72** (117 mg, 0.2705 mmol) in 2.7 mL THF. The resulting yellow solution was stirred 45 minutes at -78°C , then Tf_2O (1 mL of a 0.29M solution in Et_2O) was slowly added over 15 minutes. Stirring was continued at -78°C for 1 hour, then another solution of LiHMDS (114.5 mg, 0.6637 mmol) in 2 mL THF was charged and the reaction stirred for 45 minutes. HMPA (0.17 mL, 0.98 mmol) was added to the reaction mixture, which was stirred another 45 minutes, then ZnCl_2 (1M solution in Et_2O , 0.67 mL) was added and the reaction stirred a final hour at -78°C . The reaction was quenched by pouring into a cold (0°C) biphasic mixture of saturated aqueous NH_4Cl and Et_2O . This biphasic mixture was separated and the aqueous fraction extracted twice with Et_2O . The combined organic fractions were washed with brine, dried with MgSO_4 and concentrated. The residue was chromatographed on silica gel with 2% EtOAc /hexanes to isolate **73** as a colourless oil (59.1 mg, 52.7% yield). IR (neat, cm^{-1}): 3435, 2968, 2818, 1969, 1939, 1701.

^1H NMR (400 MHz, CDCl_3) δ = 7.24 (dd, J = 2.0, 7.4 Hz, 1 H), 7.20 (dd, J = 2.1, 7.6 Hz, 1 H), 7.13 (t, J = 7.4 Hz, 1 H), 5.27 (t, J = 6.6 Hz, 1 H), 5.03 (dt, J = 1.0, 3.0 Hz, 2 H), 4.55 (dd, J = 5.4, 7.9 Hz, 1 H), 3.75 (s, 3 H), 3.32 (spt, J = 7.0 Hz, 1 H), 3.24 (s, 2 H), 2.52 - 2.35 (m, 2 H), 2.25 (d, J = 9.1 Hz, 2 H), 2.10 (t, J = 8.3 Hz, 2 H), 1.54 (s, 3 H), 1.47 (s, 9 H), 1.26 (d, J = 6.9 Hz, 3 H), 1.23 (d, J = 6.9 Hz, 3 H). ^{13}C NMR (101 MHz, CDCl_3) δ = 213.7, 166.5, 155.4, 141.6, 136.2, 135.0, 125.8, 124.6, 124.6, 121.3, 101.4, 80.7, 78.5, 77.9, 62.2, 56.7, 38.1, 36.1, 28.1, 26.7, 26.2, 24.2, 23.9, 16.1. HRMS (EI) m/z calcd for $\text{C}_{26}\text{H}_{38}\text{O}_4$ (M) $^+$ 414.2770, found 326.1879 (M-88)



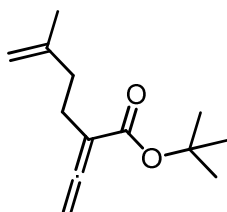
(±)-(E)-3-(6-(3-Isopropyl-2-methoxyphenyl)-6-methoxy-3-methylhex-3-enyl)furan-2(5H)-one (74):

To **73** (22.1 mg, 0.0533mmol) in a sealed glass vial was charged a solution of AuCl (1.5 mg, 0.0065 mmol) in 1mL DCM (containing ~0.01 mL H_2O). The resulting solution was stirred at RT for 6 hours, then concentrated *in vacuo*. ^1H NMR analysis of the residue showed >90% conversion, so the residue was chromatographed on silica gel with 10% EtOAc/hexanes to isolate **74** as a waxy, colourless oil. No yield recorded. IR (neat, cm^{-1}): 3490, 2966, 2936, 1761, 1756, 1751. ^1H NMR (400 MHz, CDCl_3) δ = 7.20 (dd, J = 1.9, 6.9 Hz, 1 H), 7.22 (dd, J = 2.0, 7.0 Hz, 2 H), 7.13 (t, J = 7.4 Hz, 1 H), 7.06 (t, J = 1.7 Hz, 1 H), 5.27 (dt, J = 1.2, 7.1 Hz, 1 H), 4.74 (q, J = 2.0 Hz, 2 H), 4.55 (dd, J = 5.4, 7.6 Hz, 1 H), 3.75 (s, 3 H), 3.32 (spt, J = 6.8 Hz, 1 H), 3.24 (s, 3 H), 2.53 - 2.36 (m, 4 H), 2.24 (t, J = 7.7 Hz, 2 H), 1.56 (s, 3 H), 1.26 (d, J = 7.0 Hz, 3 H), 1.23 (d, J = 7.0 Hz, 3 H). ^{13}C NMR (101 MHz, CDCl_3) δ = 174.4, 155.4, 144.3, 141.7, 135.2, 134.8, 133.9, 125.9, 124.6, 124.5, 122.0, 77.8, 70.1, 62.2, 56.7, 37.1, 36.0, 26.2, 24.2, 23.8, 23.4, 16.0. HRMS (EI) m/z calcd for $\text{C}_{22}\text{H}_{30}\text{O}_4$ (M) $^+$ 358.2144, found 326.1872 (M-32)



(±)-(E)-4-[(Triphenylphosphino)gold]-3-(6-(3-isopropyl-2-methoxyphenyl)-6-methoxy-3-methylhex-3-enyl)furan-2(5H)-one (75):

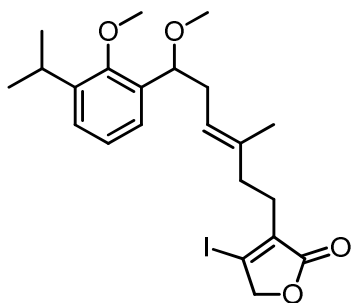
To a solution of **73** (321 mg, 0.770 mmol) in 20 mL dry DCM was added 2,6-di-*tert*-butyl-4-methylpyridine (771 mg, 3.75 mmol) and (PPh₃AuNTf₂)₂•PhMe (605.1 mg, 0.770 mmol Au). This solution was stirred at RT for 1.75 hours, then silica gel was added and the slurry concentrated to a dry-pack, which was chromatographed on silica gel with 10-30% EtOAc/hexanes to isolate **75** as a semicrystalline white solid (486 mg, 77.3% yield). ¹H NMR (300 MHz, CDCl₃) δ = 7.59 - 7.43 (m, 15 H), 7.21 (dd, *J* = 2.1, 7.2 Hz, 1 H), 7.17 (dd, *J* = 2.1, 7.7 Hz, 1 H), 7.10 (t, *J* = 7.6 Hz, 1 H), 5.30 (t, *J* = 7.3 Hz, 1 H), 4.86 (s, 1 H), 4.52 (dd, *J* = 5.8, 8.0 Hz, 1 H), 3.71 (s, 2 H), 3.31 (spt, *J* = 7.2 Hz, 1 H), 3.20 (s, 2 H), 2.54 - 2.35 (m, 4 H), 1.54 (s, 3 H), 1.23 (t, *J* = 7.2 Hz, 6 H). ¹³C NMR (101 MHz, CDCl₃) δ = 141.6, 136.8, 135.1, 134.3, 134.1, 131.5, 130.2, 129.7, 129.3, 129.2, 125.7, 124.5, 121.0, 77.9, 62.2, 56.7, 40.3, 36.3, 26.2, 24.1, 23.9, 16.3. ³¹P NMR (122 MHz, CDCl₃) δ = 44.20.



***tert*-Butyl 5-methyl-2-vinylidenehex-5-enoate (76):**

To a solution of LiHMDS (2.08 g, 12.0 mmol) in THF (0.36M) at -78°C was charged **56** (1.24 g, 5.47 mmol) dropwise. The resulting yellow solution was stirred for 45 minutes at -78°C, then Tf₂O (0.95 mL, 5.59 mmol) was added dropwise over 5 minutes. Stirring was continued for 1 hour at -78°C, then another solution of LiHMDS (1.05 g, 6.09 mmol) in THF

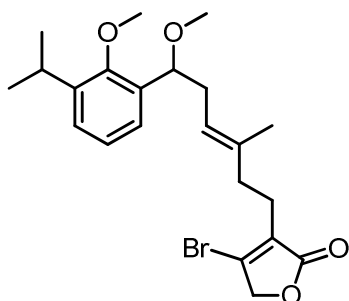
(1M) was added. Stirring was continued at -78°C for 30 minutes, then HMPA (3.4 mL, 19.5 mmol) was added and the mixture stirred for another 30 minutes. A solution of ZnCl_2 (1M in Et_2O , 6.6 mL) was added and the mixture was stirred a final 30 minutes at -78°C . The reaction was quenched by pouring into a cold (0°C) biphasic mixture of saturated aqueous NH_4Cl and Et_2O . Layers were separated and the aqueous fraction extracted twice with Et_2O . The combined organic fractions were washed with brine, dried with MgSO_4 and concentrated. The residue was purified by column chromatography on silica gel with 2% EtOAc /hexanes to isolate **76** as a colourless oil (444 mg, 39% yield). ^1H NMR (400 MHz, CDCl_3) δ = 5.08 (t, J = 2.9 Hz, 2 H), 4.77 - 4.66 (m, 2 H), 2.39 - 2.26 (m, 2 H), 2.21 - 2.10 (m, 2 H), 1.74 (s, 3 H), 1.48 (s, 9 H). ^{13}C NMR (101 MHz, CDCl_3) δ = 213.6, 166.4, 145.0, 110.4, 80.8, 78.7, 36.0, 28.1, 26.3, 22.4.



(±)-(E)-4-Iodo-3-(6-(3-isopropyl-2-methoxyphenyl)-6-methoxy-3-methylhex-3-enyl)furan-2(5H)-one (77):

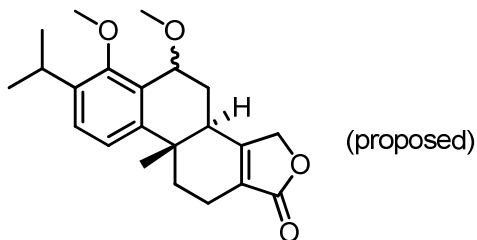
To a solution of **75** (148.9 mg, 0.1823 mmol) in 5 mL acetone was added *N*-iodosuccinimide (44.8 mg, 0.193 mmol) in one portion. The resulting solution was stirred at RT 10 minutes, by which time TLC showed complete consumption of starting material. The mixture was concentrated, then flushed through a silica gel plug with 20% EtOAc /hexanes. After concentration, **77** was isolated as a colourless, waxy oil (82.7 mg, 93.6% yield). ^1H NMR (400 MHz, CDCl_3) δ = 7.25 - 7.17 (m, 2 H), 7.17 - 7.11 (m, 1 H), 5.24 (t, J = 6.9 Hz, 1 H), 4.73 (s, 2 H), 4.54 (dd, J = 5.5, 7.4 Hz, 1 H), 3.75 (s, 3 H), 3.33 (spt, J = 6.9 Hz, 1 H), 3.24 (s, 3 H), 2.51 - 2.33 (m, 4 H), 2.26 - 2.14 (m, 2 H), 1.62 - 1.58 (m, 3 H), 1.26 (d, J = 6.9 Hz, 3 H), 1.24 (d, J = 6.9 Hz, 3 H). ^{13}C NMR (101 MHz, CDCl_3) δ = 169.9, 155.4, 141.7,

138.4, 134.9, 134.9, 125.9, 124.6, 124.5, 122.4, 114.2, 77.7, 76.3, 62.2, 56.7, 36.6, 36.2, 26.2, 25.6, 24.2, 23.9, 16.2.



(±)-(E)-4-Bromo-3-(6-(3-isopropyl-2-methoxyphenyl)-6-methoxy-3-methylhex-3-enyl)furan-2(5H)-one (78):

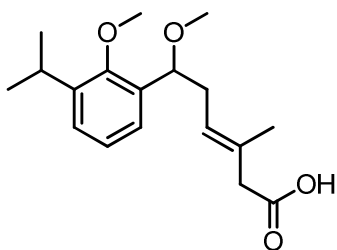
Experimental procedure as per the synthesis of **77**, utilizing *N*-bromosuccinimide as the halogen source. Incomplete conversion and some protodeauration were observed by TLC, likely due to residual HBr in the commercial *N*-bromosuccinimide, which was not recrystallized before use. The title compound was isolated as a colourless, waxy oil (17.2 mg, 45.6% yield). ¹H NMR (400 MHz, CDCl₃) δ = 7.25 - 7.18 (m, 2 H), 7.13 (t, *J* = 7.6 Hz, 1 H), 5.24 (t, *J* = 6.9 Hz, 1 H), 4.74 (s, 2 H), 4.54 (dd, *J* = 5.5, 7.5 Hz, 1 H), 3.75 (s, 3 H), 3.32 (spt, *J* = 7.0 Hz, 1 H), 3.24 (s, 3 H), 2.50 - 2.33 (m, 4 H), 2.27 - 2.17 (m, 2 H), 1.60 (s, 3 H), 1.26 (d, *J* = 7.0 Hz, 3 H), 1.23 (d, *J* = 7.0 Hz, 3 H). ¹³C NMR (101 MHz, CDCl₃) δ = 166.7, 155.4, 134.9, 124.6, 124.5, 122.3, 77.7, 72.8, 62.2, 56.7, 36.4, 36.2, 26.2, 24.2, 23.9, 23.3, 16.0.



(±)-(3bR,9bS)-7-Isopropyl-5,6-dimethoxy-9b-methyl-3b,4,5,9b,10,11-hexahydrophenanthro[2,1-c]furan-1(3H)-one (79):

A solution of either **77** or **78** and [Au] (10 mol%) in acetonitrile (0.05 M) was degassed by sparging with Ar at RT for 15 minutes in a sealed Pyrex tube equipped with a

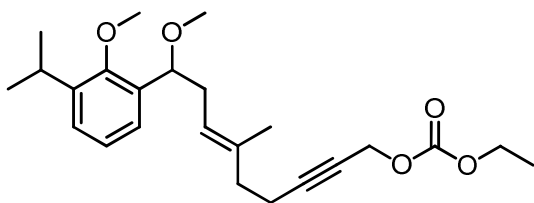
septum. DIPEA (2 equivalents) was charged to the reaction mixture, which was then taken outdoors and exposed to sunlight (Moderate to High UV Index) for 2.5 hours. Upon exposure to light, the solution turned from colourless to yellow (**77**) or orange (**78**) within 2 minutes. After the reaction was deemed complete, the mixture was concentrated, then reconstituted in Et₂O, whereby a white precipitate formed. This precipitate was removed by filtration through a plug of silica gel, washing with Et₂O. After concentration of the filtrate, the residue was chromatographed on silica gel with 30% EtOAc/hexanes to isolate a white, waxy solid believed to be **79**. Diastereomer 1: ¹H NMR (300 MHz, CDCl₃) δ = 7.27 (d, *J* = 8.4 Hz, 1 H), 7.17 (d, *J* = 8.4 Hz, 1 H), 4.95 (td, *J* = 3.0, 16.5 Hz, 1 H), 4.74 (br. dd, *J* = 3.0, 16.5 Hz, 1 H), 4.64 (td, *J* = 3.0, 9.4 Hz, 1 H), 3.85 (s, 3 H), 3.49 (s, 3 H), 3.34 (spt, *J* = 7.0 Hz, 1 H), 2.85 (d, *J* = 13.1 Hz, 1 H). Diastereomer 2: ¹H NMR (300 MHz, CDCl₃) δ = 7.24 (d, *J* = 8.7 Hz, 1 H), 7.14 (d, *J* = 8.7 Hz, 1 H), 5.00 (dd, *J* = 4.5, 16.2 Hz, 1 H), 4.65 (br. d, *J* = 15.7 Hz, 1 H), 4.42 (t, *J* = 3.9 Hz, 1 H), 3.79 (s, 3 H), 3.42 (s, 3 H), 3.31 (spt, *J* = 7.2 Hz, 2 H). ¹³C NMR (mixture of diastereomers) (DEPT-135) (126 MHz, CDCl₃) δ = 127.3, 127.3, 123.3, 121.7, 120.8, 77.2, 71.9, 71.5, 71.1, 70.9, 70.5, 70.4, 62.5, 62.3, 56.6, 56.4, 39.2, 36.6, 36.0, 35.4, 32.1, 31.9, 31.8, 30.0, 29.7, 26.2, 26.0, 25.9, 25.4, 25.1, 24.1, 24.0, 23.8, 22.7, 18.3, 17.9, 17.5, 14.1 HRMS (EI) *m/z* calcd for C₂₂H₂₈O₄ (M)⁺ 356.1988, found 356.1988



(±)-(E)-6-(3-Isopropyl-2-methoxyphenyl)-6-methoxy-3-methylhex-3-enoic acid (82**):**

A solution of alcohol **70** (857 mg, 3.12 mmol) in 20 mL acetone at 0°C was titrated with a solution of Jones' Reagent until an orange colour persisted in solution. The resulting mixture was stirred at RT for 30 minutes, then quenched by addition of 10 mL methanol, whereby the mixture turned dark green. The mixture was filtered to remove suspended solids; the filtrate was diluted with water (3 volumes), and extracted twice with EtOAc. The combined organic fractions were washed with brine, dried with Na₂SO₄ and concentrated.

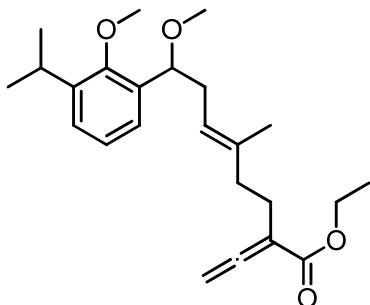
The residue was chromatographed on silica gel with 10-40% EtOAc/hexanes to isolate **82** as a yellow, viscous oil (411 mg, 43% yield). ^1H NMR (300 MHz, CDCl_3) δ = 7.24 (dd, J = 2.2, 7.4 Hz, 1 H), 7.21 (dd, J = 1.9, 8.4 Hz, 1 H), 7.14 (t, J = 7.6 Hz, 1 H), 5.42 (t, J = 7.6 Hz, 1 H), 4.58 (dd, J = 5.6, 7.4 Hz, 1 H), 3.75 (s, 3 H), 3.32 (spt, J = 6.9 Hz, 1 H), 3.25 (s, 3 H), 3.03 (s, 2 H), 2.63 - 2.35 (m, 2 H), 1.62 (d, J = 1.0 Hz, 3 H), 1.26 (d, J = 6.9 Hz, 3 H), 1.23 (d, J = 6.9 Hz, 3 H)



(±)-(E)-Ethyl-9-(3-isopropyl-2-methoxyphenyl)-9-methoxy-6-methylnon-6-en-2-ynyl carbonate (90):

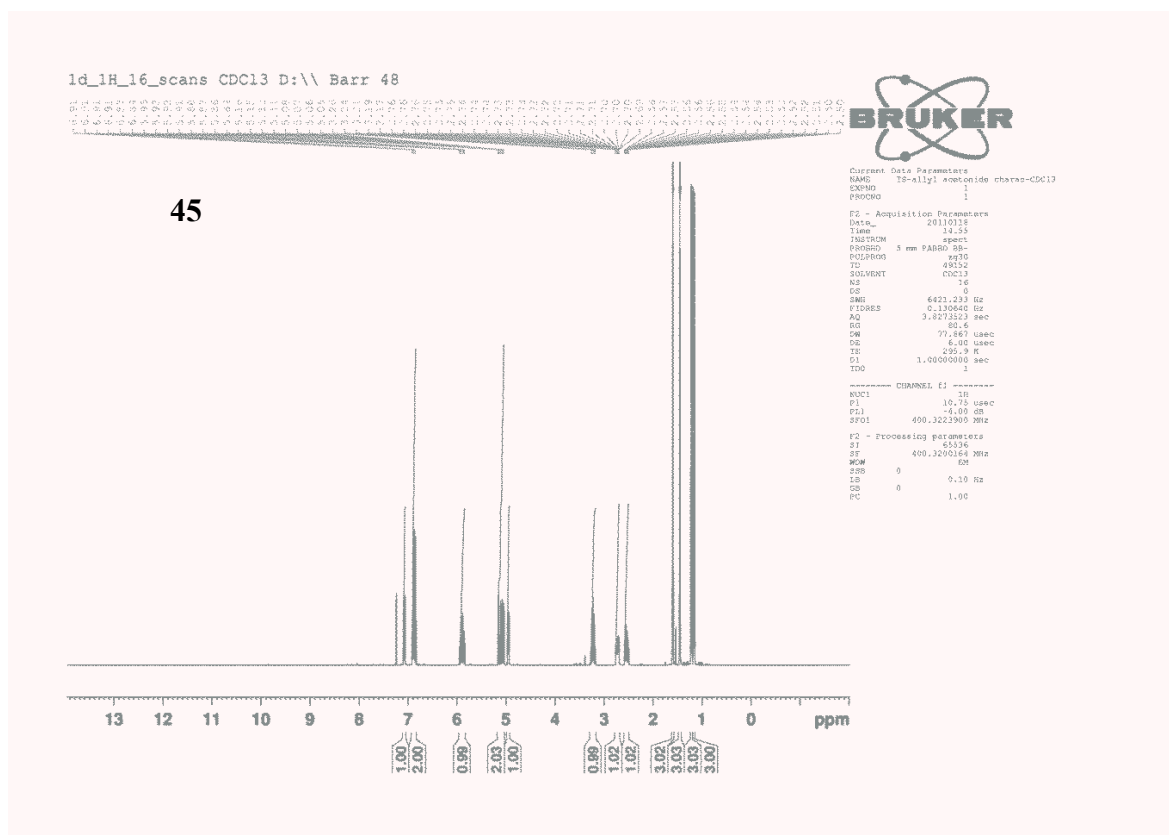
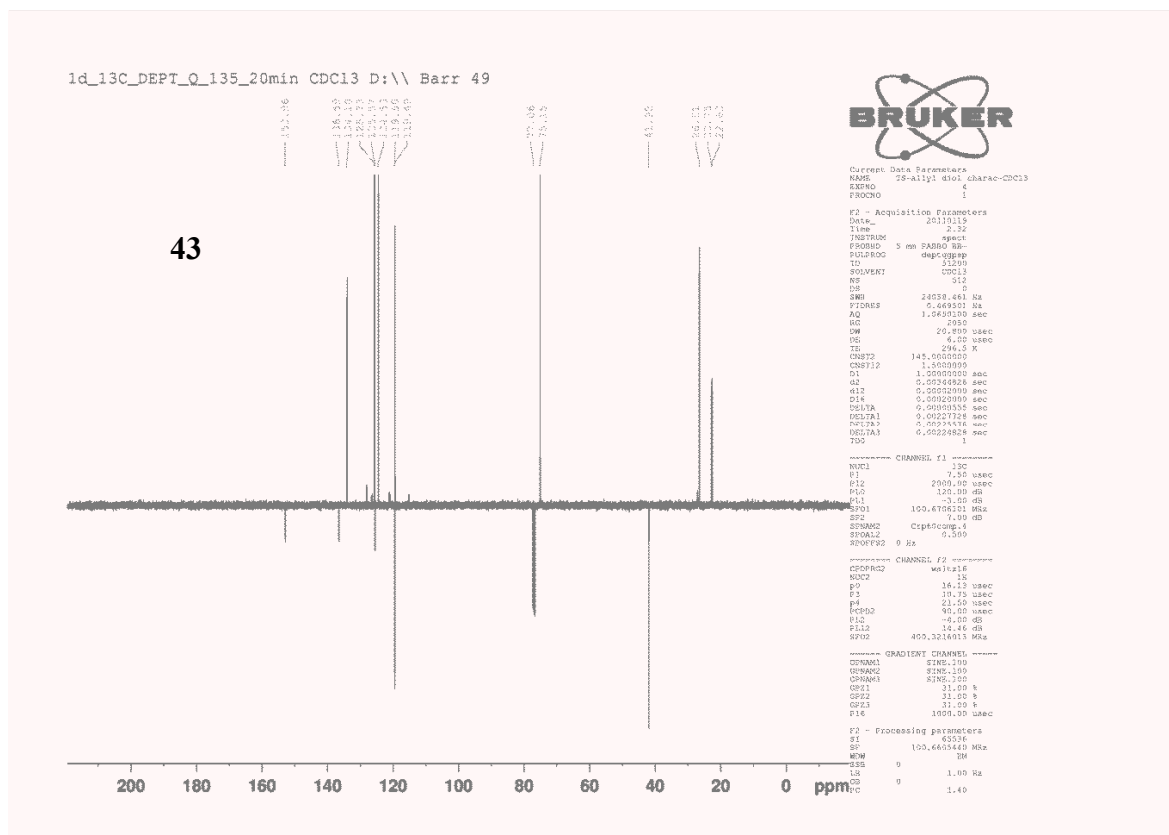
A 0.5M solution of Cy_2BH was prepared by charging cyclohexene (0.41 mL, 4.00 mmol) to a solution of $\text{BH}_3\cdot\text{DMS}$ (0.2 mL, 1.99 mmol) in THF at 0°C , stirring 1 hour to complete reaction – a white slurry indicated successful formation of Cy_2BH . To this slurry was charged a solution of diene **69** (520 mg, 1.9 mmol) as a 1M solution in THF. The reaction mixture was warmed to RT and stirred for 3.5 hours. To this mixture, 4mL N,N -dimethylacetamide was charged and the mixture re-cooled to 0°C , at which time **89** (370 mg, 2.89 mmol), $\text{Cu}(\text{OAc})_2\cdot\text{H}_2\text{O}$ (774.9 mg, 3.80 mmol) and $\text{Cu}(\text{acac})_2$ (249.6 mg, 0.95 mmol) were charged consecutively to the reaction mixture. The resulting blue-green slurry was warmed to RT and stirred overnight. The reaction was quenched by pouring into a saturated aqueous solution of Borax (20 mL) and stirring 2 hours at RT. The resulting slurry was diluted with H_2O to dissolve solids and extracted 3x with EtOAc. The combined organic fractions were washed with 1M HCl and brine, dried with Na_2SO_4 and concentrated. The residue was chromatographed on silica gel with 10% EtOAc/hexanes to isolate **90** as a clear, pale yellow oil (122.6 mg, 16% yield). ^1H NMR (400 MHz, CDCl_3) δ = 7.25 - 7.17 (m, 2 H), 7.16 - 7.08 (m, 1 H), 5.27 (t, J = 6.6 Hz, 1 H), 4.70 (t, J = 2.0 Hz, 2 H), 4.55 (dd, J = 5.4, 7.5 Hz, 1 H), 4.27 - 4.17 (m, 2 H), 3.76 - 3.70 (m, 3 H), 3.32 (spt, J = 6.9 Hz, 1 H), 3.26 - 3.19 (m, 3 H), 2.53 - 2.33 (m, 2 H), 2.32 - 2.23 (m, 2 H), 2.22 - 2.12 (m, 2 H), 1.51 (s, 3 H), 1.32 (t, J = 7.2 Hz, 3 H), 1.26 (d, J = 7.1 Hz, 3 H), 1.23 (d, J = 7.1 Hz, 3 H). ^{13}C NMR (101 MHz,

CDCl₃) δ = 155.4, 154.7, 141.6, 135.2, 134.8, 125.8, 124.6, 121.8, 88.2, 77.8, 73.6, 64.3, 62.2, 56.8, 56.0, 38.3, 36.0, 26.2, 24.2, 23.8, 17.9, 15.9, 14.2.



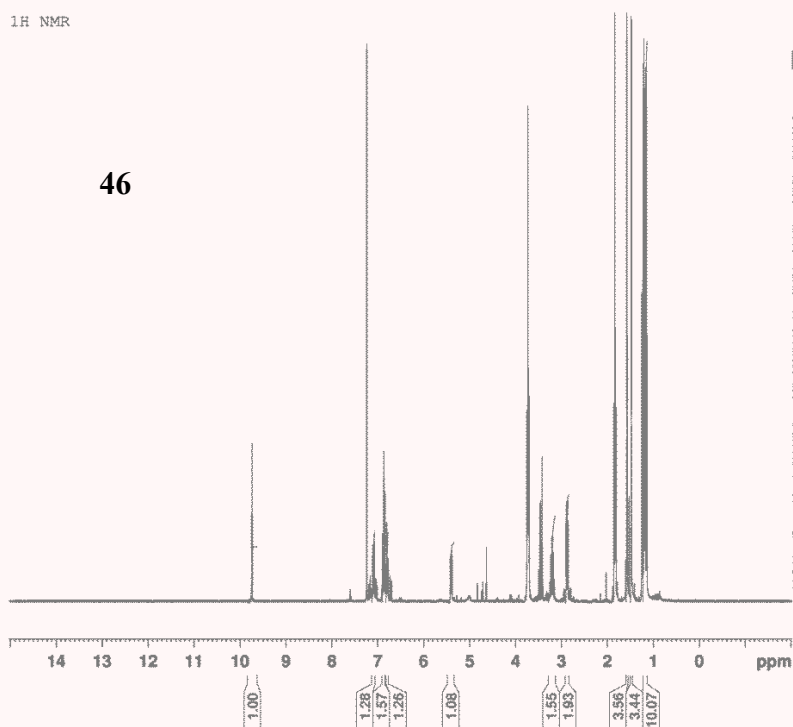
(±)-(E)-Ethyl 8-(3-isopropyl-2-methoxyphenyl)-8-methoxy-5-methyl-2-vinylideneoct-5-enoate (88):

Pd(PPh₃)₄ (40mg, 0.035mmol) was charged to a solution of **90** (172mg, 0.427mmol) in 2 mL benzene and 1 mL 99% ethanol in an autoclave glass liner, forming an orange solution. The autoclave was assembled and the atmosphere purged with CO five times, then pressurized to 400 psi with CO. The autoclave was then placed in a 50°C oil bath and stirred overnight. The resulting dark red solution was concentrated, reconstituted in hexanes, then filtered and concentrated again. ¹H NMR of the residue showed multiple products, including the desired allenolate. The residue was chromatographed on silica gel with 2-5% EtOAc/hexanes to isolated **88** as a colourless oil (~5% yield, unoptimized). Note: this yield could likely be improved by running the reaction at lower temperatures, as these allenolates are temperature sensitive. IR (neat, cm⁻¹): 3431, 2960, 2822, 1745, 1714. ¹H NMR (400 MHz, CDCl₃) δ = 7.23 (dd, J = 2.0, 7.3 Hz, 1 H), 7.20 (dd, J = 1.8, 7.7 Hz, 1 H), 7.13 (t, J = 7.5 Hz, 1 H), 5.27 (t, J = 6.7 Hz, 1 H), 5.09 (t, J = 2.7 Hz, 2 H), 4.55 (dd, J = 5.3, 7.6 Hz, 1 H), 4.20 (q, J = 7.1 Hz, 2 H), 3.74 (s, 3 H), 3.32 (spt, J = 6.9 Hz, 1 H), 3.24 (s, 3 H), 2.52 - 2.35 (m, 2 H), 2.35 - 2.26 (m, 2 H), 2.16 - 2.05 (m, 2 H), 1.54 (s, 3 H), 1.29 (t, J = 7.3 Hz, 3 H), 1.26 (d, J = 7.2 Hz, 3 H), 1.23 (d, J = 7.0 Hz, 3 H). ¹³C NMR (101 MHz, CDCl₃) δ = 213.8, 167.2, 155.4, 141.6, 136.0, 134.9, 125.8, 124.6, 124.6, 121.4, 100.0, 79.0, 77.9, 62.2, 60.9, 56.7, 37.9, 36.1, 26.5, 26.2, 24.1, 23.8, 16.1, 14.2. HRMS (EI) m/z calcd for C₂₄H₃₄O₄ (M)⁺ 386.2457, found 326.1879 (M-60)



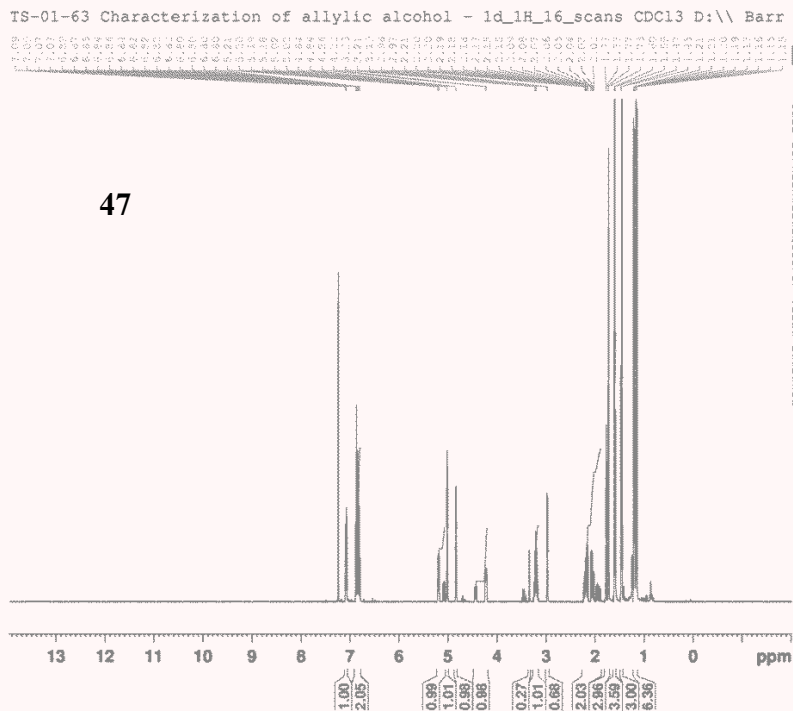
¹H NMR

46

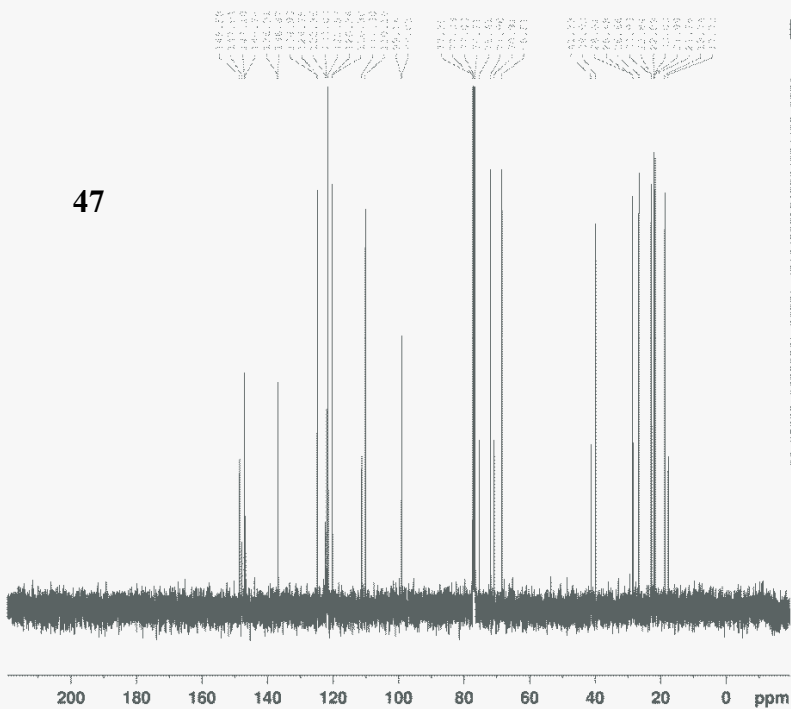


TS-01-63 Characterization of allylic alcohol - 1d_1H_16_scans CDC13 D:\ Barr

47



1d_13C_20_minutes CDC13 D:\ Barr 50



```

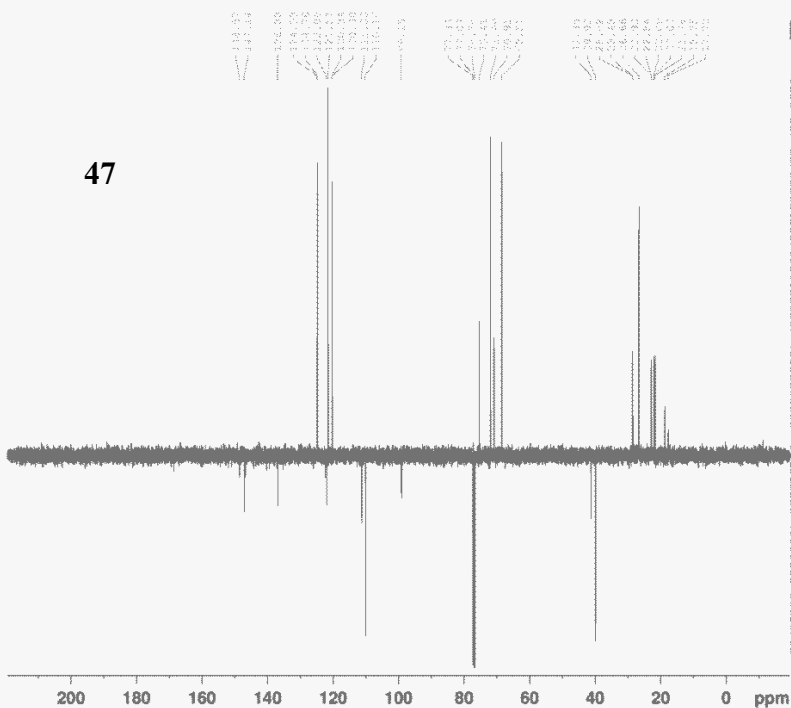
Current Data Parameters
NAME 75-leucoprophenol alcohol charew-CDC13
PROCNO 1

F2 - Acquisition Parameters
DATE_ 20111114
TIME 17.24
INSTRUM spect
PROBHD 5 mm PA100 1H
PULPROG zgpg30
PC 1300
SOLVENT CDCl3
NS 1312
DS 4
SFO 200.136101 MHz
FIDRES 0.449901 Hz
AQ 1.093100 sec
RG 133
SF 200.136101 MHz
WDW EM
SS 30.000 usec
DE 4.00 usec
TE 293.2 K
D1 1.0000000 sec
d11 0.0000000 sec
DELTA 0.8999998 sec
DDE 1

----- CHANNEL f1 -----
NUC1 13C
P1 1.00 usec
PL1 0.00 dB
PL12 19.00 dB
PL13 19.00 dB
PL14 19.00 dB
PL15 19.00 dB
PL16 19.00 dB
PL17 19.00 dB
PL18 19.00 dB
PL19 19.00 dB
PL20 19.00 dB
PL21 19.00 dB
PL22 19.00 dB
PL23 19.00 dB
PL24 19.00 dB
PL25 19.00 dB
PL26 19.00 dB
PL27 19.00 dB
PL28 19.00 dB
PL29 19.00 dB
PL30 19.00 dB
PL31 19.00 dB
PL32 19.00 dB
PL33 19.00 dB
PL34 19.00 dB
PL35 19.00 dB
PL36 19.00 dB
PL37 19.00 dB
PL38 19.00 dB
PL39 19.00 dB
PL40 19.00 dB
PL41 19.00 dB
PL42 19.00 dB
PL43 19.00 dB
PL44 19.00 dB
PL45 19.00 dB
PL46 19.00 dB
PL47 19.00 dB
PL48 19.00 dB
PL49 19.00 dB
PL50 19.00 dB
PL51 19.00 dB
PL52 19.00 dB
PL53 19.00 dB
PL54 19.00 dB
PL55 19.00 dB
PL56 19.00 dB
PL57 19.00 dB
PL58 19.00 dB
PL59 19.00 dB
PL60 19.00 dB
PL61 19.00 dB
PL62 19.00 dB
PL63 19.00 dB
PL64 19.00 dB
PL65 19.00 dB
PL66 19.00 dB
PL67 19.00 dB
PL68 19.00 dB
PL69 19.00 dB
PL70 19.00 dB
PL71 19.00 dB
PL72 19.00 dB
PL73 19.00 dB
PL74 19.00 dB
PL75 19.00 dB
PL76 19.00 dB
PL77 19.00 dB
PL78 19.00 dB
PL79 19.00 dB
PL80 19.00 dB
PL81 19.00 dB
PL82 19.00 dB
PL83 19.00 dB
PL84 19.00 dB
PL85 19.00 dB
PL86 19.00 dB
PL87 19.00 dB
PL88 19.00 dB
PL89 19.00 dB
PL90 19.00 dB
PL91 19.00 dB
PL92 19.00 dB
PL93 19.00 dB
PL94 19.00 dB
PL95 19.00 dB
PL96 19.00 dB
PL97 19.00 dB
PL98 19.00 dB
PL99 19.00 dB
PL100 19.00 dB

F2 - Processing parameters
SI 32768
SF 100.626100 MHz
WDW EM
SS 30.000 usec
DE 4.00 usec
TE 293.2 K
D1 1.0000000 sec
d11 0.0000000 sec
DELTA 0.8999998 sec
DDE 1
DD 1.40
  
```

1d_13C_DEPT_Q_135_20min CDC13 D:\ Barr 50



```

Current Data Parameters
NAME 75-leucoprophenol alcohol charew-CDC13
PROCNO 1

F2 - Acquisition Parameters
DATE_ 20111114
TIME 17.24
INSTRUM spect
PROBHD 5 mm PA100 1H
PULPROG zgpg30
PC 1300
SOLVENT CDCl3
NS 1312
DS 4
SFO 200.136101 MHz
FIDRES 0.449901 Hz
AQ 1.093100 sec
RG 133
SF 200.136101 MHz
WDW EM
SS 30.000 usec
DE 4.00 usec
TE 293.2 K
D1 1.0000000 sec
d11 0.0000000 sec
DELTA 0.8999998 sec
DDE 1

----- CHANNEL f1 -----
NUC1 13C
P1 1.00 usec
PL1 0.00 dB
PL12 19.00 dB
PL13 19.00 dB
PL14 19.00 dB
PL15 19.00 dB
PL16 19.00 dB
PL17 19.00 dB
PL18 19.00 dB
PL19 19.00 dB
PL20 19.00 dB
PL21 19.00 dB
PL22 19.00 dB
PL23 19.00 dB
PL24 19.00 dB
PL25 19.00 dB
PL26 19.00 dB
PL27 19.00 dB
PL28 19.00 dB
PL29 19.00 dB
PL30 19.00 dB
PL31 19.00 dB
PL32 19.00 dB
PL33 19.00 dB
PL34 19.00 dB
PL35 19.00 dB
PL36 19.00 dB
PL37 19.00 dB
PL38 19.00 dB
PL39 19.00 dB
PL40 19.00 dB
PL41 19.00 dB
PL42 19.00 dB
PL43 19.00 dB
PL44 19.00 dB
PL45 19.00 dB
PL46 19.00 dB
PL47 19.00 dB
PL48 19.00 dB
PL49 19.00 dB
PL50 19.00 dB
PL51 19.00 dB
PL52 19.00 dB
PL53 19.00 dB
PL54 19.00 dB
PL55 19.00 dB
PL56 19.00 dB
PL57 19.00 dB
PL58 19.00 dB
PL59 19.00 dB
PL60 19.00 dB
PL61 19.00 dB
PL62 19.00 dB
PL63 19.00 dB
PL64 19.00 dB
PL65 19.00 dB
PL66 19.00 dB
PL67 19.00 dB
PL68 19.00 dB
PL69 19.00 dB
PL70 19.00 dB
PL71 19.00 dB
PL72 19.00 dB
PL73 19.00 dB
PL74 19.00 dB
PL75 19.00 dB
PL76 19.00 dB
PL77 19.00 dB
PL78 19.00 dB
PL79 19.00 dB
PL80 19.00 dB
PL81 19.00 dB
PL82 19.00 dB
PL83 19.00 dB
PL84 19.00 dB
PL85 19.00 dB
PL86 19.00 dB
PL87 19.00 dB
PL88 19.00 dB
PL89 19.00 dB
PL90 19.00 dB
PL91 19.00 dB
PL92 19.00 dB
PL93 19.00 dB
PL94 19.00 dB
PL95 19.00 dB
PL96 19.00 dB
PL97 19.00 dB
PL98 19.00 dB
PL99 19.00 dB
PL100 19.00 dB

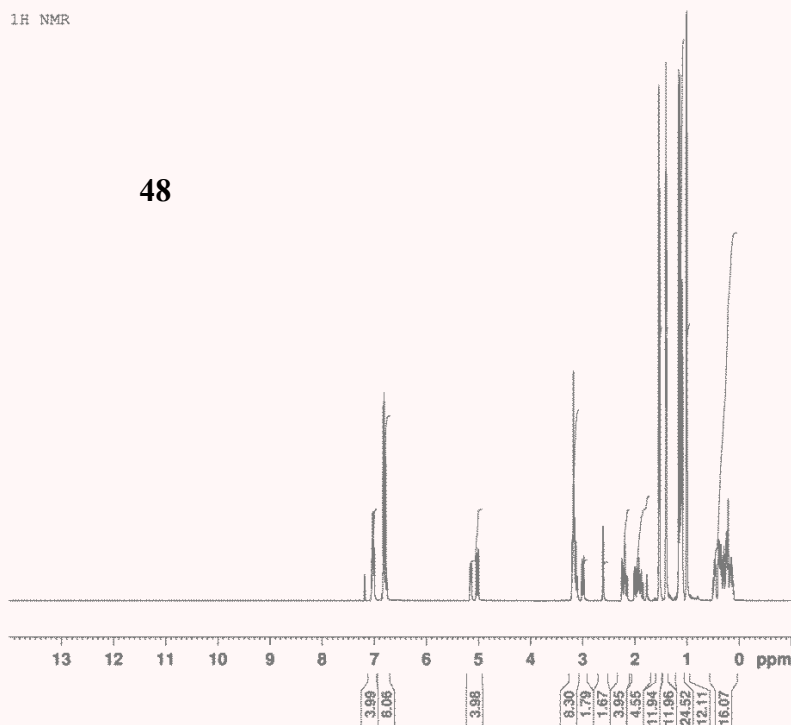
F2 - Processing parameters
SI 32768
SF 100.626100 MHz
WDW EM
SS 30.000 usec
DE 4.00 usec
TE 293.2 K
D1 1.0000000 sec
d11 0.0000000 sec
DELTA 0.8999998 sec
DDE 1
DD 1.40

----- CHANNEL f2 -----
NAME1 13C
P1 1.00 usec
PL1 0.00 dB
PL12 19.00 dB
PL13 19.00 dB
PL14 19.00 dB
PL15 19.00 dB
PL16 19.00 dB
PL17 19.00 dB
PL18 19.00 dB
PL19 19.00 dB
PL20 19.00 dB
PL21 19.00 dB
PL22 19.00 dB
PL23 19.00 dB
PL24 19.00 dB
PL25 19.00 dB
PL26 19.00 dB
PL27 19.00 dB
PL28 19.00 dB
PL29 19.00 dB
PL30 19.00 dB
PL31 19.00 dB
PL32 19.00 dB
PL33 19.00 dB
PL34 19.00 dB
PL35 19.00 dB
PL36 19.00 dB
PL37 19.00 dB
PL38 19.00 dB
PL39 19.00 dB
PL40 19.00 dB
PL41 19.00 dB
PL42 19.00 dB
PL43 19.00 dB
PL44 19.00 dB
PL45 19.00 dB
PL46 19.00 dB
PL47 19.00 dB
PL48 19.00 dB
PL49 19.00 dB
PL50 19.00 dB
PL51 19.00 dB
PL52 19.00 dB
PL53 19.00 dB
PL54 19.00 dB
PL55 19.00 dB
PL56 19.00 dB
PL57 19.00 dB
PL58 19.00 dB
PL59 19.00 dB
PL60 19.00 dB
PL61 19.00 dB
PL62 19.00 dB
PL63 19.00 dB
PL64 19.00 dB
PL65 19.00 dB
PL66 19.00 dB
PL67 19.00 dB
PL68 19.00 dB
PL69 19.00 dB
PL70 19.00 dB
PL71 19.00 dB
PL72 19.00 dB
PL73 19.00 dB
PL74 19.00 dB
PL75 19.00 dB
PL76 19.00 dB
PL77 19.00 dB
PL78 19.00 dB
PL79 19.00 dB
PL80 19.00 dB
PL81 19.00 dB
PL82 19.00 dB
PL83 19.00 dB
PL84 19.00 dB
PL85 19.00 dB
PL86 19.00 dB
PL87 19.00 dB
PL88 19.00 dB
PL89 19.00 dB
PL90 19.00 dB
PL91 19.00 dB
PL92 19.00 dB
PL93 19.00 dB
PL94 19.00 dB
PL95 19.00 dB
PL96 19.00 dB
PL97 19.00 dB
PL98 19.00 dB
PL99 19.00 dB
PL100 19.00 dB

F2 - Processing parameters
SI 32768
SF 100.626100 MHz
WDW EM
SS 30.000 usec
DE 4.00 usec
TE 293.2 K
D1 1.0000000 sec
d11 0.0000000 sec
DELTA 0.8999998 sec
DDE 1
DD 1.40
  
```

1H NMR

48



Current Data Parameters
 NAME TS-02-85-char1
 EXPNO 1
 PROCNO 1

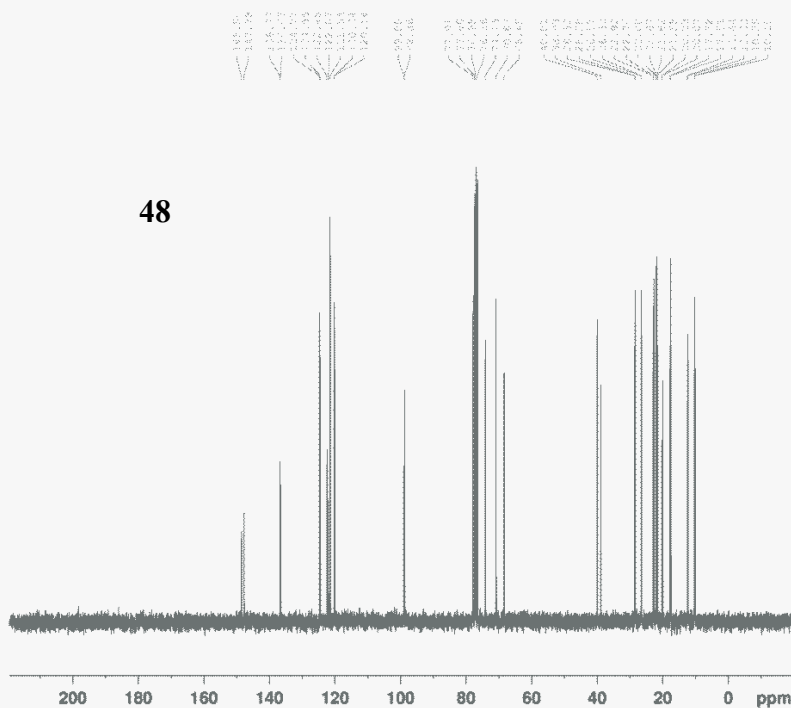
F2 - Acquisition Parameters
 Date_ 20120827
 Time_ 8.08
 INSTRUM spect
 PROBHD 5 mm PABBO BB-
 PULPROG zg30
 TD 32768
 SOLVENT CDCl3
 NS 16
 DS 0
 SMH 4507.211 Hz
 FIDRES 0.137549 Hz
 AQ 3.6351135 sec
 RG 14.2
 DW 110.933 usec
 DE 6.00 usec
 TE 294.0 K
 D1 0.01000000 sec
 TDO 1

===== CHANNEL f1 =====
 NUC1 1H
 P1 11.75 usec
 PL1 0 dB
 SFO1 300.3319506 MHz

F2 - Processing parameters
 SI 32768
 SF 300.3300000 MHz
 WDW EM
 SSB 0
 LB 0 Hz
 GB 0
 PC 1.00

13C NMR with 1H decoupling

48



Current Data Parameters
 NAME TS-02-85-char1
 EXPNO 2
 PROCNO 1

F2 - Acquisition Parameters
 Date_ 20120827
 Time_ 8.24
 INSTRUM spect
 PROBHD 5 mm PABBO BB-
 PULPROG zgpg30
 TD 32768
 SOLVENT CDCl3
 NS 256
 DS 2
 SMH 18028.846 Hz
 FIDRES 0.550197 Hz
 AQ 0.9088159 sec
 RG 575
 DW 27.733 usec
 DE 6.00 usec
 TE 295.0 K
 D1 1.00000000 sec
 d11 0.03000000 sec
 DELTA 0.89999998 sec
 TDO 1

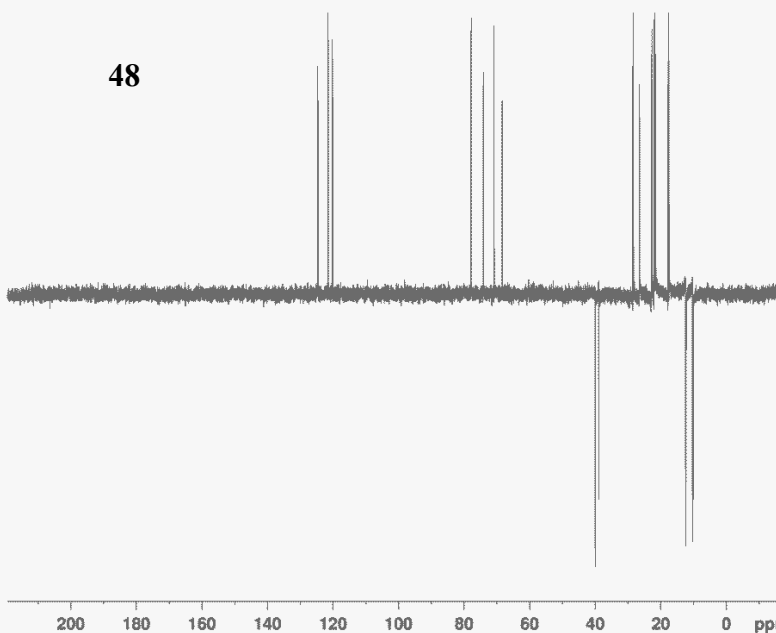
===== CHANNEL f1 =====
 NUC1 13C
 P1 6.65 usec
 PL1 -4.00 dB
 SFO1 75.5255699 MHz

===== CHANNEL f2 =====
 CPDPRG2 waltz16
 NUC2 1H
 FCPD2 80.00 usec
 PL2 0 dB
 PL12 16.66 dB
 PL13 17.00 dB
 SFO2 300.3312013 MHz

F2 - Processing parameters
 SI 32768
 SF 75.5180390 MHz
 WDW EM
 SSB 0
 LB 1.00 Hz
 GB 0
 PC 1.40

13C DEPT 135

48



```

Current Data Parameters
NAME      TS-02-05-char1
EXPNO     3
PROCNO    1

F2 - Acquisition Parameters
Date_     20120827
Time      8.28
INSTRUM   spect
PROBHD    5 mm PABBO BB-
PULPROG   dept135
TD         32768
SOLVENT   CDCl3
NS         64
DS         0
SWH        18028.846 Hz
FIDRES     0.550197 Hz
AQ         0.9088159 sec
RG         16384
DW         27.733 usec
DE         6.00 usec
TE         294.7 K
CWST2     145.000000
D1         2.0000000 sec
J2         0.00344828 sec
J12        0.00002000 sec
DELTA     0.0000847 sec
TD0        1

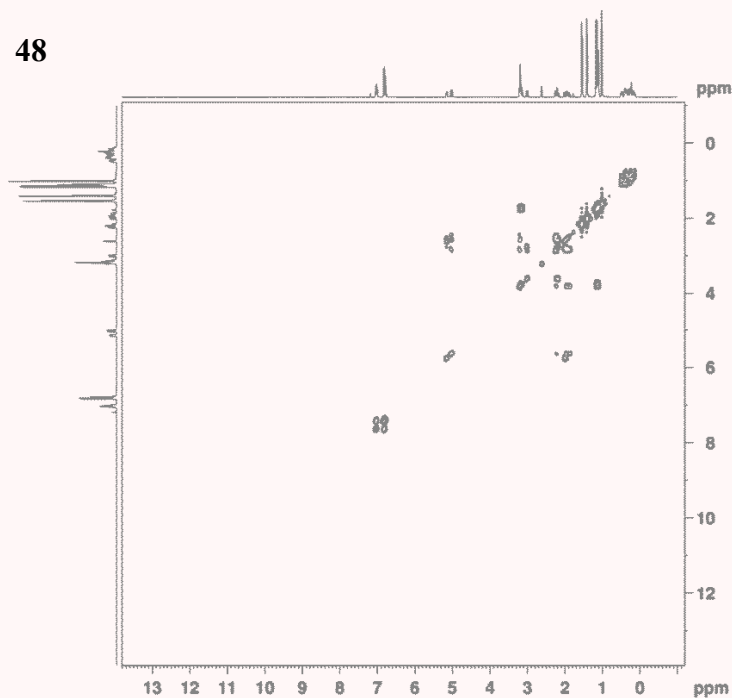
===== CHANNEL f1 =====
NUC1       13C
P1         6.65 usec
P2         13.30 usec
PL1        -4.00 dB
SFO1       75.5255899 MHz

===== CHANNEL f2 =====
CPDPRG2    waltz16
NUC2        1H
P3         11.75 usec
P4         23.50 usec
PCPD2      80.00 usec
PL2         0 dB
PL12       16.66 dB
SFO2       300.3312013 MHz

F2 - Processing parameters
SI         32768
SF         75.5180390 MHz
WDW        EM
SSB        0
LB         1.00 Hz
GB         0
PC         1.40
  
```

1H COSY 45

48



```

Current Data Parameters
NAME      TS-02-05-char1
EXPNO     4
PROCNO    1

F2 - Acquisition Parameters
Date_     20120827
Time      8.28
INSTRUM   spect
PROBHD    5 mm PABBO BB-
PULPROG   cosyqpcq45
TD         1024
SOLVENT   CDCl3
NS         1
DS         0
SWH        4507.211 Hz
FIDRES     4.401574 Hz
AQ         0.1136457 sec
RG         181
DW         110.933 usec
DE         6.00 usec
TE         294.6 K
AQ         0.0000300 sec
D1         1.0000000 sec
D12        0.00000400 sec
D15        0.00000000 sec
IND        0.0022185 sec

===== CHANNEL f1 =====
NUC1       1H
P1         11.75 usec
PL1         0 dB
SFO1       300.3319506 MHz

===== GRADIENT CHANNEL =====
OPNAM1     SINE_100
OPNAM2     SINE_100
QP1        20.00 %
QP2        20.00 %
P16        1090.00 usec

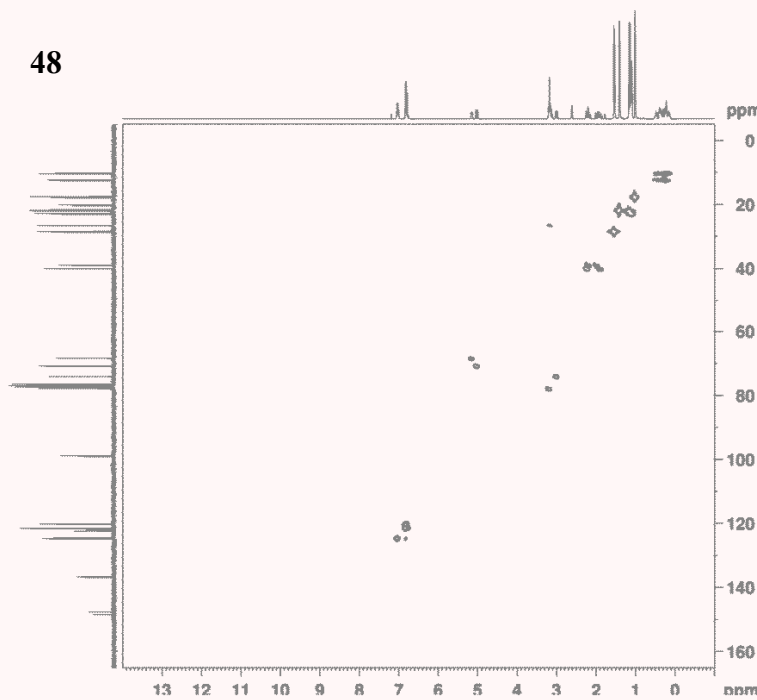
F1 - Acquisition parameters
TD         256
SFO1       300.3315 MHz
FIDRES     17.007618 Hz
SN         15.003 ppm
PreMODE    QF

F2 - Processing parameters
SI         1024
SF         300.3300000 MHz
WDW        SINC
SSB        0
LB         0 Hz
GB         0
PC         1.00

F1 - Processing parameters
SI         1024
MC2        0
SF         300.3293695 MHz
WDW        <gauss>
PreSPNAM1  <gauss>
SSB        0
LB         0 Hz
GB         0
  
```

1H - 13C HMQC

48



```

Current Data Parameters
NAME 75-02-85-0001
EXPNO 2
PROCNO 1

P2 - Acquisition Parameters
Date_ 20120111
Time 8.13
INSTRUM spect
PROBHD 5 mm PABBO BO
PULPROG zgpg30
TD 65536
SOLVENT ccdcl3
NS 2
DS 2
SWH 4507.314 Hz
FIDRES 4.401274 Hz
AQ 0.1198451 sec
RG 320
SQ 0.132
WDW EM
SSB 0
LB 110.000 usec
GB 0
PC 1.00
TE 294.2 K
DQ 4.00 usec
DE 0.0000000 sec
D1 3.0000000 sec
D11 1.0000000 sec
D12 2.0000000 sec
D13 3.0000000 sec
D14 0.0000000 sec
DELTA1 3.0000000 sec
JNO 3.0000000 sec

----- CHANNEL f1 -----
NUC1 13
P1 11.75 usec
RF 23.50 usec
SF01 300.31506 MHz
SF02 0

----- CHANNEL f2 -----
CPDPRG2 gpg30
NUC2 1
P2 8.00 usec
RF2 4.00 usec
SF02 75.00000 MHz
SF03 14.00 usec
SF04 75.00000 MHz

----- MAGNET CHANNEL -----
CPDPRG1 sine102
NUC1 13
P1 8.00 usec
RF 4.00 usec
SF01 500.13630 MHz
SF02 40.11 Hz
P14 1005.00 usec

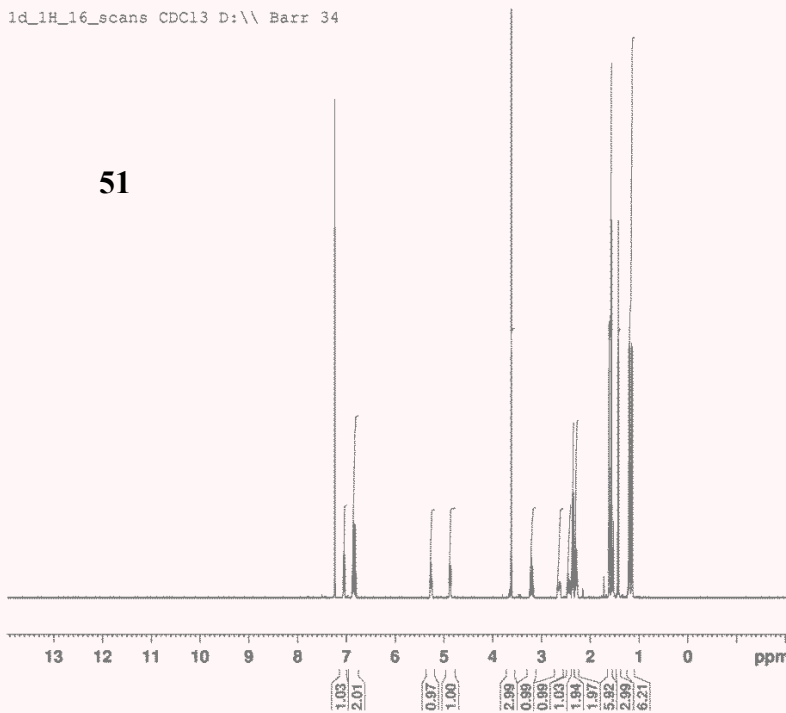
P1 - Acquisition parameters
TD 65536
SF01 75.32000 MHz
FIDRES 4.401274 Hz
WDW EM
SSB 0
LB 110.00 usec
GB 0
PC 1.00

P2 - Processing parameters
SI 32768
SF 300.3150600 MHz
WDW EM
SSB 0
LB 0 Hz
GB 0
PC 1.00

P1 - Processing parameters
SI 65536
SF 75.3186934 MHz
WDW EM
SSB 0
LB 0 Hz
GB 0
PC 1.00
    
```

1d_1H_16_scans CDC13 D:\ Barr 34

51



```

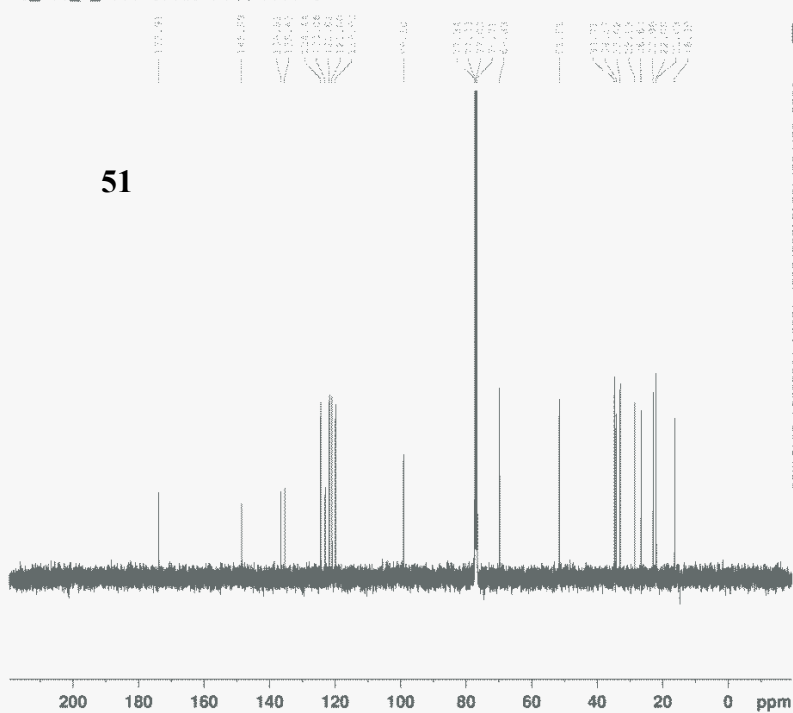
Current Data Parameters
NAME 75-06-01char - Ma ester JC rrangr
EXPNO 1
PROCNO 1

P2 - Acquisition Parameters
Date_ 20120809
Time 14.42
INSTRUM spect
PROBHD 5 mm PABBO BO
PULPROG zgpg30
TD 65536
SOLVENT ccdcl3
NS 16
DS 16
SWH 6421.233 Hz
FIDRES 0.120640 Hz
AQ 3.8273323 sec
RG 320
SQ 0.132
WDW EM
SSB 0
LB 110.000 usec
GB 0
PC 1.00
TE 294.2 K
DQ 4.00 usec
DE 0.0000000 sec
D1 1.0000000 sec

----- CHANNEL f1 -----
NUC1 13
P1 10.75 usec
RF 23.50 usec
SF01 400.3223900 MHz

P2 - Processing parameters
SI 65536
SF 400.3200144 MHz
WDW EM
SSB 0
LB 0 Hz
GB 0
PC 1.00
    
```

1d_13C_1_hour CDC13 D:\ Barr 34



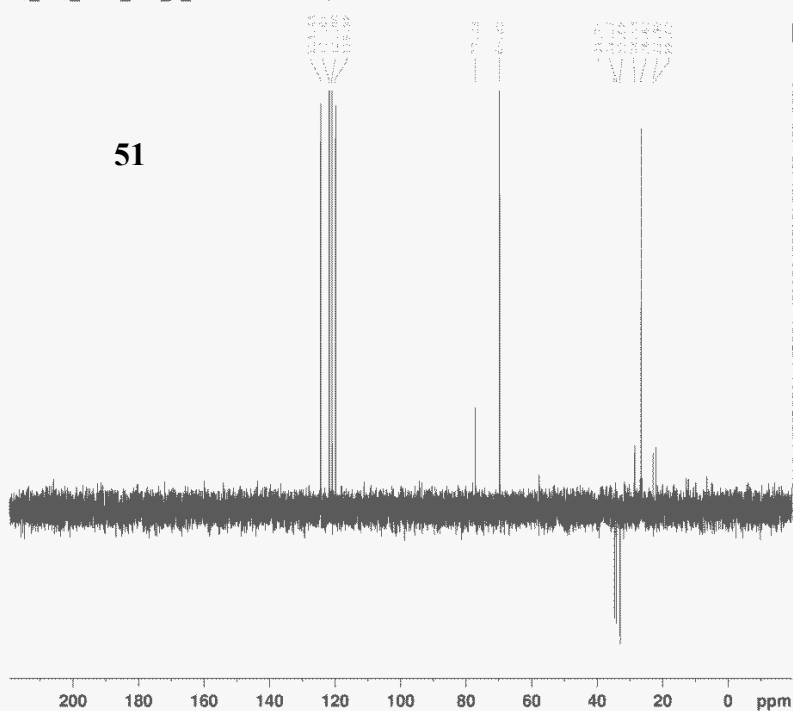
Current Data Parameters
NAME: T2-26-Dichlor - Mx ester JC string
EXPNO: 1
PROCNO: 1

F2 - Acquisition Parameters
Date_ 20120907
Time 22.51
INSTRUM spect
PROBHD 5 mm VAMBI 90
PULPROG zgpg30
TD 51200
SOLVENT CDCl3
NS 1634
DS 4
SWH 24038.461 Hz
FIDRES 0.468901 Hz
AQ 1.0650190 sec
RG 501
DM 20.000 usec
DE 1.00 usec
TE 299.2 K
D1 1.0000000 sec
dL1 0.0100000 sec
DELTA 0.8999999 sec
D2

----- CHANNEL F1 -----
NUC1 13C
P1 7.50 usec
PL1 -1.00 dB
AF01 100.6190191 MHz
----- CHANNEL F2 -----
P3 10.75 usec
PL3 1.00 dB
PL2 90.00 usec
PL4 -1.00 dB
PL5 14.00 dB
PL6 14.00 dB
PL7 14.00 dB
PL8 14.00 dB
SF02 400.1324013 MHz

F2 - Processing parameters
SI 65536
SF 100.6190191 MHz
WDW EM
SSB 0
LB 1.00 Hz
GB 0
PC 1.40

1d_13C_DEPT_135_1_hour CDC13 D:\ Barr 34



Current Data Parameters
NAME: T2-26-Dichlor - Mx ester JC string
EXPNO: 1
PROCNO: 1

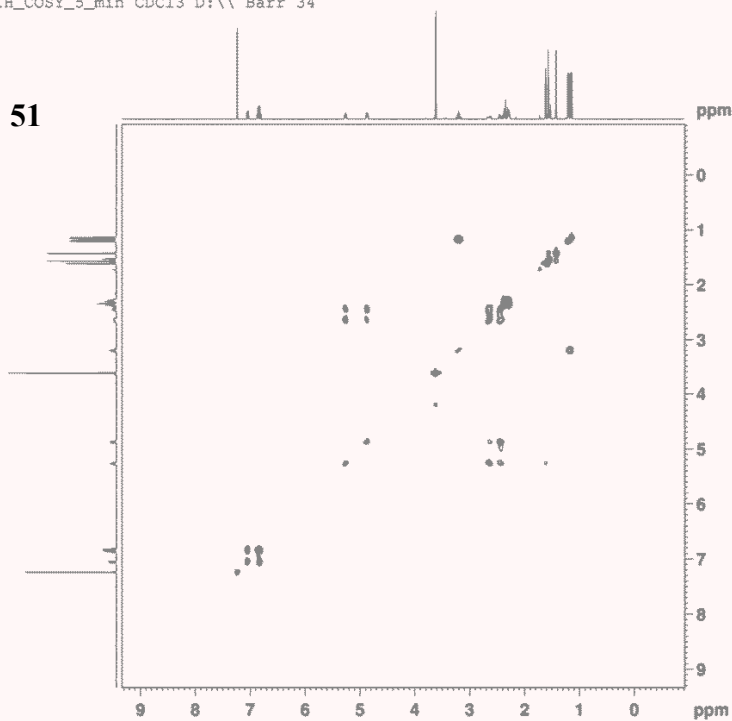
F2 - Acquisition Parameters
Date_ 20120907
Time 22.46
INSTRUM spect
PROBHD 5 mm VAMBI 90
PULPROG zgpg30
TD 51200
SOLVENT CDCl3
NS 1634
DS 4
SWH 24038.461 Hz
FIDRES 0.468901 Hz
AQ 1.0650190 sec
RG 501
DM 20.000 usec
DE 1.00 usec
TE 299.2 K
D1 1.0000000 sec
dL1 0.0100000 sec
DELTA 0.8999999 sec
D2

----- CHANNEL F1 -----
NUC1 13C
P1 7.50 usec
PL1 -1.00 dB
PL2 90.00 usec
PL3 1.00 dB
PL4 14.00 dB
PL5 14.00 dB
PL6 14.00 dB
PL7 14.00 dB
PL8 14.00 dB
SF02 400.1324013 MHz

F2 - Processing parameters
SI 65536
SF 100.6190191 MHz
WDW EM
SSB 0
LB 1.00 Hz
GB 0
PC 1.40

2d_1H-COSY_5_min CDC13 D:\ Barr 34

51



Current Data Parameters
NAME: 75-06-Dichlor - Me ester JC program
EXPER: 1
PROCNO: 1

P2 - Acquisition Parameters
Date_: 20120909
Time: 14.43
INSTRUM: spect
PROBHD: 5 mm PABBO BB-
PULPROG: zgpg30
TD: 1024
SOLVENT: CDCl3
NS: 1
DS: 4
SWH: 4105.090 Hz
F2PRES: 4.008877 Hz
AQ: 0.1247732 sec
RG: 5050
DM: 121.000 usec
DE: 1.00 usec
TE: 294.2 K
D1: 0.0000000 sec
D2: 1.0000000 sec
D15: 0.0002000 sec
D18: 0.0002000 sec
D19: 0.0002430 sec

----- CHANNEL f1 -----
NUC1: 1H
Q1: 6.00 usec
P1: 10.75 usec
PL1: -1.00 dB
SFO1: 400.3217014 MHz

----- GRADIENT CHANNEL -----

OPAM1: size:100
OPAM2: size:100
GFC1: 10.00 %
GFC2: 10.00 %
P15: 1000.00 usec

P1 - Acquisition parameters

TD: 256
SFO1: 400.3217014 MHz
F2PRES: 4.008877 Hz
SW: 10.250 ppm
FREQ0R: 0

P2 - Processing parameters

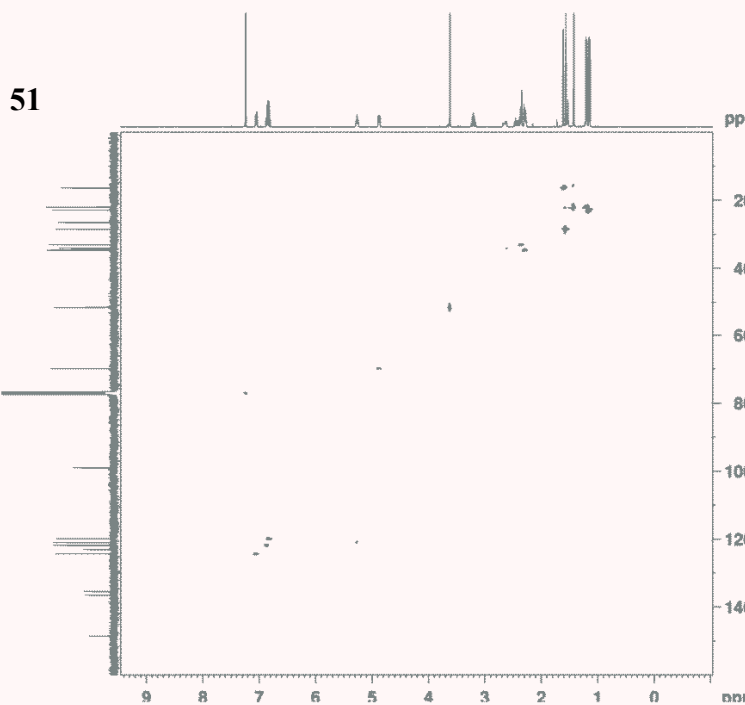
SF: 400.3200444 MHz
WDW: 0
SSB: 0
LB: 0 Hz
GB: 0
PC: 1.00

P1 - Processing parameters

SF: 400.3200444 MHz
WDW: 0
SSB: 0
LB: 0 Hz
GB: 0

2d_HMQC_1_hour CDC13 D:\ Barr 34

51



Current Data Parameters
NAME: 75-06-Dichlor - Me ester JC program
EXPER: 1
PROCNO: 1

P2 - Acquisition Parameters
Date_: 20120909
Time: 22.08
INSTRUM: spect
PROBHD: 5 mm PABBO BB-
PULPROG: zgpg30
TD: 1024
SOLVENT: CDCl3
NS: 1
DS: 4
SWH: 5001.620 Hz
F2PRES: 4.103204 Hz
AQ: 0.1219645 sec
RG: 4050
DM: 119.100 usec
DE: 1.00 usec
TE: 294.2 K
D15: 145.0000000 sec
D1: 1.0000000 sec
D2: 2.0000000 sec
D12: 0.0000000 sec
D13: 2.0000000 sec
D16: 2.0000000 sec
D18: 2.0000000 sec
D19: 2.0000000 sec

----- CHANNEL f1 -----

NUC1: 13C
Q1: 10.75 usec
P1: 21.52 usec
PL1: -1.00 dB
SFO1: 400.3217014 MHz

----- CHANNEL f2 -----

OPAM1: size:100
OPAM2: size:100
GFC1: 10.00 %
GFC2: 10.00 %
P15: 1000.00 usec

P1 - Acquisition parameters

TD: 256
SFO1: 100.62636 MHz
F2PRES: 4.103204 Hz
SW: 159.961 ppm
FREQ0R: 0

P2 - Processing parameters

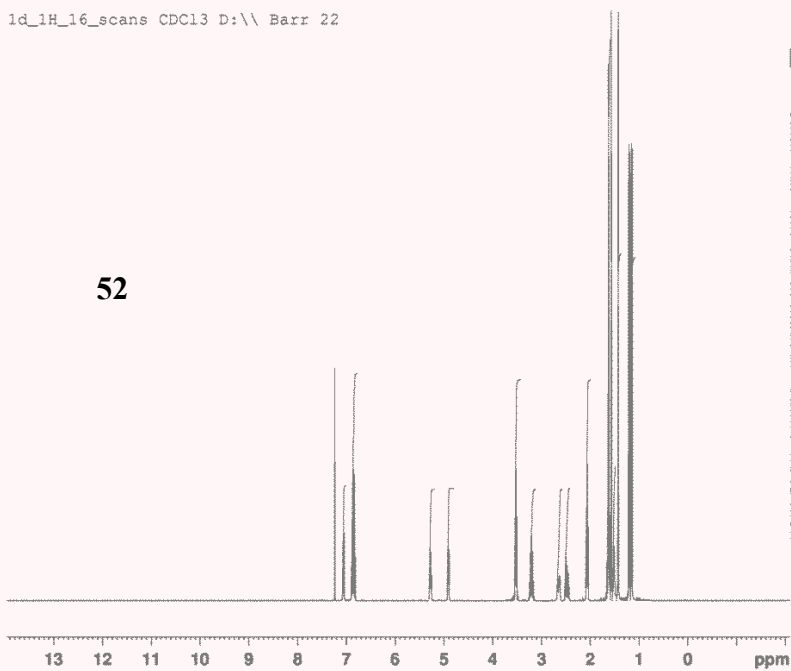
SF: 400.3200444 MHz
WDW: 0
SSB: 0
LB: 0 Hz
GB: 0
PC: 1.00

P1 - Processing parameters

SF: 100.62636 MHz
WDW: 0
SSB: 0
LB: 0 Hz
GB: 0

1d_1H_16_scans CDC13 D:\ Barr 22

52



Current Data Parameters
 NAME TS-06-04char - alcohol
 EXPHO 1
 PROCNO 1

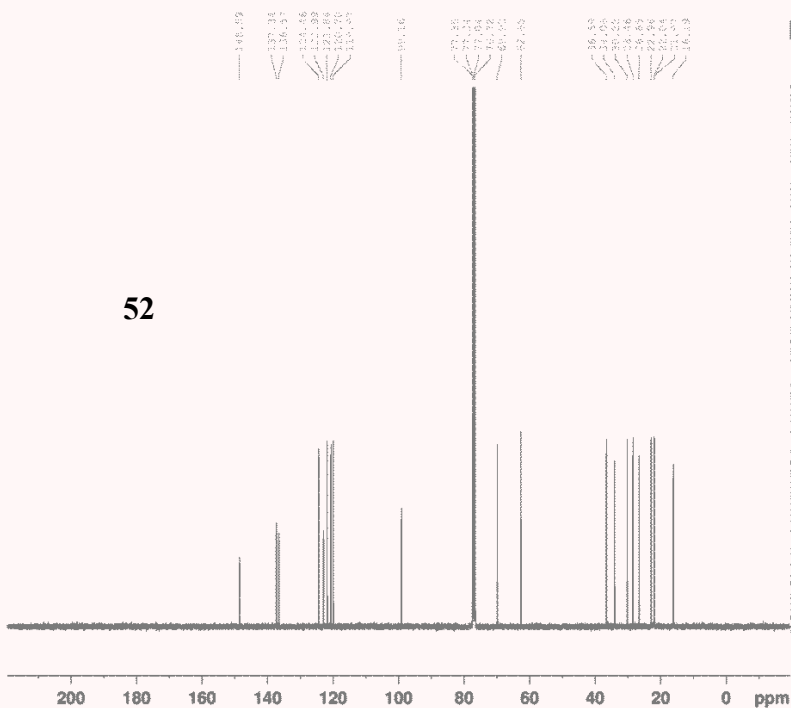
F2 - Acquisition Parameters
 Date_ 20120404
 Time 15.41
 INSTRUM spect
 PROBHD 5 mm PABBO B9-
 PULPROG zg30
 ID 49152
 SOLVENT CDC13
 NS 16
 DS 0
 SMH 6421.233 Hz
 FIDRES 0.130640 Hz
 AQ 3.827323 sec
 RG 228
 DW 77.867 usec
 DE 6.00 usec
 TE 294.8 K
 D1 1.0000000 sec
 TD0 1

===== CHANNEL f1 =====
 NUC1 1H
 P1 10.75 usec
 PL1 -4.00 dB
 SFO1 400.323900 MHz

F2 - Processing parameters
 SI 65536
 SF 400.320164 MHz
 WDW EM
 SSB 0
 LB 0.10 Hz
 GB 0
 PC 1.00

1d_13C_1_hour CDC13 D:\ Barr 22

52



Current Data Parameters
 NAME TS-06-04char - alcohol
 EXPHO 2
 PROCNO 1

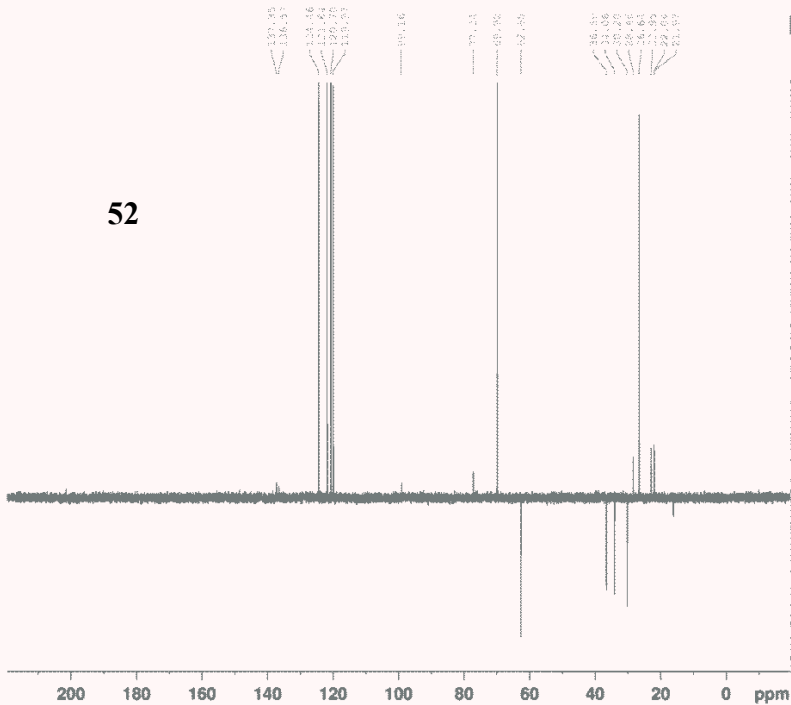
F2 - Acquisition Parameters
 Date_ 20120405
 Time 5.23
 INSTRUM spect
 PROBHD 5 mm PABBO B9-
 PULPROG zgpg30
 ID 51200
 SOLVENT CDC13
 NS 1664
 DS 0
 SMH 24038.461 Hz
 FIDRES 0.465501 Hz
 AQ 1.0630100 sec
 RG 228
 DW 20.800 usec
 DE 6.00 usec
 TE 295.9 K
 D1 1.0000000 sec
 d11 0.6300000 sec
 DELTA 0.89959998 sec
 TD0 1

===== CHANNEL f1 =====
 NUC1 13C
 P1 7.50 usec
 PL1 -3.00 dB
 SFO1 100.6706101 MHz

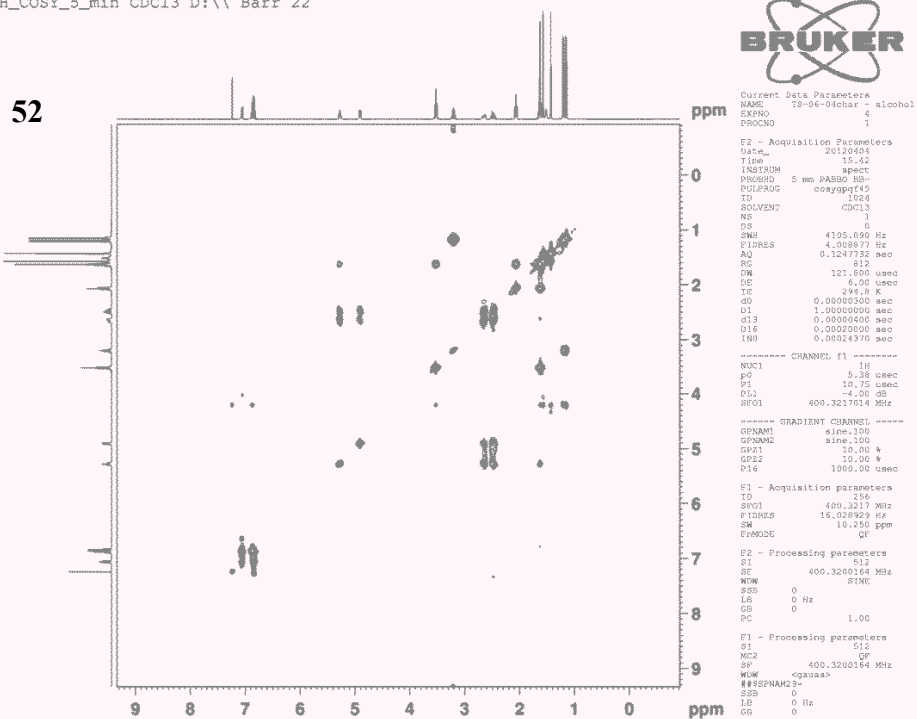
===== CHANNEL f2 =====
 CPDPRG2 waltz16
 NUC2 1H
 FCPD2 90.00 usec
 PL2 -4.00 dB
 PL12 18.46 dB
 PL13 18.01 dB
 SFO2 400.3216013 MHz

F2 - Processing parameters
 SI 65536
 SF 100.6605440 MHz
 WDW EM
 SSB 0
 LB 1.00 Hz
 GB 0
 PC 1.40

1d_13C_DEPT_135_1_hour CDC13 D:\ Barr 22

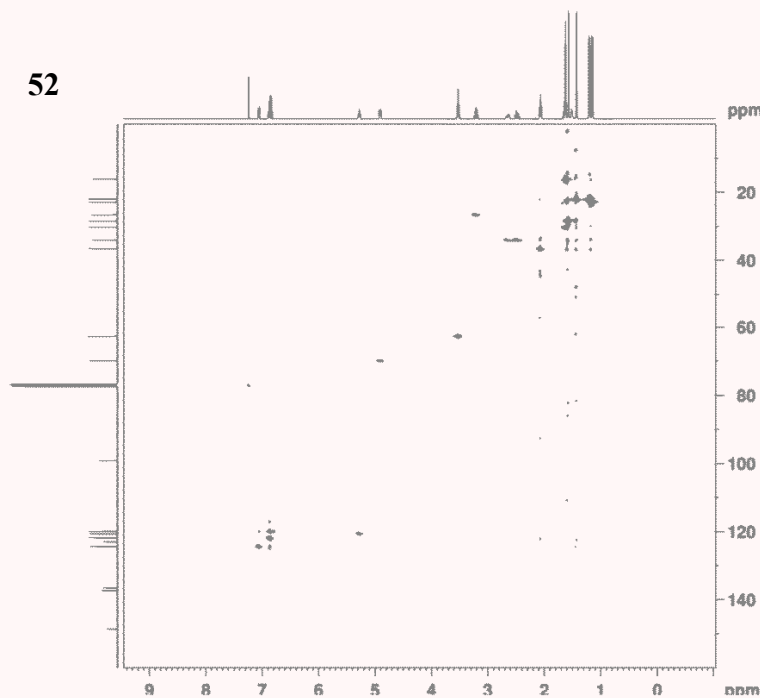


2d_1H_COSY_5_min CDC13 D:\ Barr 22



2d_HMQC_1_hour CDC13 D:\ Barr 22

52



Current Data Parameters
NAME 18-06-07-F2- nitrile char
EXPNO 1
PROCNO 1

F2 - Acquisition Parameters
Date_ 20120411
Time 9.13
INSTRUM spect
PROBHD 5 mm PABBO BB-
PULPROG zgpg30
TD 49152
SOLVENT CDCl3
NS 16
DS 0
SWH 6421.233 Hz
FIDRES 0.1130810 Hz
AQ 3.8272523 sec
RG 406
RW 77.667 usec
DE 6.00 usec
TE 294.2 K
D1 1.0000000 sec
D10 1

***** CHANNEL f1 *****
NUC1 13
P1 10.75 usec
PL1 -4.00 dB
SFO1 400.3229900 MHz

***** CHANNEL f2 *****
CPDPRG2 gpg
NUC2 1H
PCPD2 86.01 usec
PL2 -3.00 dB
PL12 17.36 dB
SFO2 100.6263700 MHz

***** CHANNEL f3 *****
CPDPRG3 sine107
NUC3 1H
PCPD3 50.00 usec
PL3 0.00 dB
SFO3 50.0000000 MHz

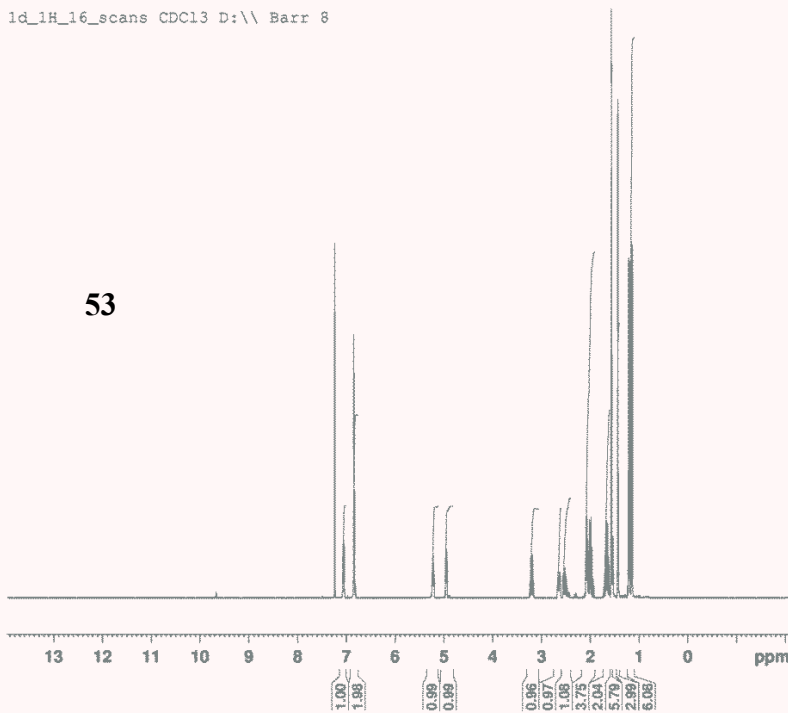
F1 - Acquisition parameters
TD 65536
SFO1 100.6263700 MHz
FIDRES 0.1130810 Hz
AQ 3.8272523 sec
RG 406

F2 - Processing parameters
SI 32768
SF 400.3229900 MHz
WV 0 SINE
SSB 0 Hz
LB 0 Hz
GB 0
PC 1.00

F1 - Processing parameters
SI 65536
SF 100.6263700 MHz
WV 0 P1
SSB 0 Hz
LB 0 Hz
GB 0
PC 0

1d_1H_16_scans CDC13 D:\ Barr 8

53



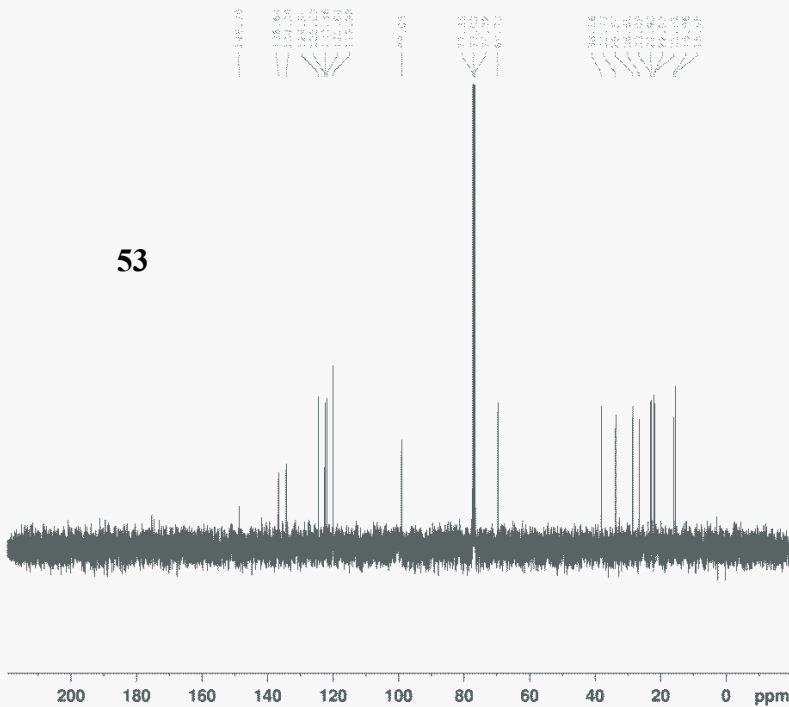
Current Data Parameters
NAME 18-06-07-F2- nitrile char
EXPNO 1
PROCNO 1

F2 - Acquisition Parameters
Date_ 20120411
Time 9.13
INSTRUM spect
PROBHD 5 mm PABBO BB-
PULPROG zgpg30
TD 49152
SOLVENT CDCl3
NS 16
DS 0
SWH 6421.233 Hz
FIDRES 0.1130810 Hz
AQ 3.8272523 sec
RG 406
RW 77.667 usec
DE 6.00 usec
TE 294.2 K
D1 1.0000000 sec
D10 1

***** CHANNEL f1 *****
NUC1 1H
P1 10.75 usec
PL1 -4.00 dB
SFO1 400.3229900 MHz

F2 - Processing parameters
SI 65536
SF 400.3229900 MHz
WV 0 EM
SSB 0 Hz
LB 0.10 Hz
GB 0
PC 1.00

1d_13C_5_minutes CDC13 D:\ Barr 8



Current Data Parameters
 NAME IS-06-07-12- nitrile char
 EXPNO 2
 PROCNO 1

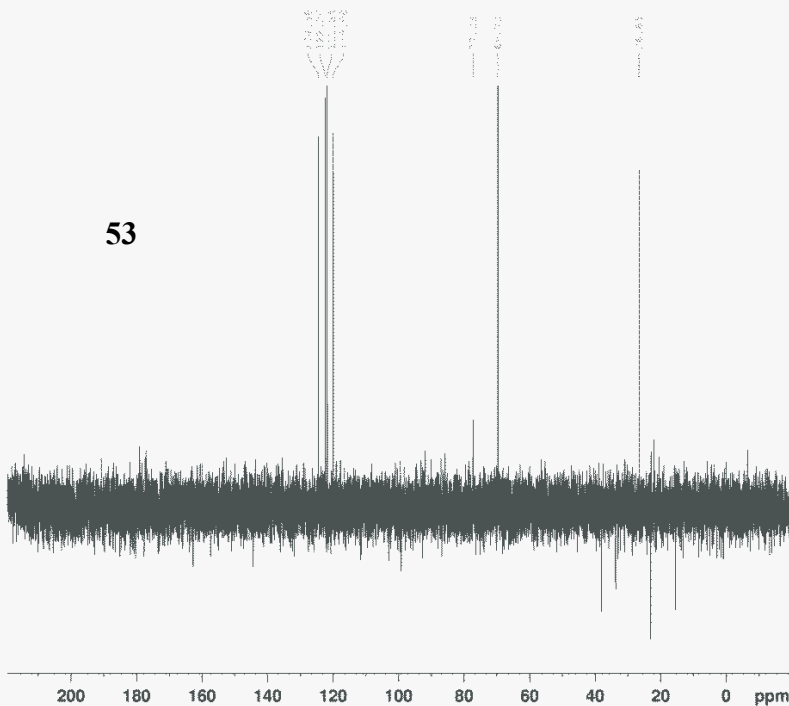
F2 - Acquisition Parameters
 Date_ 20120411
 Time 9.18
 INSTRUM spect
 PROBRD 5 mm PASAD 50-
 PULPROG zgpg30
 TD 51200
 SOLVENT CDCl3
 NS 128
 DS 0
 SFR 24038.461 Hz
 FIDRES 0.469311 Hz
 AQ 1.0650100 sec
 RG 406
 CW 20.000 usec
 DE 6.00 usec
 TE 295.3 K
 D1 1.0000000 sec
 d11 0.0300000 sec
 DELTA 0.8999999 sec
 TD0 1

===== CHANNEL f1 =====
 NU1 130
 P1 7.50 usec
 PL1 -1.00 dB
 SFO1 100.620101 MHz

===== CHANNEL f2 =====
 CPDPRG2 waltz16
 NU2 54
 PCPD2 30.00 usec
 PL2 -4.00 dB
 PL3 14.00 dB
 PL4 18.01 dB
 SFO2 400.3216013 MHz

F2 - Processing parameters
 SI 65536
 SF 100.6205440 MHz
 KW 0 DM
 SSB 0 1.00 Hz
 GB 0
 PC 1.40

1d_13C_DEPT_135_5_minutes CDC13 D:\ Barr 8



Current Data Parameters
 NAME IS-06-07-12- nitrile char
 EXPNO 2
 PROCNO 1

F2 - Acquisition Parameters
 Date_ 20120411
 Time 9.25
 INSTRUM spect
 PROBRD 5 mm PASAD 50-
 PULPROG dept135
 TD 51200
 SOLVENT CDCl3
 NS 96
 DS 2
 SFR 24038.461 Hz
 FIDRES 0.469311 Hz
 AQ 1.0650100 sec
 RG 406
 CW 20.000 usec
 DE 8.00 usec
 TE 295.4 K
 CNST2 145.0000000
 D1 2.0000000 sec
 d1 0.00344528 sec
 d12 0.0000000 sec
 DELTA 0.0000000 sec
 TD0 1

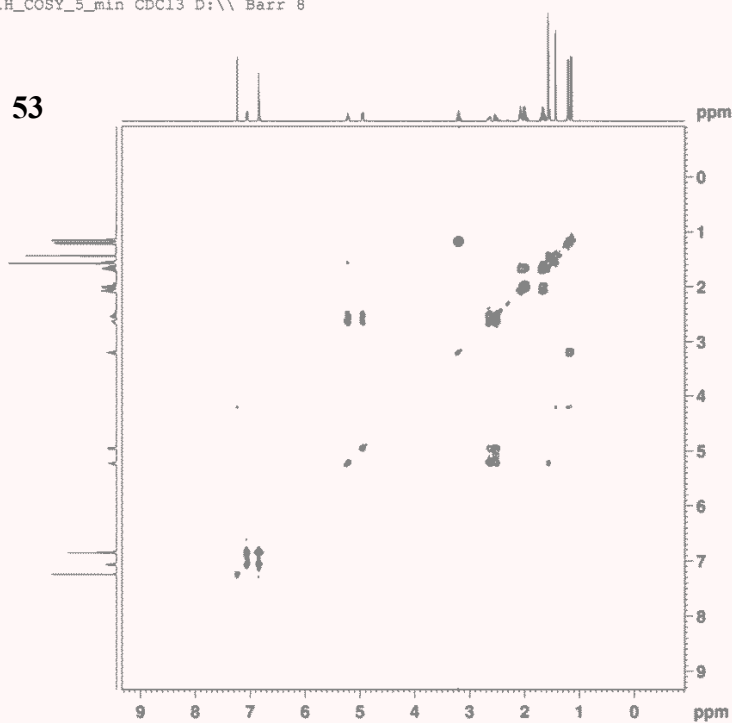
===== CHANNEL f1 =====
 NU1 130
 P1 7.50 usec
 PL1 15.00 dB
 PL2 -1.00 dB
 SFO1 100.620101 MHz

===== CHANNEL f2 =====
 CPDPRG2 waltz16
 NU2 54
 P3 10.75 usec
 P4 21.50 usec
 PCPD2 30.00 usec
 PL2 -4.00 dB
 PL3 14.00 dB
 SFO2 400.3216013 MHz

F2 - Processing parameters
 SI 65536
 SF 100.6205440 MHz
 KW 0 DM
 SSB 0 1.00 Hz
 GB 0
 PC 1.40

2d_1H_COSY_5_min CDC13 D:\ Barr 8

53



```

Current Data Parameters
NAME      TS-06-07-52- nitrile char
EXPNO    4
PROCNO    1

P2 - Acquisition Parameters
Date_     20120411
Time      3.26
INSTRUM   spect
PROBHD    5 mm PABBO 90-
PULPROG   zgpg30f45
TD         1024
SOLVENT   CDC13
NS         1
DS         0
SWH        4105.030 Hz
FIDRES    4.008877 Hz
AQ         0.1241132 sec
RG         1440
DM         121.800 usec
DE         6.0 usec
IE         235.3 Hz
SFO        400.0000000 sec
D1         1.00000000 sec
d11        0.00000000 sec
D15        0.00000000 sec
IN0        0.00024370 sec

----- CHANNEL f1 -----
NUC1       1H
P0         5.38 usec
P1         10.75 usec
PL1        -1.00 dB
SFO1       400.3217014 MHz

----- GRADIENT CHANNEL -----
GRNAM1     g1nc-100
GRNAM2     g1nc-100
GRP1       10.00 %
GRP2       10.00 %
P16        1000.00 usec

F1 - Acquisition parameters
TD         256
SFO1       400.3217 MHz
FIDRES    16.028229 Hz
SW         19.250 ppm
FWD002     ZF

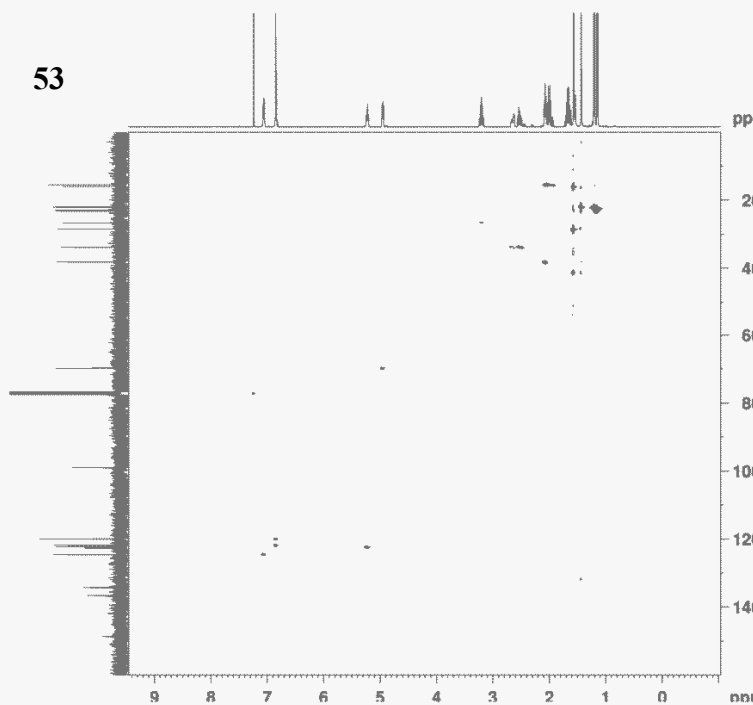
P2 - Processing parameters
SI         512
SF         400.3200164 MHz
WDW        EM
SSB        0
LB         0 Hz
GB         0
PC         1.00

F1 - Processing parameters
SI         512
MC2        ZF
SF         400.3200164 MHz
WDW        EM
SSB        0
LB         0 Hz
GB         0
PC         1.00

```

2d_HMOC_1_hour CDC13 D:\ Barr 8

53



```

Current Data Parameters
NAME      TS-04-17-12- nitrile char
EXPNO    2
PROCNO    1

P2 - Acquisition Parameters
Date_     20120411
Time      17.01
INSTRUM   spect
PROBHD    5 mm PABBO 90-
PULPROG   zgpg30f7
TD         1024
SOLVENT   CDC13
NS         14
DS         2
SWH        4201.481 Hz
FIDRES    4.103294 Hz
AQ         0.1219665 sec
RG         1440
DM         119.000 usec
DE         4.00 usec
IE         235.3 Hz
SFO        400.0000000 sec
D1         1.00000000 sec
d11        0.00000000 sec
D15        0.00000000 sec
IN0        0.00024370 sec

----- CHANNEL f1 -----
NUC1       1H
P0         5.38 usec
P1         10.75 usec
PL1        -1.00 dB
SFO1       400.3217014 MHz

----- CHANNEL f2 -----
GRNAM1     g1nc-100
GRNAM2     g1nc-100
GRP1       10.00 %
GRP2       10.00 %
P16        1000.00 usec

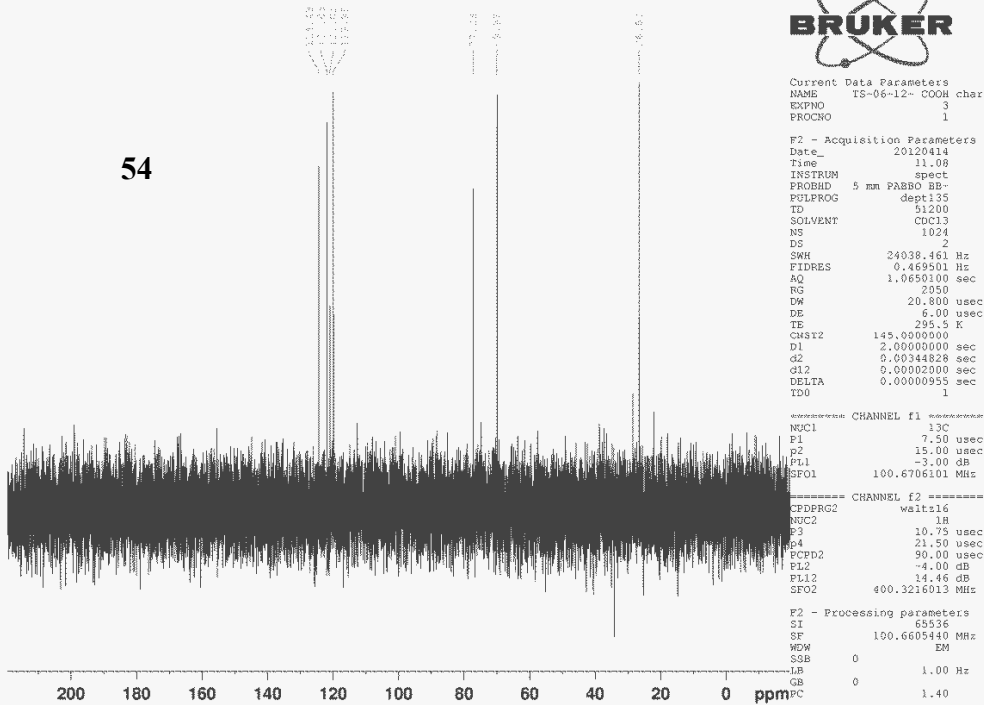
F1 - Acquisition parameters
TD         256
SFO1       400.3217 MHz
FIDRES    16.028229 Hz
SW         19.250 ppm
FWD002     ZF

P2 - Processing parameters
SI         512
SF         400.3200164 MHz
WDW        EM
SSB        0
LB         0 Hz
GB         0
PC         1.00

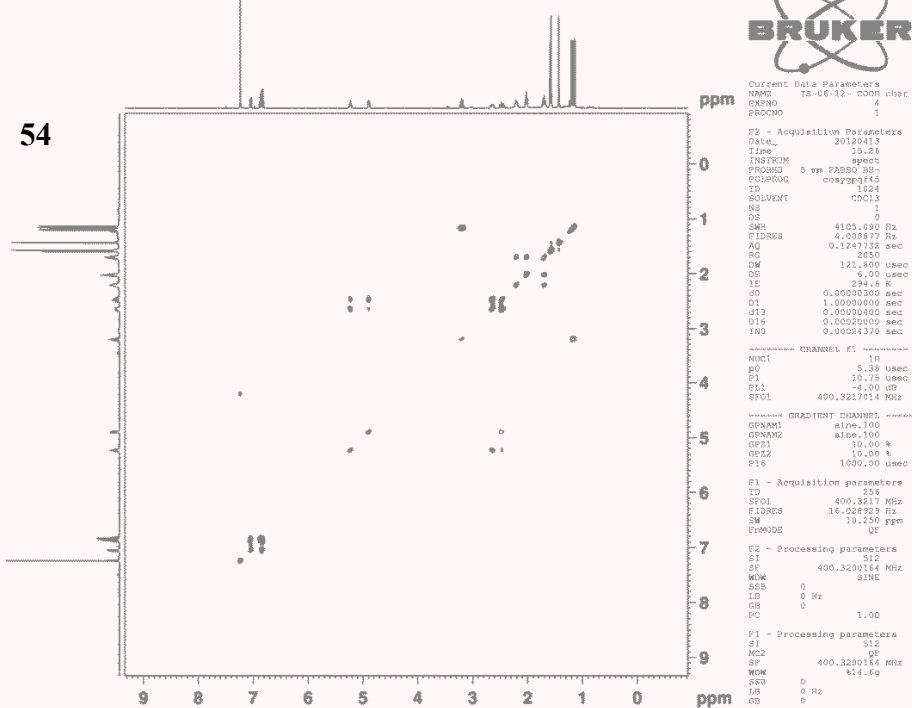
F1 - Processing parameters
SI         512
MC2        ZF
SF         400.3200164 MHz
WDW        EM
SSB        0
LB         0 Hz
GB         0
PC         1.00

```


1d_13C_DEPT_135_1_hour CDC13 D:\\ Barr 46

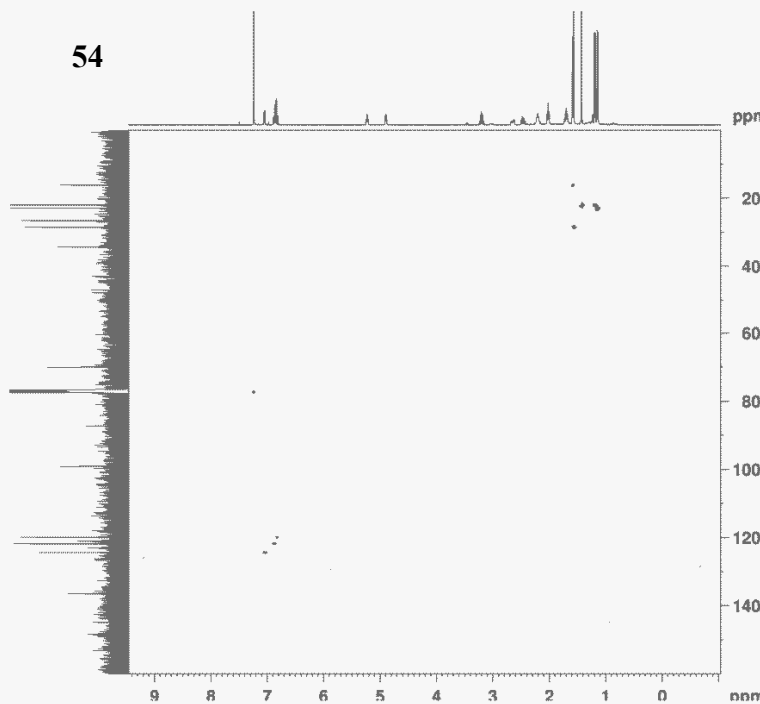


2d_1H_COSY_5_min CDC13 D:\\ Barr 46



2d_HMQC_1_hour CDC13 D:\\ Barr 46

54



Current Data Parameters
NAME TS-04-46-SM-char
EXPNO 1
PROCNO 1

F2 - Acquisition Parameters
Date_ 20120419
Time 11:10
INSTRUM spect
PROBHD 5 mm PARBO BB-
PULPROG zgpg30
TD 49152
SOLVENT CDC13
NS 16
DS 0
SWH 4201.847 Hz
FIDRES 0.132000 Hz
AQ 20.30
RG 119.4000 Hz
DE 6.00 usec
TE 294.2 K
D1 0.2000000 sec
D2 0.2000000 sec
D3 0.2000000 sec
D4 0.2000000 sec
D5 0.2000000 sec
D6 0.2000000 sec
D7 0.2000000 sec
D8 0.2000000 sec
D9 0.2000000 sec
D10 0.2000000 sec
D11 0.2000000 sec
D12 0.2000000 sec
D13 0.2000000 sec
D14 0.2000000 sec
D15 0.2000000 sec
D16 0.2000000 sec
D17 0.2000000 sec
D18 0.2000000 sec
D19 0.2000000 sec
D20 0.2000000 sec
D21 0.2000000 sec
D22 0.2000000 sec
D23 0.2000000 sec
D24 0.2000000 sec
D25 0.2000000 sec
D26 0.2000000 sec
D27 0.2000000 sec
D28 0.2000000 sec
D29 0.2000000 sec
D30 0.2000000 sec
D31 0.2000000 sec
D32 0.2000000 sec
D33 0.2000000 sec
D34 0.2000000 sec
D35 0.2000000 sec
D36 0.2000000 sec
D37 0.2000000 sec
D38 0.2000000 sec
D39 0.2000000 sec
D40 0.2000000 sec
D41 0.2000000 sec
D42 0.2000000 sec
D43 0.2000000 sec
D44 0.2000000 sec
D45 0.2000000 sec
D46 0.2000000 sec
D47 0.2000000 sec
D48 0.2000000 sec
D49 0.2000000 sec
D50 0.2000000 sec
D51 0.2000000 sec
D52 0.2000000 sec
D53 0.2000000 sec
D54 0.2000000 sec
D55 0.2000000 sec
D56 0.2000000 sec
D57 0.2000000 sec
D58 0.2000000 sec
D59 0.2000000 sec
D60 0.2000000 sec
D61 0.2000000 sec
D62 0.2000000 sec
D63 0.2000000 sec
D64 0.2000000 sec
D65 0.2000000 sec
D66 0.2000000 sec
D67 0.2000000 sec
D68 0.2000000 sec
D69 0.2000000 sec
D70 0.2000000 sec
D71 0.2000000 sec
D72 0.2000000 sec
D73 0.2000000 sec
D74 0.2000000 sec
D75 0.2000000 sec
D76 0.2000000 sec
D77 0.2000000 sec
D78 0.2000000 sec
D79 0.2000000 sec
D80 0.2000000 sec
D81 0.2000000 sec
D82 0.2000000 sec
D83 0.2000000 sec
D84 0.2000000 sec
D85 0.2000000 sec
D86 0.2000000 sec
D87 0.2000000 sec
D88 0.2000000 sec
D89 0.2000000 sec
D90 0.2000000 sec
D91 0.2000000 sec
D92 0.2000000 sec
D93 0.2000000 sec
D94 0.2000000 sec
D95 0.2000000 sec
D96 0.2000000 sec
D97 0.2000000 sec
D98 0.2000000 sec
D99 0.2000000 sec
D100 0.2000000 sec

----- CHANNEL f1 -----
NUC1 1H
P1 10.75 usec
PL1 -4.00 dB
SFO1 400.320164 MHz

----- CHANNEL f2 -----
NUC2 13C
P2 12.00 usec
PL2 -4.00 dB
SFO2 100.628150 MHz

----- GRADIENT CHANNEL -----
GPMAX1 slope:100
GPMAX2 slope:100
GPMAX3 slope:100
GPMAX4 slope:100
GPMAX5 slope:100
GPMAX6 slope:100
GPMAX7 slope:100
GPMAX8 slope:100
GPMAX9 slope:100
GPMAX10 slope:100
GPMAX11 slope:100
GPMAX12 slope:100
GPMAX13 slope:100
GPMAX14 slope:100
GPMAX15 slope:100
GPMAX16 slope:100
GPMAX17 slope:100
GPMAX18 slope:100
GPMAX19 slope:100
GPMAX20 slope:100
GPMAX21 slope:100
GPMAX22 slope:100
GPMAX23 slope:100
GPMAX24 slope:100
GPMAX25 slope:100
GPMAX26 slope:100
GPMAX27 slope:100
GPMAX28 slope:100
GPMAX29 slope:100
GPMAX30 slope:100
GPMAX31 slope:100
GPMAX32 slope:100
GPMAX33 slope:100
GPMAX34 slope:100
GPMAX35 slope:100
GPMAX36 slope:100
GPMAX37 slope:100
GPMAX38 slope:100
GPMAX39 slope:100
GPMAX40 slope:100
GPMAX41 slope:100
GPMAX42 slope:100
GPMAX43 slope:100
GPMAX44 slope:100
GPMAX45 slope:100
GPMAX46 slope:100
GPMAX47 slope:100
GPMAX48 slope:100
GPMAX49 slope:100
GPMAX50 slope:100
GPMAX51 slope:100
GPMAX52 slope:100
GPMAX53 slope:100
GPMAX54 slope:100
GPMAX55 slope:100
GPMAX56 slope:100
GPMAX57 slope:100
GPMAX58 slope:100
GPMAX59 slope:100
GPMAX60 slope:100
GPMAX61 slope:100
GPMAX62 slope:100
GPMAX63 slope:100
GPMAX64 slope:100
GPMAX65 slope:100
GPMAX66 slope:100
GPMAX67 slope:100
GPMAX68 slope:100
GPMAX69 slope:100
GPMAX70 slope:100
GPMAX71 slope:100
GPMAX72 slope:100
GPMAX73 slope:100
GPMAX74 slope:100
GPMAX75 slope:100
GPMAX76 slope:100
GPMAX77 slope:100
GPMAX78 slope:100
GPMAX79 slope:100
GPMAX80 slope:100
GPMAX81 slope:100
GPMAX82 slope:100
GPMAX83 slope:100
GPMAX84 slope:100
GPMAX85 slope:100
GPMAX86 slope:100
GPMAX87 slope:100
GPMAX88 slope:100
GPMAX89 slope:100
GPMAX90 slope:100
GPMAX91 slope:100
GPMAX92 slope:100
GPMAX93 slope:100
GPMAX94 slope:100
GPMAX95 slope:100
GPMAX96 slope:100
GPMAX97 slope:100
GPMAX98 slope:100
GPMAX99 slope:100
GPMAX100 slope:100

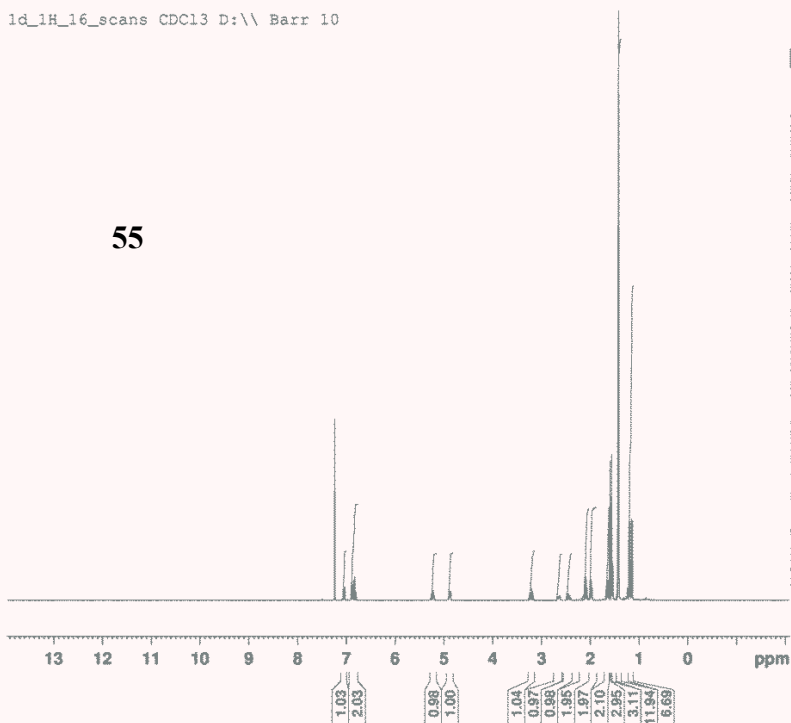
F1 - Acquisition parameters
SI 65536
SF 400.320164 MHz
WDW EM
SSB 0
LB 0.10 Hz
GB 0
PC 1.00

F2 - Processing parameters
SI 65536
SF 400.320164 MHz
WDW EM
SSB 0
LB 0.10 Hz
GB 0
PC 1.00

F1 - Processing parameters
SI 65536
SF 400.320164 MHz
WDW EM
SSB 0
LB 0.10 Hz
GB 0
PC 1.00

1d_1H_16_scans CDC13 D:\\ Barr 10

55



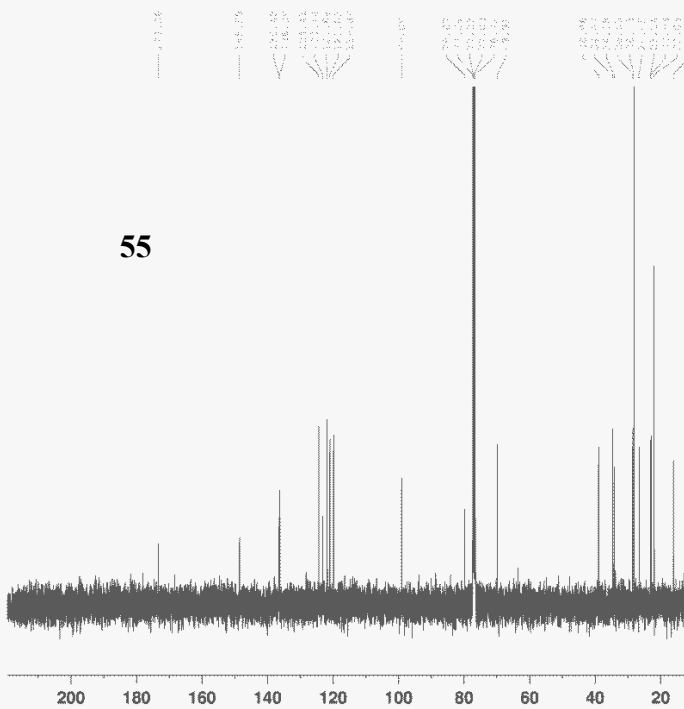
Current Data Parameters
NAME TS-04-46-SM-char
EXPNO 1
PROCNO 1

F2 - Acquisition Parameters
Date_ 20120419
Time 11:42
INSTRUM spect
PROBHD 5 mm PARBO BB-
PULPROG zg30
TD 49152
SOLVENT CDC13
NS 16
DS 0
SWH 6421.233 Hz
FIDRES 0.130640 Hz
AQ 3.8273523 sec
RG 456
DE 77.867 usec
TE 294.2 K
D1 1.0000000 sec
D2 0.2000000 sec
D3 0.2000000 sec
D4 0.2000000 sec
D5 0.2000000 sec
D6 0.2000000 sec
D7 0.2000000 sec
D8 0.2000000 sec
D9 0.2000000 sec
D10 0.2000000 sec
D11 0.2000000 sec
D12 0.2000000 sec
D13 0.2000000 sec
D14 0.2000000 sec
D15 0.2000000 sec
D16 0.2000000 sec
D17 0.2000000 sec
D18 0.2000000 sec
D19 0.2000000 sec
D20 0.2000000 sec
D21 0.2000000 sec
D22 0.2000000 sec
D23 0.2000000 sec
D24 0.2000000 sec
D25 0.2000000 sec
D26 0.2000000 sec
D27 0.2000000 sec
D28 0.2000000 sec
D29 0.2000000 sec
D30 0.2000000 sec
D31 0.2000000 sec
D32 0.2000000 sec
D33 0.2000000 sec
D34 0.2000000 sec
D35 0.2000000 sec
D36 0.2000000 sec
D37 0.2000000 sec
D38 0.2000000 sec
D39 0.2000000 sec
D40 0.2000000 sec
D41 0.2000000 sec
D42 0.2000000 sec
D43 0.2000000 sec
D44 0.2000000 sec
D45 0.2000000 sec
D46 0.2000000 sec
D47 0.2000000 sec
D48 0.2000000 sec
D49 0.2000000 sec
D50 0.2000000 sec
D51 0.2000000 sec
D52 0.2000000 sec
D53 0.2000000 sec
D54 0.2000000 sec
D55 0.2000000 sec
D56 0.2000000 sec
D57 0.2000000 sec
D58 0.2000000 sec
D59 0.2000000 sec
D60 0.2000000 sec
D61 0.2000000 sec
D62 0.2000000 sec
D63 0.2000000 sec
D64 0.2000000 sec
D65 0.2000000 sec
D66 0.2000000 sec
D67 0.2000000 sec
D68 0.2000000 sec
D69 0.2000000 sec
D70 0.2000000 sec
D71 0.2000000 sec
D72 0.2000000 sec
D73 0.2000000 sec
D74 0.2000000 sec
D75 0.2000000 sec
D76 0.2000000 sec
D77 0.2000000 sec
D78 0.2000000 sec
D79 0.2000000 sec
D80 0.2000000 sec
D81 0.2000000 sec
D82 0.2000000 sec
D83 0.2000000 sec
D84 0.2000000 sec
D85 0.2000000 sec
D86 0.2000000 sec
D87 0.2000000 sec
D88 0.2000000 sec
D89 0.2000000 sec
D90 0.2000000 sec
D91 0.2000000 sec
D92 0.2000000 sec
D93 0.2000000 sec
D94 0.2000000 sec
D95 0.2000000 sec
D96 0.2000000 sec
D97 0.2000000 sec
D98 0.2000000 sec
D99 0.2000000 sec
D100 0.2000000 sec

----- CHANNEL f1 -----
NUC1 1H
P1 10.75 usec
PL1 -4.00 dB
SFO1 400.3223900 MHz

F2 - Processing parameters
SI 65536
SF 400.320164 MHz
WDW EM
SSB 0
LB 0.10 Hz
GB 0
PC 1.00

1d_13C_20_minutes CDC13 D:\ Barr 10



Current Data Parameters
 NAME TS-04-46-SM-char
 EXPNO 2
 PROCNO 1

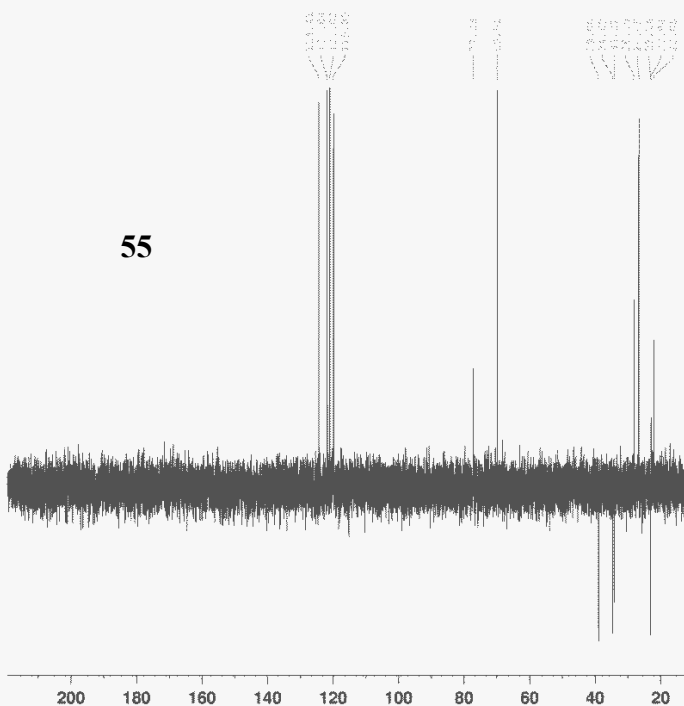
F2 - Acquisition Parameters
 Date_ 20120421
 Time_ 3.31
 INSTRUM spect
 PROBHD 5 mm PABBO BB-
 PULPROG zgpg30
 TD 51200
 SOLVENT CDC13
 NS 512
 DS 0
 SMH 24038.461 Hz
 FIDRES 0.469501 Hz
 AQ 1.0650100 sec
 RG 322
 DW 20.800 usec
 DE 6.00 usec
 TE 296.3 K
 D1 1.00000000 sec
 d11 0.03000000 sec
 DELTA 0.89999998 sec
 TD0 1

----- CHANNEL f1 -----
 NUC1 13C
 P1 7.50 usec
 PL1 -3.00 dB
 SFO1 100.6706101 MHz

----- CHANNEL f2 -----
 CPDPRG2 waltz16
 NUC2 1H
 PCPD2 90.00 usec
 PL2 -4.00 dB
 PL12 14.46 dB
 PL13 18.01 dB
 SFO2 400.3216013 MHz

F2 - Processing parameters
 SI 65536
 SF 100.6605440 MHz
 WDW EM
 SSB 0
 LB 1.00 Hz
 GB 0
 PC 1.40

1d_13C_DEPT_135_20_minutes CDC13 D:\ Barr 10



Current Data Parameters
 NAME TS-04-46-SM-char
 EXPNO 3
 PROCNO 1

F2 - Acquisition Parameters
 Date_ 20120421
 Time_ 3.55
 INSTRUM spect
 PROBHD 5 mm PABBO BB-
 PULPROG dept135
 TD 51200
 SOLVENT CDC13
 NS 416
 DS 2
 SMH 24038.461 Hz
 FIDRES 0.469501 Hz
 AQ 1.0650100 sec
 RG 2050
 DW 20.800 usec
 DE 6.00 usec
 TE 295.8 K
 CNST2 145.0000000
 D1 2.00000000 sec
 d2 0.00344828 sec
 d12 0.00002000 sec
 DELTA 0.00009955 sec
 TD0 1

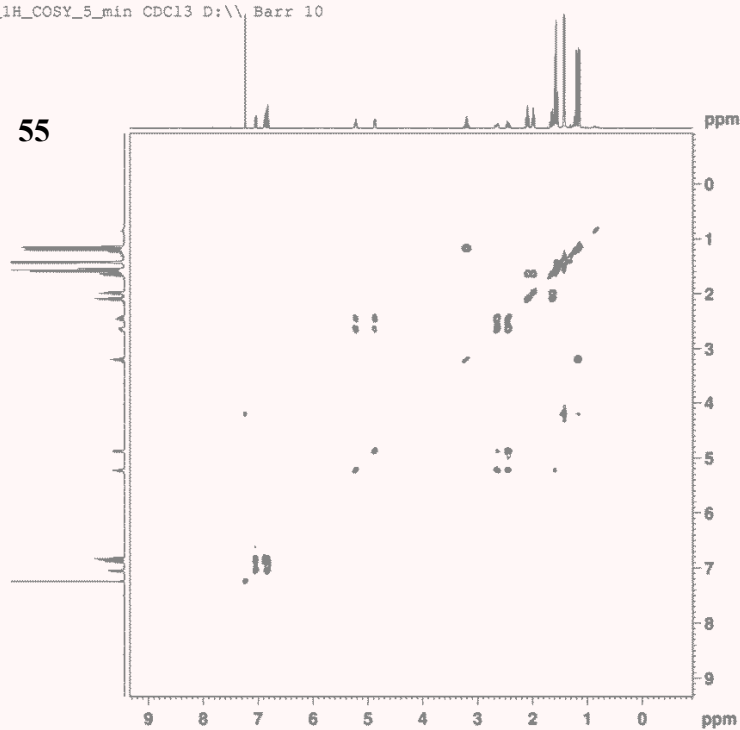
----- CHANNEL f1 -----
 NUC1 13C
 P1 7.50 usec
 PL1 -3.00 dB
 SFO1 100.6706101 MHz

----- CHANNEL f2 -----
 CPDPRG2 waltz16
 NUC2 1H
 P2 10.75 usec
 P4 21.50 usec
 PCPD2 90.00 usec
 PL2 -4.00 dB
 PL12 14.46 dB
 SFO2 400.3216013 MHz

F2 - Processing parameters
 SI 65536
 SF 100.6605440 MHz
 WDW EM
 SSB 0
 LB 1.00 Hz
 GB 0
 PC 1.40

2d_1H-COSY_5_min CDC13 D:\\ Barr 10

55



Current Data Parameters
 NAME TS-04-46-SM-char
 EXNO 4
 PROCNO 1

F2 - Acquisition Parameters
 Date_ 20120419
 Time 11:42
 INSTRUM spect
 PNCB00 5 mm BBOBO BB-
 PULPROG zgpg30f45
 TD 32768
 SOLVENT CDCl3
 NS 1
 DS 0
 SFO1 4105.090 Hz
 FIDRES 4.002877 Hz
 AQ 0.1247725 sec
 RG 2050
 DW 121.000 usec
 DE 6.00 usec
 TE 300.2 K
 D0 0.0000000 sec
 D1 1.0000000 sec
 d13 0.0000000 sec
 D16 0.0002000 sec
 INU 0.0024370 sec

----- CHANNEL f1 -----
 NU1 16
 p0 0.30 usec
 P1 10.70 usec
 PL1 -4.00 dB
 SFO1 400.3217014 MHz

----- GRADIENT CHANNEL -----
 GPRAM1 sine,100
 GPRAM2 sine,100
 GPC1 10.00 %
 GPC2 10.00 %
 P16 1000.00 usec

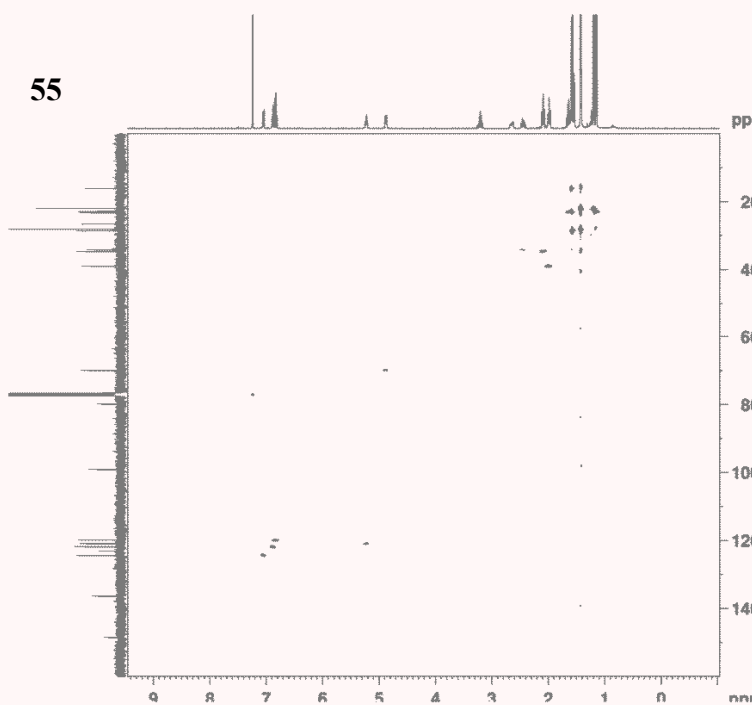
F1 - Acquisition parameters
 TD 32768
 SFO1 400.3217 MHz
 FIDRES 16.028920 Hz
 SW 10.740 ppm
 FREQ00 QF

F2 - Processing parameters
 SI 512
 SF 400.3200164 MHz
 NWDW 0 SINC
 SSB 0
 LB 0 Hz
 GB 0
 PC 1.00

F1 - Processing parameters
 SI 512
 NCS2 QF
 SF 400.3200164 MHz
 HSW <Gauss>
 ##\$PNAME\$
 SSB 0
 LB 0 Hz
 GB 0

2d_HMQC_1_hour CDC13 D:\\ Barr 10

55



Current Data Parameters
 NAME TS-04-46-SM-char
 EXNO 4
 PROCNO 1

F2 - Acquisition Parameters
 Date_ 20120419
 Time 11:51
 INSTRUM spect
 PNCB00 5 mm BBOBO BB-
 PULPROG zgpg30f
 TD 32768
 SOLVENT CDCl3
 NS 1
 DS 0
 SFO1 4201.487 Hz
 FIDRES 4.156204 Hz
 AQ 0.1219000 sec
 RG 2030
 DW 119.000 usec
 DE 6.00 usec
 TE 300.2 K
 D0 0.0000000 sec
 D1 1.0000000 sec
 d1 0.0034000 sec
 d12 0.0002000 sec
 d13 0.0000000 sec
 D15 0.0000000 sec
 D16 0.0022000 sec
 INU 0.0012100 sec

----- CHANNEL f1 -----
 NU1 16
 p0 0.30 usec
 P1 10.70 usec
 PL1 -4.00 dB
 SFO1 400.3217014 MHz

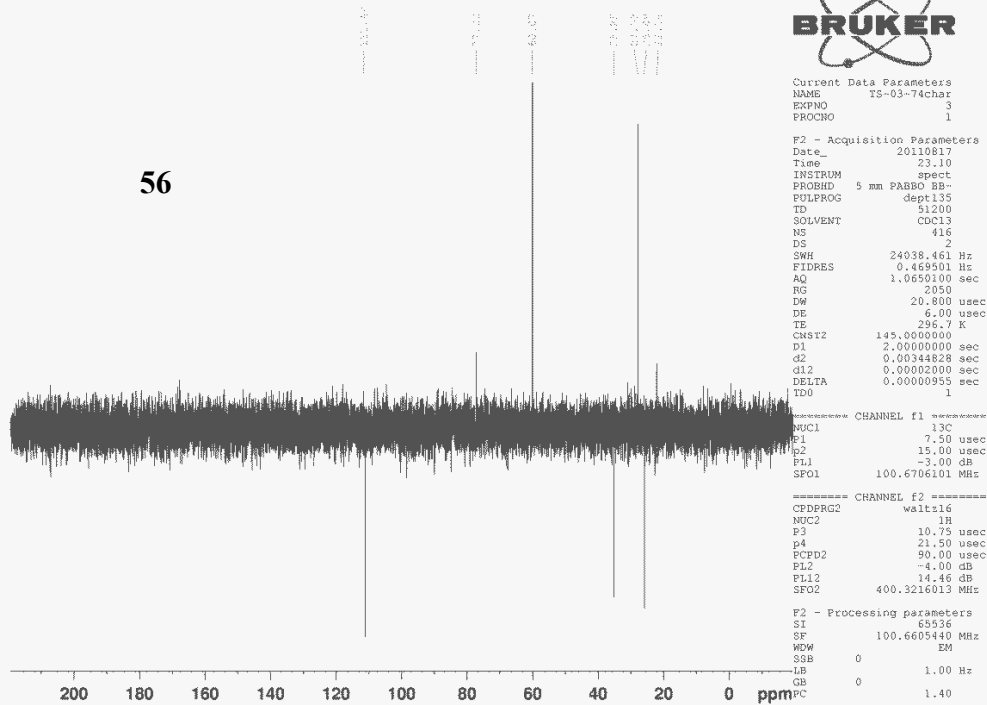
----- CHANNEL f2 -----
 GPRAM1 sine,100
 GPRAM2 sine,100
 GPC1 10.00 %
 GPC2 10.00 %
 GPC3 10.00 %
 GPC4 10.00 %
 P16 1000.00 usec

F1 - Acquisition parameters
 TD 32768
 SFO1 400.3217 MHz
 FIDRES 42.342376 Hz
 SW 10.740 ppm
 FREQ00 QF

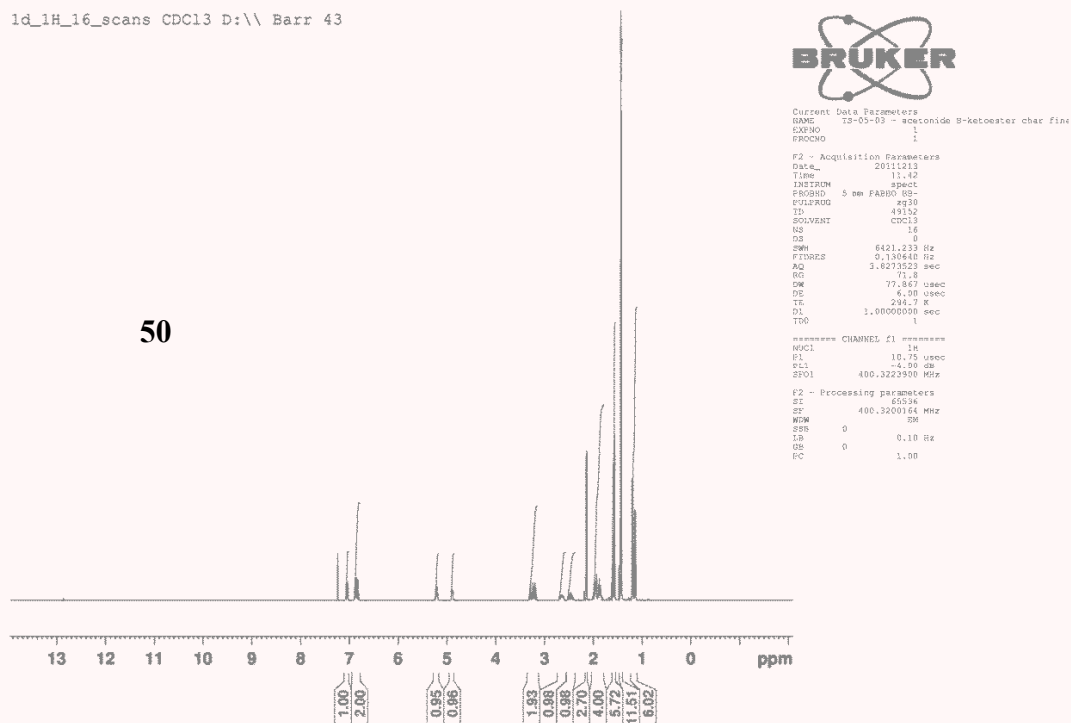
F2 - Processing parameters
 SI 3074
 SF 400.3200164 MHz
 NWDW 0 SINC
 SSB 0
 LB 0 Hz
 GB 0
 PC 1.00

F1 - Processing parameters
 SI 3074
 NCS2 QF
 SF 400.3200164 MHz
 HSW <Gauss>
 ##\$PNAME\$
 SSB 0
 LB 0 Hz
 GB 0

1d_13C_DEPT_135_20_minutes CDC13 D:\ Barr 4



1d_1H_16_scans CDC13 D:\ Barr 43



1d_13C_5_minutes CDC13 D:\\ Barr 43

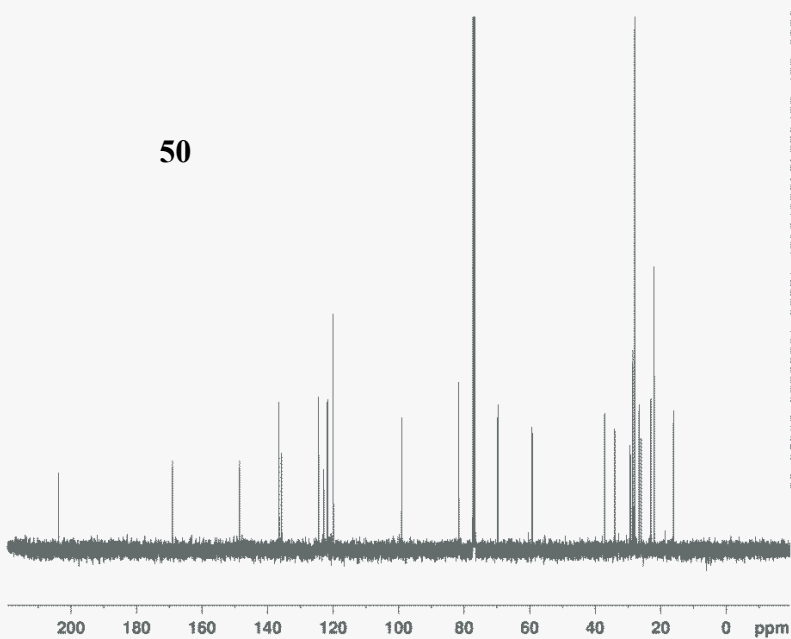


Current Data Parameters
 NAME TS-05-03 - acetamide B-kechoester char 1
 EXPNO 2
 PROCNO 1

F2 - Acquisition Parameters
 Date_ 20111213
 Time 11.48
 INSTRUM spect
 PROBP02 5 mm PABBO BA-
 PULPROG zgpg30
 TD 31200
 SOLVENT CDC13
 NS 128
 DS 0
 SWS 24028.461 Hz
 FIDRES 0.468501 Hz
 AQ 1.0650100 sec
 RG 456
 DM 29.900 usec
 DD 6.00 usec
 DE 295.5 K
 D1 1.00500000 sec
 d11 0.03000000 sec
 DELTA 0.58999998 sec
 TDO 1

----- CHANNEL f1 -----
 NUCL1 13C
 P1 7.00 usec
 PL1 -1.00 dB
 SFO1 100.6760101 MHz
 ----- CHANNEL f2 -----
 CPDPRG2 waltz16
 NS2 18
 PCPD2 90.00 usec
 PL2 1.00 dB
 PL12 14.40 dB
 PL13 18.01 dB
 SFO2 400.3216013 MHz

F2 - Processing parameters
 SI 65336
 SF 100.6604440 MHz
 NWDW 0
 SSB 0
 LB 1.00 Hz
 GB 0
 PC 1.40



1d_13C_DEPT_Q_135_5min CDC13 D:\\ Barr 43



Current Data Parameters
 NAME TS-05-03 - acetamide B-kechoester char final
 EXPNO 2
 PROCNO 1

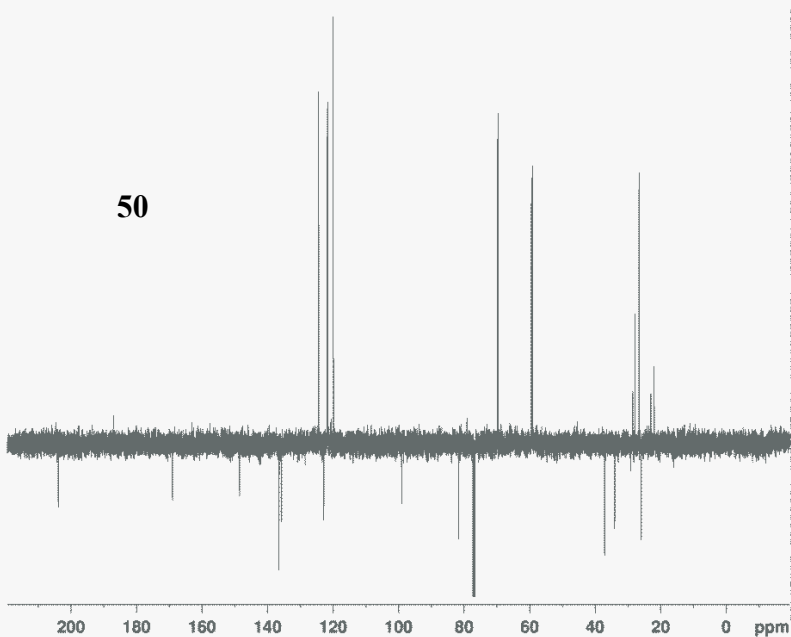
F2 - Acquisition Parameters
 Date_ 20111213
 Time 11.50
 INSTRUM spect
 PROBP02 5 mm PABBO BA-
 PULPROG zgpg30
 TD 31200
 SOLVENT CDC13
 NS 128
 DS 0
 SWS 24028.461 Hz
 FIDRES 0.468501 Hz
 AQ 1.0650100 sec
 RG 456
 DM 29.900 usec
 DD 6.00 usec
 DE 295.5 K
 D1 1.00500000 sec
 D12 1.00000000 sec
 D13 0.00048200 sec
 D14 0.00020600 sec
 D15 0.00000000 sec
 DELTA 0.00000000 sec
 DELTA1 0.00007200 sec
 DELTA2 0.00025378 sec
 DELTA3 0.00000000 sec
 TDO 1

----- CHANNEL f1 -----
 NUCL1 13C
 P1 7.00 usec
 PL1 2000.00 usec
 PL2 100.00 dB
 PL3 -1.00 dB
 SFO1 100.6760101 MHz
 SFO2 400.3216013 MHz
 SFO3 0 Hz
 SFO4 0 Hz
 SFO5 0 Hz

----- CHANNEL f2 -----
 CPDPRG2 waltz16
 NS2 18
 PCPD2 90.00 usec
 PL2 1.00 dB
 PL12 14.40 dB
 PL13 18.01 dB
 SFO2 400.3216013 MHz

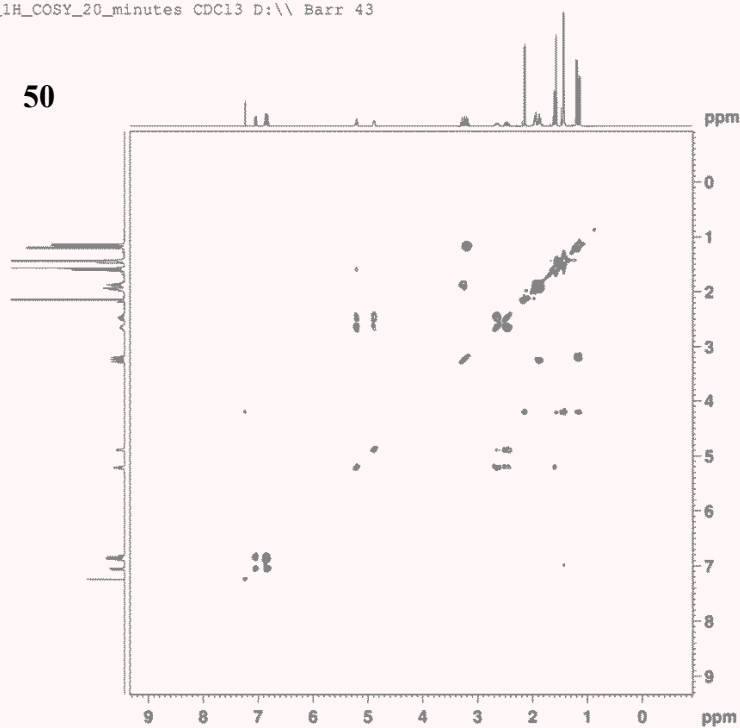
----- GRABENT CHANNEL -----
 GRAB1 0 Hz
 GRAB2 0 Hz
 GRAB3 0 Hz
 SFO1 0 Hz
 SFO2 0 Hz
 SFO3 0 Hz
 SFO4 0 Hz
 SFO5 0 Hz

F2 - Processing parameters
 SI 65336
 SF 100.6604440 MHz
 NWDW 0
 SSB 0
 LB 1.00 Hz
 GB 0
 PC 1.40



2d_1H_COSY_20_minutes CDC13 D:\ Barr 43

50



```

Current Data Parameters
NAME      T6-05-03char
EXPNO    4
PROCNO   1

F2 - Acquisition Parameters
Date_    20111213
Time     17.08
INSTRUM  spect
PROBHD   5 mm PABBO 90-
PULPROG  zgpg30f45
TD       1024
SOLVENT  CDC13
NS       4
DS       0
SFO1     4105.090 Hz
FIDRES   4.008877 Hz
AQ       0.1241132 sec
RG       124
DM       121.800 usec
DE       6.00 usec
TE       295.1 K
d0       0.00000000 sec
d1       1.00000000 sec
d12      0.00000000 sec
d15      0.00000000 sec
IN0      0.00024370 sec

----- CHANNEL f1 -----
NUC1     1H
P0       5.38 usec
P1       10.76 usec
P12      -1.00 dB
SFO1     400.321714 MHz

----- GRADIENT CHANNEL -----
GRNAM1   s1ne-100
GRNAM2   s1ne-100
GE21     10.00 %
GF22     10.00 %
P16      1000.00 usec

F1 - Acquisition parameters
TD       256
SFO1     400.3217 MHz
FIDRES   16.028299 Hz
SW       19.250 ppm
F2NAME    OF

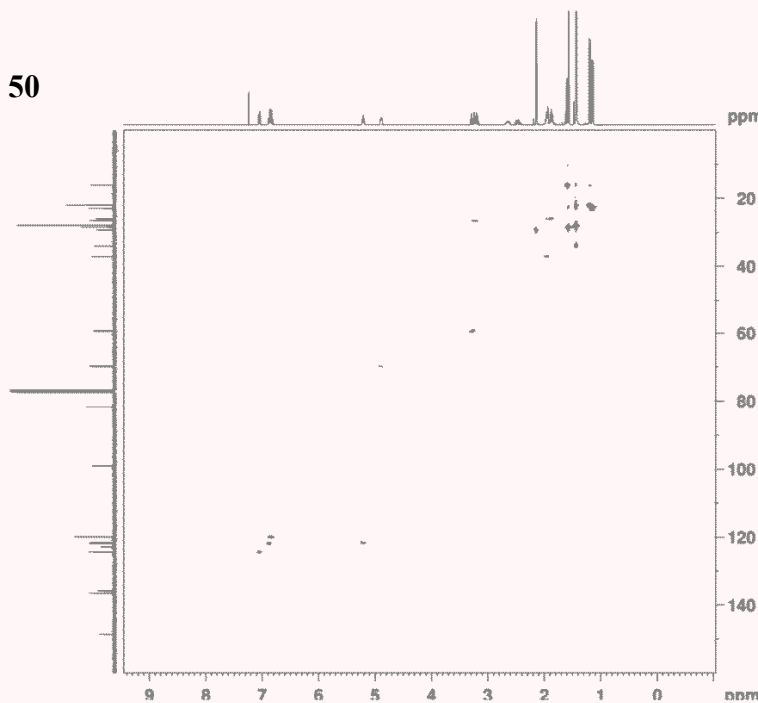
F2 - Processing parameters
SI       512
SF       400.320164 MHz
WDW      SINC
SSB      0
LB       0 Hz
GB       0
PC       1.00

F1 - Processing parameters
SI       512
MC2      OF
SF       400.320164 MHz
WDW      OF
SSB      0
LB       0 Hz
GB       0
PC       1.00

```

2d_HMQC_1_hour CDC13 D:\ Barr 43

50



```

Current Data Parameters
NAME      T6-05-03char
EXPNO    3
PROCNO   1

F2 - Acquisition Parameters
Date_    20111213
Time     17.08
INSTRUM  spect
PROBHD   5 mm PABBO 90-
PULPROG  zgpg30f45
TD       1024
SOLVENT  CDC13
NS       14
DS       0
SFO1     400.141 Hz
FIDRES   4.103204 Hz
AQ       0.1311000 sec
RG       7032
DM       131.000 usec
DE       4.00 usec
TE       295.1 K
d0       0.00000000 sec
d1       1.00000000 sec
d12      1.00000000 sec
d15      0.00000000 sec
IN0      0.00024370 sec

----- CHANNEL f1 -----
NUC1     1H
P0       5.38 usec
P1       10.76 usec
P12      -1.00 dB
SFO1     400.321714 MHz

----- CHANNEL f2 -----
CFPRG2   s1ne-100
NUC2     13C
P0       9.10 usec
P1       18.20 usec
P12      -3.00 dB
P122     17.36 dB
SFO2     100.626370 MHz

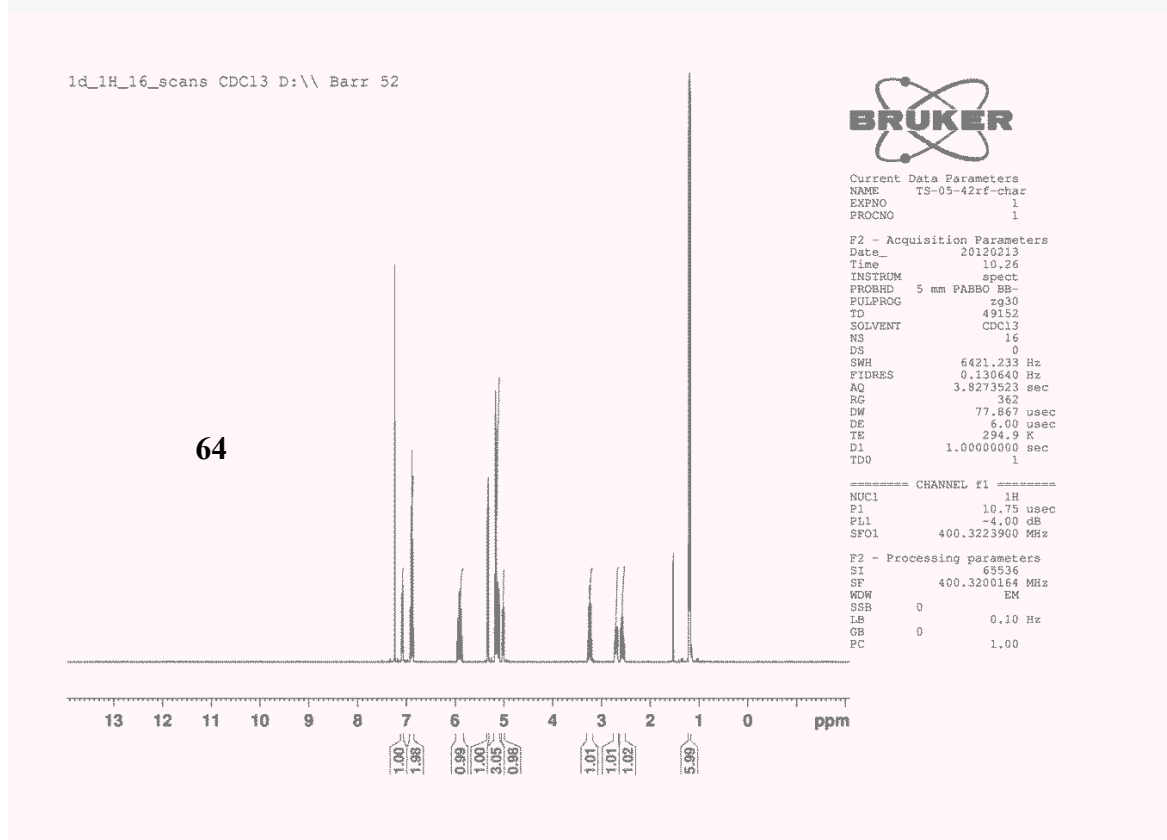
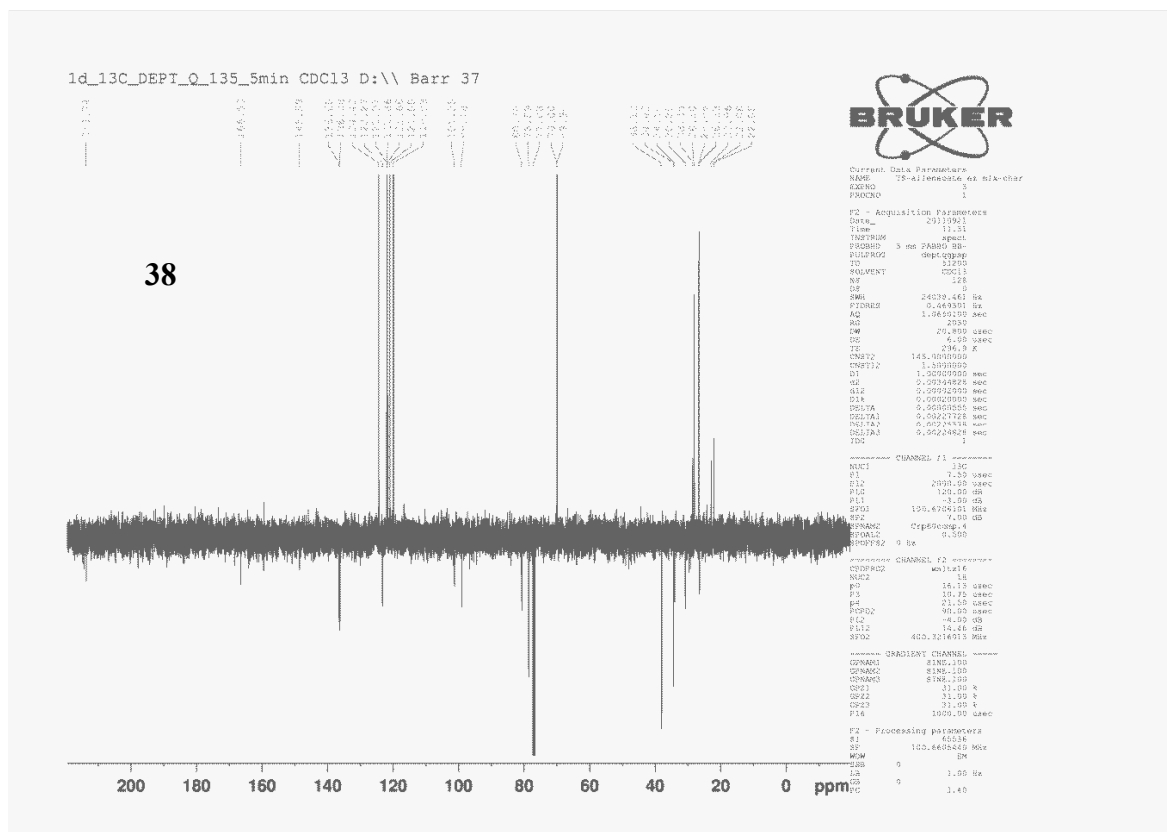
----- GRADIENT CHANNEL -----
GRNAM1   s1ne-100
GRNAM2   s1ne-100
GE21     50.00 %
GF22     50.00 %
P16      1000.00 usec

F1 - Acquisition parameters
TD       256
SFO1     100.62636 MHz
FIDRES   6.300276 Hz
SW       159.961 ppm
F2NAME    OF

F2 - Processing parameters
SI       1024
SF       100.6250431 MHz
WDW      SINC
SSB      0
LB       0 Hz
GB       0
PC       1.00

F1 - Processing parameters
SI       1024
MC2      OF
SF       100.6250431 MHz
WDW      OF
SSB      0
LB       0 Hz
GB       0
PC       1.00

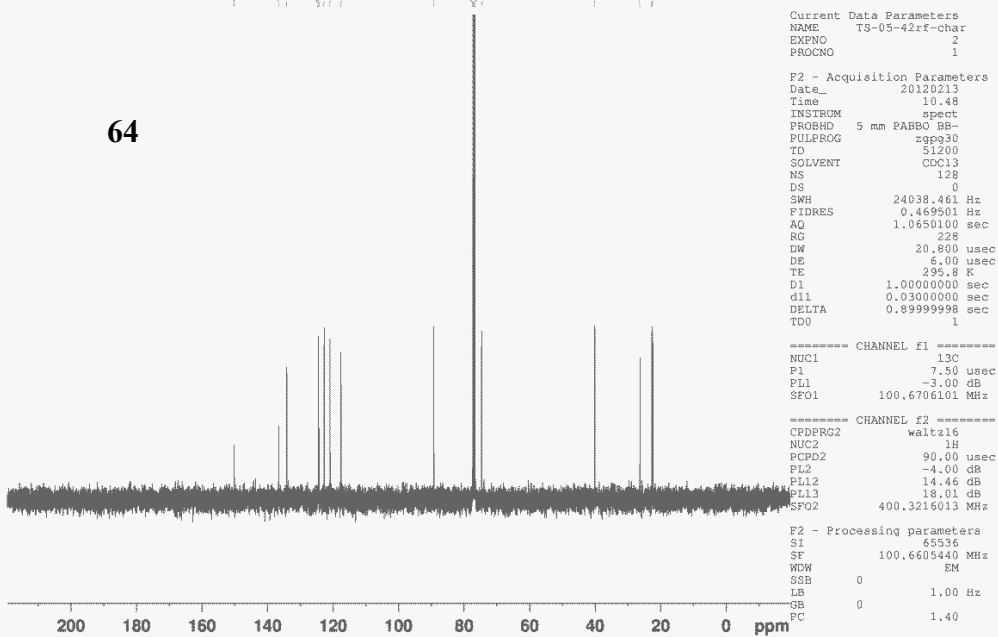
```

1d_13C_5_minutes CDC13 D:\\ Barr 52



64



Current Data Parameters
 NAME TS-05-42rf-char
 EXPNO 2
 PROCNO 1

F2 - Acquisition Parameters
 Date_ 20120213
 Time_ 10.48
 INSTRUM spect
 PROBHD 5 mm PABBO BB-
 PULPROG zgpg30
 TD 51200
 SOLVENT CDC13
 NS 128
 DS 0
 SMH 24038.461 Hz
 FIDRES 0.469501 Hz
 AQ 1.0650100 sec
 RG 228
 DW 20.800 usec
 DE 6.00 usec
 TE 295.8 K
 D1 1.0000000 sec
 d11 0.0300000 sec
 DELTA 0.89999998 sec
 TD0 1

----- CHANNEL f1 -----
 NUC1 13C
 P1 7.50 usec
 PL1 -3.00 dB
 SFO1 100.6706101 MHz

----- CHANNEL f2 -----
 CPDPRG2 waltz16
 NUC2 1H
 PCPD2 90.00 usec
 PL2 -4.00 dB
 PL12 14.46 dB
 PL13 18.01 dB
 SFO2 400.3216013 MHz

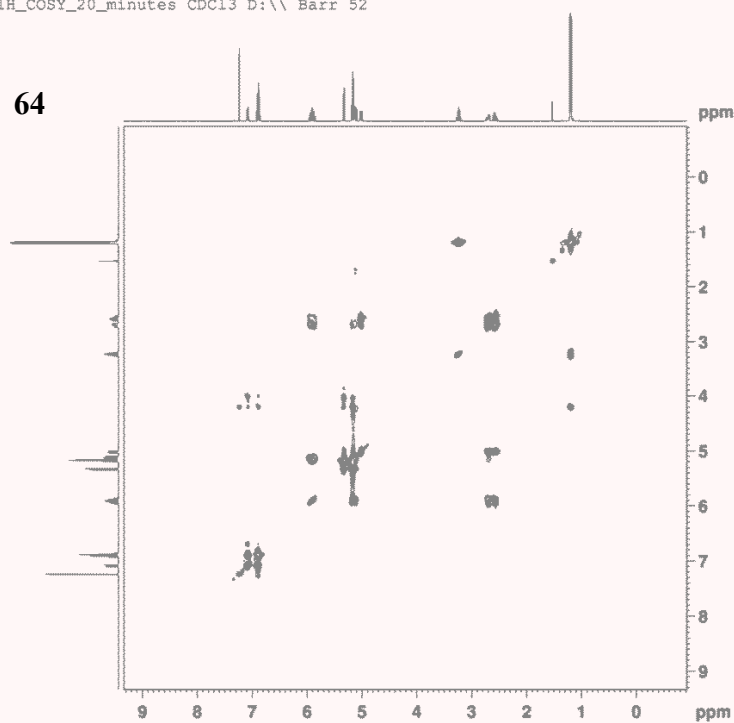
F2 - Processing parameters
 SI 65536
 SF 100.6605440 MHz
 WDW EM
 SSB 0
 LB 1.00 Hz
 GB 0
 PC 1.40

1d_13C_DEPT_135_5_minutes CDC13 D:\\ Barr 52



2d_1H_COSY_20_minutes CDC13 D:\ Barr 52

64



```

Current Data Parameters
NAME 75-05-42rf-char
EXPNO 4
PROCNO 1

F2 - Acquisition Parameters
Date_ 20120214
Time 0.07
INSTRUM spect
PROBHD 5 mm PABBO BH-
PULPROG cosyzgpg15
TD 1024
SOLVENT cdcl3
NS 4
DS 0
SWH 4105.090 Hz
FIDRES 4.008877 Hz
AQ 0.1241132 sec
RG 2050
DM 121.800 usec
DE 6.00 usec
TE 295.3 K
D0 0.00000000 sec
D1 1.00000000 sec
d11 0.00000000 sec
D12 0.00000000 sec
D15 0.00024370 sec
IN0 0.00024370 sec

----- CHANNEL f1 -----
NUC1 1H
P0 5.38 usec
P1 10.75 usec
P11 -1.00 dB
SFO1 400.321714 MHz

----- GRADIENT CHANNEL -----
GPNAM1 gline-100
GPNAM2 gline-100
GPE1 10.00 %
GPE2 10.00 %
P16 1000.00 usec

F1 - Acquisition parameters
TD 256
SFO1 400.321714 MHz
FIDRES 16.028299 Hz
SW 19.250 ppm
FREQ02 0F

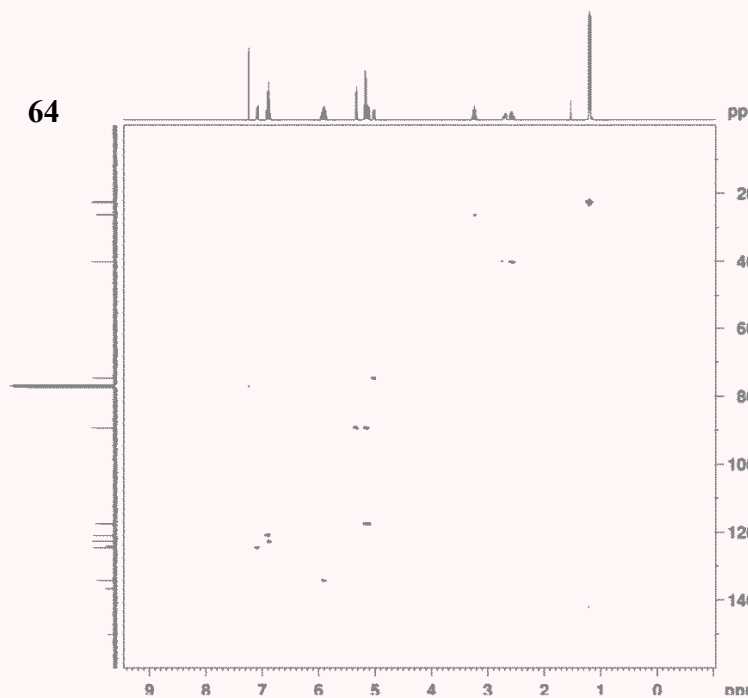
F2 - Processing parameters
SI 512
SF 400.320164 MHz
WDW SINC
SSB 0
LB 0 Hz
GB 0
PC 1.00

F1 - Processing parameters
SI 512
MC2 0F
SF 400.320164 MHz
WDW 0
SSB 0
LB 0 Hz
GB 0
PC 1.00

```

2d_HMQC_1_hour CDC13 D:\ Barr 49

64



```

Current Data Parameters
NAME 75-05-42-char2
EXPNO 1
PROCNO 1

F2 - Acquisition Parameters
Date_ 20120214
Time 0.07
INSTRUM spect
PROBHD 5 mm PABBO BH-
PULPROG hmqcpgf
TD 1024
SOLVENT cdcl3
NS 4
DS 0
SWH 4201.481 Hz
FIDRES 4.103204 Hz
AQ 0.1218657 sec
RG 2050
DM 121.800 usec
DE 6.00 usec
TE 295.3 K
D0 0.00000000 sec
D1 1.00000000 sec
d11 0.00000000 sec
D12 0.00000000 sec
D15 0.00024370 sec
IN0 0.00024370 sec

----- CHANNEL f1 -----
NUC1 1H
P0 5.38 usec
P1 10.75 usec
P11 -1.00 dB
SFO1 400.321714 MHz

----- CHANNEL f2 -----
CPDPRG2 gpc1
NUC2 13C
P02 91.00 usec
P03 91.00 usec
P04 91.00 usec
P05 91.00 usec
P06 91.00 usec
P07 91.00 usec
P08 91.00 usec
P09 91.00 usec
P10 91.00 usec
P11 91.00 usec
P12 91.00 usec
P13 91.00 usec
P14 91.00 usec
P15 91.00 usec
P16 91.00 usec
P17 91.00 usec
P18 91.00 usec
P19 91.00 usec
P20 91.00 usec
P21 91.00 usec
P22 91.00 usec
P23 91.00 usec
P24 91.00 usec
P25 91.00 usec
P26 91.00 usec
P27 91.00 usec
P28 91.00 usec
P29 91.00 usec
P30 91.00 usec
P31 91.00 usec
P32 91.00 usec
P33 91.00 usec
P34 91.00 usec
P35 91.00 usec
P36 91.00 usec
P37 91.00 usec
P38 91.00 usec
P39 91.00 usec
P40 91.00 usec
P41 91.00 usec
P42 91.00 usec
P43 91.00 usec
P44 91.00 usec
P45 91.00 usec
P46 91.00 usec
P47 91.00 usec
P48 91.00 usec
P49 91.00 usec
P50 91.00 usec
P51 91.00 usec
P52 91.00 usec
P53 91.00 usec
P54 91.00 usec
P55 91.00 usec
P56 91.00 usec
P57 91.00 usec
P58 91.00 usec
P59 91.00 usec
P60 91.00 usec
P61 91.00 usec
P62 91.00 usec
P63 91.00 usec
P64 91.00 usec
P65 91.00 usec
P66 91.00 usec
P67 91.00 usec
P68 91.00 usec
P69 91.00 usec
P70 91.00 usec
P71 91.00 usec
P72 91.00 usec
P73 91.00 usec
P74 91.00 usec
P75 91.00 usec
P76 91.00 usec
P77 91.00 usec
P78 91.00 usec
P79 91.00 usec
P80 91.00 usec
P81 91.00 usec
P82 91.00 usec
P83 91.00 usec
P84 91.00 usec
P85 91.00 usec
P86 91.00 usec
P87 91.00 usec
P88 91.00 usec
P89 91.00 usec
P90 91.00 usec
P91 91.00 usec
P92 91.00 usec
P93 91.00 usec
P94 91.00 usec
P95 91.00 usec
P96 91.00 usec
P97 91.00 usec
P98 91.00 usec
P99 91.00 usec
P100 91.00 usec

----- GRADIENT CHANNEL -----
GPNAM1 gline-100
GPNAM2 gline-100
GPE1 10.00 %
GPE2 10.00 %
P16 1000.00 usec

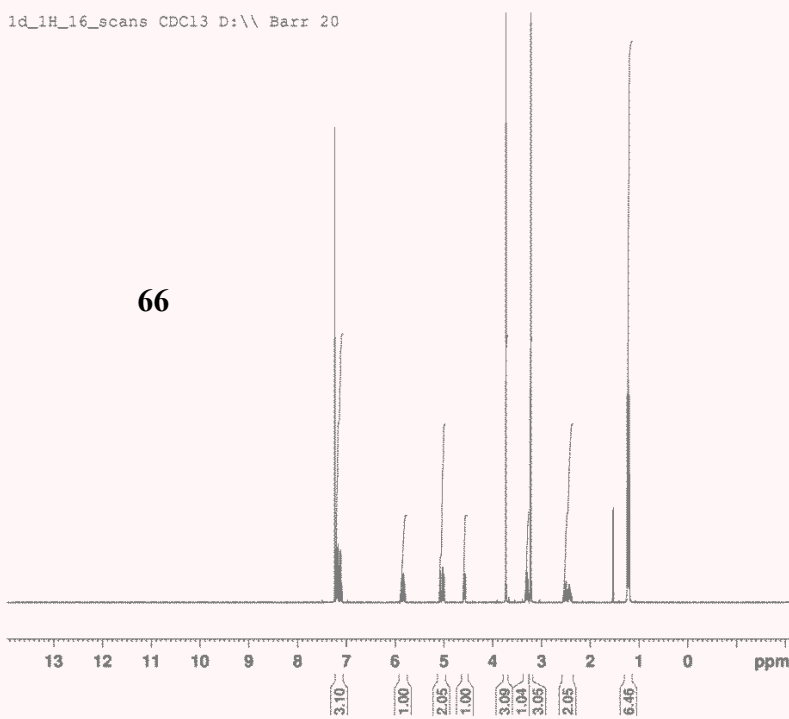
F1 - Acquisition parameters
TD 256
SFO1 400.321714 MHz
FIDRES 16.028299 Hz
SW 19.250 ppm
FREQ02 0F

F2 - Processing parameters
SI 1024
SF 400.320164 MHz
WDW SINC
SSB 0
LB 0 Hz
GB 0
PC 1.00

F1 - Processing parameters
SI 1024
MC2 0F
SF 400.320164 MHz
WDW 0
SSB 0
LB 0 Hz
GB 0
PC 1.00

```

1d_1H_16_scans CDC13 D:\\ Barr 20



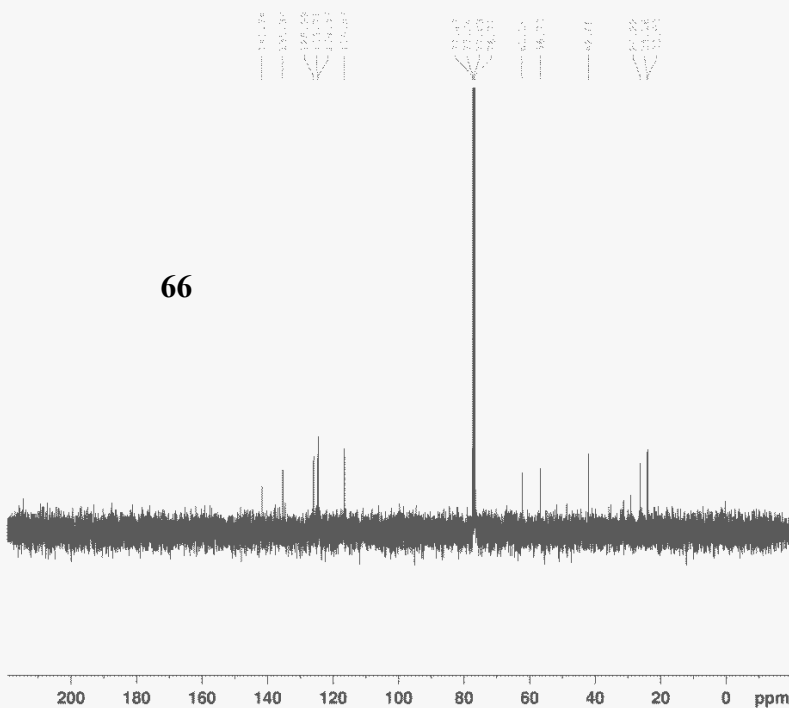
Current Data Parameters
 NAME TS-05-60char
 EXPNO 1
 PROCNO 1

F2 - Acquisition Parameters
 Date_ 20120222
 Time_ 10.40
 INSTRUM spect
 FROBHD 5 mm PABBO BB-
 PULPROG zg30
 TD 49152
 SOLVENT CDC13
 NS 16
 DS 0
 SMH 6421.233 Hz
 FIDRES 0.130640 Hz
 AQ 3.8273523 sec
 RG 512
 DW 77.867 usec
 DE 6.00 usec
 TE 295.0 K
 D1 1.00000000 sec
 TDO 1

===== CHANNEL f1 =====
 NUC1 1H
 P1 10.75 usec
 PL1 -4.00 dB
 SFO1 400.3223900 MHz

F2 - Processing parameters
 SI 65536
 SF 400.3200164 MHz
 WDW EM
 SSB 0
 LB 0.10 Hz
 GB 0
 PC 1.00

1d_13C_5_minutes CDC13 D:\\ Barr 20



Current Data Parameters
 NAME TS-05-60char
 EXPNO 2
 PROCNO 1

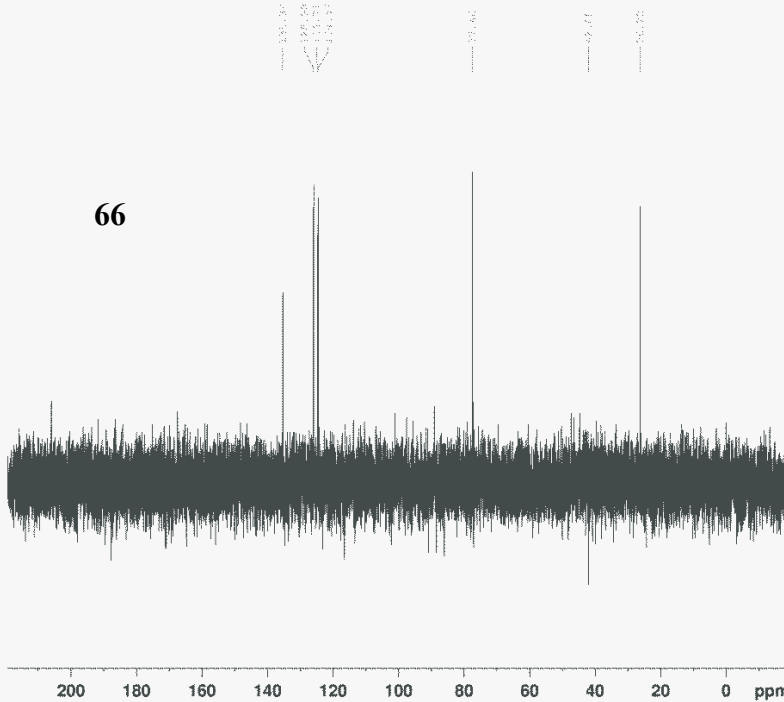
F2 - Acquisition Parameters
 Date_ 20120222
 Time_ 10.47
 INSTRUM spect
 FROBHD 5 mm PABBO BB-
 PULPROG zgpg30
 TD 51200
 SOLVENT CDC13
 NS 128
 DS 0
 SMH 24038.461 Hz
 FIDRES 0.469501 Hz
 AQ 1.0650100 sec
 RG 322
 DW 20.800 usec
 DE 6.00 usec
 TE 295.9 K
 D1 1.00000000 sec
 d11 0.03000000 sec
 DELTA 0.89999998 sec
 TDO 1

===== CHANNEL f1 =====
 NUC1 13C
 P1 7.50 usec
 PL1 -3.00 dB
 SFO1 100.6706101 MHz

===== CHANNEL f2 =====
 CPDPRG2 waltz16
 NUC2 1H
 BCPD2 90.00 usec
 PL2 -4.00 dB
 PL12 14.46 dB
 PL13 18.01 dB
 SFO2 400.3216013 MHz

F2 - Processing parameters
 SI 65536
 SF 100.6605440 MHz
 WDW EM
 SSB 0
 LB 1.00 Hz
 GB 0
 PC 1.40

1d_13C_DEPT_135_5_minutes CDC13 D:\ Barr 20



Current Data Parameters
 NAME TS-05-60char
 EXPNO 3
 PROCNO 1

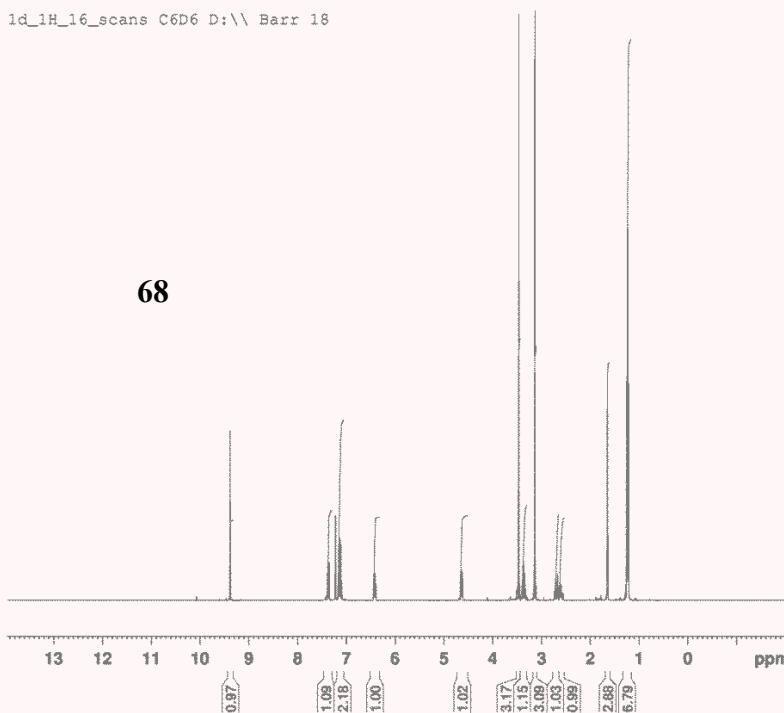
F2 - Acquisition Parameters
 Date_ 20120222
 Time 10.54
 INSTRUM spect
 PROBHD 5 mm PABBO BB-
 PULPROG dept135
 ID 51200
 SOLVENT CDC13
 NS 96
 DS 2
 SWH 24038.461 Hz
 FIDRES 0.469501 Hz
 AQ 1.0650100 sec
 RG 2050
 DW 20.800 usec
 DE 6.00 usec
 TE 295.5 K
 CHST2 145.000000
 D1 2.00000000 sec
 J2 0.00344828 sec
 J12 0.00020000 sec
 DELTA 0.0000955 sec
 TD0 1

===== CHANNEL f1 =====
 NUC1 13C
 P1 7.50 usec
 P2 15.00 usec
 PL1 -3.00 dB
 SFO1 100.6706101 MHz

===== CHANNEL f2 =====
 CPDPRG2 waitz16
 NUC2 1H
 P3 10.75 usec
 P4 21.50 usec
 PCPD2 90.00 usec
 PL2 -4.00 dB
 PL12 14.45 dB
 SFO2 400.3216013 MHz

F2 - Processing parameters
 SI 65536
 SF 100.6605440 MHz
 WDW EM
 SSB 0
 LB 1.00 Hz
 GB 0
 PC 1.40

1d_1H_16_scans C6D6 D:\ Barr 18



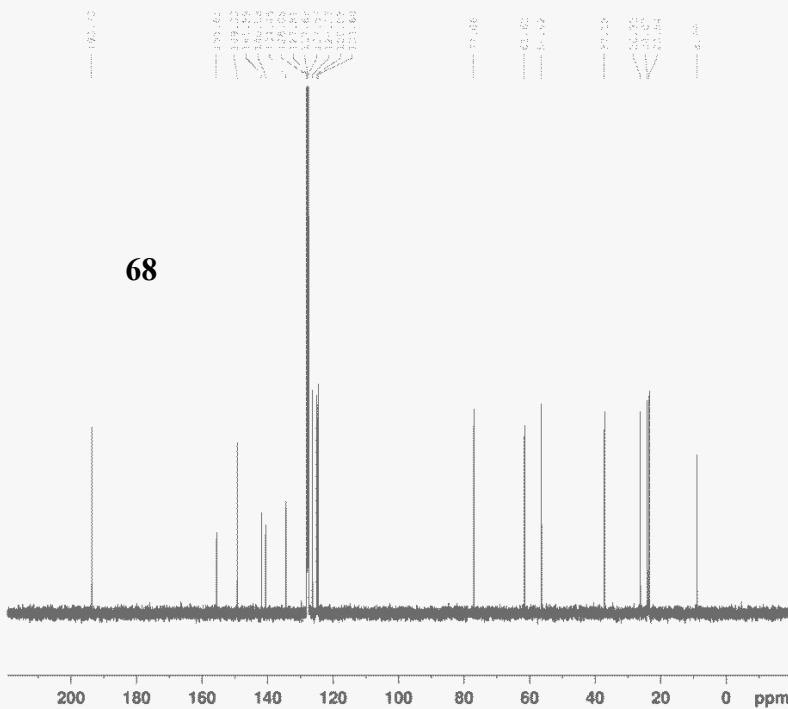
Current Data Parameters
 NAME TS-06-23-char-aldehyde
 EXPNO 1
 PROCNO 1

F2 - Acquisition Parameters
 Date_ 20120426
 Time 7.02
 INSTRUM spect
 PROBHD 5 mm PABBO BB-
 PULPROG zg30
 ID 49152
 SOLVENT C6D6
 NS 16
 DS 0
 SWH 6421.233 Hz
 FIDRES 0.130640 Hz
 AQ 3.8273523 sec
 RG 90.5
 DW 77.867 usec
 DE 6.00 usec
 TE 284.7 K
 D1 1.00000000 sec
 TD0 1

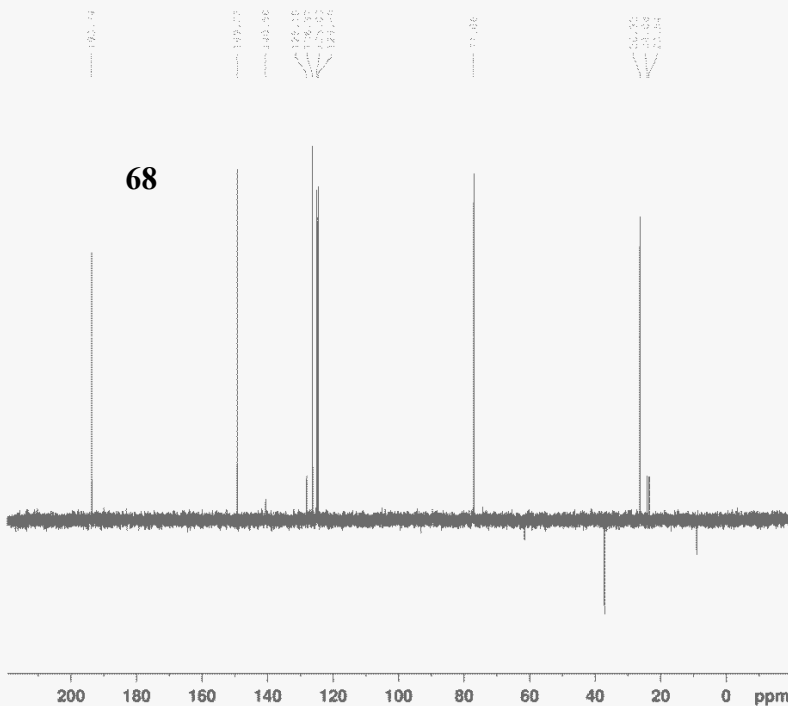
===== CHANNEL f1 =====
 NUC1 1H
 P1 10.75 usec
 PL1 -4.00 dB
 SFO1 400.3223900 MHz

F2 - Processing parameters
 SI 65536
 SF 400.3200164 MHz
 WDW EM
 SSB 0
 LB 0.10 Hz
 GB 0
 PC 1.00

1d_13C_5_minutes C6D6 D:\ Barr 18

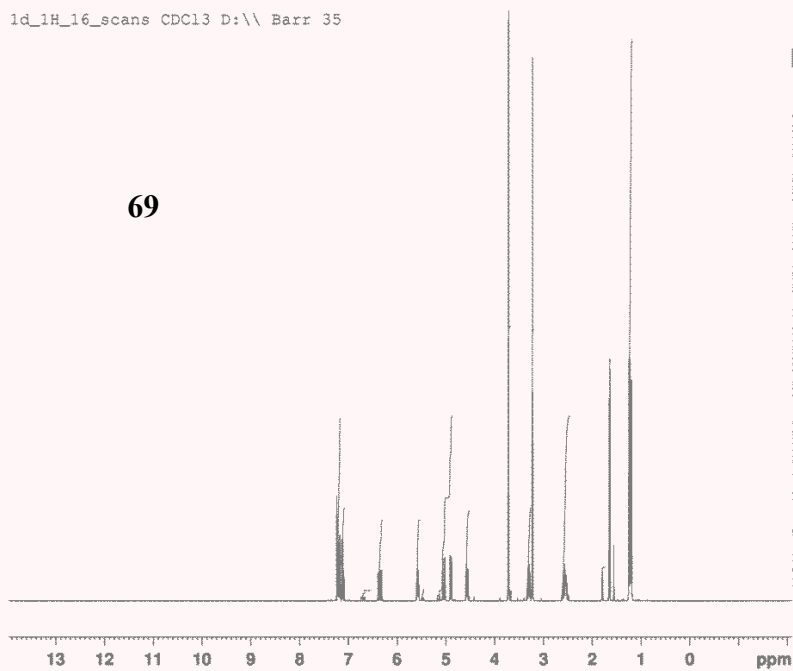


1d_13C_DEPT_135_5_minutes C6D6 D:\ Barr 18



1d_1H_16_scans CDC13 D:\\ Barr 35

69



Current Data Parameters
 NAME TS-05-65char
 EXPNO 1
 PROCNO 1

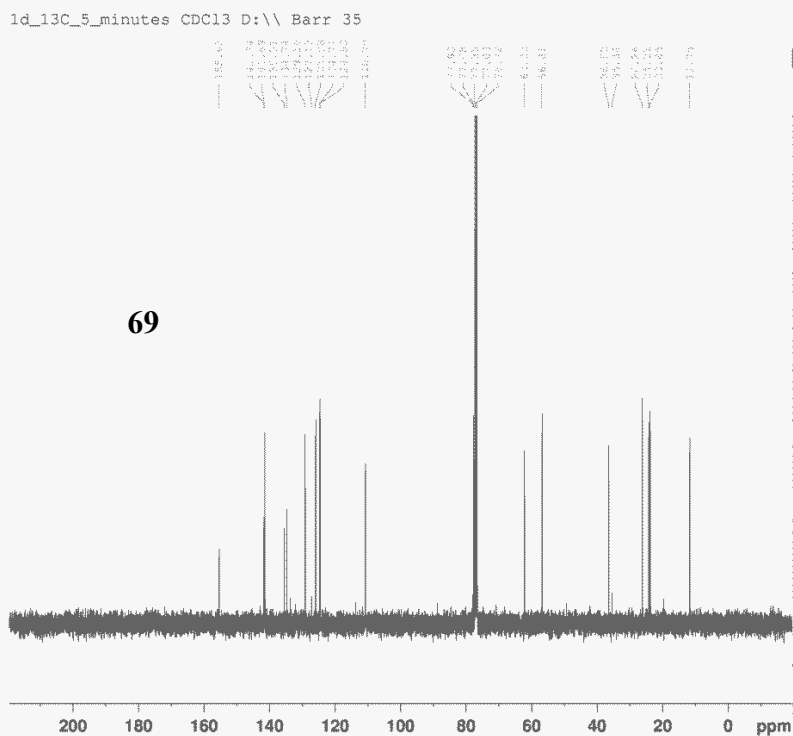
F2 - Acquisition Parameters
 Date_ 20120227
 Time_ 12.09
 INSTRUM spect
 PROBHD 5 mm PABBO BB-
 PULPROG zg30
 TD 49152
 SOLVENT CDC13
 NS 16
 DS 0
 SMH 6421.233 Hz
 FIDRES 0.130640 Hz
 AQ 3.8273523 sec
 RG 144
 DW 77.867 usec
 DE 6.00 usec
 TE 295.7 K
 D1 1.0000000 sec
 TDO 1

===== CHANNEL f1 =====
 NUC1 1H
 P1 10.75 usec
 PL1 -4.00 dB
 SFO1 400.3223900 MHz

F2 - Processing parameters
 SI 65536
 SF 400.3200164 MHz
 WDW EM
 SSB 0
 LB 0.10 Hz
 GB 0
 PC 1.00

1d_13C_5_minutes CDC13 D:\\ Barr 35

69



Current Data Parameters
 NAME TS-05-65char
 EXPNO 2
 PROCNO 1

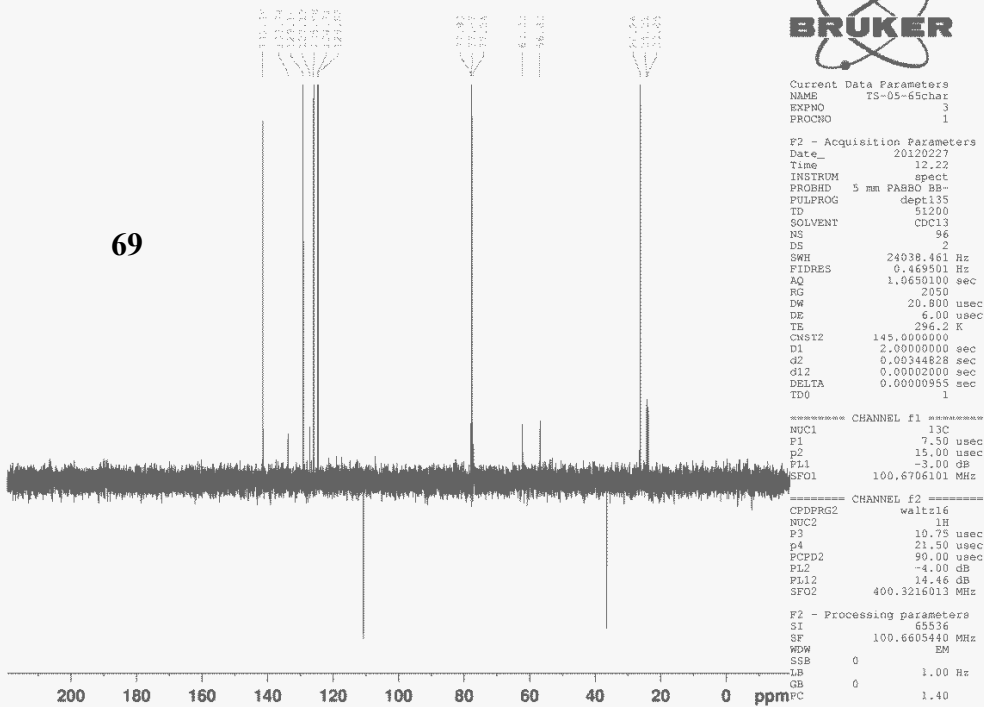
F2 - Acquisition Parameters
 Date_ 20120227
 Time_ 12.15
 INSTRUM spect
 PROBHD 5 mm PABBO BB-
 PULPROG zgpg30
 TD 51200
 SOLVENT CDC13
 NS 128
 DS 0
 SMH 24038.461 Hz
 FIDRES 0.469501 Hz
 AQ 1.0650100 sec
 RG 405
 DW 20.800 usec
 DE 6.00 usec
 TE 296.6 K
 D1 1.0000000 sec
 d11 0.0300000 sec
 DELTA 0.89999998 sec
 TDO 1

===== CHANNEL f1 =====
 NUC1 13C
 P1 7.50 usec
 PL1 -3.00 dB
 SFO1 100.6706101 MHz

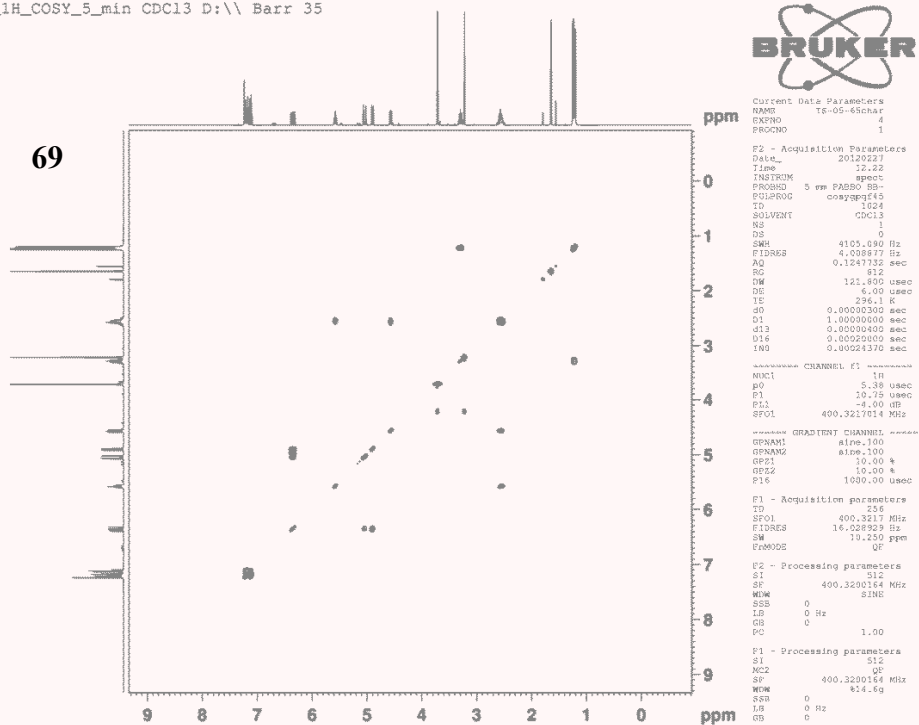
===== CHANNEL f2 =====
 CPDPRG2 waltz16
 NUC2 1H
 FCPD2 90.00 usec
 PL2 -4.00 dB
 PL12 14.46 dB
 PL13 16.01 dB
 SFO2 400.3216013 MHz

F2 - Processing parameters
 SI 65536
 SF 100.6608440 MHz
 WDW EM
 SSB 0
 LB 1.00 Hz
 GB 0
 PC 1.40

1d_13C_DEPT_135_5_minutes CDC13 D:\\ Barr 35

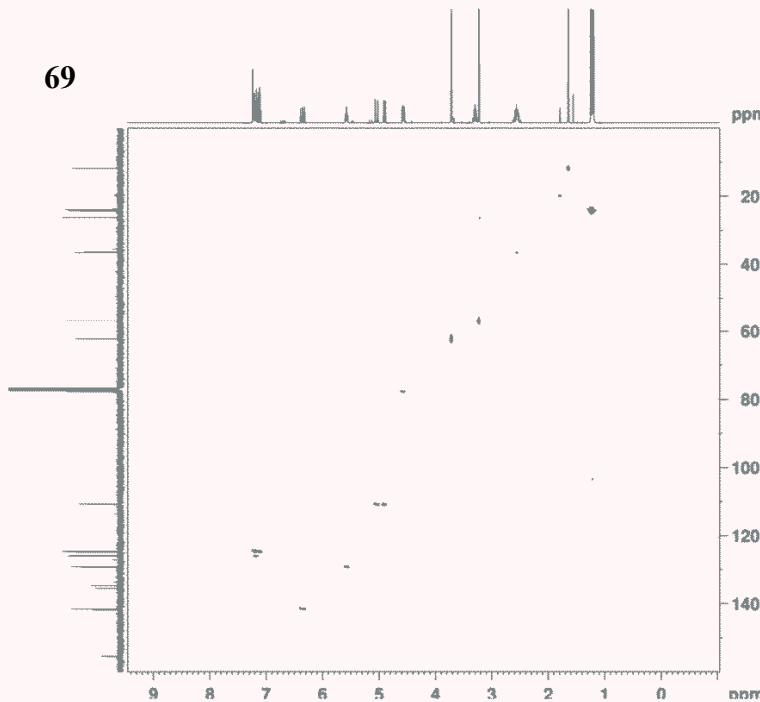


2d_1H_COSY_5_min CDC13 D:\\ Barr 35



2d_HMQC_10_minutes CDC13 D:\ Barr 35

69



```

Output Data Parameters
NAME      TS-01-63day
EXPNO    2
PROCNO   1

F2 - Acquisition Parameters
Date_    20121217
Time     12.24
INSTRUM  spect
PROBHD   5 mm PABBO 1H1
PULPROG  zgpg30
TD        65536
SOLVENT  CDCl3
NS        2
DS        4
SWH       6201.622 Hz
FIDRES   0.1319625 Hz
AQ        0.1219625 sec
RG         320
RW         7.238 Hz
RM         0.1319625 Hz
DE         6.05 usec
TE        295.2 K
DSTRT2   145.000000 sec
d0        0.2000000 sec
d1        1.2000000 sec
d2        0.2000000 sec
d3        0.2000000 sec
d4        0.2000000 sec
DELTA1   0.2000000 sec
DELTA2   0.2000000 sec
SFO      400.1464010 MHz

===== CHANNEL f1 =====
NUC1      13
P1        19.75 usec
PC        215.52 usec
PL1       -1.00 dB
PL2       400.3217134 MHz

===== CHANNEL f2 =====
CPDPRG2  zgpg
NUC2      13
P2        9.25 usec
PC        80.01 usec
PL2       -1.00 dB
PL3       17.36 dB
PL4       100.4883019 MHz

===== SPINLOCK CHANNEL =====
SPINLOCK  sfo-100
GSPIN1    sfo-100
GSPIN2    sfo-100
GSPIN3    sfo-100
CPDPRG3   zgpg
GFL1      30.00 kHz
GFL2      30.00 kHz
GFL3      40.13 kHz
D16       1005.01 usec

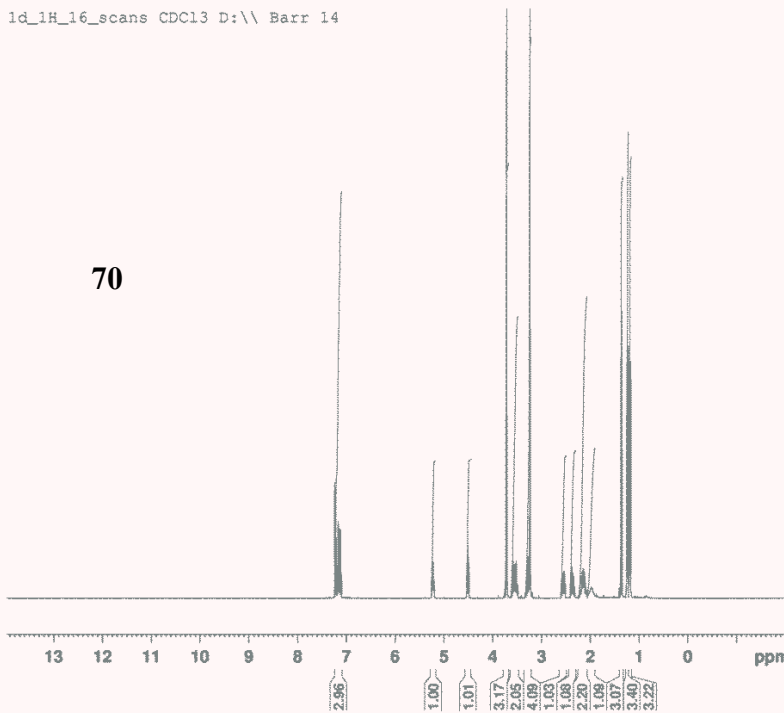
F1 - Acquisition parameters
TD        65536
SFO1     100.6263 MHz
FIDRES   6.392376 Hz
SW        159.961 ppm
FNUC1    13

F2 - Processing parameters
SI        3274
SF        400.1464010 MHz
WDW       EM
SSB       0
LB        0 Hz
GB        0
PC        1.00

F1 - Processing parameters
SI        3274
SF        400.1464010 MHz
WDW       EM
SSB       0
LB        0 Hz
GB        0
PC        1.00
    
```

1d_1H_16_scans CDC13 D:\ Barr 14

70



```

Output Data Parameters
NAME      TS-01-63day - bis-OH-alcohol - done
EXPNO    1
PROCNO   1

F2 - Acquisition Parameters
Date_    20120315
Time     12.04
INSTRUM  spect
PROBHD   5 mm PABBO 1H1
PULPROG  zgpg30
TD        65536
SOLVENT  CDCl3
NS        2
DS        4
SWH       6421.733 Hz
FIDRES   0.1319625 Hz
AQ        0.1219625 sec
RG         320
RW         7.238 Hz
RM         0.1319625 Hz
DE         6.05 usec
TE        295.2 K
DSTRT2   145.000000 sec
d0        0.2000000 sec
d1        1.2000000 sec
d2        0.2000000 sec
d3        0.2000000 sec
DELTA1   0.2000000 sec
DELTA2   0.2000000 sec
SFO      400.1464010 MHz

===== CHANNEL f1 =====
NUC1      13
P1        19.75 usec
PC        215.52 usec
PL1       -1.00 dB
PL2       400.3217134 MHz

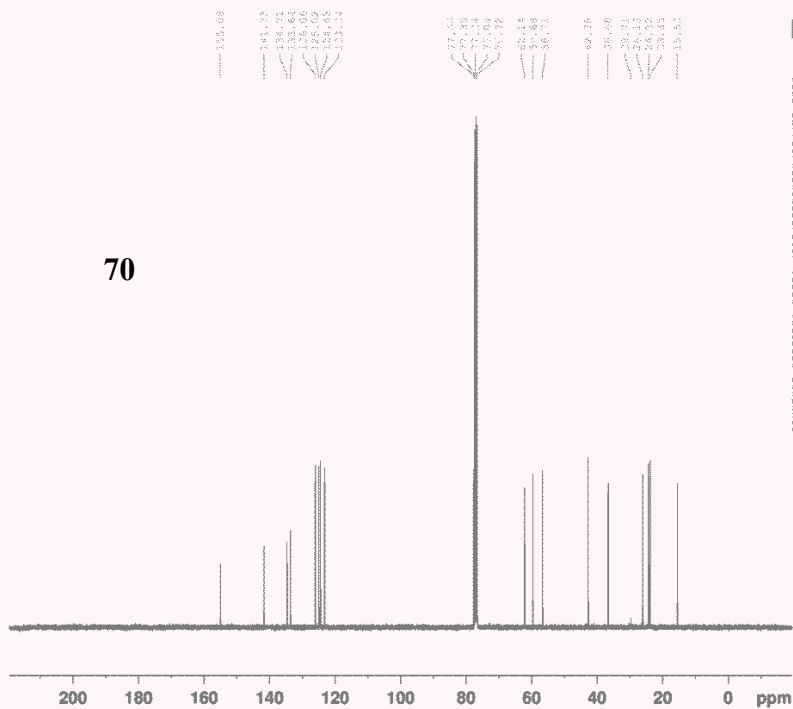
===== CHANNEL f2 =====
CPDPRG2  zgpg
NUC2      13
P2        9.25 usec
PC        80.01 usec
PL2       -1.00 dB
PL3       17.36 dB
PL4       100.4883019 MHz

===== SPINLOCK CHANNEL =====
SPINLOCK  sfo-100
GSPIN1    sfo-100
GSPIN2    sfo-100
GSPIN3    sfo-100
CPDPRG3   zgpg
GFL1      30.00 kHz
GFL2      30.00 kHz
GFL3      40.13 kHz
D16       1005.01 usec

F1 - Acquisition parameters
TD        65536
SFO1     100.6263 MHz
FIDRES   6.392376 Hz
SW        159.961 ppm
FNUC1    13

F2 - Processing parameters
SI        3274
SF        400.1464010 MHz
WDW       EM
SSB       0
LB        0 Hz
GB        0
PC        1.00
    
```

1d_13C_1_hour CDC13 D:\ Barr 14



70



Current Data Parameters
 NAME 1d_13C_1hour - his-00m-alcohol - done
 EXPNO 1
 PROCNO 1

F2 - Acquisition Parameters
 Date_ 20120316
 Time 17:24
 INSTRUM spect
 PULPROG zgpg30
 FIDRES 5.00 #3000 Hz
 AQ 0.00000000
 TD 32768
 SFO 125.130
 SOLVENT CDCl3
 NS 1664
 DS 2
 SWH 24536.441 Hz
 FWHM 0.600001 Hz
 AQ 1.0426166 sec
 RG 256
 DM 30.846 MHz
 DE 4.00 MHz
 TE 300.2 K
 D1 1.00000000 sec
 DELT 0.00000000 sec
 DELTA 0.00000000 sec
 TDC 1

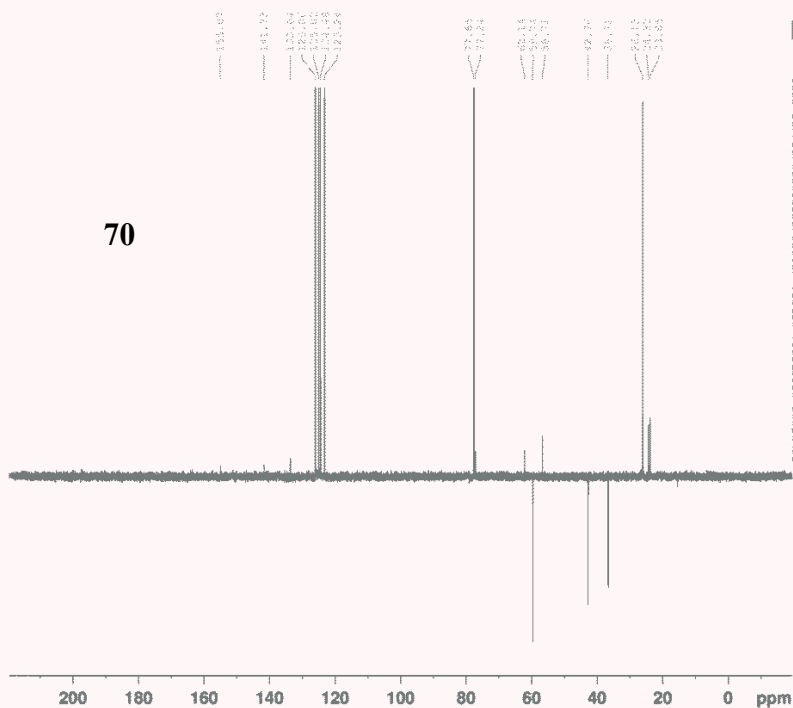
===== CHANNEL f1 =====
 NUC1 13C
 P1 1.00 usec
 PL 0.00 dB
 SFO1 101.6261001 MHz

===== CHANNEL f2 =====
 NUC2 13C
 P2 1.00 usec
 PL 0.00 dB
 SFO2 101.6261001 MHz

===== CHANNEL f3 =====
 NUC3 13C
 P3 1.00 usec
 PL 0.00 dB
 SFO3 101.6261001 MHz

F2 - Processing parameters
 SI 65536
 SF 101.6261001 MHz
 NW 1.00 MHz
 SFO 101.6261001 MHz
 DS 2
 DM 30.846 MHz
 DE 4.00 MHz
 TE 300.2 K
 PC 1.46

1d_13C_DEPT_135_1_hour CDC13 D:\ Barr 14



70



Current Data Parameters
 NAME 1d_13C_DEPT_135_1hour - his-00m-alcohol - done
 EXPNO 1
 PROCNO 1

F2 - Acquisition Parameters
 Date_ 20120316
 Time 17:29
 INSTRUM spect
 PULPROG zgpg30
 FIDRES 5.00 #3000 Hz
 AQ 0.00000000
 TD 32768
 SFO 125.130
 SOLVENT CDCl3
 NS 1024
 DS 2
 SWH 24536.441 Hz
 FWHM 0.600001 Hz
 AQ 1.0426166 sec
 RG 256
 DM 30.846 MHz
 DE 4.00 MHz
 TE 300.2 K
 D1 1.00000000 sec
 DELT 0.00000000 sec
 DELTA 0.00000000 sec
 TDC 1

===== CHANNEL f1 =====
 NUC1 13C
 P1 1.00 usec
 PL 0.00 dB
 SFO1 101.6261001 MHz

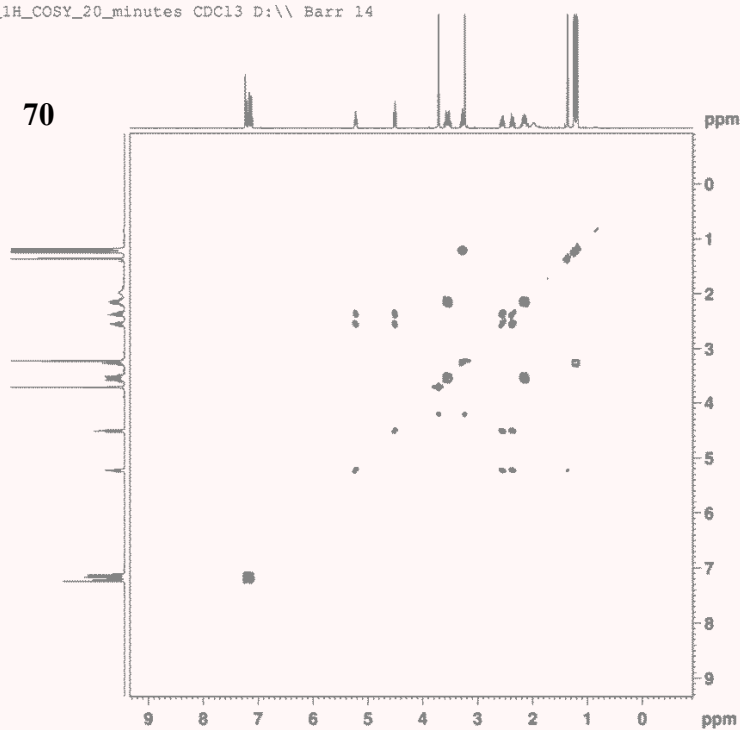
===== CHANNEL f2 =====
 NUC2 13C
 P2 1.00 usec
 PL 0.00 dB
 SFO2 101.6261001 MHz

===== CHANNEL f3 =====
 NUC3 13C
 P3 1.00 usec
 PL 0.00 dB
 SFO3 101.6261001 MHz

F2 - Processing parameters
 SI 65536
 SF 101.6261001 MHz
 NW 1.00 MHz
 SFO 101.6261001 MHz
 DS 2
 DM 30.846 MHz
 DE 4.00 MHz
 TE 300.2 K
 PC 1.46

2d_1H_COSY_20_minutes CDC13 D:\ Barr 14

70



```

Current Data Parameters
NAME      T6-05-74char
EXPNO    4
PROCNO    1

F2 - Acquisition Parameters
Date_     20120316
Time      15.00
INSTRUM   spect
PROBHD    5 mm PABBO 90-
PULPROG   zgpg30f4f5
TD        1024
SOLVENT   CDC13
NS         4
DS         0
SWH        4105.090 Hz
FIDRES    4.008877 Hz
AQ         0.1241732 sec
RG         612
DM         121.800 usec
DE         6.20 usec
TE         295.3 K
AQ        0.0000300 sec
D1         1.00000000 sec
d11        0.00000000 sec
D12        0.00020100 sec
IN0        0.0024370 sec

----- CHANNEL f1 -----
NUC1       1H
P0         5.38 usec
P1         10.76 usec
PL1        -1.00 dB
SFO1       400.3217014 MHz

----- GRADIENT CHANNEL -----
GRNAM1     gline-100
GRNAM2     sline-100
GRP1       10.00 %
GRP2       10.00 %
P16        1000.00 usec

F1 - Acquisition parameters
TD         256
SFO1       400.3217 MHz
FIDRES    16.028229 Hz
SW         10.250 ppm
F2NAME     OF

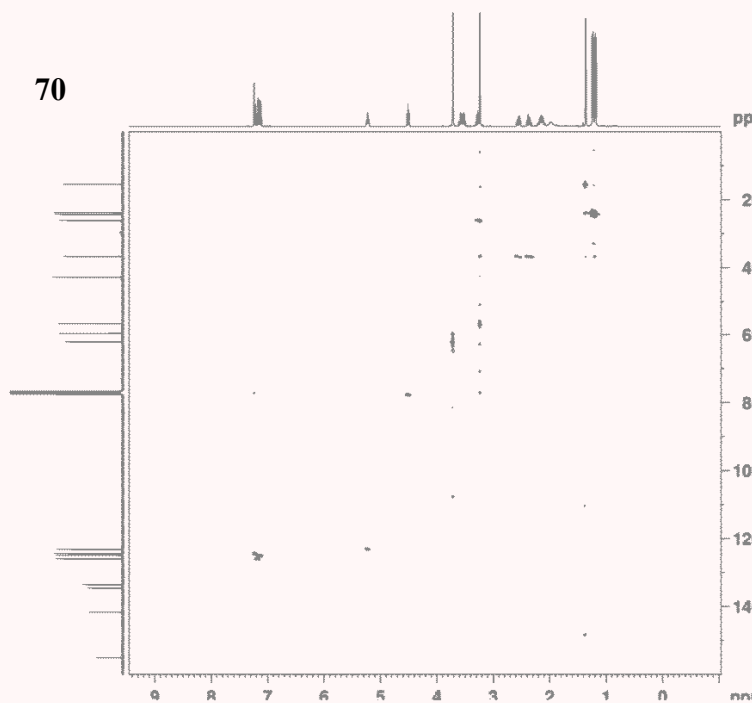
F2 - Processing parameters
SI         512
SF         400.3201164 MHz
WDW        SINC
SSB        0
LB         0 Hz
GB         0
PC         1.00

F1 - Processing parameters
SI         512
MC2        OF
SF         400.3201164 MHz
WDW        SINC
SSB        0
LB         0 Hz
GB         0
PC         1.00

```

2d_HMQC_1_hour CDC13 D:\ Barr 14

70



```

Current Data Parameters
NAME      T6-05-74char
EXPNO    3
PROCNO    1

F2 - Acquisition Parameters
Date_     20120316
Time      15.00
INSTRUM   spect
PROBHD    5 mm PABBO 90-
PULPROG   zgpg30f4f5
TD        1024
SOLVENT   CDC13
NS         4
DS         0
SWH        4201.481 Hz
FIDRES    4.103204 Hz
AQ         0.1218655 sec
RG         7232
DM         131.000 usec
DE         4.00 usec
TE         295.3 K
AQ        0.0000300 sec
D1         1.00000000 sec
d11        0.00000000 sec
D12        2.00000000 sec
D13        3.00000000 sec
D14        0.00020000 sec
IN0        0.00221000 sec

----- CHANNEL f1 -----
NUC1       1H
P0         5.38 usec
P1         10.76 usec
PL1        -1.00 dB
SFO1       400.3217014 MHz

----- CHANNEL f2 -----
CPDPRG2   gpc2
NUC2       13C
P0         91.00 usec
P1         31.28 usec
PCPD0     80.00 vppp
PL2        -3.00 dB
PL12       17.36 dB
SFO2       100.6263970 MHz

----- GRADIENT CHANNEL -----
GRNAM1     sline-100
GRNAM2     sline-100
GRNAM3     sline-100
GRP1       30.00 %
GRP2       30.00 %
GRP3       60.75 %
P16        1000.00 usec

F1 - Acquisition parameters
TD         256
SFO1       100.62636 MHz
FIDRES    6.302076 Hz
SW         159.961 ppm
F2NAME     OF

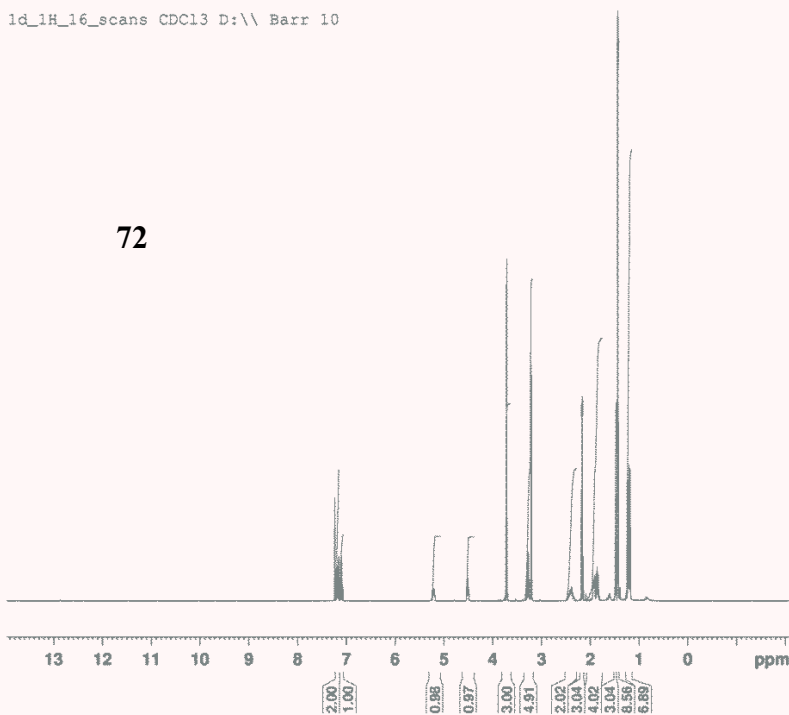
F2 - Processing parameters
SI         1024
SF         100.6263970 MHz
WDW        SINC
SSB        0
LB         0 Hz
GB         0
PC         1.00

F1 - Processing parameters
SI         1024
MC2        OF
SF         100.6263970 MHz
WDW        SINC
SSB        0
LB         0 Hz
GB         0
PC         1.00

```

1d_1H_16_scans CDC13 D:\\ Barr 10

72



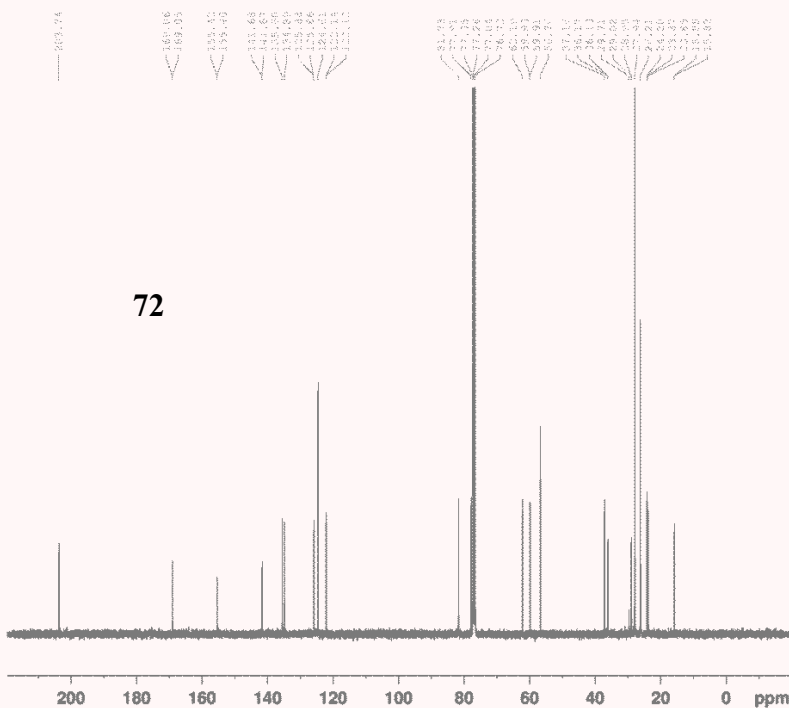
Current Data Parameters
 Name: 16-03-85 - dimethyl 3-hydroxybut-3-ene diol
 ExpNo: 5
 F2 - Acquisition Parameters
 Date_: 20121208
 Time: 07:19
 Larmor: 400.146
 PRGMRG: 5 nm HMRG0 82-
 PULPROG: zgpg30
 ID: 40255
 SOLVENT: CDCl3
 NS: 16
 DS: 4
 SWH: 4421.832 Hz
 FIDRES: 0.120000 Hz
 AQ: 3.6271212 sec
 RG: 327
 RBW: 13.53 Hz
 RE: 77.825 kHz
 RF: 100.626151 MHz
 TE: 300.2 K
 DE: 1.0000000 sec
 TO: 2

----- CHANNEL f1 -----
 NUC1: 13C
 P1: 12.00 usec
 PL1: 0.00 dB
 SFO1: 100.626151 MHz

F2 - Processing parameters
 SI: 32768
 SF: 100.626151 MHz
 WDM: 0
 SFO: 0.00 Hz
 GB: 0
 PC: 1.99

1d_13C_1_hour CDC13 D:\\ Barr 10

72



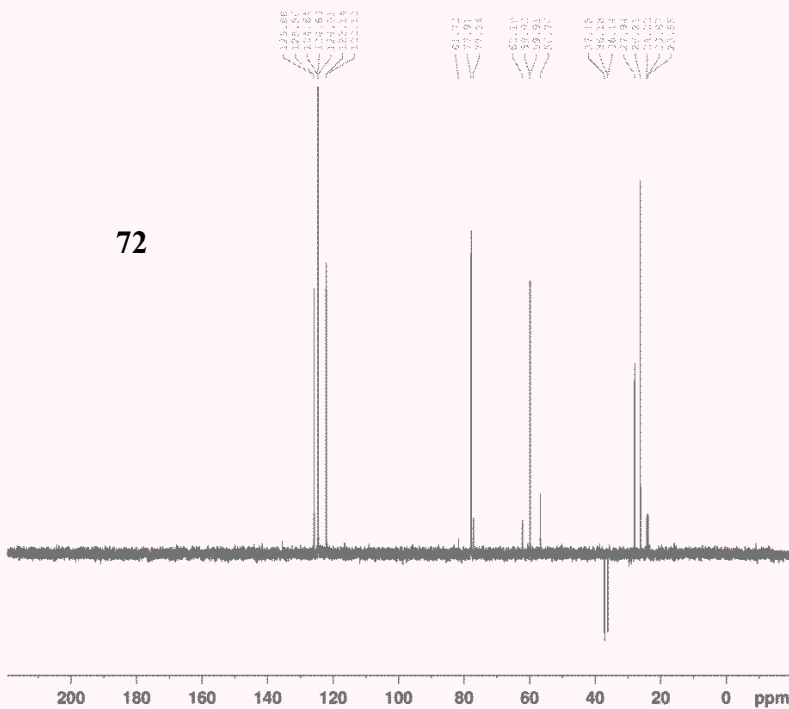
Current Data Parameters
 Name: 16-03-85 - dimethyl 3-hydroxybut-3-ene diol
 ExpNo: 5
 F2 - Acquisition Parameters
 Date_: 20121208
 Time: 07:49
 Larmor: 400.146
 PRGMRG: 5 nm HMRG0 82-
 PULPROG: zgpg30
 ID: 40255
 SOLVENT: CDCl3
 NS: 16
 DS: 4
 SWH: 24038.641 Hz
 FIDRES: 0.440000 Hz
 AQ: 1.0000000 sec
 RG: 327
 RBW: 25.485 kHz
 RE: 77.825 kHz
 RF: 100.626151 MHz
 TE: 300.2 K
 DE: 1.0000000 sec
 TO: 2

----- CHANNEL f1 -----
 NUC1: 13C
 P1: 12.00 usec
 PL1: 0.00 dB
 SFO1: 100.626151 MHz

----- CHANNEL f2 -----
 NUC2: 1H
 P2: 30.00 usec
 PL2: 14.00 dB
 SFO2: 400.146151 MHz

F2 - Processing parameters
 SI: 65536
 SF: 100.626151 MHz
 WDM: 0
 SFO: 0.00 Hz
 GB: 0
 PC: 1.99

1d_13C_DEPT_135_1_hour CDC13 D:\\ Barr 10



Current Data Parameters
 NAME 1d-13-45 - dimethyl 3-oxocamphor chex final
 EXPNO 5
 PROCNO 1

F2 - Acquisition Parameters
 DATE_ 20120705
 TIME 13.44
 LATEST 46464
 PROBRG 5 nm PASSED 5C
 F2PROC 002115
 ID 13390
 SOLVENT cdcl3
 NS 1048
 DS 2
 SFO 1409.440 Hz
 FIDRES 0.440091 Hz
 AQ 1.0000000 sec
 RG 256.000
 SF 250.130 MHz
 EQ 1.0000000 sec
 EX 260.7 Hz
 CK1Z 145.000000 sec
 D1 7.0000000 sec
 d2 0.0000000 sec
 FID 0.0000000 sec
 DELTA 0.0000000 sec
 ZD 0.0000000 sec

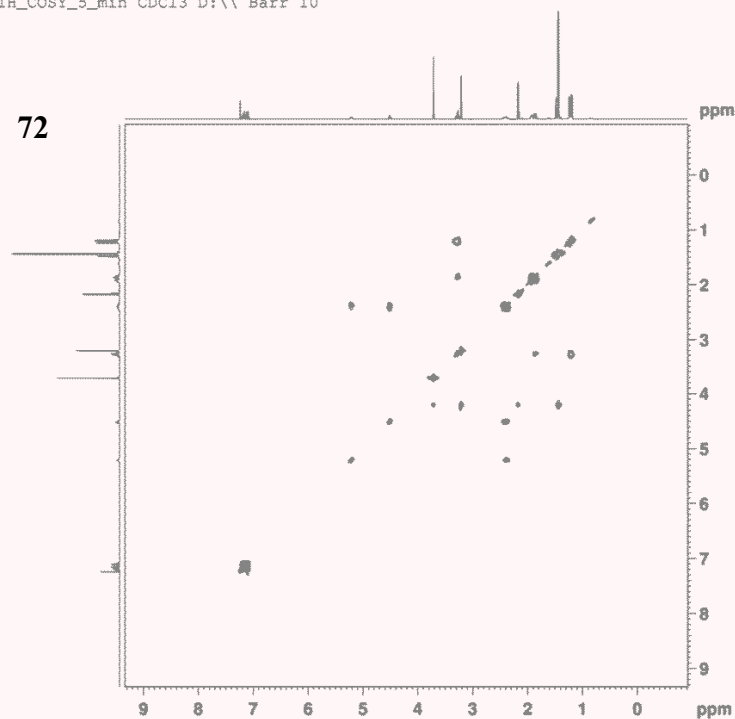
----- CHANNEL f1 -----
 NUC1 13C
 P1 13.00 usec
 PL 0.00 dB
 SFO1 100.626115 MHz

----- CHANNEL f2 -----
 CPDPRG2 waltz16
 NUC2 1H
 P2 10.00 usec
 PL 2.00 dB
 SFO2 400.146000 MHz
 SFO12 400.146000 MHz
 SFO13 400.146000 MHz

F1 - Processing parameters
 SI 32768
 SF 100.626115 MHz
 WF 0.0000000 Hz
 GB 0
 LB 1.00 Hz
 DS 9
 SS 0.400

72

2d_1H-COSY_5_min CDC13 D:\\ Barr 10



Current Data Parameters
 NAME 2d-1H-COSY-5 min
 EXPNO 5
 PROCNO 1

F2 - Acquisition Parameters
 DATE_ 20120705
 TIME 13.44
 LATEST 46464
 PROBRG 5 nm PASSED 5C
 F2PROC 002115
 ID 13390
 SOLVENT cdcl3
 NS 1048
 DS 2
 SFO 1409.440 Hz
 FIDRES 0.440091 Hz
 AQ 1.0000000 sec
 RG 256.000
 SF 250.130 MHz
 EQ 1.0000000 sec
 EX 260.7 Hz
 CK1Z 145.000000 sec
 D1 7.0000000 sec
 d2 0.0000000 sec
 FID 0.0000000 sec
 DELTA 0.0000000 sec
 ZD 0.0000000 sec

----- CHANNEL f1 -----
 NUC1 1H
 P1 10.00 usec
 PL 0.00 dB
 SFO1 400.146000 MHz

----- CHANNEL f2 -----
 CPDPRG2 waltz16
 NUC2 13C
 P2 13.00 usec
 PL 0.00 dB
 SFO2 100.626115 MHz
 SFO12 100.626115 MHz
 SFO13 100.626115 MHz

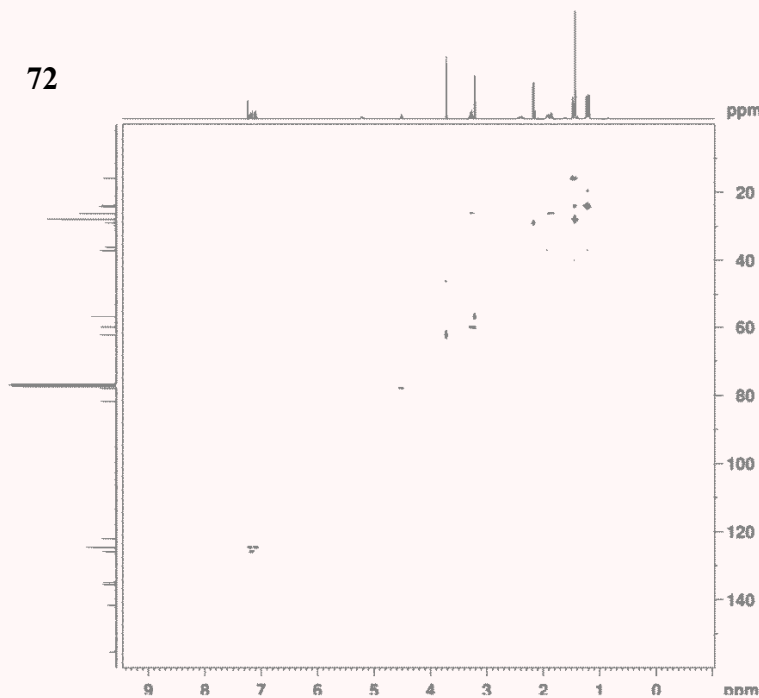
F1 - Acquisition Parameters
 DATE_ 20120705
 TIME 13.44
 LATEST 46464
 PROBRG 5 nm PASSED 5C
 F1PROC 002115
 ID 13390
 SOLVENT cdcl3
 NS 1048
 DS 2
 SFO 1409.440 Hz
 FIDRES 0.440091 Hz
 AQ 1.0000000 sec
 RG 256.000
 SF 250.130 MHz
 EQ 1.0000000 sec
 EX 260.7 Hz
 CK1Z 145.000000 sec
 D1 7.0000000 sec
 d2 0.0000000 sec
 FID 0.0000000 sec
 DELTA 0.0000000 sec
 ZD 0.0000000 sec

F1 - Processing parameters
 SI 32768
 SF 100.626115 MHz
 WF 0.0000000 Hz
 GB 0
 LB 1.00 Hz
 DS 9
 SS 0.400

72

2d_HMQC_1_hour CDC13 D:\ Barr 10

72



```

Current Data Parameters
NAME      TS-05-85 - dimethyl 2-bromosuccinate char final
EXPNO    1
PROCNO   1

F2 - Acquisition Parameters
Date_    20120403
Time     7.46
INSTRUM  spect
PROBHD   5 mm PABBO BB-
PULPROG  zg30
TD       49152
SOLVENT  CDCl3
NS       16
DS       0
SWH      6421.233 Hz
FIDRES   0.130640 Hz
AQ       3.8279523 sec
RG       436
DM       77.867 usec
DE       6.00 usec
TE       294.7 K
D2       1.00000000 sec
TDO      1

===== CHANNEL f1 =====
NUC1     1H
P1       10.75 usec
PL1      -4.00 dB
SFO1     400.3223900 MHz

===== CHANNEL f2 =====
CPDPRG2  gpc
NUC2     13C
P2       7.30 usec
PL2      -1.90 dB
SFO2     100.6261500 MHz

===== CHANNEL f3 =====
CPDPRG3  gpc
NUC3     13C
P3       7.30 usec
PL3      -1.90 dB
SFO3     100.6261500 MHz

===== CHANNEL f4 =====
CPDPRG4  gpc
NUC4     13C
P4       7.30 usec
PL4      -1.90 dB
SFO4     100.6261500 MHz

===== CHANNEL f5 =====
CPDPRG5  gpc
NUC5     13C
P5       7.30 usec
PL5      -1.90 dB
SFO5     100.6261500 MHz

===== CHANNEL f6 =====
CPDPRG6  gpc
NUC6     13C
P6       7.30 usec
PL6      -1.90 dB
SFO6     100.6261500 MHz

===== CHANNEL f7 =====
CPDPRG7  gpc
NUC7     13C
P7       7.30 usec
PL7      -1.90 dB
SFO7     100.6261500 MHz

===== CHANNEL f8 =====
CPDPRG8  gpc
NUC8     13C
P8       7.30 usec
PL8      -1.90 dB
SFO8     100.6261500 MHz

===== CHANNEL f9 =====
CPDPRG9  gpc
NUC9     13C
P9       7.30 usec
PL9      -1.90 dB
SFO9     100.6261500 MHz

===== CHANNEL f10 =====
CPDPRG10 gpc
NUC10    13C
P10      7.30 usec
PL10     -1.90 dB
SFO10    100.6261500 MHz

===== CHANNEL f11 =====
CPDPRG11 gpc
NUC11    13C
P11      7.30 usec
PL11     -1.90 dB
SFO11    100.6261500 MHz

===== CHANNEL f12 =====
CPDPRG12 gpc
NUC12    13C
P12      7.30 usec
PL12     -1.90 dB
SFO12    100.6261500 MHz

===== CHANNEL f13 =====
CPDPRG13 gpc
NUC13    13C
P13      7.30 usec
PL13     -1.90 dB
SFO13    100.6261500 MHz

===== CHANNEL f14 =====
CPDPRG14 gpc
NUC14    13C
P14      7.30 usec
PL14     -1.90 dB
SFO14    100.6261500 MHz

===== CHANNEL f15 =====
CPDPRG15 gpc
NUC15    13C
P15      7.30 usec
PL15     -1.90 dB
SFO15    100.6261500 MHz

===== CHANNEL f16 =====
CPDPRG16 gpc
NUC16    13C
P16      7.30 usec
PL16     -1.90 dB
SFO16    100.6261500 MHz

===== CHANNEL f17 =====
CPDPRG17 gpc
NUC17    13C
P17      7.30 usec
PL17     -1.90 dB
SFO17    100.6261500 MHz

===== CHANNEL f18 =====
CPDPRG18 gpc
NUC18    13C
P18      7.30 usec
PL18     -1.90 dB
SFO18    100.6261500 MHz

===== CHANNEL f19 =====
CPDPRG19 gpc
NUC19    13C
P19      7.30 usec
PL19     -1.90 dB
SFO19    100.6261500 MHz

===== CHANNEL f20 =====
CPDPRG20 gpc
NUC20    13C
P20      7.30 usec
PL20     -1.90 dB
SFO20    100.6261500 MHz

===== CHANNEL f21 =====
CPDPRG21 gpc
NUC21    13C
P21      7.30 usec
PL21     -1.90 dB
SFO21    100.6261500 MHz

===== CHANNEL f22 =====
CPDPRG22 gpc
NUC22    13C
P22      7.30 usec
PL22     -1.90 dB
SFO22    100.6261500 MHz

===== CHANNEL f23 =====
CPDPRG23 gpc
NUC23    13C
P23      7.30 usec
PL23     -1.90 dB
SFO23    100.6261500 MHz

===== CHANNEL f24 =====
CPDPRG24 gpc
NUC24    13C
P24      7.30 usec
PL24     -1.90 dB
SFO24    100.6261500 MHz

===== CHANNEL f25 =====
CPDPRG25 gpc
NUC25    13C
P25      7.30 usec
PL25     -1.90 dB
SFO25    100.6261500 MHz

===== CHANNEL f26 =====
CPDPRG26 gpc
NUC26    13C
P26      7.30 usec
PL26     -1.90 dB
SFO26    100.6261500 MHz

===== CHANNEL f27 =====
CPDPRG27 gpc
NUC27    13C
P27      7.30 usec
PL27     -1.90 dB
SFO27    100.6261500 MHz

===== CHANNEL f28 =====
CPDPRG28 gpc
NUC28    13C
P28      7.30 usec
PL28     -1.90 dB
SFO28    100.6261500 MHz

===== CHANNEL f29 =====
CPDPRG29 gpc
NUC29    13C
P29      7.30 usec
PL29     -1.90 dB
SFO29    100.6261500 MHz

===== CHANNEL f30 =====
CPDPRG30 gpc
NUC30    13C
P30      7.30 usec
PL30     -1.90 dB
SFO30    100.6261500 MHz

===== CHANNEL f31 =====
CPDPRG31 gpc
NUC31    13C
P31      7.30 usec
PL31     -1.90 dB
SFO31    100.6261500 MHz

===== CHANNEL f32 =====
CPDPRG32 gpc
NUC32    13C
P32      7.30 usec
PL32     -1.90 dB
SFO32    100.6261500 MHz

===== CHANNEL f33 =====
CPDPRG33 gpc
NUC33    13C
P33      7.30 usec
PL33     -1.90 dB
SFO33    100.6261500 MHz

===== CHANNEL f34 =====
CPDPRG34 gpc
NUC34    13C
P34      7.30 usec
PL34     -1.90 dB
SFO34    100.6261500 MHz

===== CHANNEL f35 =====
CPDPRG35 gpc
NUC35    13C
P35      7.30 usec
PL35     -1.90 dB
SFO35    100.6261500 MHz

===== CHANNEL f36 =====
CPDPRG36 gpc
NUC36    13C
P36      7.30 usec
PL36     -1.90 dB
SFO36    100.6261500 MHz

===== CHANNEL f37 =====
CPDPRG37 gpc
NUC37    13C
P37      7.30 usec
PL37     -1.90 dB
SFO37    100.6261500 MHz

===== CHANNEL f38 =====
CPDPRG38 gpc
NUC38    13C
P38      7.30 usec
PL38     -1.90 dB
SFO38    100.6261500 MHz

===== CHANNEL f39 =====
CPDPRG39 gpc
NUC39    13C
P39      7.30 usec
PL39     -1.90 dB
SFO39    100.6261500 MHz

===== CHANNEL f40 =====
CPDPRG40 gpc
NUC40    13C
P40      7.30 usec
PL40     -1.90 dB
SFO40    100.6261500 MHz

===== CHANNEL f41 =====
CPDPRG41 gpc
NUC41    13C
P41      7.30 usec
PL41     -1.90 dB
SFO41    100.6261500 MHz

===== CHANNEL f42 =====
CPDPRG42 gpc
NUC42    13C
P42      7.30 usec
PL42     -1.90 dB
SFO42    100.6261500 MHz

===== CHANNEL f43 =====
CPDPRG43 gpc
NUC43    13C
P43      7.30 usec
PL43     -1.90 dB
SFO43    100.6261500 MHz

===== CHANNEL f44 =====
CPDPRG44 gpc
NUC44    13C
P44      7.30 usec
PL44     -1.90 dB
SFO44    100.6261500 MHz

===== CHANNEL f45 =====
CPDPRG45 gpc
NUC45    13C
P45      7.30 usec
PL45     -1.90 dB
SFO45    100.6261500 MHz

===== CHANNEL f46 =====
CPDPRG46 gpc
NUC46    13C
P46      7.30 usec
PL46     -1.90 dB
SFO46    100.6261500 MHz

===== CHANNEL f47 =====
CPDPRG47 gpc
NUC47    13C
P47      7.30 usec
PL47     -1.90 dB
SFO47    100.6261500 MHz

===== CHANNEL f48 =====
CPDPRG48 gpc
NUC48    13C
P48      7.30 usec
PL48     -1.90 dB
SFO48    100.6261500 MHz

===== CHANNEL f49 =====
CPDPRG49 gpc
NUC49    13C
P49      7.30 usec
PL49     -1.90 dB
SFO49    100.6261500 MHz

===== CHANNEL f50 =====
CPDPRG50 gpc
NUC50    13C
P50      7.30 usec
PL50     -1.90 dB
SFO50    100.6261500 MHz

===== CHANNEL f51 =====
CPDPRG51 gpc
NUC51    13C
P51      7.30 usec
PL51     -1.90 dB
SFO51    100.6261500 MHz

===== CHANNEL f52 =====
CPDPRG52 gpc
NUC52    13C
P52      7.30 usec
PL52     -1.90 dB
SFO52    100.6261500 MHz

===== CHANNEL f53 =====
CPDPRG53 gpc
NUC53    13C
P53      7.30 usec
PL53     -1.90 dB
SFO53    100.6261500 MHz

===== CHANNEL f54 =====
CPDPRG54 gpc
NUC54    13C
P54      7.30 usec
PL54     -1.90 dB
SFO54    100.6261500 MHz

===== CHANNEL f55 =====
CPDPRG55 gpc
NUC55    13C
P55      7.30 usec
PL55     -1.90 dB
SFO55    100.6261500 MHz

===== CHANNEL f56 =====
CPDPRG56 gpc
NUC56    13C
P56      7.30 usec
PL56     -1.90 dB
SFO56    100.6261500 MHz

===== CHANNEL f57 =====
CPDPRG57 gpc
NUC57    13C
P57      7.30 usec
PL57     -1.90 dB
SFO57    100.6261500 MHz

===== CHANNEL f58 =====
CPDPRG58 gpc
NUC58    13C
P58      7.30 usec
PL58     -1.90 dB
SFO58    100.6261500 MHz

===== CHANNEL f59 =====
CPDPRG59 gpc
NUC59    13C
P59      7.30 usec
PL59     -1.90 dB
SFO59    100.6261500 MHz

===== CHANNEL f60 =====
CPDPRG60 gpc
NUC60    13C
P60      7.30 usec
PL60     -1.90 dB
SFO60    100.6261500 MHz

===== CHANNEL f61 =====
CPDPRG61 gpc
NUC61    13C
P61      7.30 usec
PL61     -1.90 dB
SFO61    100.6261500 MHz

===== CHANNEL f62 =====
CPDPRG62 gpc
NUC62    13C
P62      7.30 usec
PL62     -1.90 dB
SFO62    100.6261500 MHz

===== CHANNEL f63 =====
CPDPRG63 gpc
NUC63    13C
P63      7.30 usec
PL63     -1.90 dB
SFO63    100.6261500 MHz

===== CHANNEL f64 =====
CPDPRG64 gpc
NUC64    13C
P64      7.30 usec
PL64     -1.90 dB
SFO64    100.6261500 MHz

===== CHANNEL f65 =====
CPDPRG65 gpc
NUC65    13C
P65      7.30 usec
PL65     -1.90 dB
SFO65    100.6261500 MHz

===== CHANNEL f66 =====
CPDPRG66 gpc
NUC66    13C
P66      7.30 usec
PL66     -1.90 dB
SFO66    100.6261500 MHz

===== CHANNEL f67 =====
CPDPRG67 gpc
NUC67    13C
P67      7.30 usec
PL67     -1.90 dB
SFO67    100.6261500 MHz

===== CHANNEL f68 =====
CPDPRG68 gpc
NUC68    13C
P68      7.30 usec
PL68     -1.90 dB
SFO68    100.6261500 MHz

===== CHANNEL f69 =====
CPDPRG69 gpc
NUC69    13C
P69      7.30 usec
PL69     -1.90 dB
SFO69    100.6261500 MHz

===== CHANNEL f70 =====
CPDPRG70 gpc
NUC70    13C
P70      7.30 usec
PL70     -1.90 dB
SFO70    100.6261500 MHz

===== CHANNEL f71 =====
CPDPRG71 gpc
NUC71    13C
P71      7.30 usec
PL71     -1.90 dB
SFO71    100.6261500 MHz

===== CHANNEL f72 =====
CPDPRG72 gpc
NUC72    13C
P72      7.30 usec
PL72     -1.90 dB
SFO72    100.6261500 MHz

===== CHANNEL f73 =====
CPDPRG73 gpc
NUC73    13C
P73      7.30 usec
PL73     -1.90 dB
SFO73    100.6261500 MHz

===== CHANNEL f74 =====
CPDPRG74 gpc
NUC74    13C
P74      7.30 usec
PL74     -1.90 dB
SFO74    100.6261500 MHz

===== CHANNEL f75 =====
CPDPRG75 gpc
NUC75    13C
P75      7.30 usec
PL75     -1.90 dB
SFO75    100.6261500 MHz

===== CHANNEL f76 =====
CPDPRG76 gpc
NUC76    13C
P76      7.30 usec
PL76     -1.90 dB
SFO76    100.6261500 MHz

===== CHANNEL f77 =====
CPDPRG77 gpc
NUC77    13C
P77      7.30 usec
PL77     -1.90 dB
SFO77    100.6261500 MHz

===== CHANNEL f78 =====
CPDPRG78 gpc
NUC78    13C
P78      7.30 usec
PL78     -1.90 dB
SFO78    100.6261500 MHz

===== CHANNEL f79 =====
CPDPRG79 gpc
NUC79    13C
P79      7.30 usec
PL79     -1.90 dB
SFO79    100.6261500 MHz

===== CHANNEL f80 =====
CPDPRG80 gpc
NUC80    13C
P80      7.30 usec
PL80     -1.90 dB
SFO80    100.6261500 MHz

===== CHANNEL f81 =====
CPDPRG81 gpc
NUC81    13C
P81      7.30 usec
PL81     -1.90 dB
SFO81    100.6261500 MHz

===== CHANNEL f82 =====
CPDPRG82 gpc
NUC82    13C
P82      7.30 usec
PL82     -1.90 dB
SFO82    100.6261500 MHz

===== CHANNEL f83 =====
CPDPRG83 gpc
NUC83    13C
P83      7.30 usec
PL83     -1.90 dB
SFO83    100.6261500 MHz

===== CHANNEL f84 =====
CPDPRG84 gpc
NUC84    13C
P84      7.30 usec
PL84     -1.90 dB
SFO84    100.6261500 MHz

===== CHANNEL f85 =====
CPDPRG85 gpc
NUC85    13C
P85      7.30 usec
PL85     -1.90 dB
SFO85    100.6261500 MHz

===== CHANNEL f86 =====
CPDPRG86 gpc
NUC86    13C
P86      7.30 usec
PL86     -1.90 dB
SFO86    100.6261500 MHz

===== CHANNEL f87 =====
CPDPRG87 gpc
NUC87    13C
P87      7.30 usec
PL87     -1.90 dB
SFO87    100.6261500 MHz

===== CHANNEL f88 =====
CPDPRG88 gpc
NUC88    13C
P88      7.30 usec
PL88     -1.90 dB
SFO88    100.6261500 MHz

===== CHANNEL f89 =====
CPDPRG89 gpc
NUC89    13C
P89      7.30 usec
PL89     -1.90 dB
SFO89    100.6261500 MHz

===== CHANNEL f90 =====
CPDPRG90 gpc
NUC90    13C
P90      7.30 usec
PL90     -1.90 dB
SFO90    100.6261500 MHz

===== CHANNEL f91 =====
CPDPRG91 gpc
NUC91    13C
P91      7.30 usec
PL91     -1.90 dB
SFO91    100.6261500 MHz

===== CHANNEL f92 =====
CPDPRG92 gpc
NUC92    13C
P92      7.30 usec
PL92     -1.90 dB
SFO92    100.6261500 MHz

===== CHANNEL f93 =====
CPDPRG93 gpc
NUC93    13C
P93      7.30 usec
PL93     -1.90 dB
SFO93    100.6261500 MHz

===== CHANNEL f94 =====
CPDPRG94 gpc
NUC94    13C
P94      7.30 usec
PL94     -1.90 dB
SFO94    100.6261500 MHz

===== CHANNEL f95 =====
CPDPRG95 gpc
NUC95    13C
P95      7.30 usec
PL95     -1.90 dB
SFO95    100.6261500 MHz

===== CHANNEL f96 =====
CPDPRG96 gpc
NUC96    13C
P96      7.30 usec
PL96     -1.90 dB
SFO96    100.6261500 MHz

===== CHANNEL f97 =====
CPDPRG97 gpc
NUC97    13C
P97      7.30 usec
PL97     -1.90 dB
SFO97    100.6261500 MHz

===== CHANNEL f98 =====
CPDPRG98 gpc
NUC98    13C
P98      7.30 usec
PL98     -1.90 dB
SFO98    100.6261500 MHz

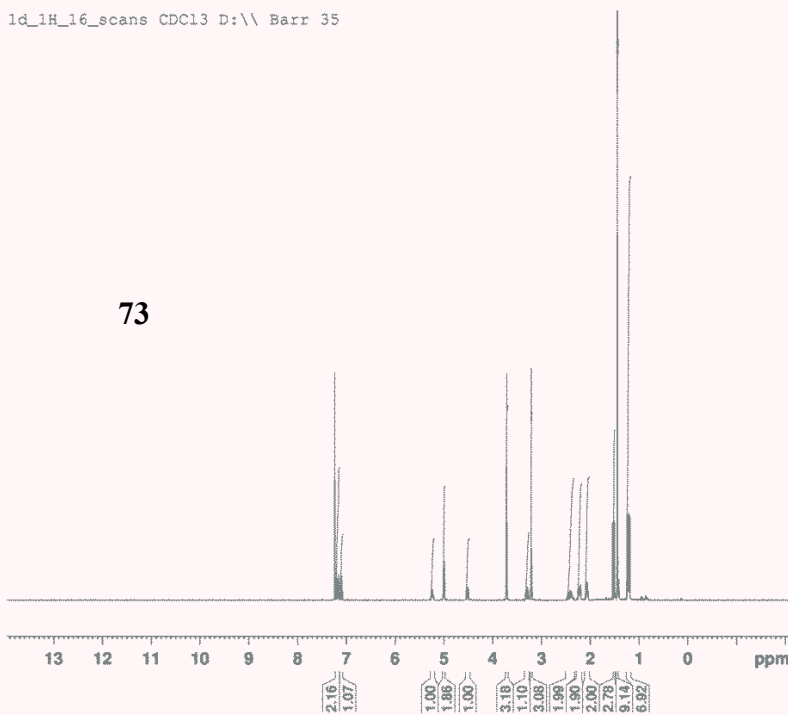
===== CHANNEL f99 =====
CPDPRG99 gpc
NUC99    13C
P99      7.30 usec
PL99     -1.90 dB
SFO99    100.6261500 MHz

===== CHANNEL f100 =====
CPDPRG100 gpc
NUC100   13C
P100     7.30 usec
PL100    -1.90 dB
SFO100   100.6261500 MHz

```

1d_1H_16_scans CDC13 D:\ Barr 35

73



```

Current Data Parameters
NAME      TS-05-95char - allene
EXPNO    1
PROCNO   1

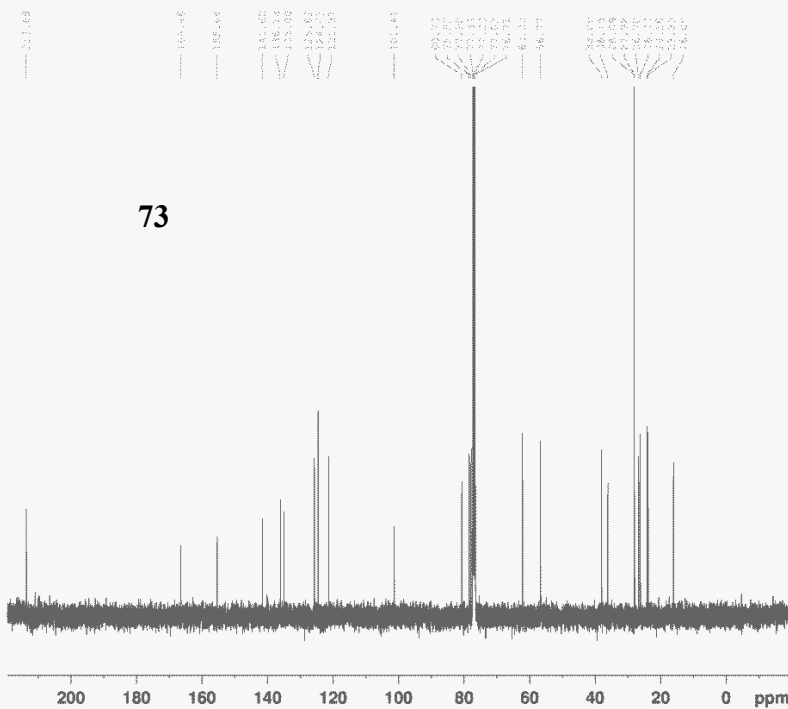
F2 - Acquisition Parameters
Date_    20120403
Time     7.46
INSTRUM  spect
PROBHD   5 mm PABBO BB-
PULPROG  zg30
TD       49152
SOLVENT  CDCl3
NS       16
DS       0
SWH      6421.233 Hz
FIDRES   0.130640 Hz
AQ       3.8279523 sec
RG       436
DM       77.867 usec
DE       6.00 usec
TE       294.7 K
D2       1.00000000 sec
TDO      1

===== CHANNEL f1 =====
NUC1     1H
P1       10.75 usec
PL1      -4.00 dB
SFO1     400.3223900 MHz

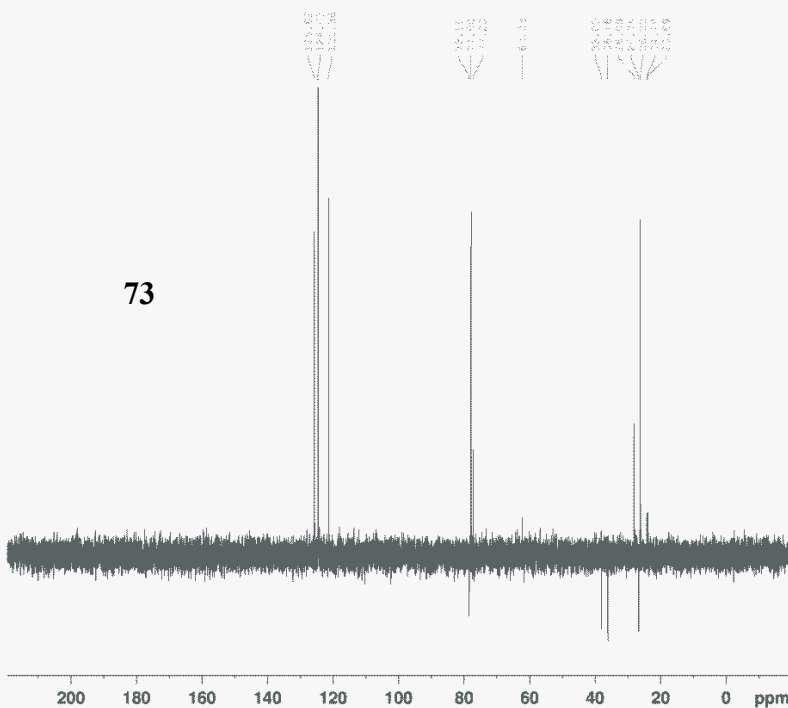
F2 - Processing parameters
SI       65536
SF       400.3200164 MHz
WDW      EM
SSB      0
LB       0.10 Hz
GB       0
PC       1.00

```

1d_13C_1_hour CDC13 D:\\ Barr 35

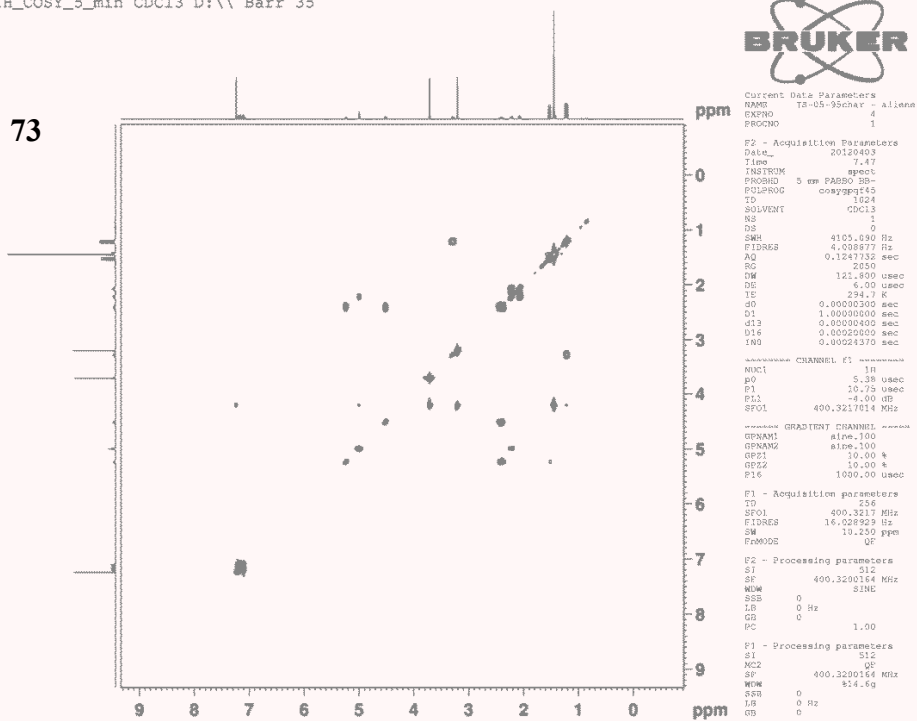


1d_13C_DEPT_135_1_hour CDC13 D:\\ Barr 35



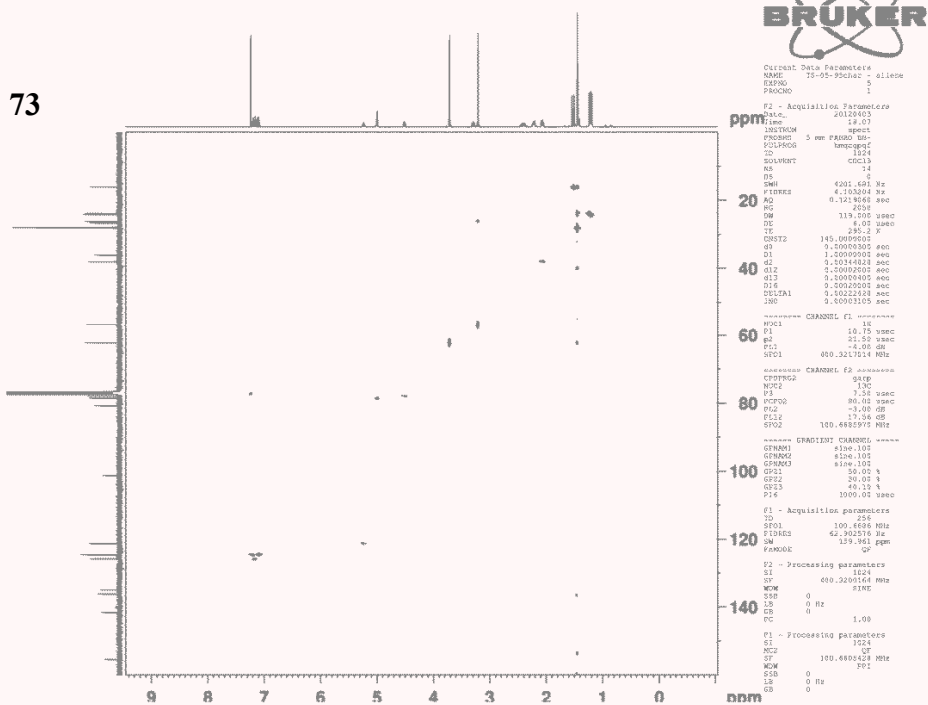
2d_1H_COSY_5_min CDC13 D:\\ Barr 35

73



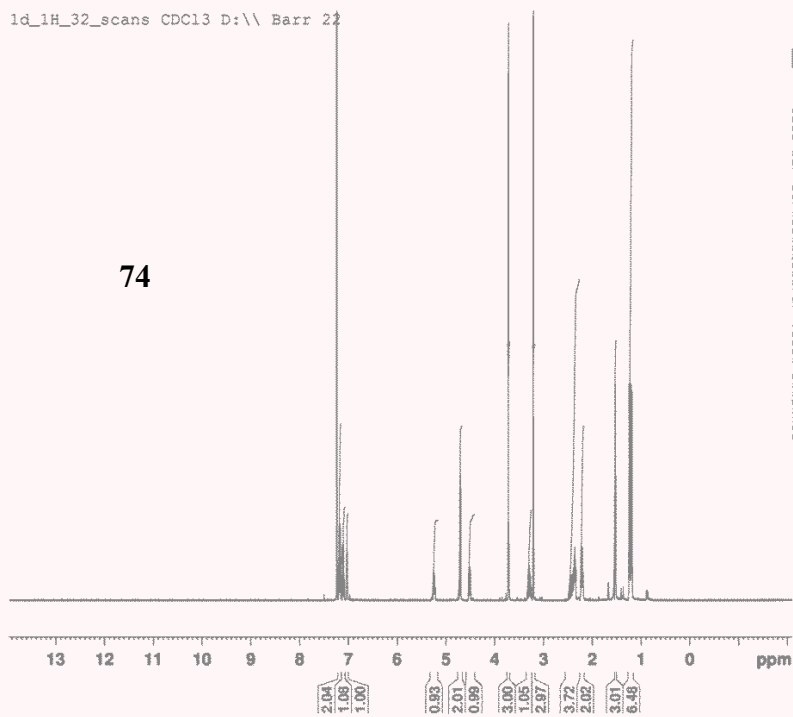
2d_HMQC_1_hour CDC13 D:\\ Barr 35

73



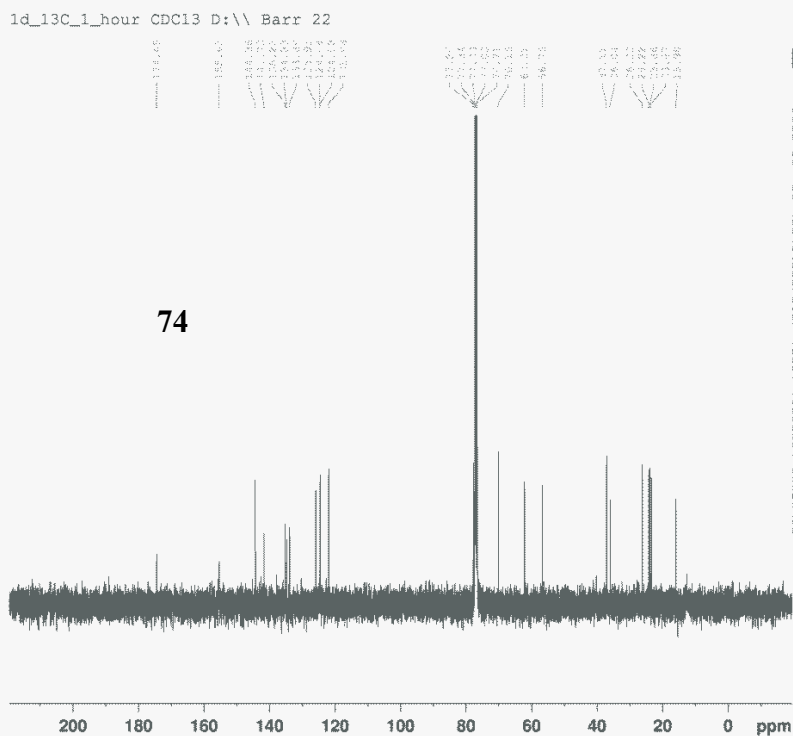
1d_1H_32_scans CDC13 D:\ Barr 22

74

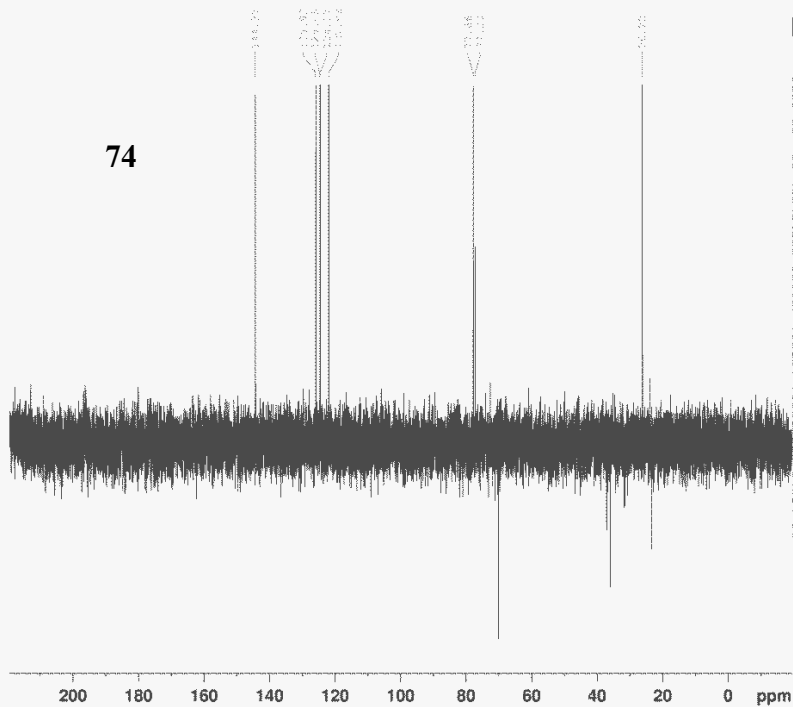


1d_13C_1_hour CDC13 D:\ Barr 22

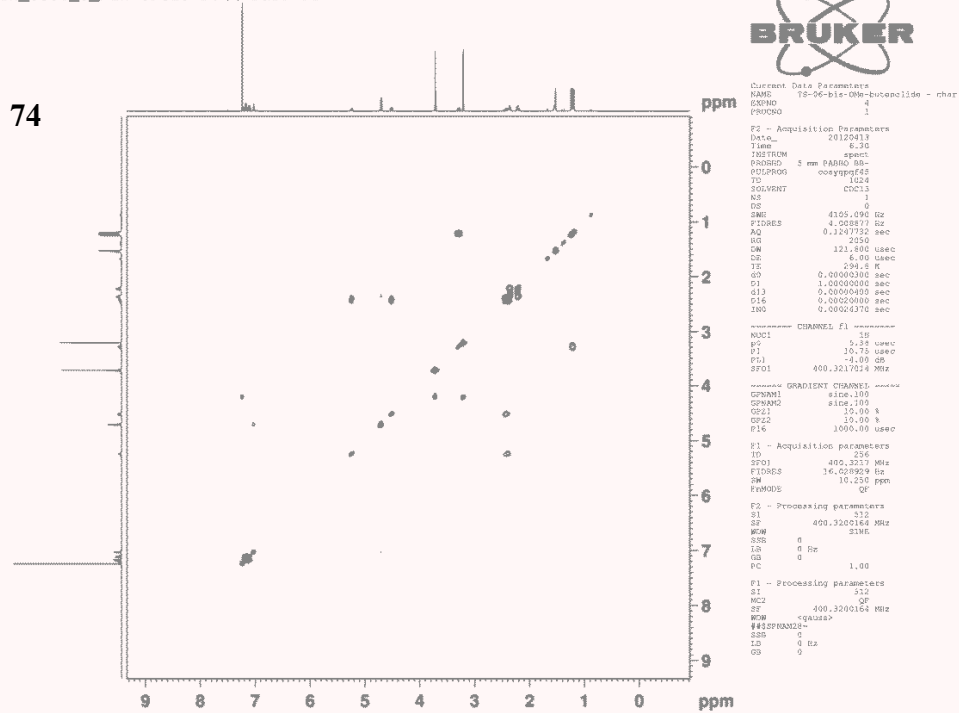
74



1d_13C_DEPT_135_1_hour CDC13 D:\ Barr 22

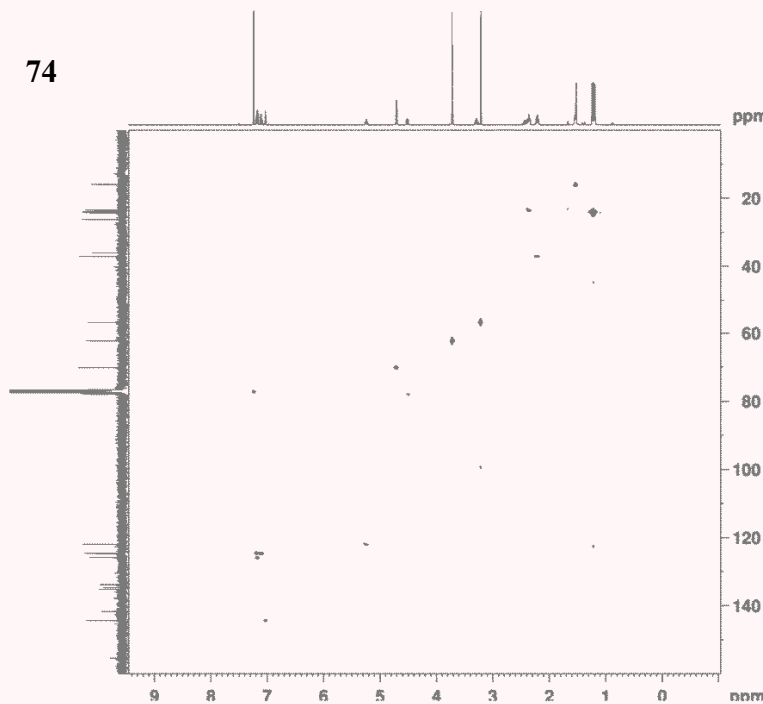


2d_1H-COSY_5_min CDC13 D:\ Barr 22



2d_HMQC_1_hour CDC13 D:\ Barr 22

74



Current Data Parameters
 NAME TS-06-01a-00a-00a-00a-00a - char
 EXPNO 2
 PROCNO 1

F2 - Acquisition Parameters
 Date_ 20120513
 Time 18.05
 INSTRUM spect
 FPROBHD 5 mm PABBO BB-
 PULPROG zgpg30
 TD 32768
 SOLVENT CDC13
 NS 26
 DS 0
 SWH 4507.421 Hz
 FIDRES 0.137549 Hz
 AQ 3.6351135 sec
 RG 128
 DW 110.933 usec
 DE 6.00 usec
 TE 298.2 K
 D1 0.01000000 sec
 D11 0.00220000 sec
 D12 0.00220000 sec
 D13 0.00220000 sec
 DELTAT 0.00220000 sec
 JNO 0.00000000 sec

===== CHANNEL f1 =====
 NUC1 13
 P1 10.75 usec
 PL1 21.52 dB
 SFO1 400.3217514 MHz

===== CHANNEL f2 =====
 CPDPRG2 90pg
 NUC2 1H
 P2 12.55 usec
 PL2 19.36 dB
 SFO2 500.1362670 MHz

===== CHANNEL f3 =====
 CPDPRG3 90pg
 NUC3 13
 P3 10.75 usec
 PL3 21.52 dB
 SFO3 400.3217514 MHz

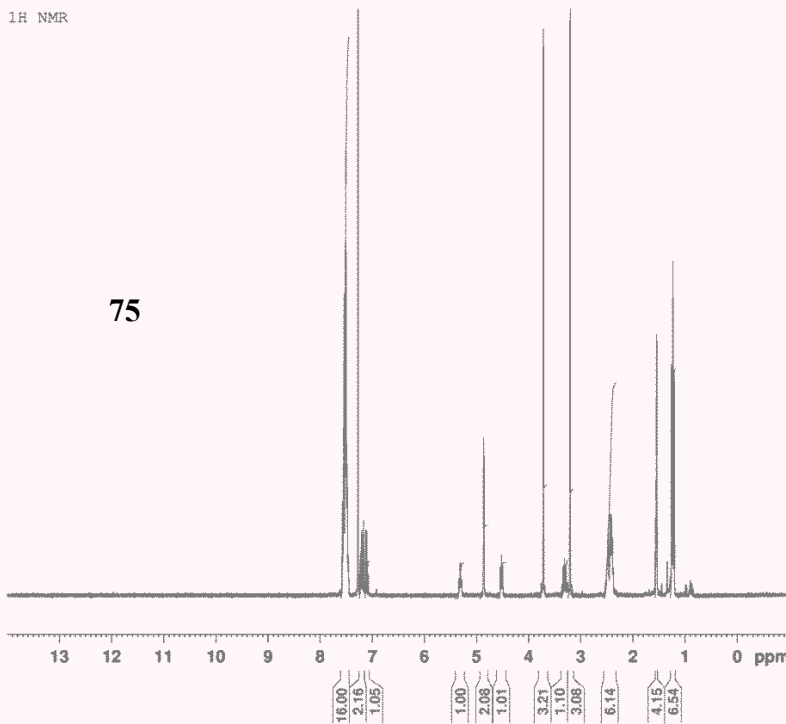
D1 - Acquisition parameters
 SI 32768
 SF 300.3319506 MHz
 SW 309.961 ppm
 FREQ00 0F

D2 - Processing parameters
 SI 32768
 SF 300.3319506 MHz
 SW 309.961 ppm
 FREQ00 0F

D3 - Processing parameters
 SI 32768
 SF 300.3319506 MHz
 SW 309.961 ppm
 FREQ00 0F

1H NMR

75



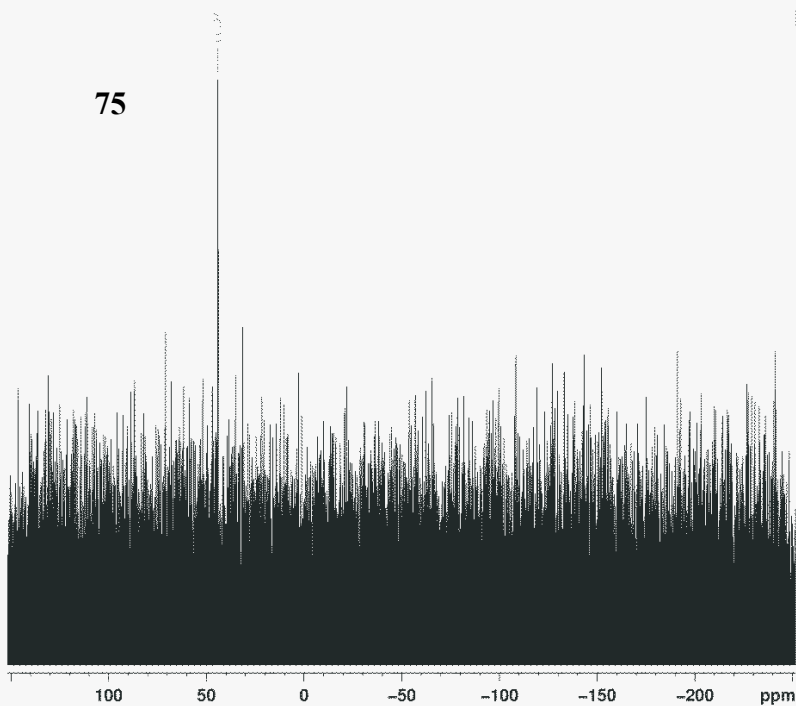
Current Data Parameters
 NAME TS-06-36
 EXPNO 2
 PROCNO 1

F2 - Acquisition Parameters
 Date_ 20120515
 Time 15.23
 INSTRUM spect
 FPROBHD 5 mm PABBO BB-
 PULPROG zg30
 TD 32768
 SOLVENT CDC13
 NS 26
 DS 0
 SWH 4507.211 Hz
 FIDRES 0.137549 Hz
 AQ 3.6351135 sec
 RG 128
 DW 110.933 usec
 DE 6.00 usec
 TE 298.2 K
 D1 0.01000000 sec
 TD0 1

===== CHANNEL f1 =====
 NUC1 1H
 P1 11.75 usec
 PL1 0 dB
 SFO1 300.3319506 MHz

F2 - Processing parameters
 SI 32768
 SF 300.3300000 MHz
 SW 309.961 ppm
 FREQ00 0F

31P NMR no decoupling



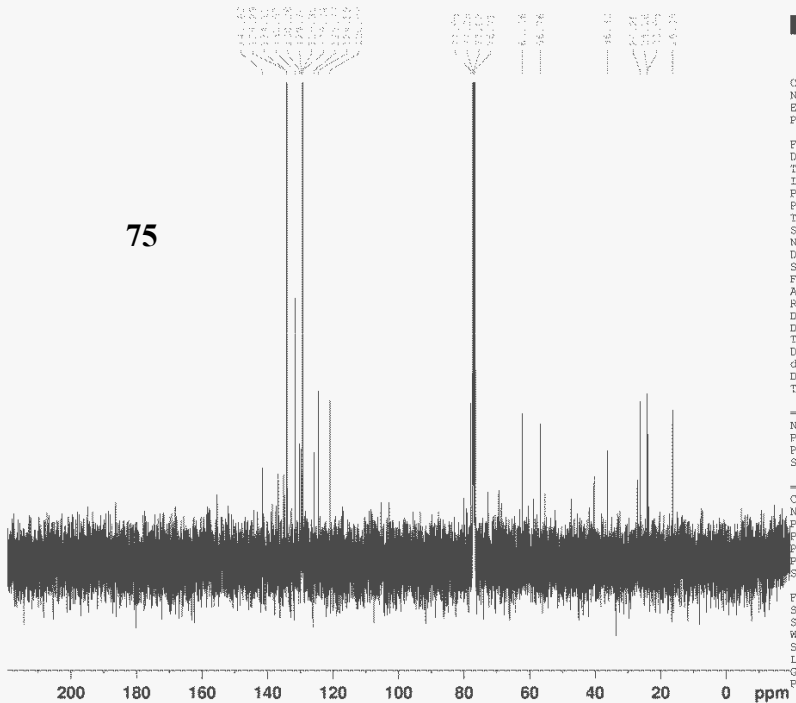
Current Data Parameters
 NAME TS-06-36
 EXPNO 3
 PROCNO 1

F2 - Acquisition Parameters
 Date_ 20120515
 Time 15.28
 INSTRUM spect
 PROBHD 5 mm PABBO BB-
 PULPROG zg30
 TD 65536
 SOLVENT Acetone
 NS 64
 DS 0
 SMH 49019.609 Hz
 FIDRES 0.747980 Hz
 AQ 0.668312 sec
 RG 312
 DW 10.200 usec
 DE 6.00 usec
 TE 299.1 K
 D1 1.0000000 sec
 TDC 1

----- CHANNEL f1 -----
 NUC1 31P
 P1 5.16 usec
 PL1 -3.00 dB
 SFO1 121.5697334 MHz

F2 - Processing parameters
 S1 65536
 SF 121.5758120 MHz
 WDW EM
 SSB 0
 LB 1.00 Hz
 GB 0
 PC 1.40

1d_13C_20_minutes CDC13 D:\ Barr 22



Current Data Parameters
 NAME TS-06-36char
 EXPNO 2
 PROCNO 1

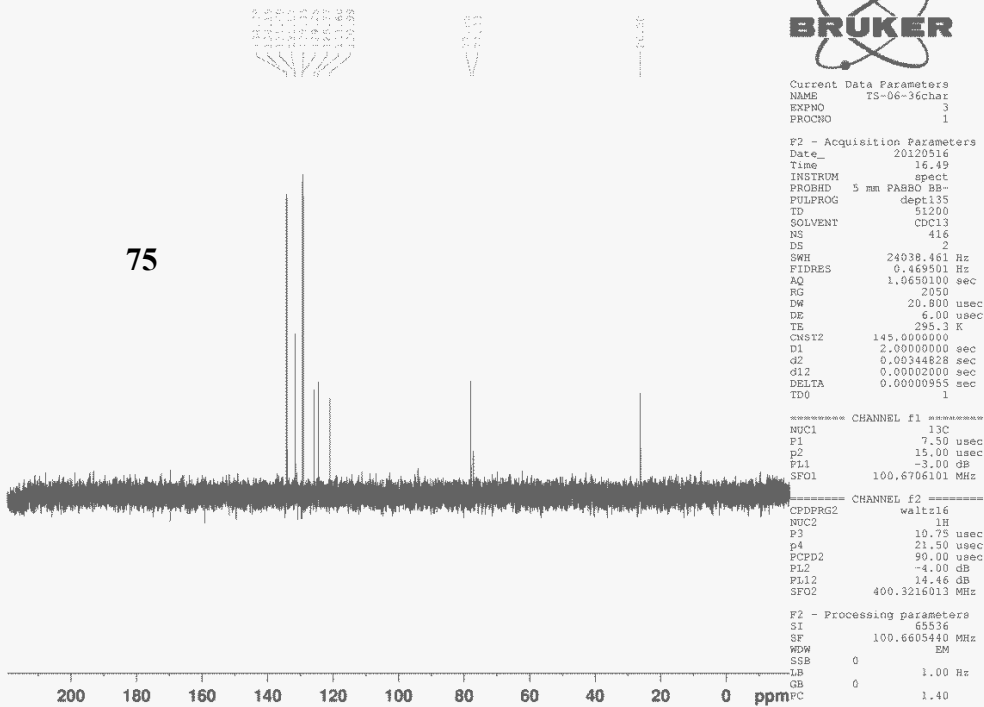
F2 - Acquisition Parameters
 Date_ 20120516
 Time 16.25
 INSTRUM spect
 PROBHD 5 mm PABBO BB-
 PULPROG zgpg30
 TD 51200
 SOLVENT CDC13
 NS 512
 DS 0
 SMH 24038.461 Hz
 FIDRES 0.469501 Hz
 AQ 1.0650100 sec
 RG 322
 DW 20.800 usec
 DE 6.00 usec
 TE 299.8 K
 D1 1.0000000 sec
 d11 0.0300000 sec
 DELTA 0.89999998 sec
 TDC 1

----- CHANNEL f1 -----
 NUC1 13C
 P1 7.50 usec
 PL1 -3.00 dB
 SFO1 100.6706101 MHz

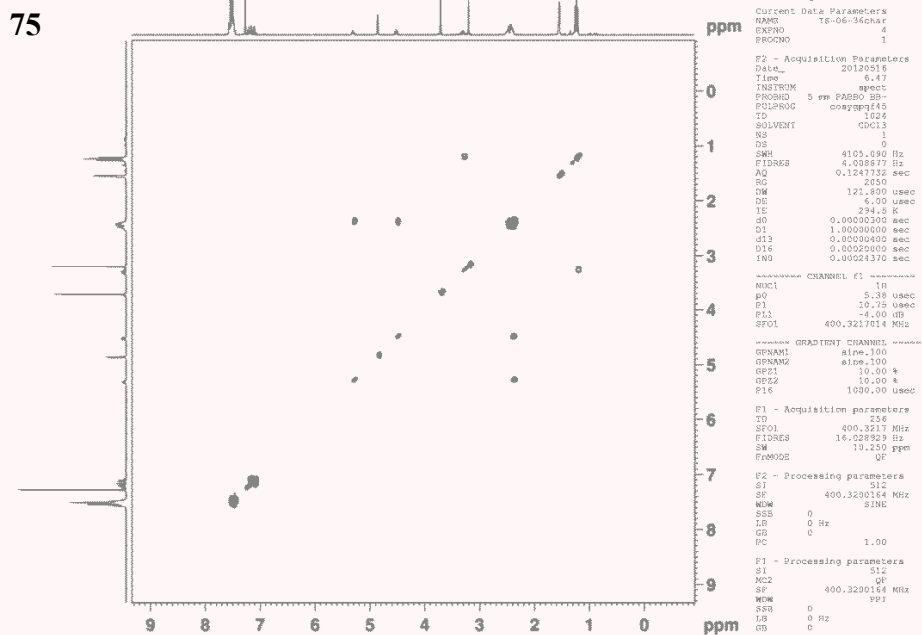
----- CHANNEL f2 -----
 CDPGR2 waltz16
 WDC2 18
 PCPD2 90.00 usec
 PL2 -4.00 dB
 PLL2 14.46 dB
 PLL3 18.01 dB
 SFO2 400.3216013 MHz

F2 - Processing parameters
 S1 65536
 SF 100.6609440 MHz
 WDW EM
 SSB 0
 LB 1.00 Hz
 GB 0
 PC 1.40

1d_13C_DEPT_135_20_minutes CDC13 D:\\ Barr 22

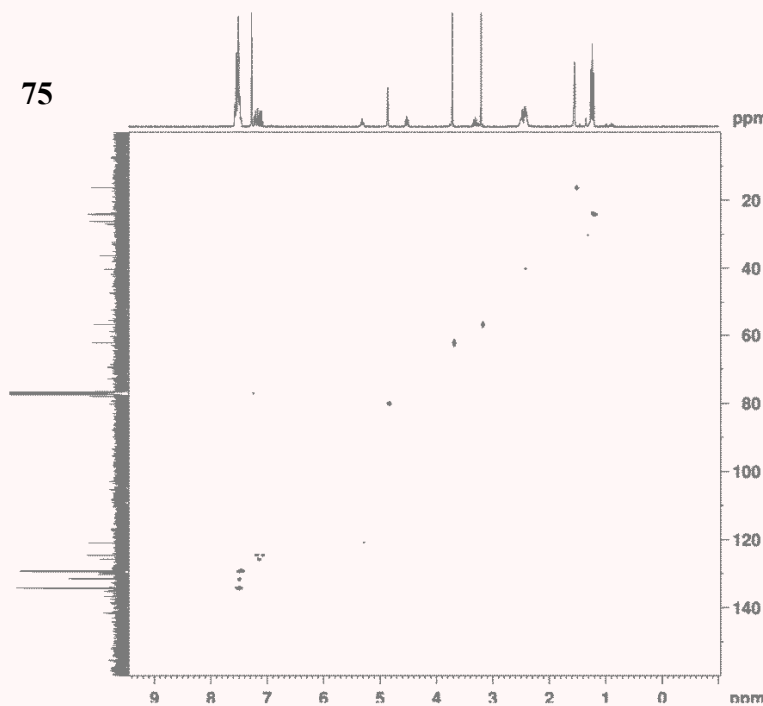


2d_1H_COSY_5_min CDC13 D:\\ Barr 22



2d_HMQC_1_hour CDC13 D:\ Barr 22

75



Current Data Parameters
 NAME TS-06-13char
 EXPNO 1
 PROCNO 1

F2 - Acquisition Parameters
 Date_ 20120115
 Time 15:31
 INSTRUM spect
 FPROBHD 5 mm F4000 90
 PULPROG zgpg30
 TD 32768
 SOLVENT CDC13
 NS 14
 DS 14
 SWH 4201.187 Hz
 FIDRES 4.115204 Hz
 AQ 0.1218060 sec
 RG 2030
 DW 119.2000 usec
 DE 6.00 usec
 TE 293.2 K
 D1 145.000000 sec
 d11 0.0000000 sec
 d12 1.0000000 sec
 d13 0.0000000 sec
 d14 0.0000000 sec
 d15 0.0000000 sec
 d16 0.0000000 sec
 DELTAC 0.0000000 sec
 JMR 0.0000000 sec

===== CHANNEL f1 =====
 NUC1 13
 P1 10.10 usec
 PL1 23.50 dB
 PL1 -4.00 dB
 SFO1 400.3217014 MHz

===== CHANNEL f2 =====
 CPDPRG2 gmg
 NUC2 13C
 P2 7.00 usec
 PL2 0.00 dB
 PL2 -2.00 dB
 PL2 17.50 dB
 SFO2 100.626370 MHz

===== GRADIENT CHANNEL =====
 GPMAX1 size:100
 GPMAX2 size:100
 GPMAX3 size:100
 GPC1 30.00 V
 GPC2 30.00 V
 GPC3 30.00 V
 P1 1000.00 usec

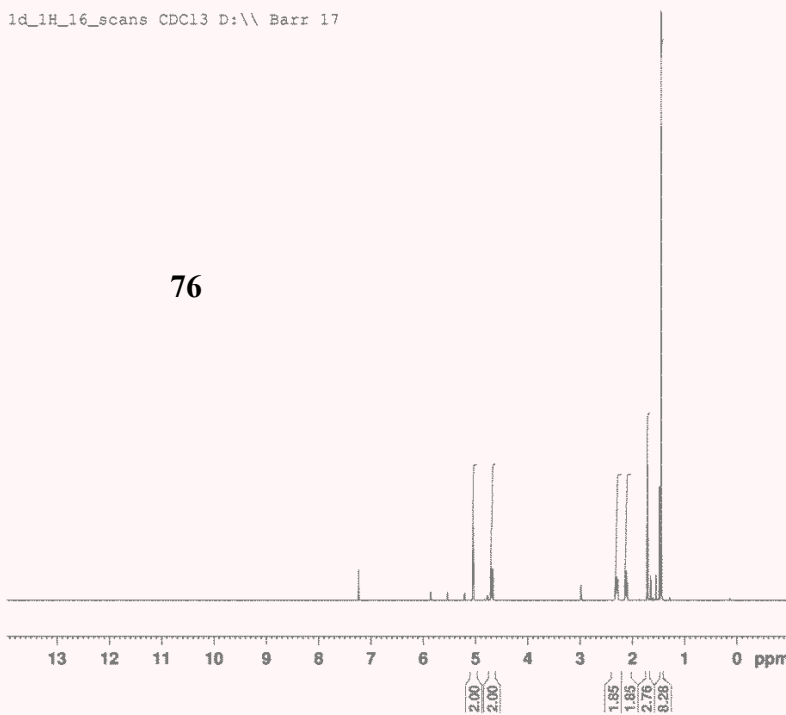
F1 - Acquisition Parameters
 Date_ 2012
 Time 16:45:46
 INSTRUM spect
 FPROBHD 5 mm F4000 90
 PULPROG zgpg30
 TD 32768
 SOLVENT CDC13
 NS 14
 DS 14
 SWH 6421.233 Hz
 FIDRES 0.130640 Hz
 AQ 3.8273523 sec
 RG 2037
 DW 77.867 usec
 DE 6.00 usec
 TE 294.2 K
 D1 1.00000000 sec
 D11 0.00000000 sec
 D12 0.00000000 sec
 D13 0.00000000 sec
 D14 0.00000000 sec
 D15 0.00000000 sec
 D16 0.00000000 sec
 DELTAC 0.00000000 sec
 JMR 0.00000000 sec

F2 - Processing parameters
 SI 3074
 SF 400.3220164 MHz
 NMR EM
 SSB 0
 LB 0 Hz
 GB 0
 PC 1.00

F1 - Processing parameters
 SI 3074
 SF 400.3220164 MHz
 NMR EM
 SSB 0
 LB 0 Hz
 GB 0
 PC 1.00

1d_1H_16_scans CDC13 D:\ Barr 17

76



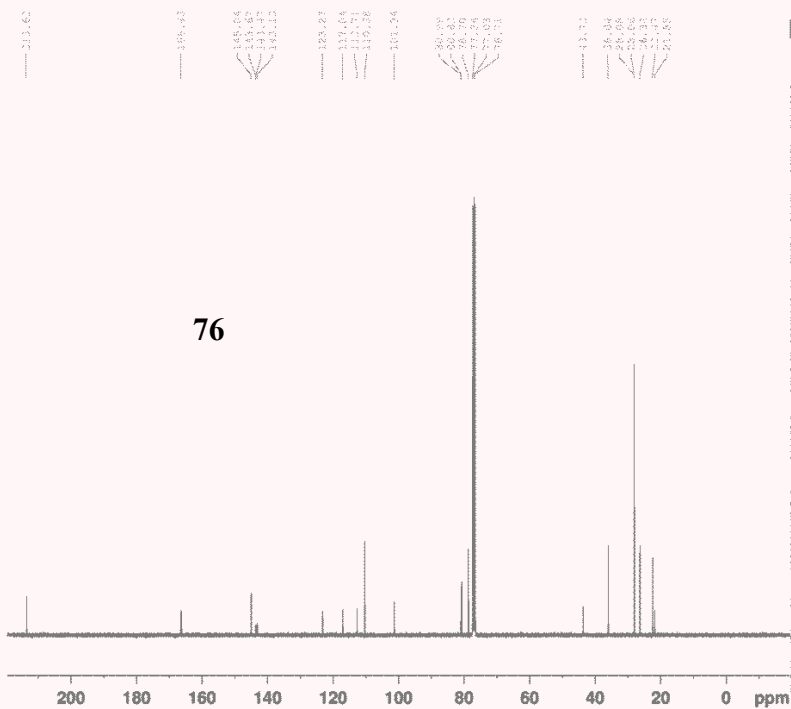
Current Data Parameters
 NAME TS-07-17char
 EXPNO 1
 PROCNO 1

F2 - Acquisition Parameters
 Date_ 20120720
 Time 14:39
 INSTRUM spect
 FPROBHD 5 mm DUL 13C-1
 PULPROG zg30
 TD 49152
 SOLVENT CDC13
 NS 16
 DS 0
 SWH 6421.233 Hz
 FIDRES 0.130640 Hz
 AQ 3.8273523 sec
 RG 2037
 DW 77.867 usec
 DE 6.00 usec
 TE 294.2 K
 D1 1.00000000 sec
 D11 0.00000000 sec
 D12 0.00000000 sec
 D13 0.00000000 sec
 D14 0.00000000 sec
 D15 0.00000000 sec
 D16 0.00000000 sec
 DELTAC 0.00000000 sec
 JMR 0.00000000 sec

===== CHANNEL f1 =====
 NUC1 1H
 P1 9.70 usec
 PL1 -4.00 dB
 SFO1 400.3223900 MHz

F2 - Processing parameters
 SI 65536
 SF 400.3200164 MHz
 NMR EM
 SSB 0
 LB 0.10 Hz
 GB 0
 PC 1.00

1d_13C_1_hour CDC13 D:\ Barr 17



Current Data Parameters
 NAME TS-07-17char
 EXPNO 2
 PROCNO 1

F2 - Acquisition Parameters
 Date_ 20120720
 Time_ 23.06
 INSTRUM spect
 PROBHD 5 mm DUL 13C-1
 PULPROG zgpg30
 TD 51200
 SOLVENT CDC13
 NS 1664
 DS 0
 SMH 24038.461 Hz
 FIDRES 0.469501 Hz
 AQ 1.0650100 sec
 RG 322
 DW 20.800 usec
 DE 6.00 usec
 TE 295.0 K
 D1 1.0000000 sec
 d11 0.0300000 sec
 DELTA 0.89999998 sec
 TD0 1

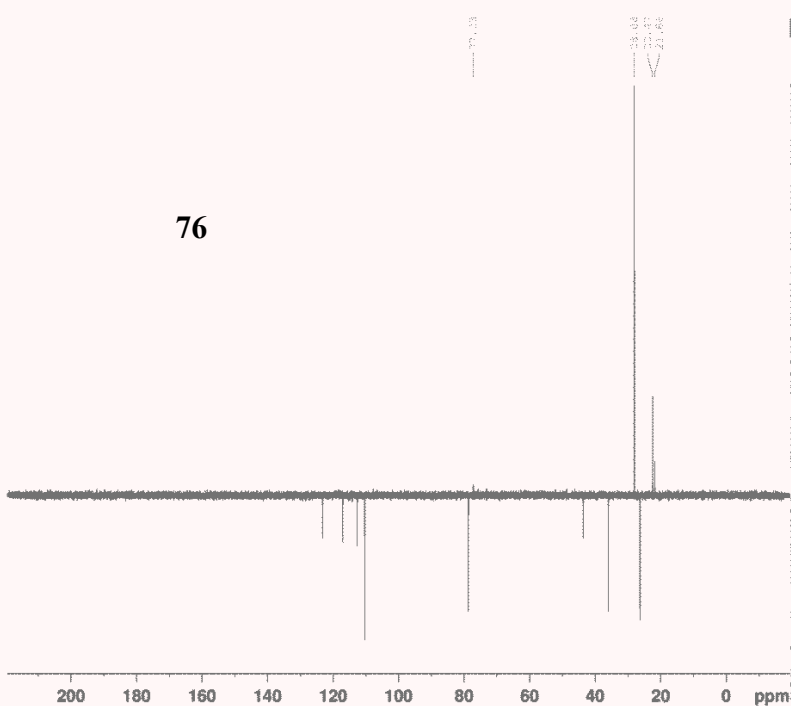
===== CHANNEL f1 =====
 NUC1 13C
 P1 7.00 usec
 PL1 -3.00 dB
 SFO1 100.6706101 MHz

===== CHANNEL f2 =====
 CPDPRG2 waltz16
 NUC2 1H
 FCPD2 80.00 usec
 PL2 -4.00 dB
 PL12 11.78 dB
 PL13 17.00 dB
 SFO2 400.3216013 MHz

F2 - Processing parameters
 SI 65536
 SF 100.6605440 MHz
 MDW EM
 SSB 0
 LB 1.00 Hz
 GB 0
 PC 1.40

76

1d_13C_DEPT_135_20_minutes CDC13 D:\ Barr 17



Current Data Parameters
 NAME TS-07-17char
 EXPNO 3
 PROCNO 1

F2 - Acquisition Parameters
 Date_ 20120720
 Time_ 23.28
 INSTRUM spect
 PROBHD 5 mm DUL 13C-1
 PULPROG dept135
 TD 51200
 SOLVENT CDC13
 NS 416
 DS 2
 SMH 24038.461 Hz
 FIDRES 0.469501 Hz
 AQ 1.0650100 sec
 RG 2050
 DW 20.800 usec
 DE 6.00 usec
 TE 295.0 K
 CRST2 145.0000000 sec
 D1 2.00000000 sec
 d2 0.00344828 sec
 d12 0.00002000 sec
 DELTA 0.00000891 sec
 TD0 1

===== CHANNEL f1 =====
 NUC1 13C
 P1 7.00 usec
 PL1 14.00 dB
 PL1 -3.00 dB
 SFO1 100.6706101 MHz

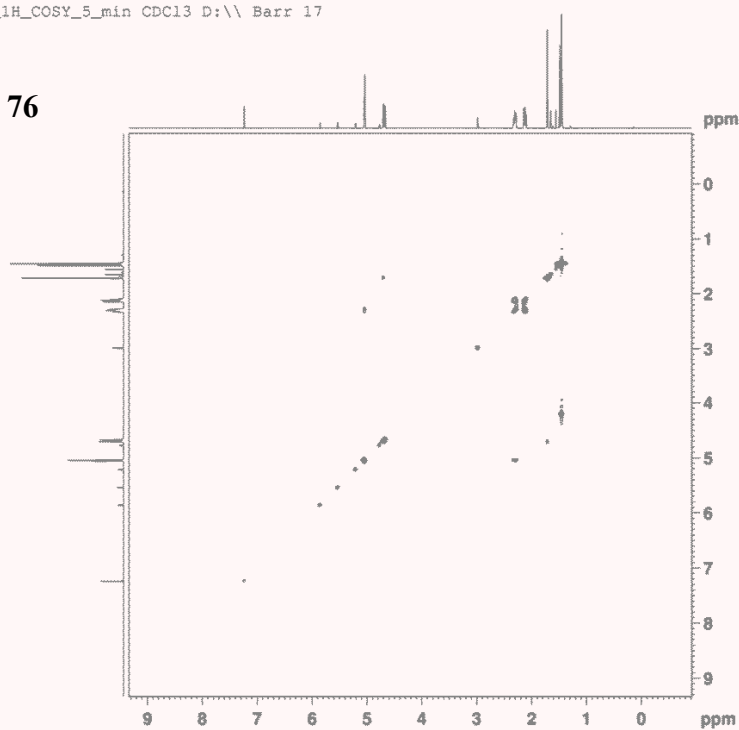
===== CHANNEL f2 =====
 CPDPRG2 waltz16
 NUC2 1H
 P3 13.00 usec
 P4 26.00 usec
 FCPD2 80.00 usec
 PL2 -4.00 dB
 PL12 11.78 dB
 SFO2 400.3216013 MHz

F2 - Processing parameters
 SI 65536
 SF 100.6605440 MHz
 MDW EM
 SSB 0
 LB 1.00 Hz
 GB 0
 PC 1.40

76

2d_1H-COSY_5_min CDC13 D:\\ Barr 17

76



```

Current Data Parameters
NAME      T6-07-17char
EXPNO    4
PROCNO   1

F2 - Acquisition Parameters
Date_    20120720
Time     11.40
INSTRUM  spect
PROBHD   5 mm DDZ 13C-1
PULPROG  zgpg30
TD        1024
SOLVENT  CDCl3
NS        1
DS        0
SWH       4105.090 Hz
FIDRES   4.008877 Hz
AQ        0.1241132 sec
RG         612
DM         121.800 usec
DE         6.00 usec
IE         274.0 K
SFO       0.0000300 sec
D1         1.0000000 sec
d11       0.0000400 sec
D12       0.0002000 sec
IN0       0.00024370 sec

----- CHANNEL f1 -----
NUC1      1H
P0        4.85 usec
P1        -1.00 dB
P2        400.321714 MHz

----- GRADIENT CHANNEL -----
GRNAM1   s1ne-100
GRNAM2   s1ne-100
GP21     10.00 %
GP22     10.00 %
P16      1000.00 usec

F1 - Acquisition parameters
TD        256
SFO1     400.3217 MHz
FIDRES   16.028229 Hz
SW        19.250 ppm
FREQ002  QF

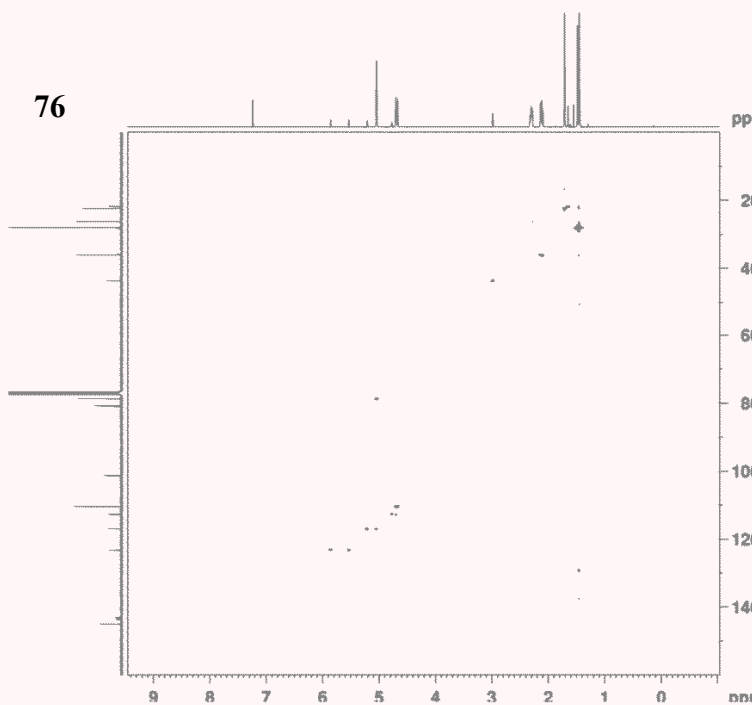
F2 - Processing parameters
SI        512
SF        400.3200164 MHz
WDW       0
SSB       0 Hz
LB        0
GB        0
PC        1.00

F1 - Processing parameters
SI        512
MC2       0
SF        400.3200164 MHz
WDW       0
SSB       0 Hz
LB        0
GB        0
PC        1.00

```

2d_HMQC_1_hour CDC13 D:\\ Barr 17

76



```

Current Data Parameters
NAME      T6-07-17char
EXPNO    3
PROCNO   1

F2 - Acquisition Parameters
Date_    20120720
Time     12.24
INSTRUM  spect
PROBHD   5 mm DDZ 13C-1
PULPROG  zgpg30
TD        1024
SOLVENT  CDCl3
NS        14
DS        0
SWH       4201.401 Hz
FIDRES   4.103804 Hz
AQ        0.1219656 sec
RG         728
DM         139.000 usec
DE         6.00 usec
IE         294.1 K
SFO       0.0000300 sec
D1         1.0000000 sec
d11       1.0000000 sec
d12       1.0000000 sec
D13       1.0000000 sec
D14       1.0000000 sec
D15       1.0002000 sec
IN0       1.0000000 sec

----- CHANNEL f1 -----
NUC1      1H
P0        8.75 usec
P1        -1.00 dB
P2        400.321714 MHz

----- CHANNEL f2 -----
CPDPRG2  s1ne-100
NUC2      13C
P0        3.00 usec
P1        80.00 usec
P2        -1.00 dB
P3        13.75 dB
SFO2     100.6263970 MHz

----- GRADIENT CHANNEL -----
GRNAM1   s1ne-100
GRNAM2   s1ne-100
GP21     10.00 %
GP22     10.00 %
GP23     10.00 %
P16      1000.00 usec

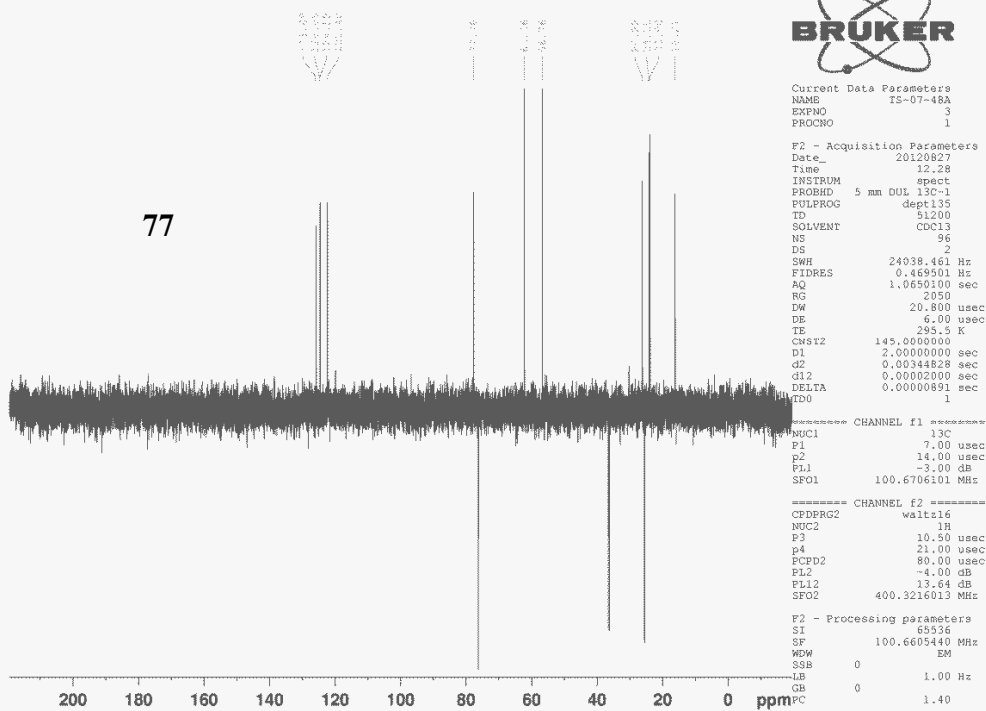
F1 - Acquisition parameters
TD        256
SFO1     100.62636 MHz
FIDRES   6.302076 Hz
SW        159.961 ppm
FREQ002  QF

F2 - Processing parameters
SI        1024
SF        100.6263636 MHz
WDW       0
SSB       0 Hz
LB        0
GB        0
PC        1.00

F1 - Processing parameters
SI        1024
MC2       0
SF        100.6263636 MHz
WDW       0
SSB       0 Hz
LB        0
GB        0
PC        1.00

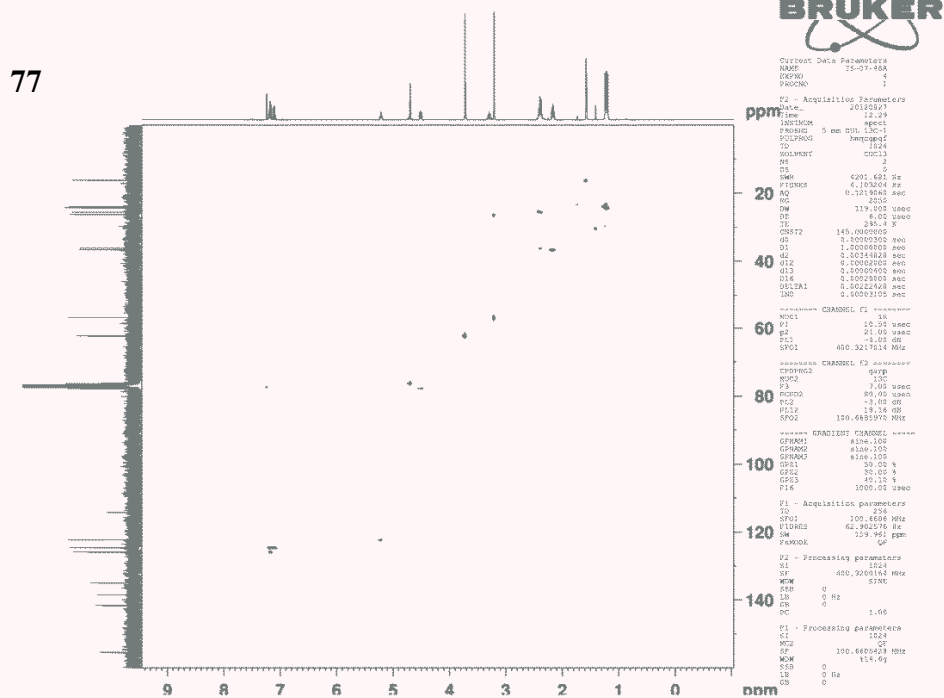
```


1d_13C_DEPT_135_5_minutes CDC13 D:\ Barr 34

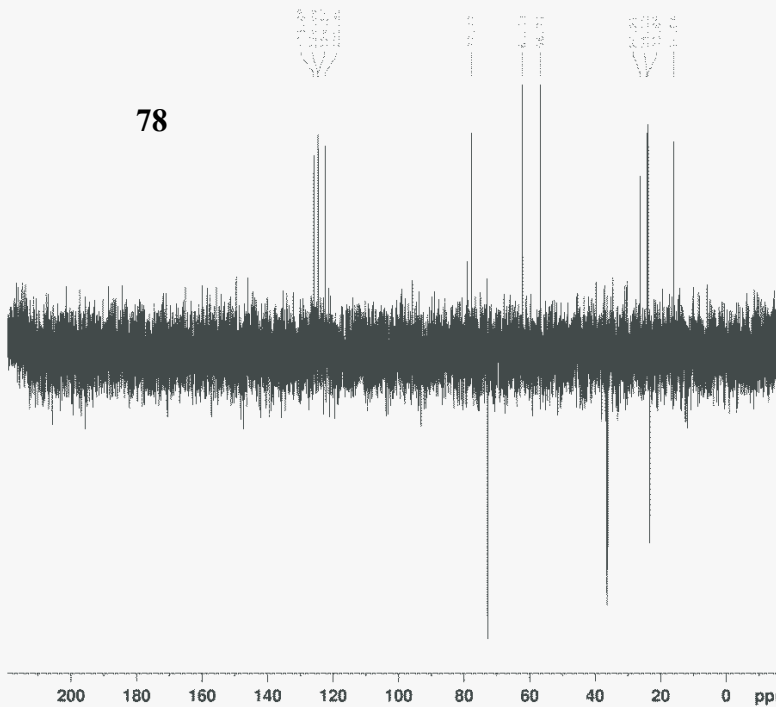


2d_HMQC_10_minutes CDC13 D:\ Barr 34

77



1d_13C_DEPT_135_5_minutes CDC13 D:\ Barr 35



```

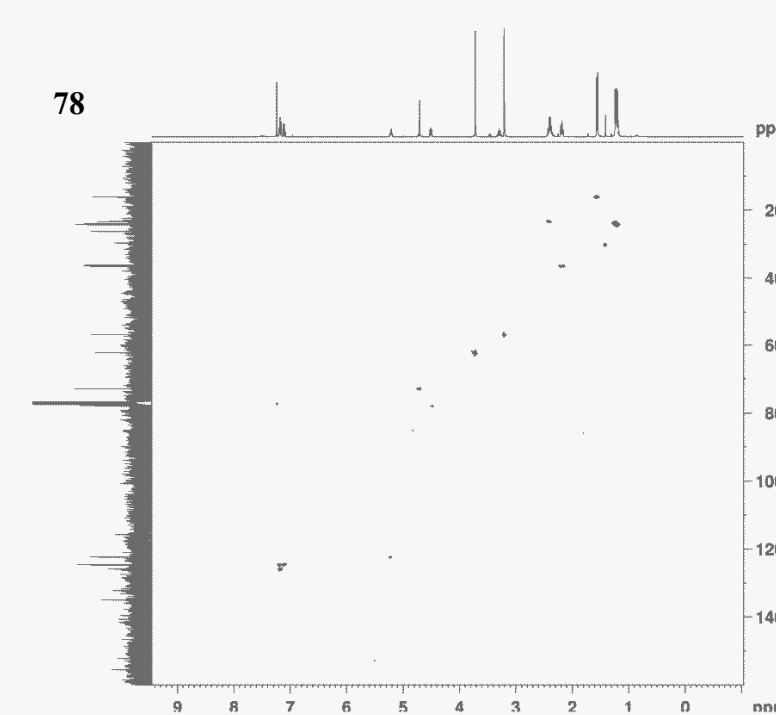
Current Data Parameters
NAME      15-07-48B
EXPNO     3
PROCNO    1

F2 - Acquisition Parameters
Date_     20120827
Time      12.54
INSTRUM   spect
PROBHD    5 mm DUL 13C-1
PULPROG   dept135
ID        51200
SOLVENT   CDC13
NS         96
DS         2
SWH        24038.461 Hz
FIDRES     0.469501 Hz
AQ         1.0650100 sec
RG         2050
DM         20.800 usec
DE         6.00 usec
TE         295.6 K
===== CHANNEL f1 =====
NUC1       13C
P1         7.00 usec
P2         14.00 usec
PL1        -3.00 dB
PL2        -3.00 dB
SFO1       100.6706101 MHz

===== CHANNEL f2 =====
CPDPRG2   waltz16
NUC2       1H
P3         10.50 usec
P4         21.00 usec
PCPD2     80.00 usec
PL2        -4.00 dB
PL12       13.64 dB
SFO2       400.3216013 MHz

F2 - Processing parameters
SI         65536
SF         100.6605440 MHz
WDW        EM
SSB        0
LB         1.00 Hz
GB         0
PC         1.40
    
```

2d_HMQC_10_minutes CDC13 D:\ Barr 35



```

Current Data Parameters
NAME      15-07-48B
EXPNO     3
PROCNO    1

F2 - Acquisition Parameters
Date_     20120827
Time      12.54
INSTRUM   spect
PROBHD    5 mm DUL 13C-1
PULPROG   hmqc
ID        51200
SOLVENT   CDC13
NS         96
DS         2
SWH        24038.461 Hz
FIDRES     0.469501 Hz
AQ         1.0650100 sec
RG         2050
DM         20.800 usec
DE         6.00 usec
TE         295.6 K
===== CHANNEL f1 =====
NUC1       13C
P1         7.00 usec
P2         14.00 usec
PL1        -3.00 dB
PL2        -3.00 dB
SFO1       100.6706101 MHz

===== CHANNEL f2 =====
CPDPRG2   waltz16
NUC2       1H
P3         10.50 usec
P4         21.00 usec
PCPD2     80.00 usec
PL2        -4.00 dB
PL12       13.64 dB
SFO2       400.3216013 MHz

F2 - Processing parameters
SI         65536
SF         100.6605440 MHz
WDW        EM
SSB        0
LB         1.00 Hz
GB         0
PC         1.40

===== CHANNEL f1 =====
NUC1       13C
P1         7.00 usec
P2         14.00 usec
PL1        -3.00 dB
PL2        -3.00 dB
SFO1       100.6706101 MHz

===== CHANNEL f2 =====
CPDPRG2   waltz16
NUC2       1H
P3         10.50 usec
P4         21.00 usec
PCPD2     80.00 usec
PL2        -4.00 dB
PL12       13.64 dB
SFO2       400.3216013 MHz

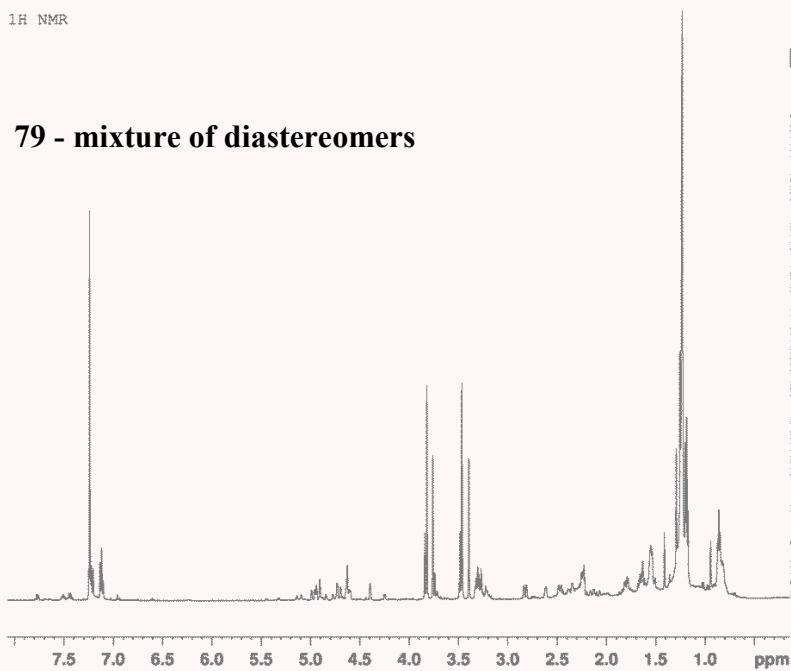
F2 - Processing parameters
SI         65536
SF         100.6605440 MHz
WDW        EM
SSB        0
LB         1.00 Hz
GB         0
PC         1.40

===== CHANNEL f1 =====
NUC1       13C
P1         7.00 usec
P2         14.00 usec
PL1        -3.00 dB
PL2        -3.00 dB
SFO1       100.6706101 MHz

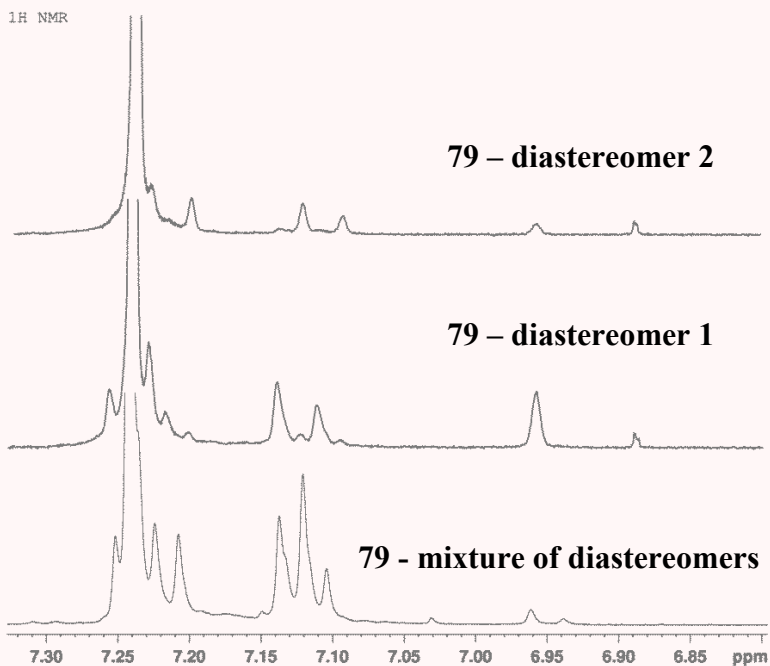
===== CHANNEL f2 =====
CPDPRG2   waltz16
NUC2       1H
P3         10.50 usec
P4         21.00 usec
PCPD2     80.00 usec
PL2        -4.00 dB
PL12       13.64 dB
SFO2       400.3216013 MHz

F2 - Processing parameters
SI         65536
SF         100.6605440 MHz
WDW        EM
SSB        0
LB         1.00 Hz
GB         0
PC         1.40
    
```

1H NMR

79 - mixture of diastereomers

1H NMR

79 - diastereomer 2**79 - diastereomer 1****79 - mixture of diastereomers**

1H NMR



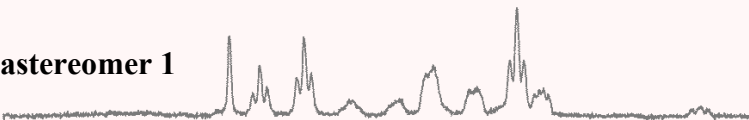
Current Data Parameters
 NAME TS-07-37-longscan
 EXPNO 1
 PROCNO 1

79 – diastereomer 2



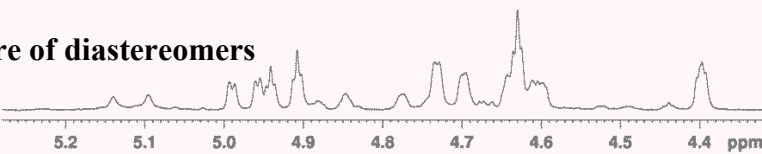
F2 - Acquisition Parameters
 Date_ 20120820
 Time_ 19.44
 INSTRUM spect
 PROBHD 5 mm TBO BB-1H
 PULPROG zg30
 TD 65536
 SOLVENT CDC13
 NS 1024
 DS 0
 SMH 8445.946 Hz
 FIDRES 0.128875 Hz
 AQ 3.8797812 sec
 RG 45.25
 DW 59.200 usec
 DE 6.50 usec
 TE 295.3 K
 D1 0.01000000 sec
 TDO 1

79 – diastereomer 1



===== CHANNEL f1 =====
 NUC1 1H
 P1 13.75 usec
 P11 0 dB
 PL1W 37.67829514 W
 SFO1 500.1320005 MHz

79 - mixture of diastereomers



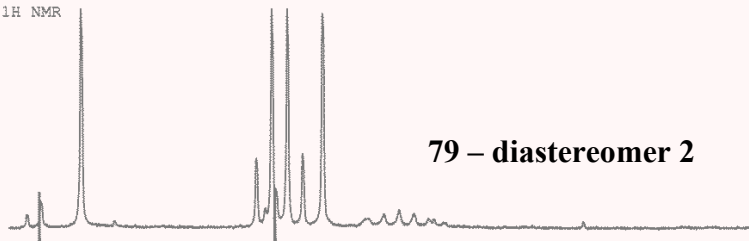
F2 - Processing parameters
 SI 65536
 SF 500.1300231 MHz
 MDW EM
 SSB 0
 LB 0 Hz
 GB 0
 PC 4.00

1H NMR



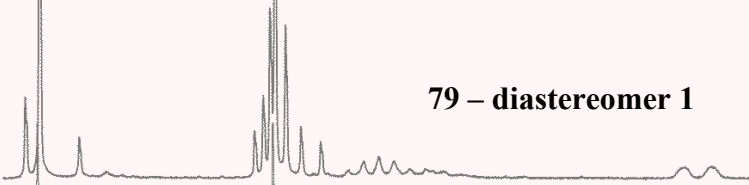
Current Data Parameters
 NAME TS-07-37-longscan
 EXPNO 1
 PROCNO 1

79 – diastereomer 2



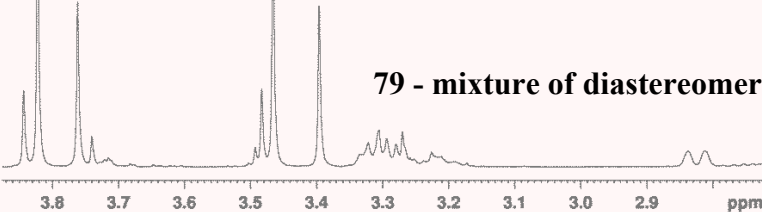
F2 - Acquisition Parameters
 Date_ 20120820
 Time_ 19.44
 INSTRUM spect
 PROBHD 5 mm TBO BB-1H
 PULPROG zg30
 TD 65536
 SOLVENT CDC13
 NS 1024
 DS 0
 SMH 8445.946 Hz
 FIDRES 0.128875 Hz
 AQ 3.8797812 sec
 RG 45.25
 DW 59.200 usec
 DE 6.50 usec
 TE 295.3 K
 D1 0.01000000 sec
 TDO 1

79 – diastereomer 1



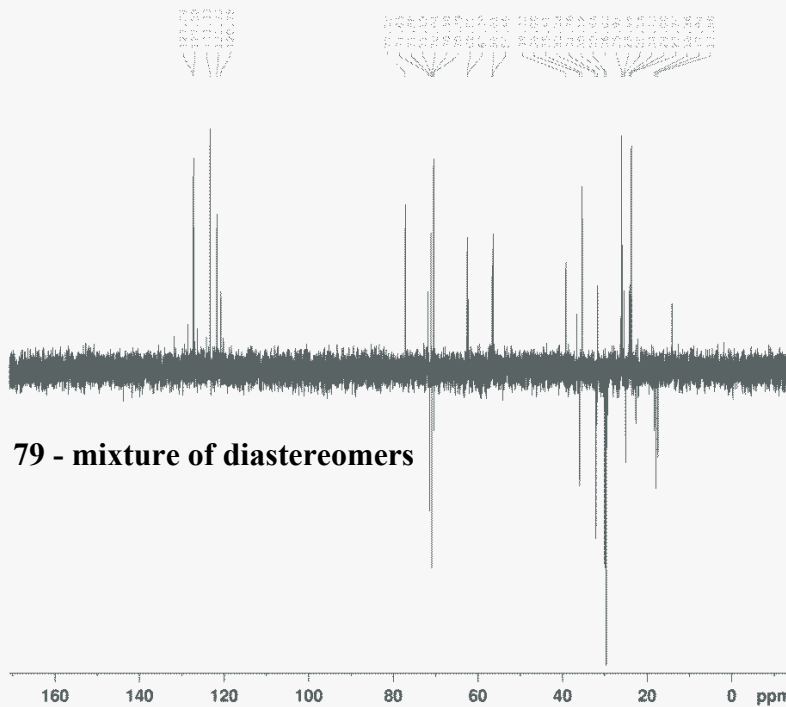
===== CHANNEL f1 =====
 NUC1 1H
 P1 13.75 usec
 P11 0 dB
 PL1W 37.67829514 W
 SFO1 500.1320005 MHz

79 - mixture of diastereomers



F2 - Processing parameters
 SI 65536
 SF 500.1300231 MHz
 MDW EM
 SSB 0
 LB 0 Hz
 GB 0
 PC 4.00

13C DEPT 135



79 - mixture of diastereomers



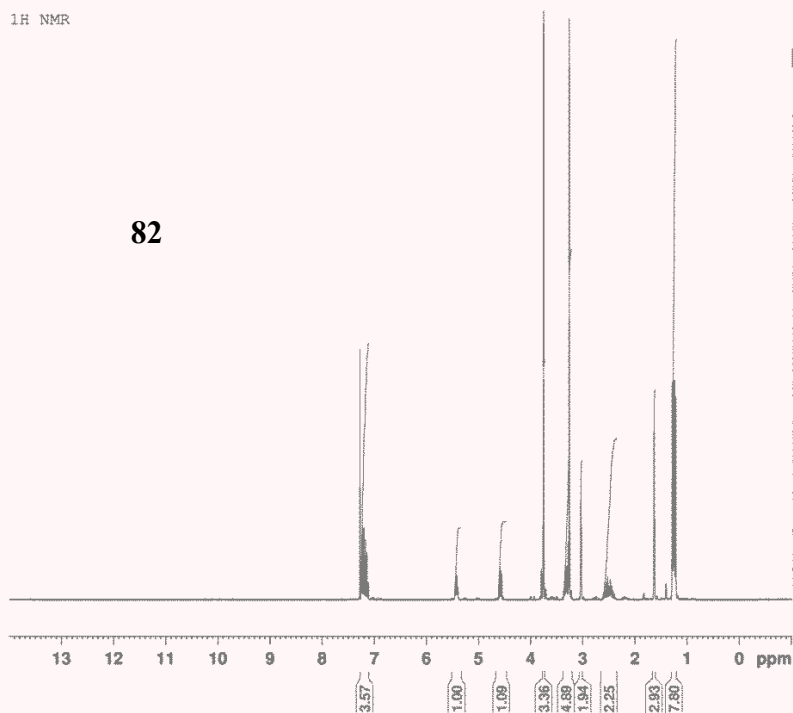
Current Data Parameters
 NAME TS-07-37-longscan
 EXPNO 3
 PROCNO 1

F2 - Acquisition Parameters
 Date_ 20120821
 Time 14.07
 INSTRUM spect
 PROBHD 5 mm TBO BB-1H
 PULPROG dept135
 TD 65536
 SOLVENT CDCl3
 NS 5000
 DS 2
 SWH 32679.738 Hz
 FIDRES 0.498653 Hz
 AQ 1.0027508 sec
 RG 4096
 DM 15.300 usec
 DE 6.50 usec
 TE 295.6 K
 CNST2 145.000000
 Z1 2.00000000 sec
 D2 0.00344828 sec
 D12 0.00002000 sec
 ID0 1

***** CHANNEL f1 *****
 NUC1 13C
 P1 8.00 usec
 P2 16.00 usec
 PL1 0 dB
 PL1W 75.35659027 W
 SF01 125.7716224 MHz
 ***** CHANNEL f2 *****
 CPDPRG2 waltz16
 NUC2 1H
 P3 13.75 usec
 P4 27.50 usec
 PCPD2 80.00 usec
 PL2 0 dB
 PL12 15.30 dB
 PL2W 37.67829514 W
 PL12W 1.11196530 W
 SF02 500.1320005 MHz

F2 - Processing parameters
 SI 65536
 SF 125.7577949 MHz
 WDW EM
 SSB 0
 LB 1.00 Hz
 GB 0
 PC 1.40

1H NMR



82



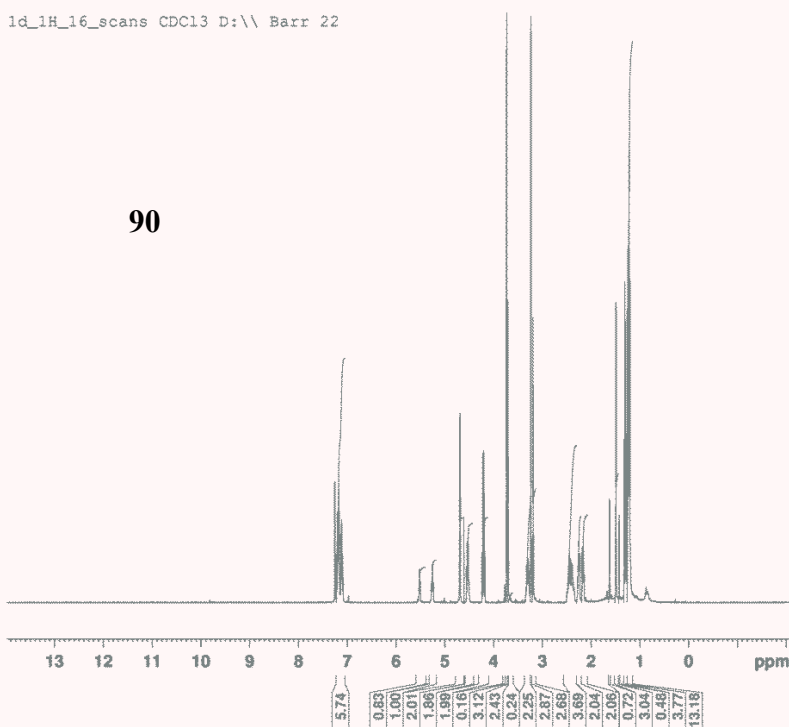
Current Data Parameters
 NAME TS-07-09
 EXPNO 2
 PROCNO 1

F2 - Acquisition Parameters
 Date_ 20120710
 Time 14.55
 INSTRUM spect
 PROBHD 5 mm PABBO BB-
 PULPROG zg30
 TD 32768
 SOLVENT CDCl3
 NS 16
 DS 0
 SWH 4507.211 Hz
 FIDRES 0.137549 Hz
 AQ 3.6351135 sec
 RG 90.5
 DM 110.933 usec
 DE 6.00 usec
 TE 298.2 K
 D1 0.01000000 sec
 TD0 1

***** CHANNEL f1 *****
 NUC1 1H
 P1 11.75 usec
 PL1 0 dB
 SF01 300.3319506 MHz
 F2 - Processing parameters
 SI 32768
 SF 300.3300000 MHz
 WDW EM
 SSB 0
 LB 0 Hz
 GB 0
 PC 1.00

1d_1H_16_scans CDC13 D:\\ Barr 22

90



Current Data Parameters
 NAME TS-07-14-unknown product-char
 EXPNO 1
 PROCNO 1

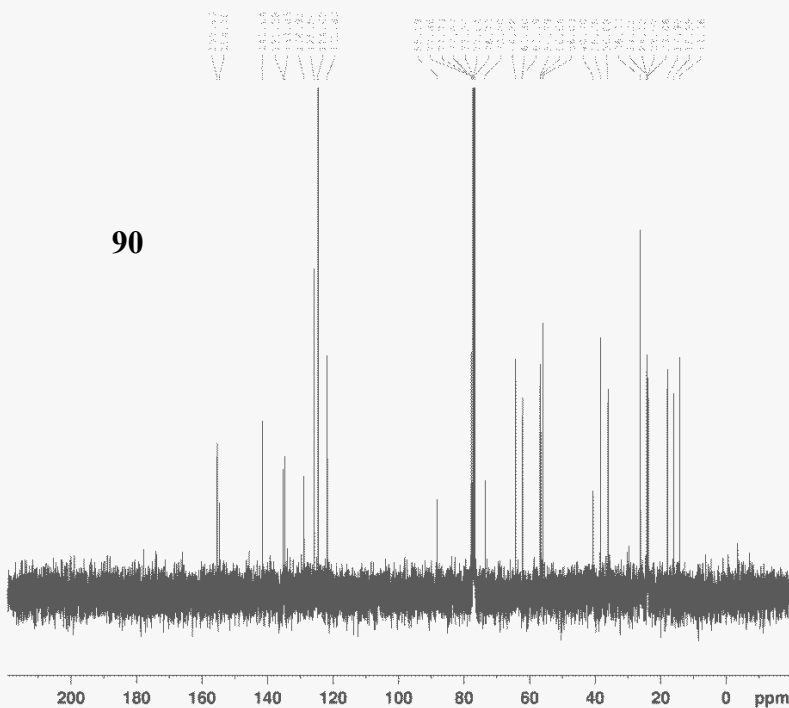
F2 - Acquisition Parameters
 Date_ 20120719
 Time 6:14
 INSTRUM spect
 PWR000 5 cm BBL 130-1
 PULPROG zg30
 TD 65536
 SOLVENT CDCl3
 NS 16
 DS 0
 SWH 6421.233 Hz
 FIDRES 0.130640 Hz
 AQ 3.6273523 sec
 RG 655
 DW 77.867 usec
 DE 6.00 usec
 TE 293.2 K
 D1 1.6000000 sec
 TD0 1

===== CHANNEL f1 =====
 NUC1 1H
 P1 9.00 usec
 PL1 -4.00 dB
 SFO1 400.3223900 MHz

F2 - Processing parameters
 SF 400.3200393 MHz
 WDW 0
 SSB 0
 GB 0 0.10 Hz
 PC 1.00

1d_13C_5_minutes CDC13 D:\\ Barr 22

90



Current Data Parameters
 NAME TS-07-14-unknown product-char
 EXPNO 2
 PROCNO 1

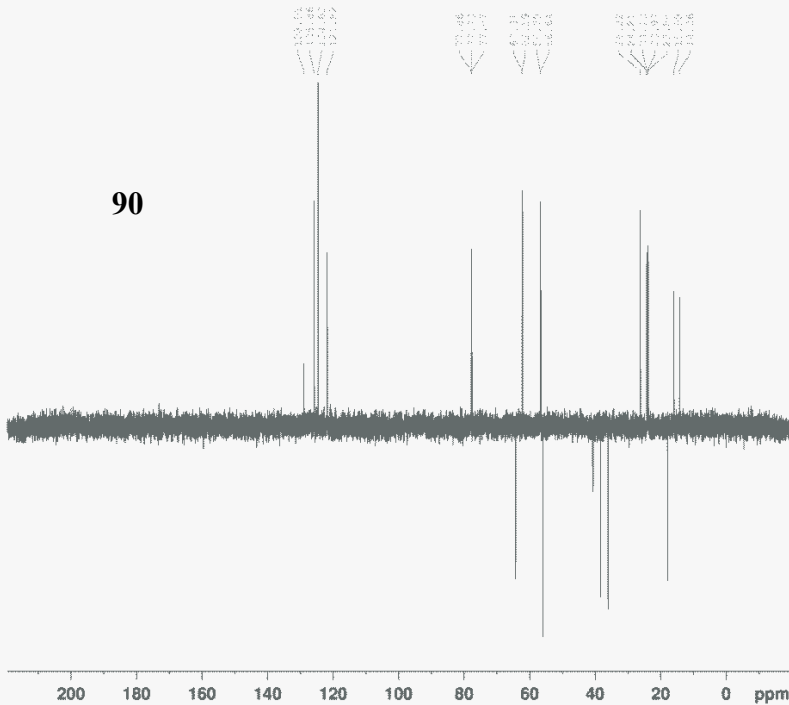
F2 - Acquisition Parameters
 Date_ 20120719
 Time 6:14
 INSTRUM spect
 PWR000 5 cm BBL 130-1
 PULPROG zgpg30
 TD 65536
 SOLVENT CDCl3
 NS 128
 DS 0
 SWH 24036.461 Hz
 FIDRES 0.144901 Hz
 AQ 1.0680100 sec
 RG 522
 DW 20.800 usec
 DE 6.00 usec
 TE 293.2 K
 D1 1.6000000 sec
 d11 0.6300000 sec
 DELTA 0.6999999 sec
 TD0 1

===== CHANNEL f1 =====
 NUC1 13C
 P1 7.00 usec
 PL1 -1.00 dB
 SFO1 100.626101 MHz

===== CHANNEL f2 =====
 NUC2 1H
 P2 90.00 usec
 PL2 -4.00 dB
 SFO2 400.322390 MHz

F2 - Processing parameters
 SF 100.626101 MHz
 WDW 0
 SSB 0
 GB 0 1.00 Hz
 PC 1.40

1d_13C_DEPT_135_5_minutes CDC13 D:\\ Barr 22



Current Data Parameters
 NAME TS-01-14-unknown product-char
 EXPNO 1
 PROCNO 1

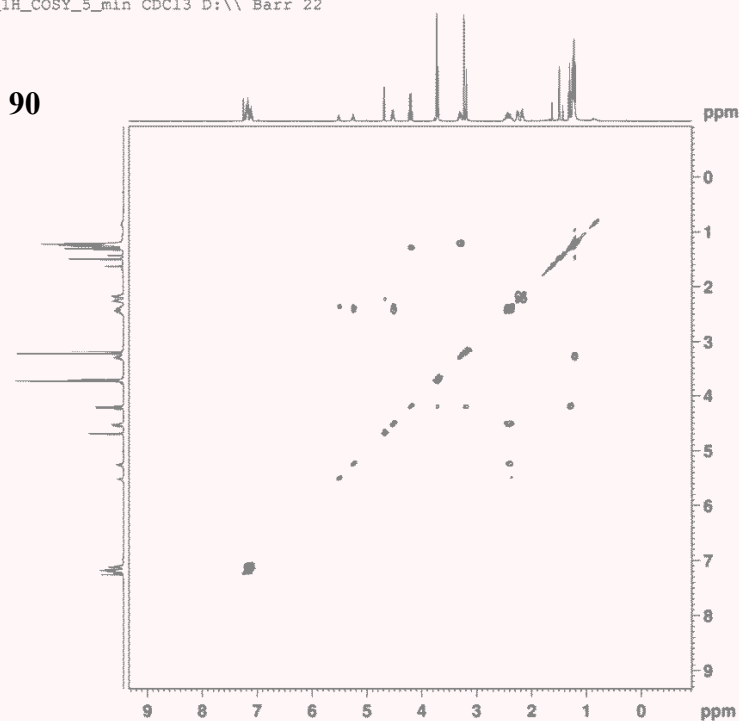
F2 - Acquisition Parameters
 Date_ 20120719
 Time 6:24
 INSTRUM spect
 PROBR0 5 mm BBI 130-1
 PULPROG dept135
 TD 32768
 SOLVENT CDCl3
 NS 96
 DS 2
 SFO1 24039.461 Hz
 FIDRES 0.163551 Hz
 AQ 1.0630100 sec
 RG 4095
 DW 20.800 usec
 DE 6.00 usec
 TE 291.2 K
 CNTRZ 148.000000
 D1 2.0000000 sec
 d2 0.0034428 sec
 d12 0.0000000 sec
 DELTA 0.0000681 sec
 TD0 1

----- CHANNEL f1 -----
 NUC1 13C
 P1 7.00 usec
 PC 14.00 usec
 PL1 -2.00 dB
 SFO1 100.626111 MHz

----- CHANNEL f2 -----
 CPDPRG2 waltz16
 EXP2 4
 NS2 33.00 usec
 DS2 1
 F4 26.00 usec
 PC22 80.00 usec
 PL2 -3.00 dB
 PL22 11.78 dB
 SFO2 400.3214111 MHz

F2 - Processing parameters
 SI 4534
 SF 100.6260640 MHz
 SSB 0
 LB 1.00 Hz
 GB 0
 DC 1.40

2d_1H_COSY_5_min CDC13 D:\\ Barr 22



Current Data Parameters
 NAME TS-01-14-unknown product-char
 EXPNO 4
 PROCNO 1

F2 - Acquisition Parameters
 Date_ 20120719
 Time 6:22
 INSTRUM spect
 PROBR0 5 mm BBI 130-1
 PULPROG cosyysg245
 TD 32768
 SOLVENT CDCl3
 NS 1
 DS 1
 SFO1 4105.030 Hz
 FIDRES 4.00877 Hz
 AQ 0.1247732 sec
 RG 121.800 usec
 DW 6.00 usec
 TE 291.2 K
 d0 0.0000000 sec
 d1 1.0000000 sec
 d13 0.0000400 sec
 d14 0.0000000 sec
 IN0 0.0002470 sec

----- CHANNEL f1 -----
 NUC1 1H
 PC 4.85 usec
 PL1 9.70 usec
 PL2 -4.00 dB
 SFO1 400.3217014 MHz

----- GRADIENT CHANNEL -----
 GPMPL sine.100
 GPRM2 sine.100
 GP21 10.00 %
 GP22 10.00 %
 P15 1000.00 usec

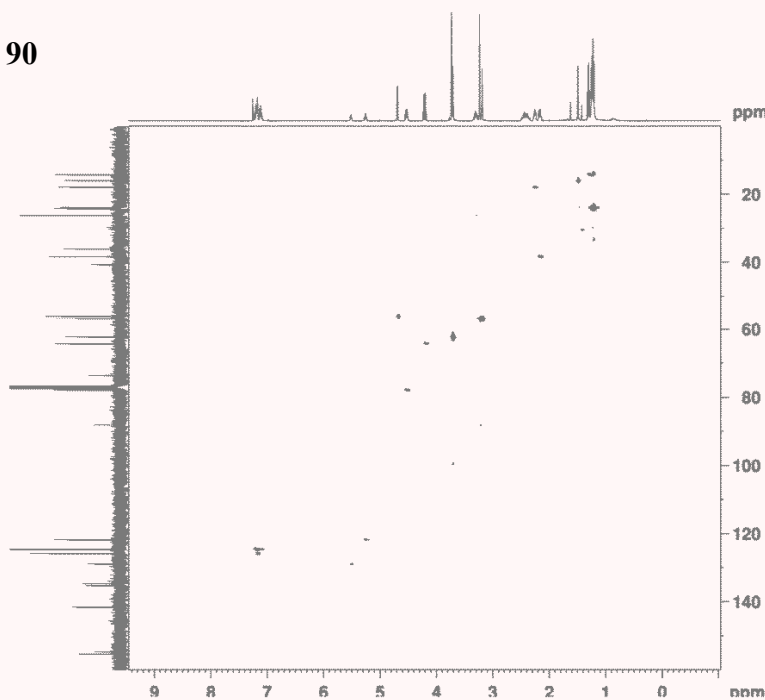
F1 - Acquisition parameters
 TD 32768
 SFO1 400.3217 MHz
 FIDRES 16.028229 Hz
 SW 10.230 ppm
 PR0MODE QF

F2 - Processing parameters
 SI 512
 SF 400.3200144 MHz
 SSB 0
 SINE
 LB 0 Hz
 GB 0
 DC 1.00

F1 - Processing parameters
 SI 512
 NUC1 1H
 SF 400.3200144 MHz
 SSB 0
 LB 411.60 Hz
 GB 0
 DC 0

2d_HMQC_10_minutes CDC13 D:\ Barr 22

90



Current Data Parameters
NAME TS-07-14-unknown product-ober
EXPNO 1
PROCNO 1

F2 - Acquisition Parameters
Date_ 201213
Time_ 8:31
INSTRUM spect
PROBHD 5 mm QNP 1H/1
PULPROG zgpg30
TD 3274
SOLVENT CDCl3
NS 1
DS 2
SWH 6301.421 Hz
FIDRES 6.133204 Hz
AQ 0.221965 sec
RG 256
DW 713.500 usec
DE 6.00 usec
TE 294.1 K
D1 145.000000 sec
d11 2.0000000 sec
d12 1.0000000 sec
d13 2.0000000 sec
d14 2.0000000 sec
d15 2.0000000 sec
d16 2.0000000 sec
d17 2.0000000 sec
d18 2.0000000 sec
d19 2.0000000 sec
d20 2.0000000 sec

===== CHANNEL f1 =====
NUC1 13
P1 9.75 usec
PL1 -1.00 dB
SFO1 400.321714 MHz

===== CHANNEL f2 =====
CPDPRG2 gfp
NUC2 13
P2 9.00 usec
PL2 -4.00 dB
SFO2 100.626150 MHz

===== CHANNEL f3 =====
CPDPRG3 gfp
NUC3 13
P3 9.00 usec
PL3 -4.00 dB
SFO3 100.626150 MHz

===== CHANNEL f4 =====
CPDPRG4 gfp
NUC4 13
P4 9.00 usec
PL4 -4.00 dB
SFO4 100.626150 MHz

D1 - Acquisition parameters
TD 3274
SFO1 400.321714 MHz
FIDRES 6.133204 Hz
SW 6301.421 Hz
PROCNO 1

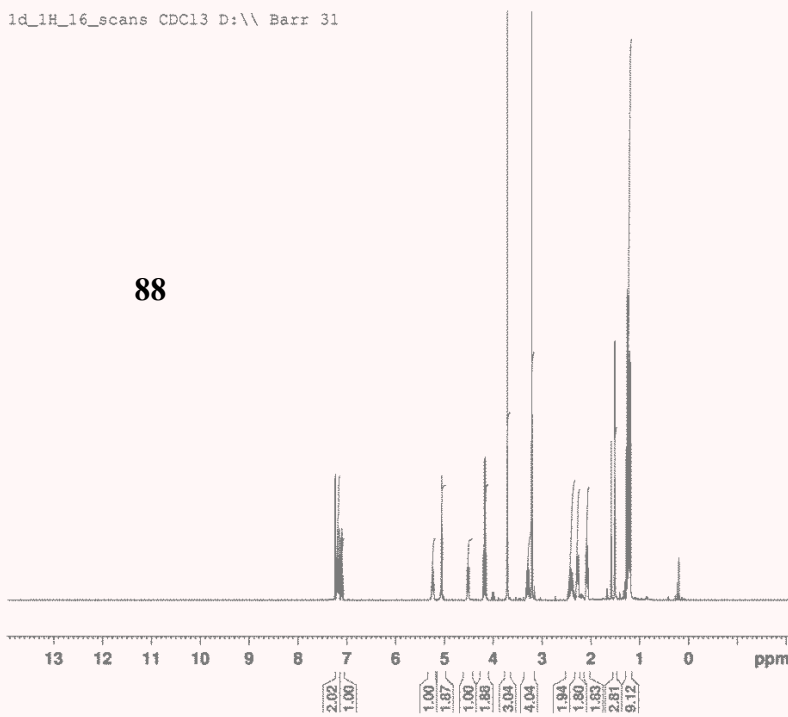
D2 - Processing parameters
SI 65536
SF 400.3200164 MHz
WDW EM
SSB 0
LB 0.10 Hz
GB 0
PC 1.00

D3 - Acquisition parameters
TD 3274
SFO1 400.321714 MHz
FIDRES 6.133204 Hz
SW 6301.421 Hz
PROCNO 1

D4 - Processing parameters
SI 65536
SF 400.3200164 MHz
WDW EM
SSB 0
LB 0.10 Hz
GB 0
PC 1.00

1d_1H_16_scans CDC13 D:\ Barr 31

88



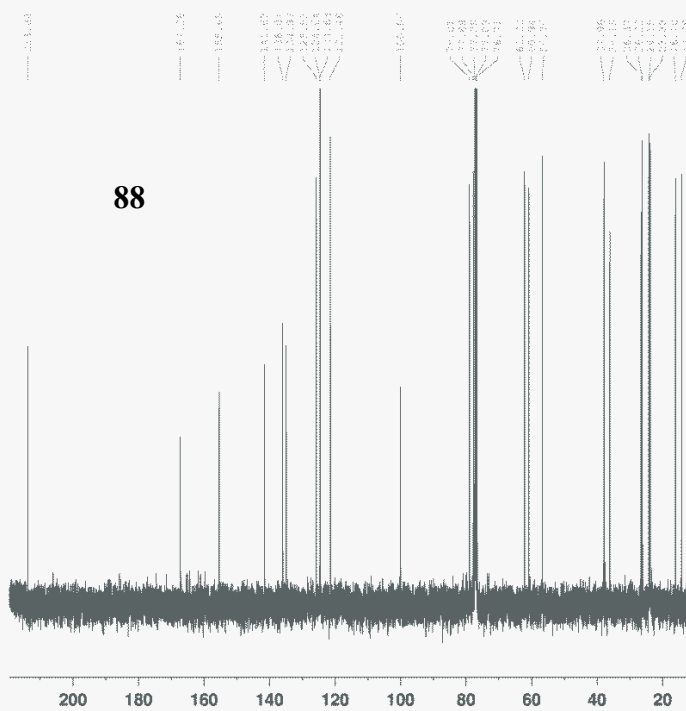
Current Data Parameters
NAME TS-06-59char
EXPNO 1
PROCNO 1

F2 - Acquisition Parameters
Date_ 20120608
Time_ 14:28
INSTRUM spect
PROBHD 5 mm PABBO BB-
PULPROG zg30
TD 49152
SOLVENT CDC13
NS 16
DS 0
SWH 6421.233 Hz
FIDRES 0.130640 Hz
AQ 3.8273523 sec
RG 256
DW 77.867 usec
DE 6.00 usec
TE 295.2 K
D1 1.00000000 sec
TDO 1

===== CHANNEL f1 =====
NUC1 1H
P1 10.75 usec
PL1 -4.00 dB
SFO1 400.3223900 MHz

F2 - Processing parameters
SI 65536
SF 400.3200164 MHz
WDW EM
SSB 0
LB 0.10 Hz
GB 0
PC 1.00

1d_13C_20_minutes CDC13 D:\ Barr 31



Current Data Parameters
 NAME TS-06-58char
 EXPNO 2
 PROCNO 1

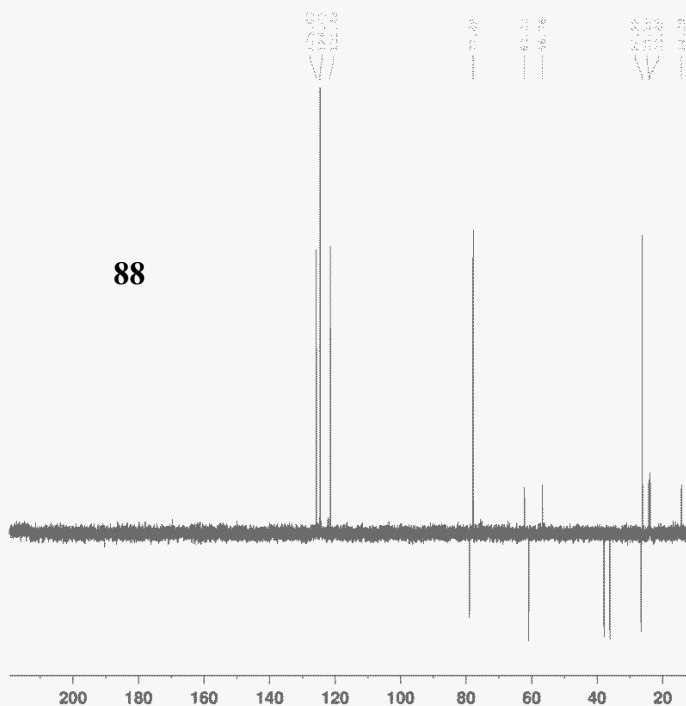
F2 - Acquisition Parameters
 Date_ 20120609
 Time_ 4.50
 INSTRUM spect
 PROBHD 5 mm PABBO BB-
 PULPROG zgpg30
 TD 51200
 SOLVENT CDC13
 NS 512
 DS 0
 SMH 24038.461 Hz
 FIDRES 0.469501 Hz
 AQ 1.0650100 sec
 RG 405
 DW 20.800 usec
 DE 6.00 usec
 TE 296.1 K
 D1 1.00000000 sec
 d11 0.03000000 sec
 DELTA 0.89999998 sec
 TD0 1

----- CHANNEL f1 -----
 NUC1 13C
 P1 7.50 usec
 PL1 -3.00 dB
 SFO1 100.6706101 MHz

----- CHANNEL f2 -----
 CPDPRG2 waltz16
 NUC2 1H
 PCPD2 90.00 usec
 PL2 -4.00 dB
 PL12 14.46 dB
 PL13 18.01 dB
 SFO2 400.3216013 MHz

F2 - Processing parameters
 S1 65536
 SF 100.6605440 MHz
 WDW EM
 SSB 0
 LB 1.00 Hz
 GB 0
 PC 1.40

1d_13C_DEPT_135_20_minutes CDC13 D:\ Barr 31



Current Data Parameters
 NAME TS-06-58char
 EXPNO 3
 PROCNO 1

F2 - Acquisition Parameters
 Date_ 20120609
 Time_ 5.14
 INSTRUM spect
 PROBHD 5 mm PABBO BB-
 PULPROG dept135
 TD 51200
 SOLVENT CDC13
 NS 416
 DS 2
 SMH 24038.461 Hz
 FIDRES 0.469501 Hz
 AQ 1.0650100 sec
 RG 2050
 DW 20.800 usec
 DE 6.00 usec
 TE 295.4 K
 CWST2 145.00000000 sec
 D1 2.00000000 sec
 Q2 0.00344828 sec
 d12 0.00002000 sec
 DELTA 0.00009955 sec
 TD0 1

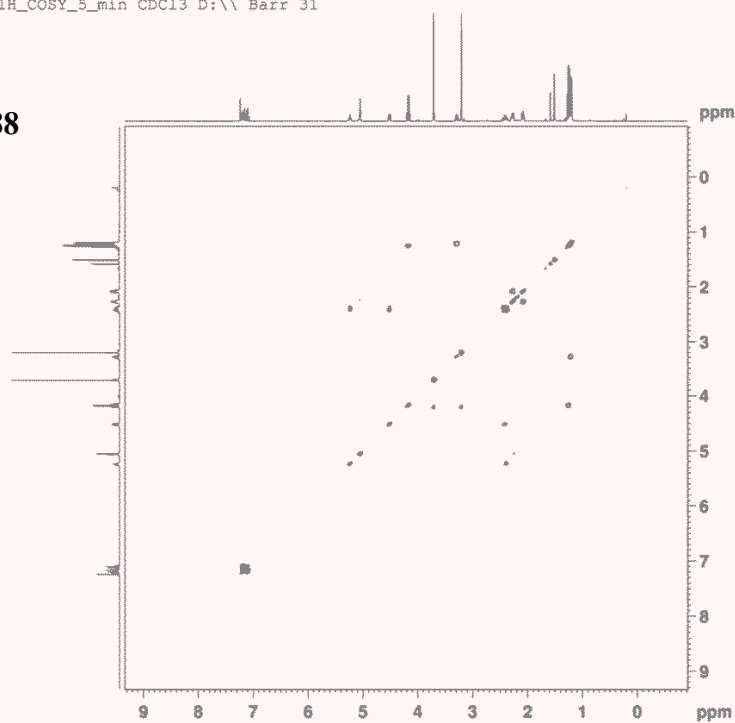
----- CHANNEL f1 -----
 NUC1 13C
 P1 7.50 usec
 P2 15.00 usec
 PL1 -3.00 dB
 SFO1 100.6706101 MHz

----- CHANNEL f2 -----
 CPDPRG2 waltz16
 NUC2 1H
 P3 10.75 usec
 P4 21.50 usec
 PCPD2 90.00 usec
 PL2 -4.00 dB
 PL12 14.46 dB
 SFO2 400.3216013 MHz

F2 - Processing parameters
 S1 65536
 SF 100.6605440 MHz
 WDW EM
 SSB 0
 LB 1.00 Hz
 GB 0
 PC 1.40

2d_1H_COSY_5_min CDC13 D:\\ Barr 31

88



```

Current Data Parameters
NAME      T5-06-58char
EXPNO    4
PROCNO    1

F2 - Acquisition Parameters
Date_     20120608
Time      11.29
INSTRUM   spect
PROBHD    5 mm PABBO BB-
PULPROG   zgpg30
TD         1024
SOLVENT   CDCl3
NS         1
DS         0
SWH        4105.090 Hz
FIDRES    4.008877 Hz
AQ         0.1241732 sec
RG         612
DM         121.800 usec
DE         6.00 usec
TE         295.2 K
AQ         0.0000300 sec
D1         1.0000000 sec
d11        0.0000000 sec
D12        0.0002000 sec
IN0        0.0024370 sec

----- CHANNEL f1 -----
NUC1       1H
P0         5.38 usec
P1         10.75 usec
PL1        -1.00 dB
SFO1       400.3217014 MHz

----- GRADIENT CHANNEL -----
GRNAM1     gline-100
GRNAM2     gline-100
GRP1       10.00 %
GRP2       10.00 %
P16        1000.00 usec

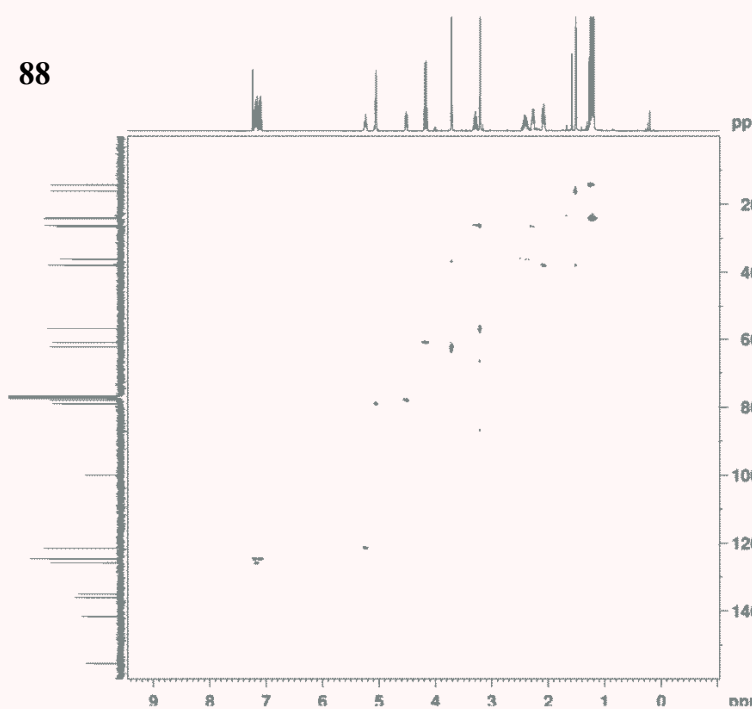
F1 - Acquisition parameters
TD         256
SFO1       400.3217 MHz
FIDRES    16.028929 Hz
SW         10.250 ppm
F0A000    0F

F2 - Processing parameters
SI         512
SF         400.320164 MHz
WDW        SINC
SSB        0
LB         0 Hz
GB         0
PC         1.00

F1 - Processing parameters
SI         512
MC2        0F
SF         400.320164 MHz
WDW        SINC
SSB        0
LB         0 Hz
GB         0
PC         1.00
    
```

2d_HMQC_1_hour CDC13 D:\\ Barr 31

88



```

Current Data Parameters
NAME      T5-06-58char
EXPNO    3
PROCNO    1

F2 - Acquisition Parameters
Date_     20120608
Time      11.05
INSTRUM   spect
PROBHD    5 mm PABBO BB-
PULPROG   zgpg30
TD         1024
SOLVENT   CDCl3
NS         14
DS         0
SWH        4001.602 Hz
FIDRES    4.103204 Hz
AQ         0.1219625 sec
RG         728
DM         121.800 usec
DE         6.00 usec
TE         295.2 K
AQ         0.0000000 sec
D1         1.0000000 sec
d1         0.0000000 sec
D12        0.0000000 sec
D13        0.0000000 sec
D16        0.0000000 sec
D18        0.0000000 sec
D19        0.0000000 sec
D20        0.0000000 sec
D21        0.0000000 sec
D22        0.0000000 sec
D23        0.0000000 sec
D24        0.0000000 sec
D25        0.0000000 sec
D26        0.0000000 sec
D27        0.0000000 sec
D28        0.0000000 sec
D29        0.0000000 sec
D30        0.0000000 sec
D31        0.0000000 sec
D32        0.0000000 sec
D33        0.0000000 sec
D34        0.0000000 sec
D35        0.0000000 sec
D36        0.0000000 sec
D37        0.0000000 sec
D38        0.0000000 sec
D39        0.0000000 sec
D40        0.0000000 sec
D41        0.0000000 sec
D42        0.0000000 sec
D43        0.0000000 sec
D44        0.0000000 sec
D45        0.0000000 sec
D46        0.0000000 sec
D47        0.0000000 sec
D48        0.0000000 sec
D49        0.0000000 sec
D50        0.0000000 sec
D51        0.0000000 sec
D52        0.0000000 sec
D53        0.0000000 sec
D54        0.0000000 sec
D55        0.0000000 sec
D56        0.0000000 sec
D57        0.0000000 sec
D58        0.0000000 sec
D59        0.0000000 sec
D60        0.0000000 sec
D61        0.0000000 sec
D62        0.0000000 sec
D63        0.0000000 sec
D64        0.0000000 sec
D65        0.0000000 sec
D66        0.0000000 sec
D67        0.0000000 sec
D68        0.0000000 sec
D69        0.0000000 sec
D70        0.0000000 sec
D71        0.0000000 sec
D72        0.0000000 sec
D73        0.0000000 sec
D74        0.0000000 sec
D75        0.0000000 sec
D76        0.0000000 sec
D77        0.0000000 sec
D78        0.0000000 sec
D79        0.0000000 sec
D80        0.0000000 sec
D81        0.0000000 sec
D82        0.0000000 sec
D83        0.0000000 sec
D84        0.0000000 sec
D85        0.0000000 sec
D86        0.0000000 sec
D87        0.0000000 sec
D88        0.0000000 sec
D89        0.0000000 sec
D90        0.0000000 sec
D91        0.0000000 sec
D92        0.0000000 sec
D93        0.0000000 sec
D94        0.0000000 sec
D95        0.0000000 sec
D96        0.0000000 sec
D97        0.0000000 sec
D98        0.0000000 sec
D99        0.0000000 sec
D100       0.0000000 sec

----- CHANNEL f1 -----
NUC1       13C
P0         9.00 usec
P1         10.75 usec
PL1        -1.00 dB
SFO1       100.6261014 MHz

----- GRADIENT CHANNEL -----
GRNAM1     gline-100
GRNAM2     gline-100
GRP1       10.00 %
GRP2       10.00 %
P16        1000.00 usec

F1 - Acquisition parameters
TD         256
SFO1       100.6261 MHz
FIDRES    6.390276 Hz
SW         19.961 ppm
F0A000    0F

F2 - Processing parameters
SI         1024
SF         100.6250164 MHz
WDW        SINC
SSB        0
LB         0 Hz
GB         0
PC         1.00

F1 - Processing parameters
SI         1024
MC2        0F
SF         100.6250164 MHz
WDW        SINC
SSB        0
LB         0 Hz
GB         0
PC         1.00
    
```